INTERFACIAL CATIONIC POLYMERIZATION AND ITS APPLICATION IN MICROENCAPSULATION

by

LAILA I. AMER
BSc, MSc (Chemistry), Cairo University

A Thesis submitted to the University of Strathclyde in partial fulfilment of the requirements for the Degree of Doctor of Philosophy

Department of Pure and Applied Chemistry
University of Strathclyde
Glasgow, Scotland

September 1990

Dedicated to Mama and my brothers,

Sultan, Sayed, Mohammed and Osama

In memory of my friend Nagah El-Korashy

CONTENTS

List of Tables

List of Figures

ACKNOWLEDGEMENT

I would like to acknowledge with deep appreciation and gratitude my advisor, Professor Neil B. Graham for his valuable guidance, friendly advice, encouragement and support throughout this work.

I would also like to express my gratitude to Strathclyde University, British Technology Group and the Egyptian Government for their financial support; and special appreciation to the National Research Centre, Egypt for granting me leave of absence to study for this Degree.

Grateful thanks are due to Dr. Marion McNeill and my colleague Christopher Moran for their valuable discussions and help in many phases of this work.

I am indebted to Dr. Zenab Abdel-Latif and Dr. David R. M. Walton, for their sincere care and support during the period of this study.

Special thanks go to technicians in the Department - Mrs. Patricia Keating, for her help and support in HPLC work, John Carruthers for his help in GPC analysis, Paul Jonquin for his expert assistance in photographic work. Thanks are also due to Dr. Bladon and staff for help with NMR analysis.

My deep appreciation to Mrs. Carole Britton for her care and support in various ways and to Mrs. Maria Lynch for her careful assistance and patience during the typing of this thesis.

I acknowledge and appreciate the help and support of all colleagues and friends.

Finally, I would like to thank my family for being patient, with special appreciation to my brother Sultan for his love, support and encouragement which has been beneficial during this study.

SUMMARY

Direct polymerization on the solid surfaces of three crystalline biologically active drugs has been carried out in this study to provide a thin polymer film (capsule wall) around the crystals. This polymer film would act as a release controlling layer of the encapsulated crystals into a surrounding fluid. To date there has not been to our knowledge, any study of release control by the encapsulation of solids by direct polymerization. This thesis describes a new technique based on solid/liquid interfacial cationic polymerization which was carried out in an entirely non-aqueous medium to encapsulate solid crystals of almost any size.

The first step of the proposed technique involved the adsorption of a surface active agent (α-monoolein) from n-heptane solution onto the surface of the three drug crystals used in this study (KCl, β-estradiol and 5-aminosalicylic acid) to form a hydroxylated (polar) surface which was able to complex an appropriate cationic catalyst, $BF_3(C_2H_5)_2O$ from solution to form a highly concentrated layer. This layer was in turn capable of polymerising the appropriate monomers used in this study namely, styrene, 3,4-dihydro-2H-pyran-2-methyl-(3,4-dihydro-2H-pyran-2-carboxylate) (abbreviated to "C1 monomer), 2,3-epoxypropylmethacrylate (GMA) and bisphenol-A diglycidylether (Epikote 828) present in the solution phase to produce the rate controlling polymer layer. Encapsulation processes were also carried out without first adsorbing a surfactant layer onto the crystal surface to investigate whether the surfactant is essential to conduct polymerization and encapsulation of the crystals by a polymer layer. Experiments proved that the encapsulation process took place on the surfaces of the three drugs used in this study even without first adsorbing a surfactant layer on their surfaces.

The studies involved measurements of the area per molecule of α–monoolein which recorded an average of 46.1 Å/M at air/water interface using the automated Lauda Surface Balance. The specific surface area of each drug powder was measured by nitrogen gas adsorption at low temperature using BET method. Values of 0.074, 3.14 and 1.69 m^2/g were obtained for KCl, β–estradiol and 5–aminosalicylic acid, respectively.

The adsorption of α–monoolein on the three drug powders was analyzed using the Lauda Surface Balance, which indicated that KCl had higher affinity towards surfactant adsorption than either β–estradiol or 5–aminosalicylic acid.

Encapsulations of the three different drugs by the polymers formed from the four previously mentioned monomers were achieved. Characterization of the polymers, their topographies and permeabilities were carried out using GPC, NMR, FTIR, IR, DSC, SEM, TEM, optical microscopy techniques. From the polymers' analyses and their release profiles, it was found that the C1 and Epikote polymers provided a continuous glassy thin layer which showed potential for release control. Polystyrene provided a microporous brittle layer which did not look practically promising, but interesting signs of tacticity were observed.

GMA polymer provided a rubbery porous layer for which further investigation is warranted.

The permeability of C1 ploymer layer (0.8% w/w of the total formulation and thickness of 0.11 μm) to KCl (very water soluble drug) was found to be 2.5 x 10^{-11} cm^2/sec.

CHAPTER I

General Introduction

Chapter I

1.1 General Introduction

The interfacial polymerization, (in particular polycondensation) came into prominence as a major technique for polymer formation about 40 years ago with the work of Schell on polycarbonates[1], Conix[2,3] on polyesters and polysulfonates and Wittbecker, Morgan and coworkers[4,5,6] on polyamides and polyurethanes. The major contribution to the excitement and interest in interfacial polymerization was its broad applicability[4,6] forming a flexible film[6] of aliphatic polyamide at the liquid-liquid interface. The film forming process[6,7] has been used to form membranes which were examined for ion-exchange properties[8]. It has been adapted for the encapsulation of inks, catalysts and insecticides[9,10]. Whitfield, Miller and Wasley developed a process for coating wool fibres in fabric form with a thin film of interfacially formed polymer to prevent fabric shrinkage during ordinary laundering[11].

Chang[12] has used interfacial polycondensation to form artificial cell-like capsules containing enzymes and other materials. These cells have possible applications in artificial kidneys, catalysis and in ion-exchange processes. Several variations of interfacial polymerization and its optimization has been reviewed[13,14] by Morgan. Additives such as surface active agents (e.g. sodium dodecylsuphate, SDS is known to enhance the degree of polymerization in the interfacial production of polymers[15,16]. The use of SDS and other emulsifiers has been the subject of optimization studies[15,16].

Morgan[17] discussed interfacial polymerization and its application to

microencapsulation processes. He disclosed that a granular polymer is obtained by a polycondensation reaction, preferably by adding an organic solution of a diacid chloride to an aqueous solution of a diamine. In such polymerization and under agitation a "thin film formed around the periphery of the liquid drop" which, when broken, exposed the fresh components in the drop to further advance the polymerization reaction. Such peripheral film around the liquid drop" is a microcapsule and the procedure is termed microencapsulation.

Microencapsulation is a process whereby small entities are encapsulated by a coating material. This would provide a means of packaging, separating and storing materials on a microscopic scale for later release under controlled conditions. The nature of the polymers and the wall thickness determine the ability of the microcapsule shell to protect the contents and to release them selectively by means of permeability, dissolution or swelling of the wall material and the diffusion profile through the wall material etc.

Increasingly, the potential applications of microencapsulation in fields such as pharmaceuticals, cosmetics, adhesives, agricultural and food industry have lead to the developments of a number of techniques and products which have been the subject of many patents and others[19-24] have contributed numerous reviews in the literature, describing the various methods of encapsulation. A variety of microencapsulation processes has been developed by a number of companies and research organizations. Some processes serve a very narrowly defined product needs, whereas others are broadly applicable. Among the many processes available, each has its advantages and drawbacks.

The methods of microencapsulation are divided into two broad classes

1. Physical–Mechanical methods
2. Chemical methods

Each of the two categories has various techniques based on their capability to produce a wide range of capsule sizes and properties using many types of nucleus materials. These two categories are broken down further into their respective sub–groups.

Physical–mechanical methods

- Air suspension coating (Wurster)
- Spray drying
- Vacuum coating
- Electrostatic aerosol
- Centrifuging

Chemical methods

- Coacervation
- Interfacial polymerization

Details of each method have been thoroughly reviewed in the literature[9,18,20,22,24–26]. Coacervation (phase separation) is one of the oldest and most common means of microencapsulation. It has been described as a process of liquid separation[27–29] and has been particularly commercialized by the pharmaceutical industry.

The production of microencapsules by interfacial polymerization is achieved by polymerization of a monomer at the interface of two immiscible liquids[30]. One may encapsulate solutions or dispersions of hydrophobic materials by the interfacial

polymerization process. It is also possible to encapsulate aqueous solutions or dispersions of hydrophilic materials. To accomplish this, a hydrophobic monomer, A, is placed in a continuous phase, and a hydrophilic monomer, B, is placed in an aqueous dispersed phase. The interfacial polymerization reaction between the said monomers is utilized to accomplish encapsulation of the dispersed phase. In the interfacial polymerization (encapsulation) process, monomers A and B are polyfunctional monomers capable of a polycondensation or a polyaddition reaction. They are selected so that one monomer is oil–soluble and the other monomer is water–soluble.

Interfacial addition polymerization may utilize only one type of monomer which homopolymerises around the core material. This method does not generally require reactants in aqueous droplets, so it is particularly suitable for enzyme microencapsulation[30,31]. Wall formation around the core material occurs because the formed polymer is insoluble in the solvent and thus phase separate at the interface.

In <u>in situ</u> polymerization the particles are dispersed in a liquid vehicle, e.g. toluene, followed by an addition of a catalyst which creates activated sides on the particles to be encapsulated. Polymerization then takes place directly on the surface[32–34] of the core material when an olefinic monomer is bubbled through. The polymer gradually surrounds the core material as the polymerization proceeds.

<u>Polymerization in monomolecular layers</u>

Since the orientation and packing density of the monomer in monomolecular layer can be varied, this method allows for the investigation of a polyreaction in such

systems[35]. The orientation of such monomer units may remain unchanged during the polymerization process. The reaction can result in a highly oriented, stable polymer film with a degree of orientation not achieved by other methods. Irradiation-initiated monolayer polymerization has been studied intensively in recent years, an extensive review was written by Ringsdorf et al[36,37]. The final polymers occupy a smaller area, their compression isotherms exhibit steeper slopes and higher collapse pressures indicating lower compressibility and higher stability[38,39]. Tieke and Lierser[40] have studied the reaction in Langmuir-Blodgett multilayers which are known to be models of biomembranes and have described the structural changes of the multilayers and the behaviour in mixed mono- and multilayer[41-43].

Based on these studies and on studies of polymerization behaviour in monomolecular layers it has been shown that this type of polymerization occurs even in *in vivo* liposomes[43-46] and Acholeplasma laidlawii cell[46]. The adsorption of diacetylenic monomer surfactants on the surface of core material followed by irradiation is a technique of encapsulation to form a solid layer which may control the release of the encapsulated core material.

Applications

The potential range of applications for encapsulation is extremely broad and offers many product opportunities and challenges. Functions served by capsules include

(1) Separation of reactive materials;

(2) Reduction of volatility and flammability;

(3) Reduced toxicity;

(4) Taste and flavour masking;

(5) Sustained, delayed or controlled release of contents;

(6) Conversion of a liquid to a solid; and

(7) Reduced odour, and environmental protection[47-50].

Encapsulation is broadly applicable to the pharmaceutical industry and offers many possibilities for producing new or improved forms of medication[51-53]. Drugs with an unpleasant taste can be masked, even for use in a chewable tablet. The release of a drug in the body can be delayed in order to achieve prolonged action and to minimize or eliminate undesirable side effects. In order to maintain a therapeutic drug concentration in the body over a prolonged period of time, sustained release formulations are used. The various drug delivery systems have been thoroughly reviewed in the literatures – such as monolithic systems of inert plastic matrices in which the drug is either dissolved or dispersed uniformly in the polymer matrices and the drug release depends upon diffusion through openings or channels in the polymer matrix[54]. Monolithic systems of inert hydrophilic matrix (hydrogel) in which the hydrogel is three dimensional network of hydrophilic polymer which absorbs water when placed in aqueous solutions[55]. Depot or (Reservoir system) in which a core of suspended drug is enclosed within an inert water insoluble polymeric material; the core serves as a reservoir from which the drug permeates out[56]. Osmotic pumping[57]devices and biodegradable polymers[58] are now widely used as drug delivery systems. The release mechanism from each system is well described in the literature[59-62]. The future of biodegradable implants and targetted, responsive and pulsed drug delivery systems has been discussed by Graham[63]. The encapsulation of titanium dioxide pigment by emulsion polymerization with a uniform polymer layer using ultrasound has also been reported[64].

There has not yet been a lot done about direct polymerization to control the release of the core species. In this study a completely novel approach by surface polymerization is described. It is based on interfacial cationic addition polymerization on crystal surfaces to provide encapsulation by a flat membrane of minimum thickness which would control the release of the encapsulated particles. This technique is suitable for the encapsulation of almost any size of solid crystals. The technique with surface chemistry studies, should provide the control of both the nature and the thickness of the capsule wall to achieve the required characteristics of the final encapsulated particle.

The technique involves the adsorption of an active layer to surround the crystals (core particles) to create active sites on the crystal surfaces. These active sites or layers should be capable of initiating a monomer to be adsorbed on the surface to initiate a polymerization process to form a polymer layer around the crystals.

The key step in the encapsulation of potassium chloride crystals, β–estradiol and 5–aminosalicylic acid was the adsorption of a layer of a fatty acid monoglyceride (α–monoolein) onto the crystal surface to form a hydroxylated surface from which the polymer layer is initiated with the help of an acid catalyst $BF_3(C_2H_5)_2O$. The monomers used in this study were styrene, C1, GMA and Epikote. The adsorption of the monoglyceride surfactant was measured using the automated Lauda Surface Balance as it provides a sensitive means to analyse the very small concentrations of the surface active agent. The adsorption study requires also the surface area of the drug powder to be accurately measured. This was achieved using the BET method of nitrogen adsorption at lower temperature. The encapsulation processes of the three drugs with the four polymers were carried out

and in some experiments the adsorption of the surfactant layer was excluded and adsorption of the catalyst directly to the crystal surfaces was carried out followed by dispersing the particles in the monomer solutions. Evaluation of the microencapsulation process and characterization of the polymer layers and their topography and permeability were carried out by GPC, NMR, FTIR, IR, SEM, TEM and optical microscopy.

The release profiles of the different drugs from the different wall materials was studied using chloride ion selective electrode to detect Cl, HPLC with a UV detector to measure the release of β–estradiol and a UV spectrophotometer to measure the release of 5–aminosalicylic acid.

1.2 References

1. Schnell, H., Angew, Chem., 68, 633 (1956): H. Schnell, L. Bottenbruch, and H. Krimm, Belgian patent 523, 543 (1954), assigned to Farbenfabriken Bayer AG.
2. Coniz, A.J., Ind. Chem. Belge, 22, 1457 (1957); Ind. Eng. Chem., 51, 147 (1959); see also I. Goodman, "Polyesters" in Encycl. Polymer Sci. Tech., ed. by N.M. Bikales, Wiley-Interscience, New York, 11, 96 (1969)
3. Conix, A.J., Belgian Patent 565, 478 (7.1.58), assigned to Gevaert Photo-pruduction N.V.; Chem. Abstr., 55, 25356 (1961)
4. Wittbecker, E.L. and Morgan, P.W., J. Polymer Sci., 40, 289 (1959)
5. Morgan, P.W., SPE (Soc. Plastic Engrs.) J., 15, 485 (1959)
6. Morgan, P.W. and Kwolek, S.L., J. Chem. ed., 36, 182, 530 (1959)
7. Morgan, P.W. "Condensation Polymer by Interfacial and Solution Methods", Interscience, New York, 1965
8. Enkelmann, V. and Wegner, G., J. Appl. Polymer Sci., 21, (4), 997, (1977)
9. Sliwka, W., Angew. Chem. Internat. Ed., 14(8), 539 (1975); Vandegaer, J.E. US Paten 3,577,515 (1963), assigned to Pennwalt Corp.
10. Vandegaer, J.E., Chem. Eng. News, July 29, P.15 (1974) and June 5, P.68 (1972)
11. Whitfield, R.E., Miller, L.A. and Wasley, W.L., Textile Res. J. 31(8), 704 (1961); J. Appl. Polymer Sci., 8, 1607 (1964)
12. Chang, T.M.S., Chemtech, 5(2), 80 (1975)
13. Morgan, P.W., Plast. Rub. Mater. Appol., 4(1), 1 (1979)
14. Carraher, C.E. and Preston, J., "Interfacial Synthesis" Vol. 3, p.3-19 Marcel Dekker, Inc., New York, 1982.
15. Korshak, V.V. and Vinogradova, S.V., Polyesters, trans. from Russian by B.J. Hazzard, Pergamon Press, Oxford (1965)
16. Eareckson, W.M., J. Polym. Sci., 40, 399 (1959)
17. Morgan, P.W., J. Polym. Sci., 60, 299 (1959)
18. Madan, P.L., Asian J. Pharm. Sci., 1, 1-46 (1979)
19. Herbig, J.A. Encyclopedia of Polym. Sci. and Tech., Interscience Publishers, N.Y. 8, 719-736, Encyclopedia of Chemical Tech. 2nd edition, John Wiley and Sons Inc. N.Y. 13, 436-456
20. Vandegaer, J.E., Editor "Microencapsulation processes and applications" Plenum Press, N.Y. (1974)

21. Luzzi, L.A., J. Pharm. Sci., 59, 1367 (1970)

22. Nixon, J.R., editor "Microencapsulation" (Drugs Pharm. Sci. Vol. 3), Marcel Dekker Inc. N.Y. (1976)

23. Salib, N.N., Pharm. Ind., 39, 506 (1977)

24. Asaji Kondo and J. Wade Van Valkenburg "Microcapsule Processing and Technology", Marcel Dekker, Inc. N.Y. & Basel, P.35 (1979)

25. Brophy, M.R., Deasy, D.B., J. Pharm. Pharmacol., 73, 495 (1981)

26. Madan, P.L., Pharm. Tech. 30, 31 (1978)

27. Bamford, C.H.; Tompa, H., Trans. Faraday Soc., 46, 310, (1949)

28. Luzzi, L.A., J. Pharm. Sci., 59,. 1367 (1970)

29. Miyazaki, S., Ishii, K., Nadai, T., Chem. Pharm. Bull. 29, 2714, (1981); 29, 3067 (1981)

30. Chang, T.M.S., Macintosh, F.C., Mason, S.G., Can. J. Phys. Pharm. 44, 115 (1966)

31. Chang, T.M.S., Nature, 218, 243 (1968)

32. Orsino, J.A., Herman, D.F. and Brancato, J.I. (to National lead Co.), Fr. Pat. 2,648,609 (April 27, 1960).

33. "Technology Newsletter", Chem. Week 91 (Nov. 24, 1962), Chem. Week 93, 43 (July 29, 1963)

34. Gorham, N.F. and Willard, H.L. (to Union Carbide Corp.), US Pat. 3,300,332 (Jan. 1967).

35. Naegele, D., Ringsdorf, H. in "Polymerization of organized systems", Midland Macromolecular Monographs. Viol. E (Elias, H.G. ed.) Gordon and Breach, New York, P.79 (1977)

36. Hupfer, B., Ringsdorf, H., in "Surface and interfacial aspects of biomedical polymers" (Andrade, J.D., ed.) Vol. 1, Plenum, N.Y. (1984)

37. Ringsdorf, H., Schlarb, B. and Venzmer, J., Angew. Chem. Int. Ed. Engl. 27, 113-158 (1988)

38. Day, D., Hub, H.H., Ringsdorf, H., Isr. J. Chem. 18, 325 (1979)

39. Day, D., Ringsdorf, H, Makromol. Chem. 180, 1059 (1979)

40. Tieke, B., Lieser, G., J. Coll. Inter. Sci., Vol. 88, No. 2, 471 (1982)

41. Lierser, G., TYieke, B. and Wegner, G., Thin Solid Films 68, 77 (1980)

42. Fonassier, J.P., Tieke, B., and Wegner, G. Isr. J. Chem., 18, 227 (1979)

43. Tieke, B., and Lieser, G., J. Coll. Interf. Sci., 83, 230 (1981)

44. Hub, H., Hupfer, B., Koch, H., Ringsdorf, H., Angew. Chem. Int. Ed.

Engl. 19, 938 (1980)

45. O'Brien, D.F., Whitesides, T.H., and Klingbiel, R.T., J. Polym. Lett. Ed. 19, 95 (1981)
46. Johnston, D.S., Sanghera, S., Pons, M., and Chapman, D., Biochem. Biophys. Acta 602, 57 (1980)
47. Encapsualtion-Application, The National Cash Register Co., Dayton, Ohio, 1965
48. Mattson, H.W., Intern. Sci. Technol. 40, 66-72 (April 1965)
49. New Scientist 25, 597-598 (Nov. 1965)
50. Packaging Design 7(2), 42-46 (March/April 1966)
51. Remington's Pharmaceutical Sciences, 13th ed., Mack Publishing Co., Easton, Pa., P.586-591 (1965)
52. J. Pharm. Sci., 54, 1719-1722 (1965)
53. Encapsulation-Pharmaceuticals, The National Cash Register Co., Dayton, Ohio, 1965
54. Tanquary, A.C. and Lacey, R.E., eds., "Controlled Release of Biologically Active Agents", Plenum Press, New York, 1974.
55. J.D. Andrade, ed., "Hydrogels for Medical and Related Applications", ACS Symposiu, Series No. 31, Amer. Chem. Soc., Washington, DC, 1976
56. Baker, R.W. and Londsdal, H.K. in "Controlled Release of Biologically Active Agents", A.C. Tanquary and R.E. Lacey eds., Plenum Press, N.Y., P.15 (1974)
57. Higuchi T. and Leeper, H., US Patent 3,7690,804 (1973)
58. Wood, D.A., Intern. J. Pharm., 7, 1 (1980)
59. Higuchi, T., J. Pharm. Sci., 50, 874, 1961
60. Ibid, 52, 1145 (1963)
61. T.J. Rosman, ibid, 61, 46, 1972
62. Chien, Y.W., ibid, 63, 515, 1974
63. Graham, N.B., Chemistry and Industry, p.482 (6 August 1990)
64. Templeton-Knight, R., Chem. Industry, p.512 (20 August 1990)

CHAPTER II

Monolayer Study of Glycerylmonooleate

Chapter II

Monolayer Study of Glycerylmonooleate

2.1 Introduction

Benjamin Franklin[1] observed that oil does not spread (as a film) on water surface thinner than 25 A. Rayleigh[2], using a technique of confining insoluble films between barriers extending over the whole width of a trough filled with water, was able to measure the relation between surface tension and the surface area quickly and reproducibly. Surface tension was found to fall steeply only when the surface was covered with a close-packed monomolecular film[2]. Devaux[3] confirmed the results of Rayleigh, and showed that the movements of the film could be made visible if it were lightly sprinkled with a fine powder. In this way he showed that even monomolecular films could become solid when compressed. Hardy[4] pointed out that monolayers are formed from molecules consisting of a hydrophobic and hydrophilic parts, and hence at the air-water interface, the molecules must be orientated with the polar, hydrophilic parts buried in the water, while the remainder of the molecules will tend to leave the water. It remained for Langmuir to provide a conclusive support for this hypothesis of orientation: he showed that monolayers of fatty acids of various chain-lengths compress to the same limiting area, an indication that the different acids must all form films in which the molecules are orientated identically with respect to the surfaces[5]. Adam has made many refinements in the technique and published comprehensive data[6]. Blodgett[7] used the so-called Langmuir Blodgett trough to deposit successive monomolecular layers, formed at the air-water interface, onto solid surfaces. This latter technique has been the object of intensive study in

recent years because of a wide variety of possible applications of these films. A critical step in many of these applications is the polymerization of the deposited film to increase its lifetime. For this approach, monomers in the reaction have generally been long–chain unsaturated carboxylic acids. A renaissance in the investigation of monomolecular layers of amphiphilic molecules has taken place in the last two decades[8–11]. Sagine and co–workers[12–15] have investigated a novel method for successively constructing organised molecular layers on solid surfaces. Surface active compounds are chemically adsorbed at the liquid/solid interface. Fendler and coworkers[16,17] have studied various kinds of polymerized surfactant vesicles. Taking advantage of the bilayered structure of vesicles, constructed of surfactants with unsaturated hydrophobic or hydrophilic moieties, it has been possible to polymerize them using heat, light or added initiators. Lando et al[18–20] performed a series of studies on the polymerization of monolayer or bilayered structures of vinyl stearate at an air–water and solid–liquid interfaces. The orientation and compatibility in monolayers and the spreading isotherm of macromolecular compounds and fatty acids were studied by Gabrielli et al[21–23]. Fluorescence microscopy is a sensitive and non–destructive optical method to directly investigate monolayers on liquid and solid substrates. This has been reported by Meller[24] to control the transfer of the monolayers on solid substrates which should help to bridge the gap between floating monolayer properties and their transfer on solid substrates.

A distinctive method for producing organized molecular films at a solid–liquid interface was reported by Wu[25]. The method is based upon the formation, by physically adsorbed surfactants, of micelle–like surfactant aggregates called admicelles[26] at the interface. As micelles incorporate other molecules into their

structure in the process of solubilization, so admicelles exhibit an analogous behaviour which was referred to as adsolubilization. The feasibility of manipulating the phenomena of admicelle formation and adsolubilization to form polymerized, organized ultrathin films of polystyrene inside the admicelles of molecular dimensions on solid surfaces was reported[25]. The application potential of this work could be unlimited.

In recent years, attention has been focussed on films of polymers at surfaces, the study of monolayers at the oil–water interfaces, electrically charged films, and the flow properties of spread and adsorbed monolayers.

2.1.1 Surface Pressure

The surface pressure of a monolayer is the lowering of surface tension due to the monolayer. The molecules constrained in the monolayer may be regarded as exerting a two–dimensional osmotic pressure; there is a repulsion in the plane of the surface, which is measured on a floating barrier acting as a semi–permeable membrane permeable to water only. It is this pressure, opposing the contractile tension of the clean interface, that is called the surface pressure as shown in the Fig. 2.1.

$$\pi = \gamma_o - \gamma \qquad (1)$$

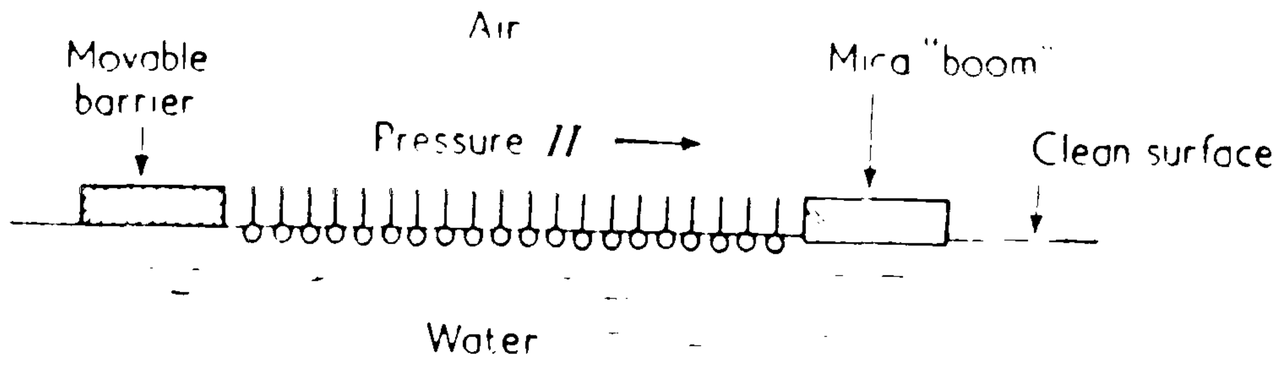

Fig. 2.1 Principle of the Langmuir Trough. The lowering of surface tension is measured directly, as a surface pressure II exerted on the mica "boom" and balanced by applying an equal pressure from a torsion wire attached to the "boom". The barrier on the left is used to compress the film as required. (See Ref. 28).

where γ_o is the surface tension of the clean interface. The variation of π with the area available to the surface-active material is represented by π-A curve (force-area curve). It is usual to express π in dynes cm^{-1} and A either in $\dot{A}^2$ for long-chain (for simple molecules) or in m^2mg^{-1} for more complex molecules and γ is the tension of the film-covered surface.

Criteria for Spreading

If a mass of some substance is placed on a liquid surface so that initially it is present in a layer of appreciable thickness, then two possibilities will exist as to what may happen. These are treated in terms of what is called spreading coefficient.

At constant temperature and pressure a small change in the surface free energy (G) of the system is given by the total differential:

$$dG = (\gamma G/\gamma A_A)dA_A + (\gamma G/\gamma A_{AB})dA_{AB} + (\gamma G/\gamma A_B)dA_B$$

but

$$dA_B = -dA_A = dA_{AB}$$

where liquid A constitutes the substrate and

$(\gamma G/\gamma A_A) = \gamma_A$ etc.

The coefficient $(\gamma G/\gamma A_B)_{area}$ gives the free energy change for the spreading of a film of liquid B over liquid A and is called the spreading coefficient of B on A. Thus,

$$S_{B/A} = \gamma_A - \gamma_B - \gamma_{AB} \qquad (2)$$

$S_{B/A}$ is positive if spreading is accompanied by a decrease in free energy, i.e., is spontaneous. From the definitions of work of adhesion and cohesion, it is seen that the spreading coefficient is the difference between the work of adhesion of A to B and the work of cohesion of B

$$S_{B/A} = W_{AB} - W_{BB} \qquad (3)$$

Generally speaking, S is positive when a liquid of low surface tension is placed on one of high surface tension. Cary and Rideal[27] found the spreading velocity of oleic acid on water to be about 20 cm/sec. Davies and Rideal[28] cited some work which suggests that spreading rates are proportional to S (presumably $S_{B/A}$) and inversely proportional to the viscosity of the bulk phase. Zisman and coworkers[29,30] have found that spreading rates can be enhanced, reduced or

even inhibited by the presence of small amounts of impurities; in particular, strongly adsorbed surfactant can form a film over which the oil will not spread.

Many substances do not spread well by themselves, and, it is more common to use a spreading solvent. Accurate measurement of the very small amounts of materials involved in the usual monolayer experiment is also facilitated by the use of a measured volume of a suitable dilute solution. It is desired that the solvent shall accomplish the dispersal of the film-forming molecules at the water-air interface, and then disappear completely. Devaux[3], Langmuir[5,19] and Adam[6,37] developed the technique of spreading with a volatile, water-insoluble solvent. This is the most generally applicable method for materials which form insoluble monolayers. Solvents must have sufficient solvent power; a spreading solution which contains much less than 0.1-1 mg/ml of film material will be impractical because of the large volume required. It must be chemically inert with respect to the film material and the subphase and be easily purified. Solvents which boil in the range of 40-80°C are generally most suitable for experiments under ordinary conditions, for example, low-boiling hydrocarbons (petroleum ether or n-hexane). Difficulty has been noted for solvents of high water solubility as some of the monolayer forming materials may then be carried into the aqueous phase and be precipitated there rather than appearing in the surface; for example, when acetone or isopropanol were used to spread perfluro acid monolayers[30]. Whether or to what extent a spreading solvent may alter the properties of the spread monolayer was discussed by Dean[33], Jones et al[34], LaMer[15], Gaines[8,36] and Langmuir[31]. The procedure[35,37] for spreading, to minimise adventitious contamination of the film during its formation, has been regarded as a satisfactory technique by LaMer[38]. The reproducibility and

consistency of the experimental results demonstrate the ultimate satisfactory control.

The Subphase

Water or other subphase upon which the monolayer is spread requires particular attention. Purity and protection from contamination are of utmost importance. Divalent cations in water interact strongly with fatty acid monolayers[39], and concentrations of Al^{3+} as low as $10^{-8}M$ may affect such films[31]. Therefore considerable precautions are required to keep impurities below this level. A number of references has been mentioned by Gaines[40] with respect to purification of water to be used as a subphase liquid. The problems with non-aqueous subphases have been discussed by Ellison[41,42], and Doyle et al[43].

Troughs and Barriers

The trough in which the subphase liquid is contained also presents certain special problems. Since it generally forms an integral part of the experimental apparatus, consideration of the trough design is necessary. The necessary developments of the trough, depending on the nature of measurements to be made, was discussed in detail by Gaines[8]. It is, however, important for us to discuss the principal of the measurements and construction of the automated Lauda Surface Balance which is used for the present study of monolayers of glyceryl monooleate at air-water and air-salt solution interfaces and subsequently for the development of an analytical technique to analyse very small concentrations of the surface active material.

2.1.2 Principle of the Measurement

The principle of measurements is based on a continuous monitoring of film pressure, π, as a function of the area A available to the spread molecules.

Using an automated Lauda Surface Balance it would be easy to measure the film pressure.

The subphase is contained in a teflonized metal trough (A) which is thermostated. The measuring barrier separates the film-clad surface from the clean surface. The difference in surface tension $\pi(\pi = \gamma_o - \gamma)$ is measured with an electronic pressure transducer (C) and amplifier (D) and fed to the Y channel of the X-Y recorder. The spread molecules are located in the enclosed surface between the fixed barrier (F) and the movable barrier (M). The movable barrier is controlled by a motor and varies the surface area of the film through compression or expansion. When the surface is reduced (the film is compressed) the film pressure π for a particular substance rises in a characteristic manner. The surface area measuring potentiometer geared to the moving barrier converts the surface into an equivalent d.c. voltage which is fed to the X channel of the recorder.

Surface Balance

The surface balance consists of four parts, the measuring unit, the circulating thermostat which maintains the subphase at the required temperature, the control unit and the X-Y recorder for plotting the π-A isotherm of the film forming material. Fig. 2.2 illustrates the construction of the surface balance.

The measuring unit consists of three main parts, the trough, the pressure barrier with the motor drive, and the area and film pressure measuring system.

The trough is made from brass which is coated with a thin film of Teflon (PTFE)

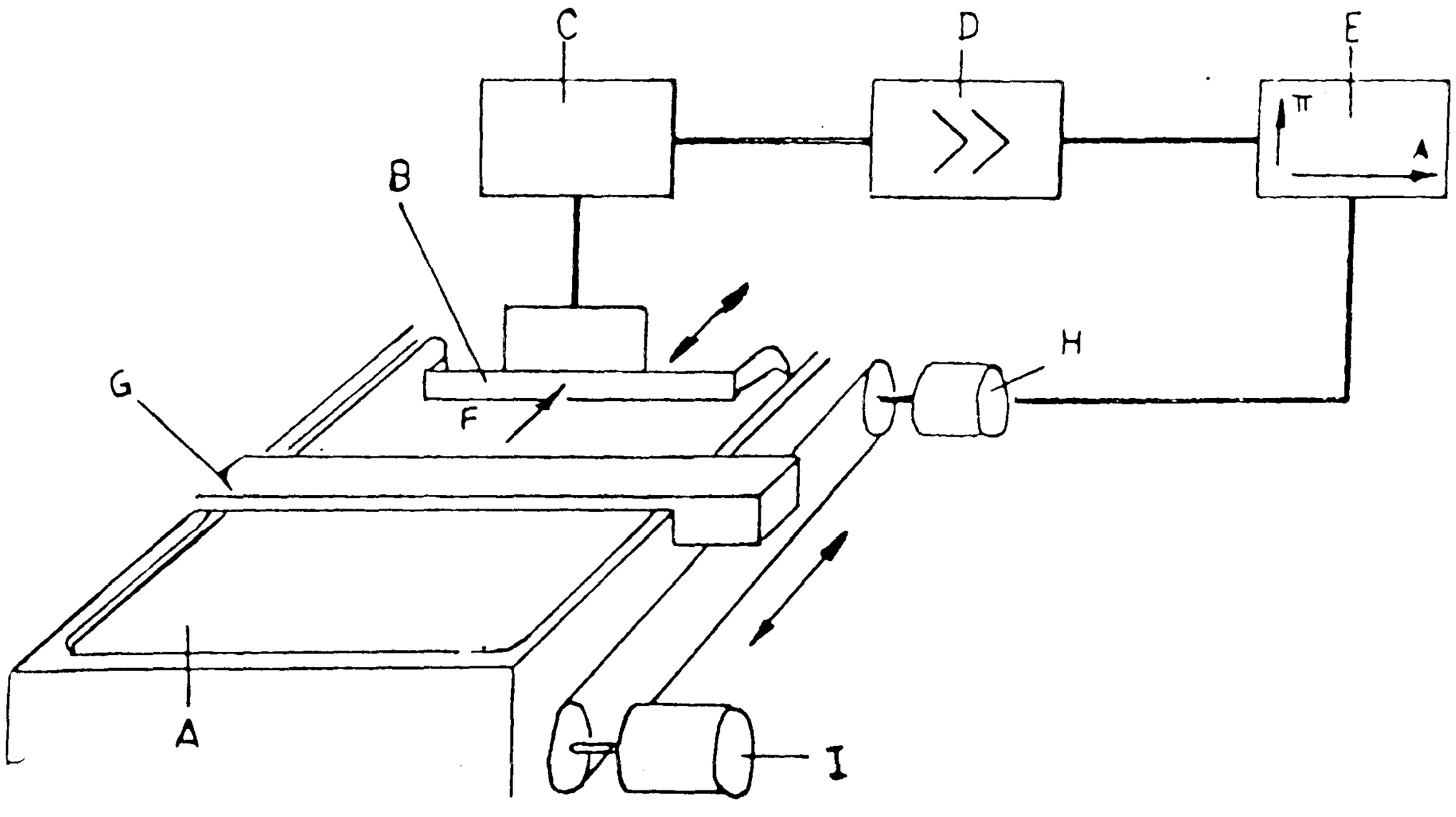

Fig. 2.2 Construction of the Lauda film balance

A = Teflonized metal trough
B = Fixed barrier
C = Electronic pressure transducer
D = Amplifier
E = X-Y recorder
F = Film pressure, $\pi = (\gamma_o - \gamma)$
G = Moveable barrier
H = Surface area potentiometer
I = Motor

to produce a hydrophobic surface which makes it possible to fill the trough with the subphase liquid to a level above the brim of the trough. This would prevent the film from slipping under the moving barrier and thereby introducing an error. The Teflon coating resists most of the organic substances, preventing any metal ion from entering the subphase and finally makes it easier to clean and drain off the subphase.

The barriers are also coated with Teflon. Compression and expansion of the film on the subphase are reversible processes and correspond to the direction of the moving barrier. The measuring system consists of the bridge piece which carries the measuring barrier.

Monolayer States and Phase Transformations

Devaux[3] pointed out that molecules in monolayers could exist in different states quite analogous to three-dimensional liquids, solids or gases. In some cases, it is possible to transform a film from "solid" to "liquid" by changing the temperature or surface pressure. It is quite certain, therefore, that various monolayer states represent different degrees of molecular freedom or order, resulting from the intermolecular forces in the film and between film and subphase. The different state of existence of a matter in monolayers are generally referred to as condensed (solid or liquid) films, expanded films[46] and gaseous films.

Gaseous Monolayers

In principle, any monolayer-forming substance will exist as a gaseous film if the molecules are sufficiently widely separated. Thermal motion will lead to such separation, and there will be a two-dimensional "surface vapour pressure". The

π–A curves of gaseous monolayers can be explained by two dimensional kinetic analysis[45] assuming that molecules in the monolayers have average translational kinetic energy of ½ kT (k = Boltzman constant) for each degree of freedom as the monolayer film behaves more or less as an ideal gas. The two dimensions in the plane of the surface lead to a total kinetic energy of kT which produces the surface pressure and leads to an ideal two–dimensional gas equation.

$$\pi A = kT \qquad (4)$$

Various expressions have been proposed to allow for the negative deviations of the π–A product from the ideal value[46,47] are given by,

$$\pi(A - A_o) = kT$$

$$\pi(A - A_o) = qkT$$

where A_o is the observed molecular area in condensed films and q is less than unity (~ 0.7). Other equations based on various assumptions have been given by other workers[48–51].

Condensed Monolayers

At the opposite extreme from gaseous monolayers in which the isolated molecules are far apart, are the condensed films, in which the molecules are arranged in almost their closest possible packing. Gaines[11] has reviewed the different approaches to account for the shape of the π–A plots of such monolayers. The π–A curves are quite straight and very steep indicating low compressibility in the condensed monolayers and strong cohesive chain–chain interaction. The presence

of polar groups or double bonds in the molecular structure may alter the packing behaviour.

Expanded Monolayer

Intermediate, in molecular area between gaseous and condensed films of simple molecules are the expanded monolayers. The π–A plots of these films show considerable curvature, although they approach the $\pi = 0$ axis at a fairly steep angle. The molecular area is typically two or three times as large as the molecular cross section. Many monolayers which are condensed at low temperature change to expanded films at higher temperatures. It was reported by Adam and Jossop[52] for myristic acid, in 0.01 N HCl at various temperatures that films are condensed at the lowest temperatures, while above 25°C the curves are of the typical expanded type. At intermediate temperatures, the film is expanded at low surface pressures, but increased surface pressure leads to condensation. Langmuir[53] introduced the concept which is now generally accepted that an expanded film is a very thin liquid phase in which the hydrophobic portions of the molecules occupy a random orientation and the polar head groups are in contact with the subphase. Langmuir derived the first equation of state for an expanded monolayer by assuming that the upper surface of the film behaved as a bulk hydrocarbon liquid and therefore exhibited a normal liquid surface tension. It was also supposed that the contribution of the polar functional groups to the surface pressure could be represented by an ideal gas equation corrected for finite molecular size. Balancing these contributions to the spreading pressure of the film leads to the equation

$$(\pi - \pi_o)(A - A_o) = kT$$

In such films the cohesion is approximately constant over a considerable range of area[6]. Films may become "gaseous" at greater areas (with shorter chains or higher temperatures). Smith[54] has made several attempts at the quantitative treatment of the π–A curves of the expanded monolayers.

2.1.3 Salt solutions as a Subphase

Some slightly polar substances which do not spread on water could spread on concentrated salt solutions because salt solutions have higher surface tension than pure water. Addition of salt to the subphase will alter the polar character of the subphase which would increase the attraction between film forming substance and the subphase. Adam, Askew and Pankhurst[32] reported that the shape of π–A curves remained unchanged on concentrated ammonium sulphate solution but the surface pressure at constant area per molecule has increased. Pankratov[55,56] observed similar results on a number of salt solutions. Dennis and Heymann[57] studied the equilibrium spreading pressure (E.S.P.) of oleic acid and ethyl sebacate on concentrated salt solutions of a number of univalent salts over a limited range of concentrations using a ring method and found a linear relationship between E.S.P. and salt activity in the subphase. Gilby and Heymann[58] later confirmed this work using a modified Langmuir–Adam surface balance.

2.1.4 Purpose of Research

In this investigation, glyceryl monooleate surfactant (α–monoolein) was chosen to study the monolayer properties at air–water and air–salt solution interfaces. Area per molecule of α–monoolein was determined using the Automated Lauda Surface Balance, described earlier on both subphases. The obtained information was important to develop an analytical technique for studying the adsorption of α–monoolein from n–heptane to the solid surfaces of three drug models with widely

different surface characteristics. Data from the adsorption investigation were used to control the encapsulation of the three drugs used in this study.

2.2 Experimental

2.2.1 Setting up of the Lauda Balance

The automated Lauda film balance type FW-1 Nr. 4012006 supplied by MGW Messgerate-Werk Lauda was placed on a well supported, essentially vibration free, separate bench where it was protected from direct sun rays. The thermostating unit, control unit and the XY recorder (Bryans 29000 A3) were connected to the film balance.

The trough was soaked in nitric acid for 8 hours to clean it from any surface active contamination, then it was sucked off using a clean glass dropper attached to a suction water pump and the trough was rinsed with double distilled water. After wiping with analar acetone applied on a wad of cotton wool and handled with clean tweezers, the trough was then filled with water to the brim and the surface was swept and all the water in the trough was sucked off. The trough was refilled with fresh double distilled water (830 ml) and a calibration of the water level (volume) in the trough was adjusted using cathetometer (The precision Tool and Instrument Co. Ltd. 2207). After adopting the cleaning procedure and adjusting the volume of water to 830 ml after sweeping the surface frequent blank runs and contamination tests were carried out.

The apparatus including the thermostat and the X-Y recorder was switched on about 30 minutes prior to the start of the experiment.

2.2.2 Handling and Care of Materials

Subphase

Water that was used in any subphase was double distilled in quartz and was kept in a clean stoppered glass flask for about 1–2 hours until it attained room temperature. These precautions were necessary as the quality of the substrate liquid is extremely crucial because the technique is very sensitive to any traces of surface active organic contaminants. Any other traces were removed by continually sweeping and sucking the surface of the subphase in the trough until no film was detected by zero pressure after maximum compression of the surface of same volume of the subphase (830 ml). That volume of the subphase was found necessary to fill the trough such that the level of the liquid was above the brim and the moving barrier was dipped into the subphase liquid, this would keep the film floating between the moving and the fixed barriers.

Spreading of Monolayer

A common method to apply a monolayer of a surface active material is to dissolve it in a volatile, non-reactive and purified organic solvent. Organic solvents with positive spreading coefficient, immiscible with subphase were found satisfactory medium for spreading experiments. The solution of film forming material were carefully delivered by a 25 μl microsyringe (Hamilton, Bonaduz, CH) with an accuracy of ± 0.05 μl. The reproducibility of the experimental results were satisfactory. The solutions were delivered very slowly to the subphase while keeping the tip of needle close to the surface of the subphase but not touching. The solution was dropped at various points on the surface for easier and quick spreading. The lid of the surface balance was kept closed after deposition of the film solution to avoid aerial contamination and surface disturbance during the

compression experiments.

2.2.3 Cleaning of the Glassware

All the glassware used were cleaned with permanganic acid followed by rinsing with plenty of tap water to remove any adsorbed ions, if any. Final rinsing with plenty of double distilled water was very important to wash off any source of contamination. Some of the glassware, especially those with small interior openings or volumetric ones, required a final rinse with distilled analar acetone to avoid drying at high temperature. The clean glassware was dried in a clean electrically heated oven above 60°C. After drying, the oven was switched off to cool the glassware gradually. Then all the glassware was stoppered and the tips were wrapped in tin foil and kept in a clean cupboard and used within a few hours.

2.2.4 Calibration of Surface Area Measuring System

The calibration is based on a calibration area of 562.68 cm^2. This area arises from the geometry of the trough and is well defined within known limits. The approach of the moveable barrier to the measuring (fixed) barrier is automatically restricted by the instrument to a distance of 0.5 cm in order to restrict the compressed film from flowing over the float and pressing it beneath the surface of the subphase. Due to this restriction and the sealing bands at the ends of the barrier, there is a residual area onto which the moving barrier can not intrude. This residual area (A_r) consists of a constant residual area (A_{rk}) and a variable residual area (A_{rv}).

i.e., $A_r = A_{rk} + A_{rv}$

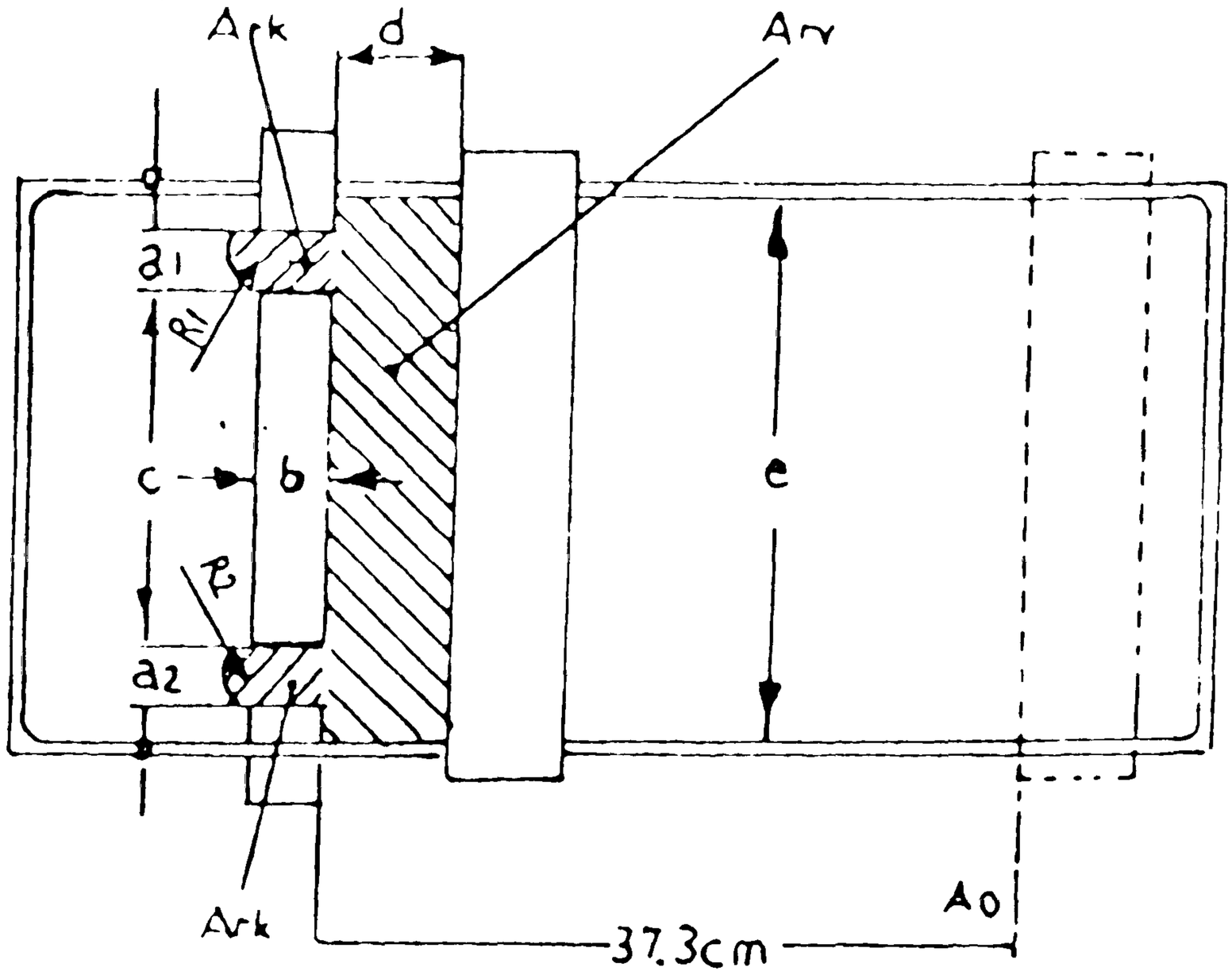

Fig. 2.3 The trough geometry and area reltionships

$a_1 = a_2 = 1$ cm
b = 1.2 cm
c = 11 cm
d = 0.5 cm
e = 15 cm
$R_1 = R_2 = 0.5$ cm

recorder pen returned to its original nil point. The recorder pen returned back to the point A_o when the surface area voltage was switched on again. This procedure was repeated few times to ensure proper calibration. Therefore, the nil point corresponds to surface area of 10.7 cm^2.

2.2.5 Calibration of the Film Pressure Measuring System

Calibration of the film pressure measuring system was achieved by simulating a film pressure by means of a calibration weight of known mass. The force is transferred to the barrier a calibration cross resting on the calibration bearing and with the lower lever pressing on the fixed barrier. The calibration was carried out by carefully placing the calibration weight on to the calibration cross which had already been zeroed without the weight. The sensitivity of the recorder was appropriately adjusted so that 1 cm of the chart paper corresponded to 2 . Since the calibration cross with the calibration weight were precalibrated by the supplier to produce a pressure of 38 mNm^{-1} on the measuring barrier, the distance of 19 cm (at Y axis) from the zero point (where π = 0.0) was adjusted. The calibration weight was then removed and the recorder pen returned to zero point. This calibration was repeated a number of times to ensure a correct reading.

The zero point was slightly changed after removal of the calibration weight and calibration cross but the necessary adjustment were made for corrections. The moveable barrier was set at the position A_o during the calibration process. The calibration was carried out just prior to the start of the experiment and recalibration was necessary whenever the subphase liquid was changed.

Finally the surface of the subphase was compressed and cleaned by sucking off the surface impurities with the help of a clean glass dropper attached to a suction

water pump and the volume of the subphase was readjusted to the right value by adding more liquid of the subphase until the calibration level was obtained. The procedure was repeated until zero pressure was observed.

2.2.6 Materials

Glycerol 1-monooleate (α-monoolein)

Anhydrous glycerol 1-monooleate was supplied by Sigma Chemical Co., contained approximately 90% of the α-isomer and the balance β-isomer. It was used without further purification and referred to as α-monoolein in the text.

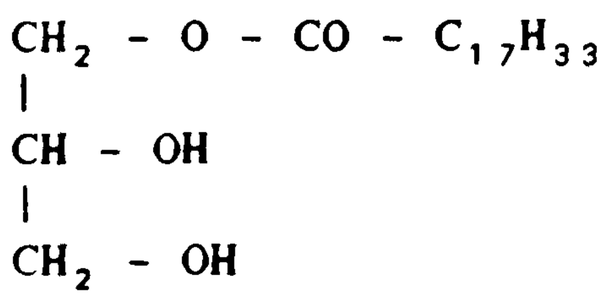

α-monoolein

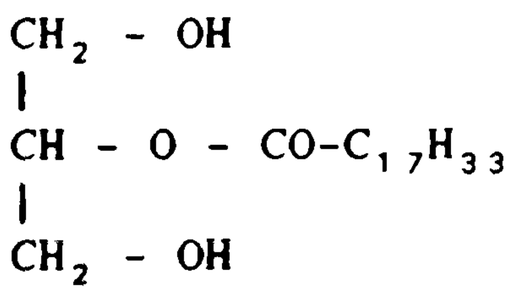

β-monoolein

Solvents

(a) n-Heptane was supplied by F.S.A. Laboratory. It was double distilled before use.

(b) Acetone, BDH of analar purity.

Sodium chloride solution

Sodium chloride of analar purity supplied by May & Baker Ltd (England) was heated in an electric furnace at 500°C for 3 hours to eliminate any organic impurities. It was cooled and kept in a clean jar to be used within 24 hours. A 20% w/v solution of this purified sodium chloride in double distilled water was

prepared. The solution was then filtered through clean glass wool to remove any traces of surface active impurities. The glass wool was cleaned first by soaking in permanganic acid for two hours followed by rinsing thoroughly with tap water and double distilled water. The salt solution was freshly prepared before use.

Experimental Procedure for Determination of Area per Molecule (A/M)

The trough of the Lauda balance was cleaned as described before and filled with 830 ml of the subphase (20% salt solution or double distilled water). The temperature of the subphase was maintained at the required value (25°C) with an accuracy of ± 0.1°C. The instrument was calibrated for surface area and film pressure measuring system and cleaned by sweeping and sucking off the surface of the subphase. The recording paper was then matched with the surface area measuring system, the barrier was set to compression mode and the points corresponding to the total surface area between the measuring and the fixed barrier were marked to indicate the area of 500–50 cm^2. The position of the barrier was then brought back to the starting point (A_0) and an accurate volume (4 – 12.5 μl) of the test solution was spread on the clean subphase surface from 25 μl capacity microsyringe. The solvent was allowed to evaporate (2–3 min) and the film was compressed with the moving barrier at its high speed (6.5 cm/min). The π–A curves were obtained on the X–Y recorder chart paper. These curves were reduced to smaller size and traced. At the end of each run, the surface was compressed and recleaned until zero pressure was observed after adjusting the subphase level to the required value (830 ml). This procedure was repeated for all the samples tested and the trough was cleaned, rinsed thoroughly and dried by sucking off all the water after rinsing the trough.

Assuming that molecules of the film spread as single molecules, the monolayer area for each sample spread was determined by extrapolating the linear portion of the compression curve (between 32–44 and 36–46 dyne/cm for water and salt solution respectively) to zero pressure and hence the area per molecule (A/m) of the film (α–monoolein) at air–water and air–20% salt solution was calculated from the equation

$$A/M = \frac{\text{Area of monolayer } (\dot{A}^2)}{\text{No. of molecules spread}}$$

The number of molecules was determined by multiplying the gram moles spread by Avogadro's number (6.023×10^{23}).

Developing an Analytical Technique

A solution of α–monoolein in n–heptane was prepared of accurate concentration (1.974×10^{-6} g/μl). Various known volumes of this solution (4 – 12.5 μl) were spread on air–water and air–20% salt solution interfaces and the π–A isotherms were recorded. Calibration curves were constructed by plotting monolayer area against the number of spread molecules.

From the calibration curves it was possible to analyse solutions of α–monoolein by spreading an accurately known volume at the subphase and determine the monolayer area from the π–A curves. The concentration of the unknown solution was then calculated from the following equations.

$$\text{Conc. of the solution (g/ml)} = \frac{\text{No.of molecules spread} \times \text{M.wt. of } \alpha\text{-monoolein}}{\text{Vol. spread } (cm^3) \times \text{Avogadro's No.}}$$

where the number of molecules spread can be determined from the appropriate calibration curve.

or

$$\text{Conc. of the solution (g/ml)} = \frac{\text{Area at monolayer } (\dot{A}^2) \times \text{M.wt. of } \alpha\text{-monoolein}}{\text{Vol. spread } (cm^3) \times A/M\ (\dot{A}) \times \text{Avogardo's No.}}$$

2.3 Results

2.3.1 Surface Pressure – Area Measurements

Figs. 2.4 and 2.5 show a series of π–A isotherms of α–monoolein at air–water and air–20% NaCl solution interfaces at temperature of 25± 0.1°C.

2.3.2 Determination of the Limiting Molecular Area of α–Monoolein

Film properties calculated from the isotherms are shown in Tables 2.1 and 2.2. These include cross–sectional area per molecule, collapse pressure and compressibility. Areas given are obtained by extrapolating the steepest part of the isotherm to the area axis at zero pressure.

Table 2.1 Monolayer properties of α-monoolein at air-water interface

Volume spread (μl)	No. of molecules spread x 10^{-16}	Area of Packed monolayer x 10^{-16} A^2	Area per molecule A^2
4.0	1.3340	66	45.0
4.5	1.5007	70	46.6
5.0	1.6675	72	43.2
7.0	2.3345	113	48.4
10.0	3.3350	155	46.5
12.0	4.0020	188	47.0
Mean			46.1

Sample standard deviation (σ_{n-1}) = 1.81

Collapse pressure = 44-45 dyne/cm

Compressibility = 0.0078 cm/dyne

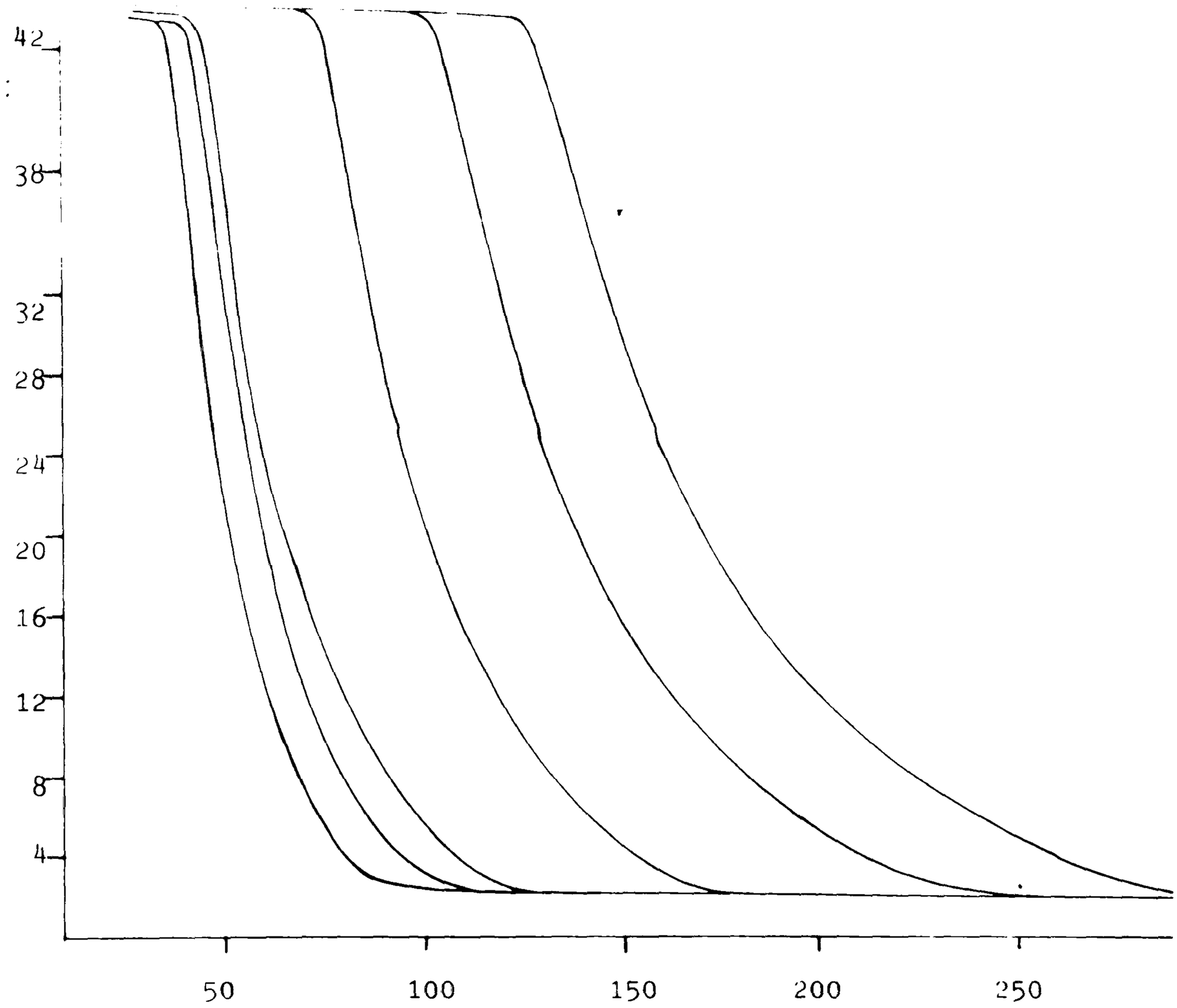

Fig. 2.4 π-A isotherms of α-monolein at air-water interface

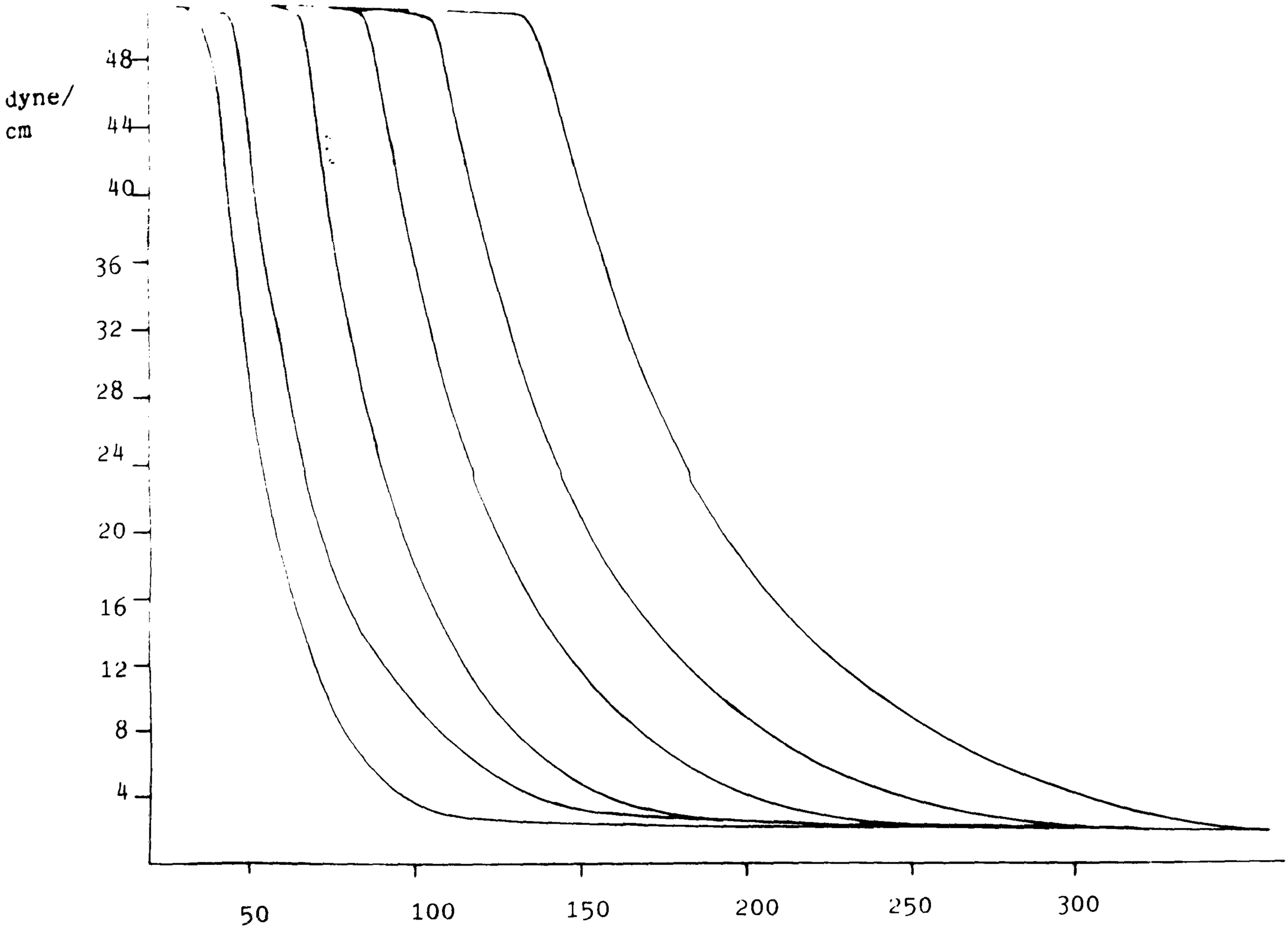

Fig. 2.5 π-A isotherms of α-monoolein at air-20% salt solution

Collapse pressure is sometimes referred to as maximum film pressure. Rigid or solid-like films usually collapse abruptly; mobile or liquid-like films gradually approach constant pressure. In the mobile films, the molecules move less suddenly from the monolayer into the upper layers.

Film compressibility is the change in area with pressure[59].

$$\frac{a_o - a_1}{a_o f_1}$$

where a_o is the extrapolated area of zero pressure, and a_1 is a smaller area of pressure f_1.

Each point on an isotherm represents pressure and an area calculated directly from measurements on the film.

Table 2.2 : Monolayer properties of α–monoolein at air–20% NaCl solution interface

Volume spread (μl)	No. of molecules spread x 10^{-16}	Area of Packed monolayer x 10^{-16} A^2	Area per molecule A^2
4.0	1.3340	65.5	49.1
5.0	1.6675	76.0	45.6
6.0	2.0010	93.0	46.5
8.0	2.6680	133.0	49.8
10.0	3.3350	163.0	48.9
12.5	4.1688	195.0	46.8
Mean			47.8

Sample standard deviation (σ_{n-1}) - 1.72

Collapse pressure - 49 dyne/cm

Compressibility - 0.0074 cm/dyne

2.3.3 Development of the Analytical Technique

Figs. 2.6 and 2.7 show the calibration plots of the packed monolayer areas of α–monoolein against the number of molecules spread from n–heptane at air–water and air–20% NaCl solution respectively.

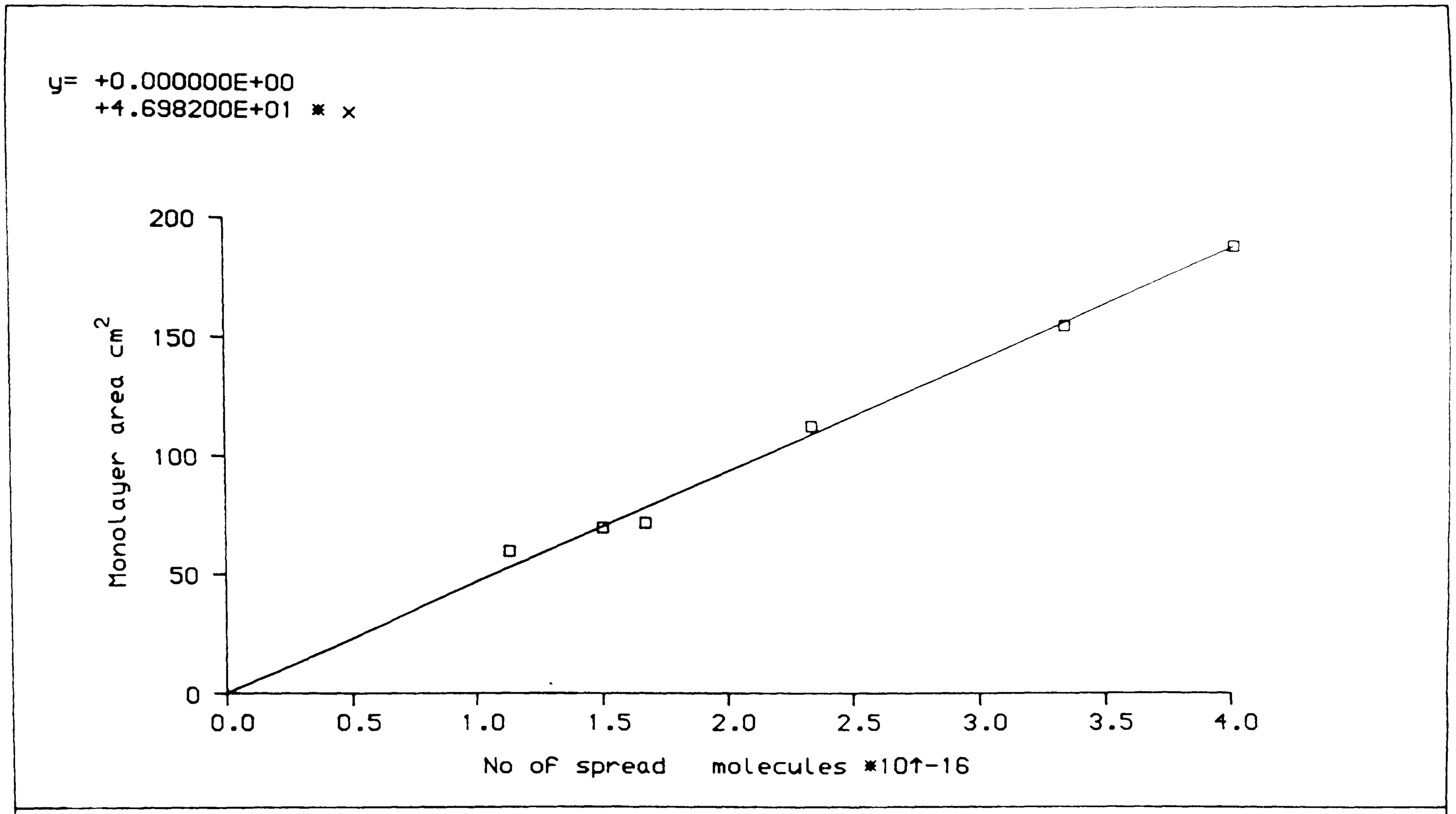

Fig. 2.6 Calibration curve of glycerylmonooleate at air-water interface

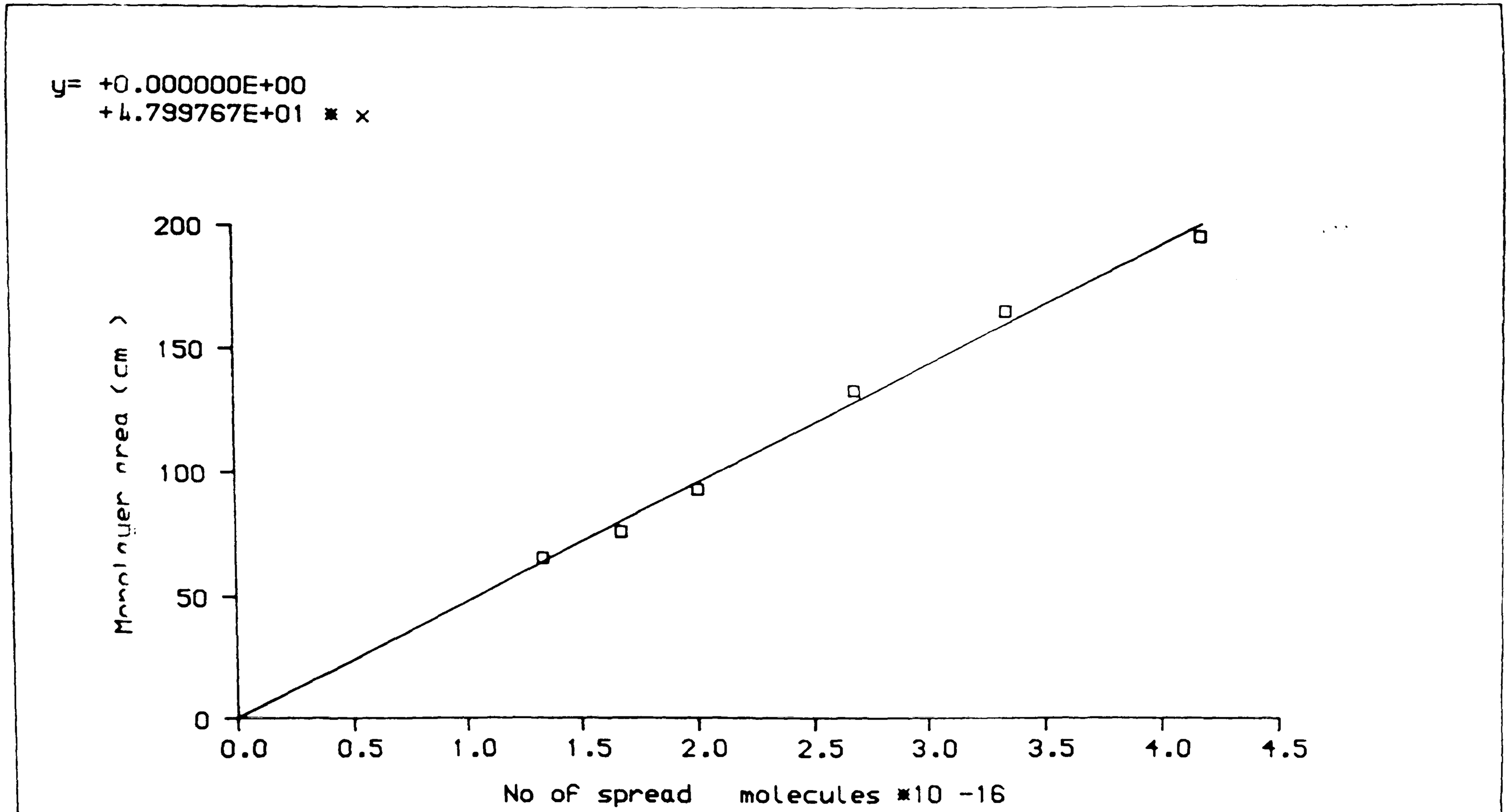

Fig. 2.7 Calibration curve of glyceryl monooleate on 20% NaCl solution

2.4 Discussion of Results and Conclusion

Isotherm characteristics are intimately related to molecular geometry and location of polar groups. The schematic drawings of Fig. 2.8 show the three possible orientations of α–monoolein and its β–isomer at air/water and air/salt solution interfaces.

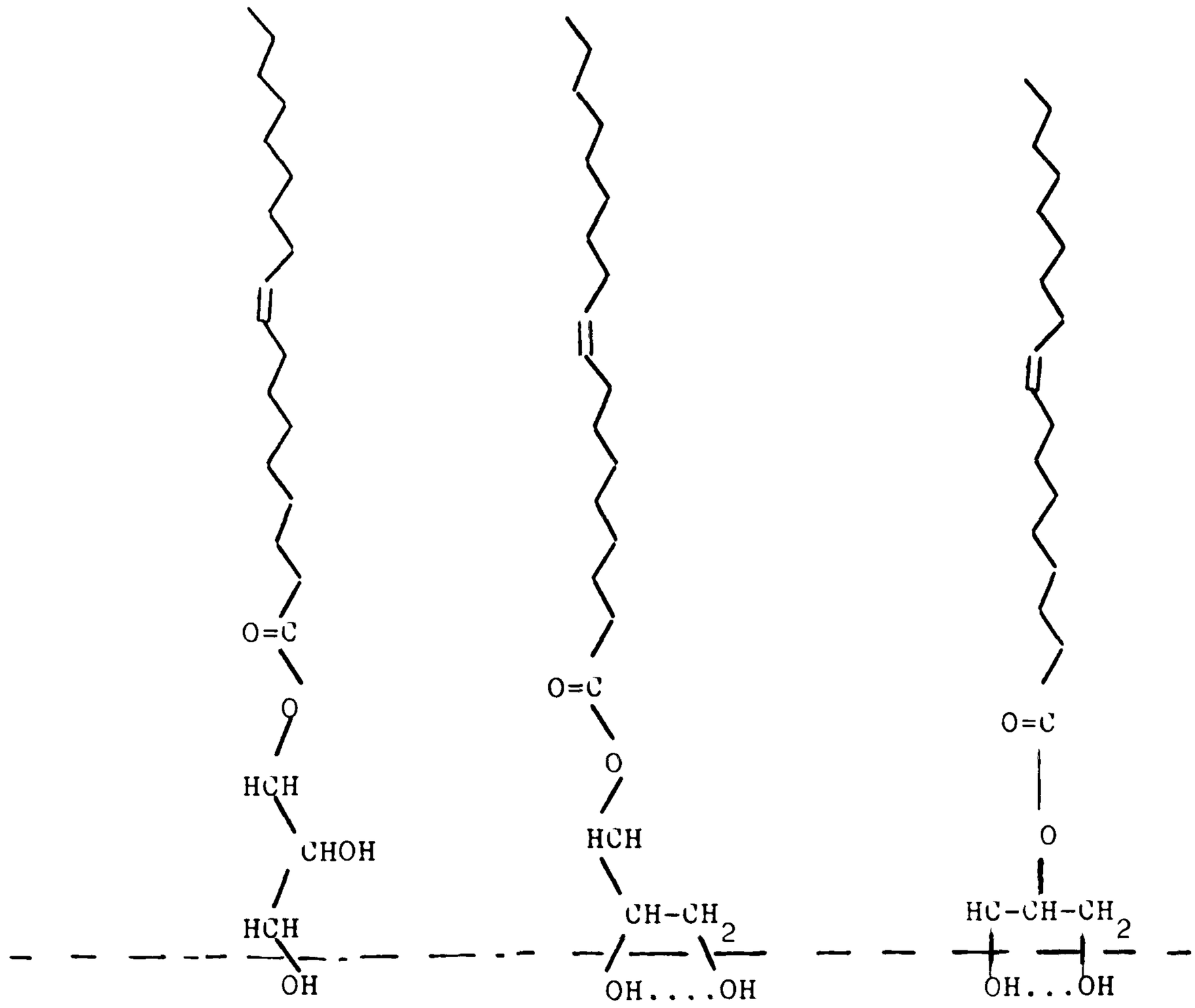

α–monoolein β–monoolein

Fig. 2.8 Molecular orientations of α– and β–monoolein

The isotherms of Figs. 2.4 and 2.5 show the gradual collapse or slow approach to

constant pressure. The film has moderate mobility and this is because the unsaturated monoglycerides and fatty acids are more stable as liquids than as solids at ordinary temperatures and pressure. The same analogy exists in the monolayer.

At zero pressure the mean value of the area per molecule of α-monoolein is 46.1 and 47.8 $\dot{A}^2$ at air-water and air-salt solution interfaces respectively as shown in table 2.1 and 2.2. These values were obtained by the usual extrapolation of the steepest upper portion of the π-A isotherms.

The area per molecule is slightly less at air-water interaface (46.1 $\dot{A}^2$) than that at air-salt solution interface (47.8 $\dot{A}^2$). This can be related to the association of the molecules in the monolayer by intra and inter hydrogen bonding of the glyceryl groups at water substrate being more than at salt solution subphase.

Merker and Danbert studied the monolayer properties of saturated[60] and unsaturated[61] monoglycerrides and reported an average cross-sectional area of 22.9 $\dot{A}^2$ for 1-monoolein calculated from its measured density in the solid state and X-ray long spacing of 49.5 $\dot{A}$. The limiting area they obtained from the force-area curve at 24.3°C and negligible pressure for 1-monoolein was 72 $\dot{A}^2$ per molecule. The limiting area per molecule of α-monoolein at 25°C reported by Rashid[62] was 67.7 and 91.2 $\dot{A}^2$ at air-water and air-20% salt solution interfaces respectively. These values were estimated from a plot of a number of molecules versus the logarithm of area per molecule obtained from the π-A compression isotherms at water and salt subphases. It is important to mention here that the area per molecule was obtained from extrapolating the linear part of the isotherm at the pressure of 21-23 dyne/cm. This was not precise as the extrapolation to

zero pressure should be done from the steepest part of the isotherm which is close to the maximum film pressure (collapse pressure) i.e. at pressure of 42 and 46 dyne/cm at water and salt solution subphases respectively.

Gander[63] measured an area of 50–55 $\dot{A}^2$ per molecule of α–monoolein at 20°C from the force–area isotherm at air–water interface. This value (50–55 $\dot{A}^2$/molecule) agrees well with the value (46.1 $\dot{A}^2$/molecule) obtained in this study considering the temperature difference of the subphase in the two studies.

α–Monoolein monolayers have a high collapse pressure of 44–45 and 49 dyne/cm at water and salt solution subphases respectively. It is slightly higher at salt solution but this is because the surface tension of a salt solution is higher than water. A high compressibility, 0.0078 and 0.0074 cm/dyne are apparent in the steeply rising isotherms at water and salt solution subphases. This indicates the mobility of α–monoolein monolayer and its high stability compared to the low compressibility of stearic acid (0.0019) and its extreme rigidity[59].

Development of the Analytical Technique

The calibration curves shown in Figs. 2.6 and 2.7 gave satisfactory linear plots passing through the origin representing the monolayer area as a function of the number of molecules. The calibration curve Fig. 2.6 will be used to analyse the unknown concentration of α–monoolein solution after adsorption on the three drug models used in this study (Chapter III). It was chosen because it was easier to use double distilled water as a subphase than salt solution.

2.5 References

1. Franklin (1765), see "The Ingenious Dr. Franklin" (ed. Goodman)(1931); "Famous American Men of Science" (ed. Crowther), Secker and Warburg, London (1937)
2. Rayleigh, Phil. Mag. 48, 321 (1899)
3. Devaux, P. V. Soc. Sci. Phys. Nat. Bordeaux, 19th Nov., 3rd Dec. (1903); ibid 7th Jan., 14th April (1904); J. Phys. Rad. 3, 450 (1904)
4. Hardy, Proc. Roy. Soc. A86, 610 (1912); A88, 303 (1913)
5. Langmuir, J. Amer. Chem. Soc. 38, 2221 (1916); 39, 1848 (1917)
6. Adam, "The Physics and Chemistry of Surfaces" (3rd ed.), Oxford University Press (1941)
7. K.B.J. Blodgett, J. Am. Chem. Soc., 57, 1007 (1935)
8. G. L. Gaines, Jr. Insoluble Monolayers at Liquid–Gas Interfaces. Interscience Publishers, New York (1966)
9. H. Kuhn, Thin Solid Films, 99, 1 (1983)
10. G.G. Roberts, Adv. Phys. 34, 475 (1985)
11. J.D. Swalen, J. Molec. Electron. 2, 155 (1986)
12. J. Sagiv, J. Am. Chem. Soc., 102, 92 (1980)
13. L. Netzer, R. Iscovia, J. Sagiv, Thin Solid Films, 99, 235 (1983)
14. L. Netzer, R. Iscovia, J. Sagiv., Thin Solid Films, 100, 67 (1983)
15. J. Gunn, R. Iscovia, J. Sagiv, J. Colloid Interface Sic. 101, 201 (1983)
16. J. H. Fendler, Chem. Eng. News, 2, 25 (1984)
17. J. H. Fendler, E.J. Fendler, G.A. Infante, P. Shih, L.K. Patterson, J. Am. Chem. Soc. 97, 89 (1975)
18. M. Puterman, T. Fort Jr., J.B.J. Lando, Colloid Interface Sci., 47,

705 (1974)

19. S.A. Letts, T. Fort, Jr., J.B.J. Lando, Colloid Interface Sci., 56, 64 (1976)

20. V. Enkelmann, J.B. Lando, J. Polym. Sci., Polym. Chem. Ed., 15, 1843 (1977)

21. G. Gabrielli and A. Maddii, J. Colloid Interface Sci., 64, 18 (1978)

22. G. Gabrielli and C. D'Aubert, Colloid Polym. Sci., 56, 258 (1980)

23. G. Gabrielli, P. Baglioni and A. Maddii, J. Colloid Interface Sic., 79, 1, 268-272 (1981)

24. P. Meller, Rev. Sci. Instrum., 59 (10), OCt. (1988)

25. J. Wu, J.H. Harwell, E.A. O'Rear, Langmuir, 3, 531-537 (1987)

26. J.H. Harwell, PhD Dissertation, The University of Texas at Austin (1983)

27. A. Cary and E. K. Rideal, Proc. Roy. Soc. (London), A109, 301 (1925)

28. J. T. Davies and E. K. Rideal, Interfacial Phenomena, Academic Press, New York, 1961

29. M. K. Bernett and W. A. Zisman, Advan. Chem., Ser. 43, 332 (1964)

30. M. K. Bernett and W. A. Zisman, J. Phys. Chem., 67, 1534 (1973)

31. I. Langmuir and V. J. Schaefer, J. Amer. Chem. Soc., 59, 2400 (1937)

32. N.K. Adam, F. A. Askew and K.J.A. Pankhurst, Proc. Roy. Soc., A170, 485 (1939)

33. R. D. Dean and F. S. Li, J. Amer. Chem. Soc., 72, 3979 (1950)

34. C. L. Cutting and D. C. Jones, J. Chem. Soc. 1955, 4067; D.C. Jones and R. H. Ottewill ibid, 1955, 4076

35. R. J. Archer and V. K. LaMer, J. Phys. Chem., 59, 200 (1955); Ann. N.Y. Acad. Sci., 58, 807 (1954)

36. G. L. Gaines, Jr., J. Phys. Chem., 65, 382 (1961)

37. J. B. Bateman and E. J. Covington, J. Colloid. Sci., 16, 531, (1961)

38. V.K. LaMer and G. T. Barnes, Proc. Natl. Acad. Sci., 45, 1275 (1959)

39. R. J. Myers and W. D. Harkins, Nature, 139, 367 (1937)

40. G. L. Gaines, Jr., J. Phys. Chem., 63, 1322 (1959)

41. A. H. Ellison, J. Phys. Chem., 66, 1867 (1962)

42. A. H. Ellison and W. A. Zisman, J. Phys. Chem., 59, 1233 (1955)

43. W. P. Doyle and A. H. Ellison in "Contact Angle, Wettability and Adhesion" Advan. Chem. Ser., 43, 268 (1963)

44. D. G. Dervichian, J. Chem. Phys., 7, 931 (1939)

45. N. K. Adam and G. Jessop, Proc. Roy. Soc. (London), A110, 323 (1926)

46. J. T. Davies, Trans. Faraday Soc., 48, 1052 (1952)

47. R. K. Schofield and E. K. Rideal, Proc. Roy. Soc. (London), A109, 57 (1925)

48. A.N. Frumkin, Z. Physik. Chem., 116, 485 (1925)

49. M. Volmer, Z. Physik. Chem., 115, 253 (1925)

50. J.S. Mitchell, Trans. Farady Soc., 31, 98 (1935)

51. D.G. Hedge, J. Colloid. Sci., 12, 417 (1957)

52. N.K. Adam and G. Jessop, Proc. Roy. Soc. (London), A112, 362 (1926)

53. I. Langmuir, J. Chem. Phys., 1, 756 (1933)

54. T. Smith, J. Colloid. Sci., 23, 27 (1967)

55. A. Pankratov, Acta Physicochim. USSR, 10, 45 (1939)

56. A. Frumkin and A. Pankratov, Acta Physicochim USSR, 10, 55 (1939)

57. Joan A. Dennison E. Heymann, Trans. Faraday Soc., 42, 1 (1946)

58. A. R. Gilby and E. Heymann, Australian J. Sci. Research, A5, 160 (1952)

59. H.E. Ries, Jr., asnd H. D. Cook, J. Colloid Sci. 9, 535 (1954)

60. D.R. Merker and B.F. Daubert, J. Am. Chem. Soc., 80, 516 (1958)

61. D. R. Merker and B.F. Daubert, J. Phys. Chem. 68, 2064 (1964)

62. A. Rashid, "Some Aspects of Surface Chemistry, Microencapsulation and *In Vitro* Evaluation of β–estradiol from an Injectable Formulation" MSc thesis, Strathclyde University (1980)

63. B. Gander and N.B. Graham, Compte rendu 5éme Congrés Internat. de Technologie Pharmacetique, APGI, Paris, 1, 251–260 (1989)

CHAPTER III

Determination of Specific Surface Area

Chapter III Determination of Specific Surface Area

3.1 Introduction

The specific surface area of a solid is one of the first things that must be determined if any detailed physical and chemical interpretation of its behaviour as an adsorbent is to be possible. Such a determination can be made through the adsorption studies themselves. The methods of area determination may be classified in three groups:

(1) Those that depend on the determination of particle size.

(2) Those that depend on the determination of the adsorption isotherm.

(3) Those that depend upon some special property other than particle size or adsorption. Most of the proposed methods fall into the first two groups, and since the adsorption methods are the simplest experimentally, most of the attention has been given to this class.

The methods of particle size determination are numerous. From the known density of the solid, the geometry of the particles and the average particle size distribution, it is relatively simple to calculate an area. Particle size determinations in general are not satisfactory for obtaining the area because if the solid is porous, i.e., possesses an internal area, the particle size measurements can not account for this area. Further difficulty of having small particles arises from their tendency to aggregate. An aggregate will appear as one particle and since a large particle has a lower area than the same weight of smaller particles, the area again will be low. The different methods of surface area determination of solids were discussed in detail by Jura[1]. The most general method for determination of the specific surface area of solids is based on adsorption of gases which is one of the oldest known phenomena.

Langmuir Method

Langmuir[2] analysed the assumptions of the theoretical relationship between the area of a solid and the adsorption of a gas on the surface. The results of the theory have met with restricted application. The treatment of Langmuir represents a simple application of the kinetic theory of gases which predict the Langmuir equation

$$S = \frac{\nu_m N \delta}{V_m} \qquad (1)$$

where S - specific surface aream^2/g

ν_m - number of molecules required to cover the surface with monomolecular layer of gas.

N - Avogadro's number

V_m - gas molar volume

δ - effective cross sectional area of adsorbate, m^2

The most important assumption made is that the adsorption is monomolecular, which Fowler and Guggenheim[3] considered essential, Langmuir made allowance[2] for the fact that in special cases the adsorbed layer may become more than monolayer, especially for high relative pressure values of P/P_o near unity in the treatment. Since in general, the adsorbed films are polymolecular then the equation will not be generally valid[2,4] The second assumption made is that the adsorption energy is independent of the concentration of molecules on the surface. The physical consequence of this assumption is that the adsorbed phase must be in a single two dimensional phase for any value of the pressure. Other workers[5,6] showed that two dimensional phase changes do exist in films adsorbed on the surface of solids. Also, the interaction between the adsorbed molecules has been

considered for films of non mobile molecules[2]. The development of Brunaner, Emmett and Teller[7] is a theory of adsorption which attempts to explain the physical adsorption characteristics where only Van der Waal's forces are the means of interaction between the solid and the gas. This theory yields substantially the same results as an empirical method developed by Brunaner and Emmett[8-11]. The results of the theory are useful as a method of area determination because one of the parameters in the resulting equation is V_m, the volume of gas required to form a monomolecular layer on the surface of the solid. The fundamental postulate of the theory of Brunaner, Emmett and Teller (BET)is that the adsorption of gases on a free surface is polymolecular.

BET Method

The measurement of the specific surface area of powders by low-temperature nitrogen adsorption is a widely used technique. The principle of the method is the measurement of the amount of nitrogen physically adsorbed by the powder at the temperature of liquid nitrogen over a range of partial pressures, so that an adsorption isotherm is obtained. The mono-layer capacity is determined by using the Brunaner, Emmett and Teller (BET) equation[7,11].

$$\frac{P}{V_a(P_o-P)} = \frac{1}{V_mC} + \frac{C-1}{V_mC} \cdot \frac{P}{P_o} \qquad (2)$$

where V_m is the monolayer capacity (S.T.P.),

V_a is the volume of gas adsorbed (S.T.P.),

P is the equilibrium pressure,

P_o is the saturation pressure of the adsorbate, and

C is a constant

A plot of $P/V_a(P_o-P)$ against P/P_o should be a straight line, of a slope $C-1/V_mC$

and intercept $1/V_mC$, from which both V_m and C can be calculated. The normal range of validity of the Brunaner, Emmett and Teller equation is for P/P_o = 0.05–0.30.

The specific surface area, S, of the powder is related to the monolayer capacity by the equations

$$S = \frac{v_m \delta N}{v_o W} \qquad (3)$$

where N is the Avogadro's number,

v_o is the ideal gas volume,

W is the weight of sample, and

δ is the area occupied per molecule of adsorbate

With nitrogen gas adsorbed at liquid nitrogen temperature, the accepted value for δ is 16.2 A^2 and equation (3) becomes

$$S = \frac{4.35}{\text{slope} + \text{intercept}} \quad m^2 g \qquad (4)$$

Adsorbates other than nitrogen may be used, e.g. argon or krypton, the only requirement is that the adsorbate should have a well defined orientation on a variety of types of surface. In this respect nitrogen is highly satisfactory and value for δ is substantially independent of the nature of the solid surface. In a volumetric apparatus, the volume of gas adsorbed is determined by difference, i.e., the initial and final equilibrium pressures of gas are measured, together with the volume of free space of the apparatus. Where the volume of gas adsorbed is small, with materials of low specific surface area, (e.g. below 0.5 m^2 per g), it is

advantageous to use a gas with a low saturation vapour pressure (P_o) at the temperature of adsorption, e.g. krypton, so that the actual volume of gas (at S.T.P) in the free space of the apparatus is greatly reduced in proportion to the volume of gas adsorbed.

Purpose of Research

The present study involves the measurements of specific surface area of the solid powder of the three chosen drug models namely, potassium chloride, β–estradiol, and 5–aminosalicylic acid by the BET adsorption method.

These surface areas will subsequently be used to calculate the adsorption area per molecule and the adsorpiton density of α–monoolein adsorbate on the surfaces of the three mentioned drugs..

3.2 Experimental

Determination of Specific Surface Area of Potassium Chloride, β–Estradiol and 5–Aminosalicylic Acid

3.2.1 Materials and Treatment

Adsorbents: Potassium Chloride (BDH Analar) of average particle 250–355 μm. It was heated at 500°C for four hours to remove any organic surface residues. The material was kept in a desiccator containing silica gel until used.

Anhydrous β–estradiol crystalline (Sigma) was dried in vacuum oven for 24 hours before use and kept dry in a dark bottle in a desiccator over silica gel. The structure of β–estradiol is

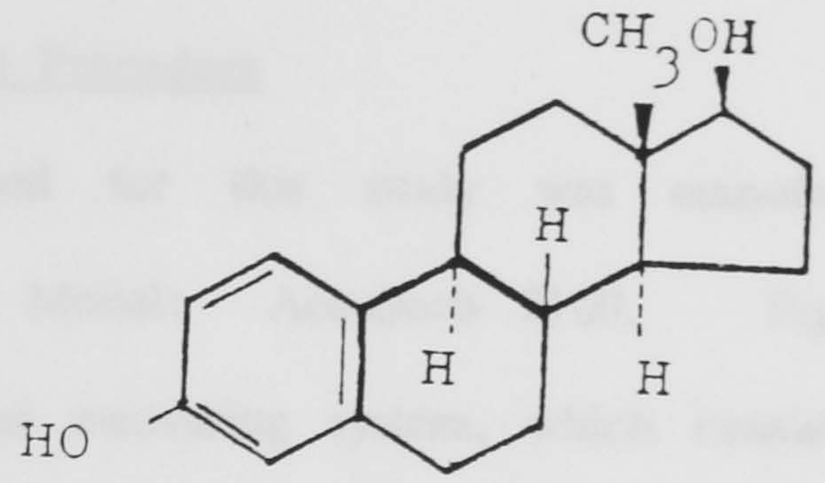

Structure of β–Estradiol

The shape and aggregation of β estradiol particles is shown below in the micrograph Figure 3.1.

Fig. 3.1 SEM micrograph of β–estradiol crystals

Crystalline 5–aminosalicylic acid (Sigma) approx. 99% used as supplied.

3.2.2 Adsorption of N_2 Gas on the Surface of the Drugs (BET Method)

This method is based on the fact that the molecules in the surface layer of a solid have a surface excess free energy which can be reduced by binding gas (nitrogen in this case) molecules in order to satisfy the unbalanced, bonding forces. The attraction in this case is physical i.e. only Van der Waal's adsorption is the

result of a relatively weak interaction between the solid and the nitrogen gas.

Apparatus and Operation Procedure

The apparatus used for this study was manufactured by Micromeritics Instrument Corporation, Model: AccuSorb 2100. Fig 3.2 shows a schematic diagram of the apparatus measuring system, which consists basically of compatible components each performing a special function. These are:

1. A manifold system which interconnects the samples, vacuum-producing equipment, pressure measuring device, and adsorbate sources;
2. The vacuum equipment;
3. The pressure detecting components;
4. A heating system to aid the sample preparation;
5. Temperature monitors for measuring both the sample outgassing and the refrigerant (liquid nitrogen) temperature;
6. A time-pressure unit that indicates the extent to which a sample has been prepared for testing; and
7. A temperature controller for the manifold and pressure transducers. The meters and monitors are all direct reading.

The basic procedure for operating the apparatus was followed to evacuate the assembled apparatus and de-gas the solid powders until satisfactory readings were reached. The dead space in the apparatus, i.e., the volume of the sample bulb and connections not occupied by powder, is determined with helium, which is not adsorbed at the temperature of liquid nitrogen. During nitrogen adsorption, the level of liquid nitrogen surrounding the adsorption bulb was kept constant. A series of points on the adsorption isotherm over a range of pressures up to $P/P_o \simeq 0.3$ was recorded. After adsorption runs were completed, the gas law

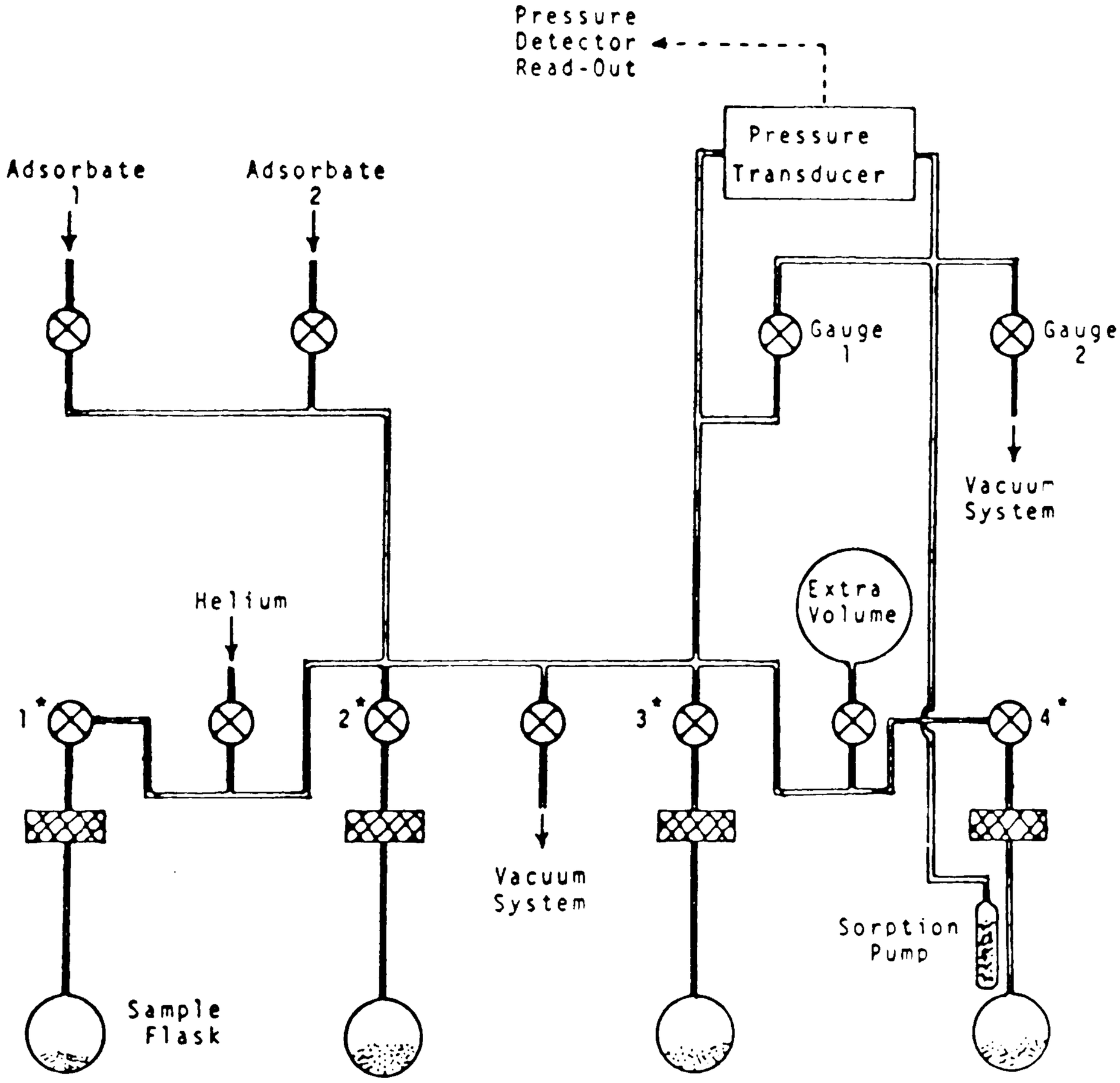

Fig. 3.2 Schematic diagram of the apparatus used for surface area mesurement of powders

calculation was applied to determine the volume of nitrogen adsorbed (va) at each equilibrium pressure, P, by using the constants for the system determined from the helium calibration. The data were fed to a computer for calculation and to plot P/P_o against $(P/V_a)P_o-P$ according to Brunauer, Emmett, and Teller equation to determine the specific surface area for each drug powder from the slope and the intercept of the straight line by substitution in equation (4).

3.2.3 Particle Size Method (Sieving)

This method was applied only for potassium chloride because β-estradiol and 5-aminosalicylic acid are sensitive to light, air and moisture; they are also in aggregated forms.

KCl was passed through a set of sieves ranging between 500 and 90 μm supplied by Endecotts Ltd (BS410) using Endecott Sieve Shaker type (E.F.L. 2MKII). Fractions of KCl powder of particle size 250 μm were collected; this value was used to calculate the surface area per gram assuming that the particle's geometry is spherical.

Calculation

Density of KCl (d) = 1.9 g/cm^3

Particle size = 250 μm

radius (r) = 125 μm

= 125 x 10^{-6} m

volume of one particle (v) = $(4/3)\pi r^3$

= 8.177 x 10^{-12} m^3

Surface area of one particle (a) $= 4\pi r^2$

$= 1.9625 \times 10^{-7}\ m^2$

$$d = \frac{\text{Weight}}{\text{Volume}}$$

$\therefore$ Volume of one gram $= 0.50505\ cm^3$

$= 0.50505 \times 10^{-6}\ m^3$

$$\therefore \text{Number of particles in 1 gram (n)} = \frac{\text{volume of one gram}}{\text{volume of one particle}}$$

$= 61765$

$\therefore$ Surface area of one gram (A) $= n \times a$

$= 1.2 \times 10^{-2}\ m^2$

3.3 Results

3.3.1 Specific Surface Area Measurements of KCl

Typical data of the adsorption of nitrogen onto the KCl solid surface are given in Table 3.1. The condition of the system at which the data were recorded is given below.

Adsorbate	:	Nitrogen
Molar cross-sectional area of N_2 (δ)	:	16.2 $Å^2$
Sample weight (KCl)	:	12.1731 g
Bath temperature	:	77.70 K
Saturation pressure of N_2 (P_o) at 77.7 K	:	791.19 mmHg

Table 3.1 Adsorption of N_2 gas onto KCl solid surface

Partial pressure of Nitrogen (P) mmHg after adsorption	Vol. adsorbed (V)cm^2/g at (S.T.P.)	X= P/P_o	Y = $X/((1-X)V)$	Y = X/V
39.370	0.004	0.050	12.188	11.581
70.300	0.007	0.089	13.185	12.013
97.990	0.009	0.124	15.541	13.615
123.110	0.011	0.156	16.164	13.649
147.350	0.012	0.186	19.067	15.516
173.750	0.011	0.220	24.051	18.769
197.440	0.017	0.249	19.106	14.339

3.3.2 Specific Surface Area Measurements of β-Estradiol

The experimental results of the adsorption of nitrogen to β-estradiol solid surface are given in Table 3.2. The condition of the system is given below:

β-Estradiol weight : 2.4563 g

Bath temperature : 77.44 K

Saturation pressure (P_o) : 767.80 mmHg

Table 3.2 Adsorption of N_2 onto β-estradiol

Partial pressure of Nitrogen (P) mmHg after adsorption	Vol. adsorbed (V) cm^3/g at (S.T.P.)	$X = P/P_o$	$Y = X/((1-X)V)$	$Y = X/V$
30.386	0.580	0.040	0.071	0.068
65.680	0.730	0.085	0.128	0.117
99.820	0.818	0.130	0.183	0.159
129.720	0.860	0.169	0.236	0.197
156.970	0.905	0.204	0.284	0.226
182.500	0.925	0.238	0.337	0.257
207.100	0.940	0.270	0.393	0.287

A plot of BET equation with $x = P/P_o$ against $Y = X/((1-X)V)$ as shown in Fig.3.3 gave a straight line of slope = $\frac{C - 1}{V_mC}$ and intercept equal $1/V_mC$ from which V_m and C were calculated for β-estradiol adsorption within a relative pressure range P/P_o between 0.04 - 0.27

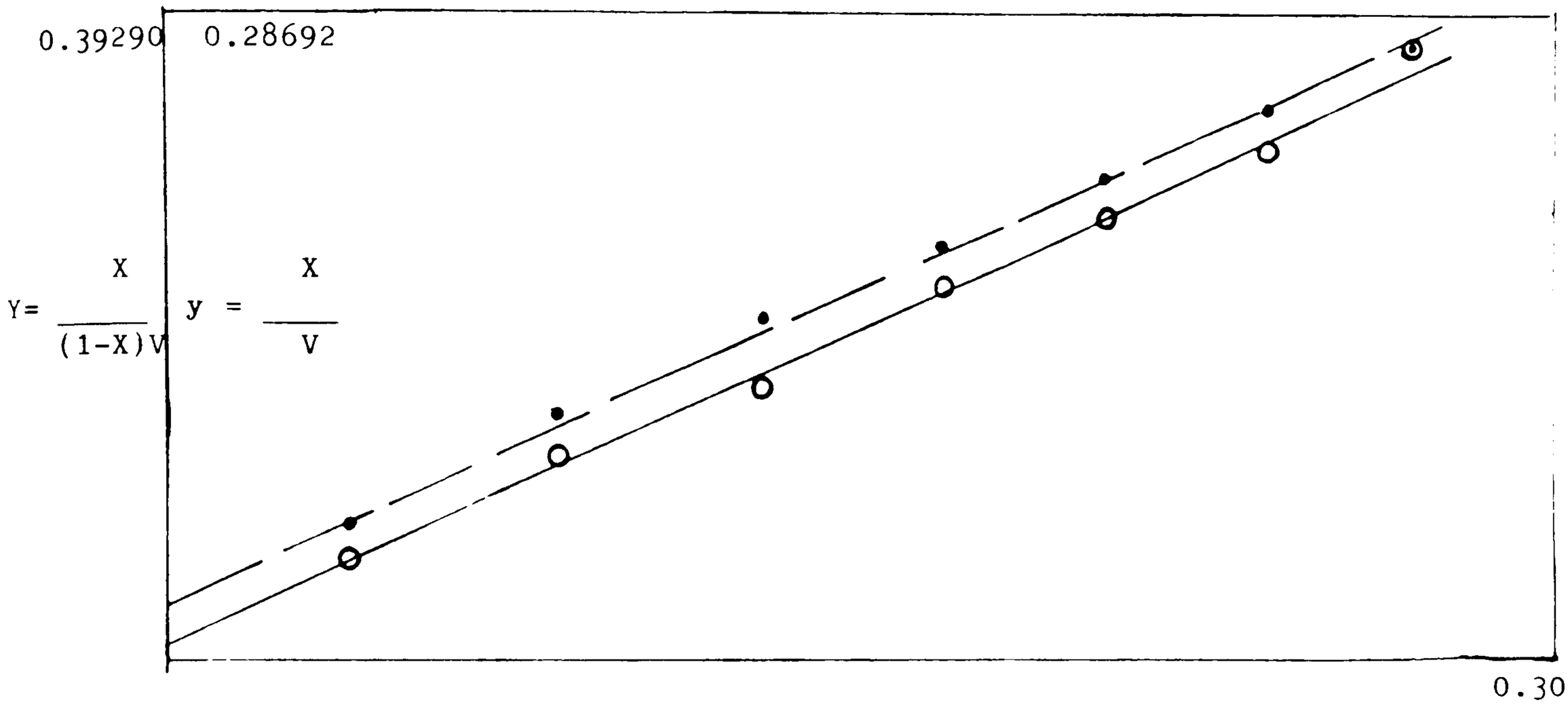

Fig.3.3 BET plot of N_2 adsorption onto -estradiol crystals

. Langmuir plot

o BET plot

3.3.3 Specific Surface Area Measurements of 5-Aminoslicylic Acid

The data are given in Table 3.3 and the condition of the adsorption system is given below:

5-Aminosalicylic acid weight	:	3.0245 g
Bath (liquid N_2) temperature	:	77.53 K
Saturation pressure (P_o)	:	775.84 mmHg

Table 3.3 Adsorption of N_2 onto 5-aminosalicylic acid

Equilibrium pressure of N_2 after adsorption (P) in mmHg	Vol. adsorbed (V)cm^3/g at (S.T.P.)	$x = P/P_o$	$Y = X/((1-X)V)$	$Y = X/V$
28.805	0.325	0.037	0.119	0.114
61.730	0.388	0.080	0.223	0.205
94.450	0.419	0.122	0.330	0.290
127.720	0.443	0.165	0.444	0.371
158.640	0.473	0.204	0.543	0.432

The straight line was obtained by plotting $X = P/P_o$ against $Y = X/V(1-X)$ from which the slope and the intercept were determined for the BET surface area calculation for each drug. For the Langmuir surface area calculation, the straight line was obtained by plotting $X = P/P_o$ against $Y = X/V$ from which the slope and intercept were determined assuming the adsorption of a monlayer onto the solid surface.

The specific surface area of each drug powder is presented in Table 3.4 based on the data obtained from BET and Langmuir adsorption isotherm plots. The surface area of potassium chloride calculated from the particle size is also given in the table.

3.4 Discussion of Results and Conclusion

The surface area of KCl obtained from BET and Langmuir adsorption isotherms was larger than that calculated from the particle size, this was because KCl particles were porous and non-spherical as shown in the micrograph below Fig. 3.4. β-Estradiol and 5-aminosalicylic acid were expected to give a larger surface areas than the values obtained from N_2 adsorption as they were quite fine powders. Experimentally the opposite was obtained and the reason could be attributed to the fact that β-estradiol and 5-aminosalicylic acid were in aggregate forms due to the cohesive forces between the particles. These aggregates exhibited smaller surface area, specially 5-aminosdalicylic acid which formed spherical aggregates. This phenomena may disappear reasonably when the adsorption is carried out from solution (Chapter IV).

The Langmuir surface area values of the three drugs were larger than those obtained from the BET ones. This is because the Langmuir calculation of the adsorption is based on the assumption[2] that it is monomolecular. This would give larger surface area than the actual surface area of the solids[2,4]. So the BET surface area values were taken as the most relevant to specific surface area of the three drugs used in this study and these values were used in all calculations of this study.

Table 3.4 Specific surface area of the three drugs

Solid Drug	BET						LANGMUIR						Particle Size Method
	Slope	Intercept	Constant C	Vm cm^3/g	Surface Area m^2/g	Corr. Coeff.	Slope	Intercept	BxP_o	Vm cm^3/g	Surface Area m^2/g	Corr. Coeff.	Surface Area m^2/g
KCl	49.70 ±12.15	9.44 ±2.03	6.26	0.02	0.074 ±0.02	0.877	25.55 ±9.69	10.31	2.48	0.04	0.17 ±0.06	0.763	0.012
β-Estradiol	1.38 ±0.04	0.009 ±0.007	156.76	0.72	3.13 ±0.09	0.998	0.94 ±0.01	0.03 ±0.00	26.95	1.06	4.64 ±0.07	0.999	-
5-Aminosalicylic acid	2.55 ±0.02	0.022 ±0.003	117.03	0.39	1.69 ±0.07	0.999	1.91 ±0.07	0.05 ±0.01	37.98	0.52	2.28 ±0.08	0.998	-

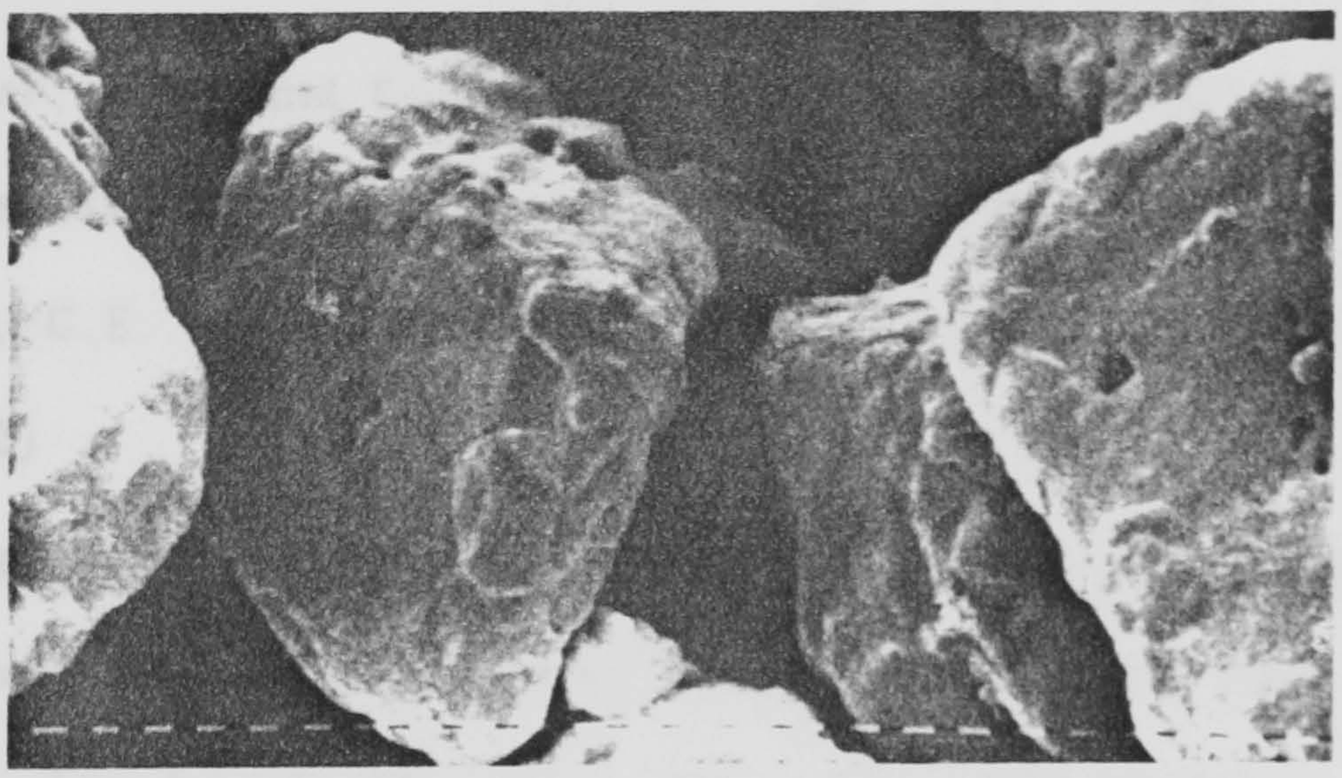

Fig. 3.5 SEM micrograph of KCl particles, scale marker - 10μm

3.5 References

1. G. Jura, "The Determination of the Area of Surfaces of Solids" in Physical Methods in Chemical Analysis, Vol. II, W. G. Berl, ed., Academic Press, New York, (1951)
2. Langmuir, I., J. Am. Chem. Soc. 54, 2798 (1932)
3. Fowler, R.H. and Guggenheim, C.A., "Statistical Thermodynamics", University Press, Cambridge, p. 429, (1939)
4. Boyd, G.E. and Livingstone, A.K., J. Am. Chem. Soc. 64, 2383 (1942)
5. Young, D.M. and Crowell, A.D., "Physical adsorption of gases", London: Butterworth & Co. (Publishers) Ltd., 1962
6. Langmuir, I., J. Am. Chem. Soc., 40, 1361 (1918)
7. Brunauer, S., Emmett, P.H., and Teller, E., J. Am. Chem. Soc., 60, 309 (1938)
8. Brunauer, S. and Emmett, P.H., J. Am. Chem. Soc., 59, 2682 (1937)
9. Emmett, P.H. and Brunauer, S., J. Am. Chem. Soc., 56, 35 (1934)
10. Emmett, P.H. and Brunauer, S., J. Am. Chem. Soc., 59, 310 (1937) and 59, 1553 (1937)
11. Emmett, P.H. and Brunauer, S., Trans. Electrochem. Soc., 71, (1937)

CHAPTER IV

Adsorption Studies of Glycerylmonooleate Surfactant at the Solid-Liquid Interface

Chapter IV

Adsorption Studies of Glycerylmonooleate Surfactant at the Solid-Liquid Interface

4.1 Introduction

Various methods have been used to measure the extent of physical adsorption but by far the most common ones involve the determination of the reduction in solution concentration of the surfactant upon addition of the solid. Clearly, for such a technique to be viable, the solid sample must present a sufficient area of surface to the solution for a readily determinable decrease in solution concentration to occur at equilibrium. The problem then reduces to selecting a sufficiently sensitive analytical technique for the determination of surfactnat concentration[1].

The use of monolayer technique[2], especially the measurement of π-A diagram, provides a sensitive analytical method for the estimation of very small amount of compounds which form insoluble monolayers. Hutchinson[3] and Crisp[4] have also used the same analytical technique, to study adsorption from solution on large solid surfaces by spreading the same volume of solution before and after adsorption on a Langmuir trough to obtain a direct comparison of the original and final equilibrium concentration. From that difference between the two, the amount of solute adsorbed on the solid powder was calculated. Giles et al[5] studied the relation between solute adsorption mechanism at solid surfaces and the types of adsorption isotherm obtained. They described a system of classification of all solution adsorption isotherms and how it can be used to diagnose the adsorption mechanism, obtain information regarding the physical nature of the solute and the substrate surface and to measure the specific surface area of the substrate. The classification system divided all the isotherms into four main classes according to

the initial slope, and sub-groups are described for each class, based on the shape of the upper parts of the curves. The four main classes are named the S, L (i.e., "Langmuir" type), H ("high affinity"), and C ("constant partition") isotherms, and the variations in each class are divided into sub-groups. Fig. 4.1 shows the system of isotherm classification.

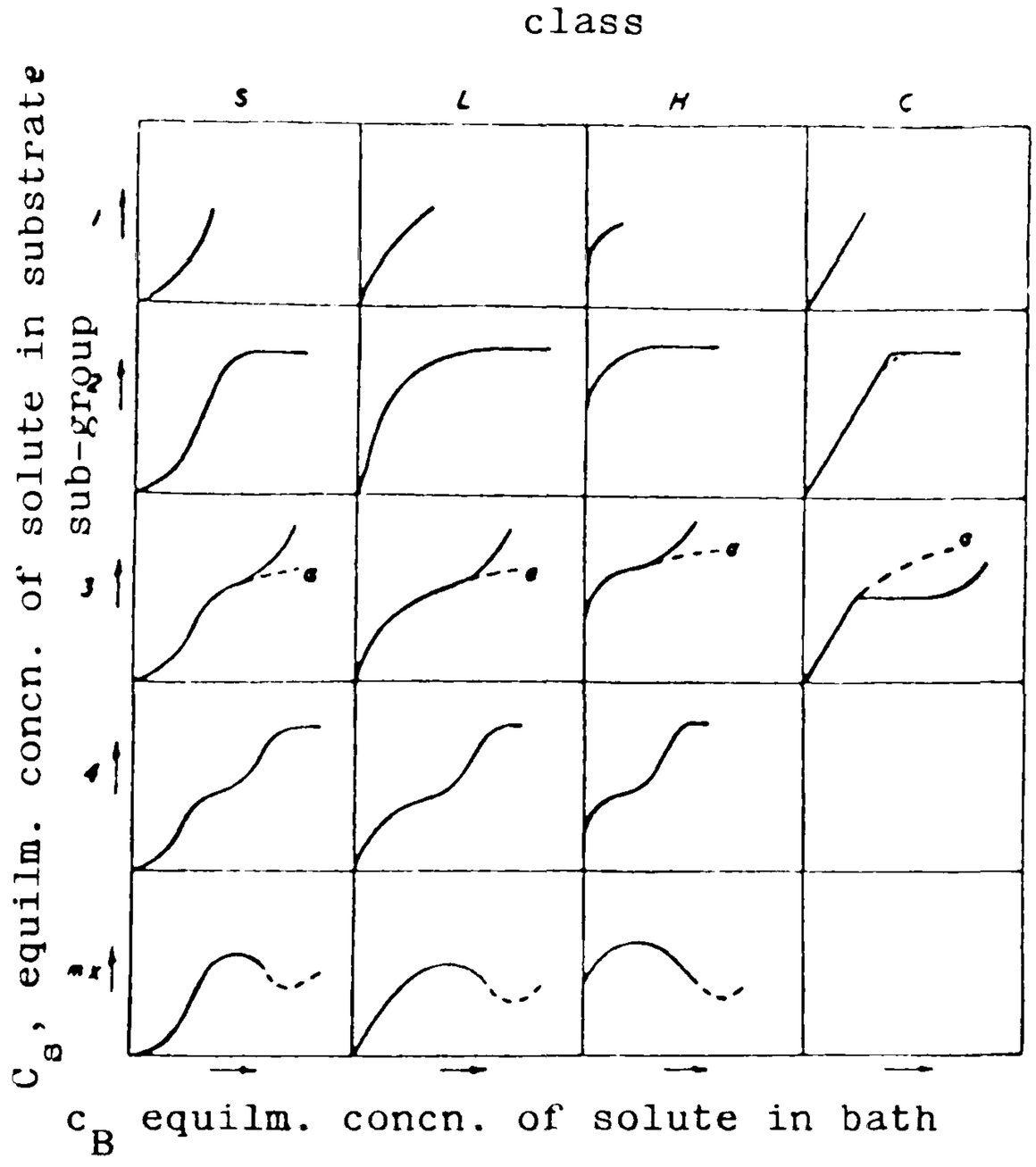

Fig. 4.1 System of isotherm classification

From the figure given and the feature of α-monoolein isotherm, it can be classified as S_2-curve. Giles stated that the S-curve usually appears when three conditions are fulfilled: the solute molecule a) has a fairly large hydrophobic residue ($> C_5$) and adsorbed as a single unit and not in the form of a micelle, b) has moderate intermolecular attraction causing it to pack vertically in regular array in the adsorbed layer, and c) meets strong competition for substrate sites from molecules of the solvent or of another adsorbed species.

Characterization of fatty materials from various natural sources has been aided by the monolayer studies of Stattberg[5] and Stenhagen[7]. The monolayer technique has been applied to the direct examination of the behaviour of molecules at liquid–gas, liquid–liquid and liquid–solid interfaces.

Physical adsorption of an adsorbate on a solid surface is a phenomenon of considerable potential in pharmaceutical science. Most of the related studies concern the adsorption of drug on adjurants or plastic containers and pertain to reduced or modified availability of the active substance[8–11]. By contrast the liquid–solid adsorption of additives on drug powders was apparently studied by Graham[12] and Rashid[13]. When a surface active agent is used as the adsorbate, a monolayer or multilayer is likely to be adsorbed on the drug crystals. This may result in modified drug properties. It also could be used as a novel technique of microencapsulation. If the adsorbate can link via a polymerization process with a monomer or prepolymer, to form a polymer membrane, the release of the encapsulated drug may be controlled.

The present work involves a study of the adsorption of glyceryl monooleate onto microcrystals of three different model drugs, namely potassium chloride, β–estradiol and 5–aminosalicylic acid. In further development of monolayer technique we have used the automated Lauda Surface Balance which apart from other improvements has a precise temperature control of the subphase to an accuracy of $\pm$ 0.1^{o}C.

The adsorption studies were carried out in clean vaccine bottles (30 cm^3 capacity) loaded with a known weight of the adsorbent plus a certain volume of surfactant solution of initially known concentration. The bottles were sealed and tumbled

mechanically for a period of 20 hours to attain equilibrium between the adsorbed molecules of surfactant, on the solid surface, and molecules remaining in the bulk phase. These adsorbed molecules may form a monolayer or multilayer depending upon the initial concentration of the surfactant.

These packing phenomenon can be visualised from the plots of the amount adsorbed at the solid surface against equilibrium concentrations after adsorption. The equilibrium concentration of the surfactant solution is determined from the π–A isotherm which is obtained by spreading an accurately known volume of the supernatant solution (after the bottles have been centrifuged after adsorption period) on a subphase (double distilled water). The solvent to be used as a dispersion medium should be a non–solvent for the solid powder, a moderate solvent for the surfactant (glyceryl monooleate) and should have a positive spreading coefficient – a criteria for spreading. (n–heptane was chosen for having such required properties).

The monolayer area was estimated by extrapolating the linear part of the condensed phase curve to the zero surface pressure. Then from the calibration curve the number of molecules at the packed monolayer was calculated from which the equilibrium concentration of the solution could be calculated.

The initial concentrations of the surfactant solutions used in the adsorption studies were accurately known and were also analysed using the monolayer technique as well as the equilibrium concentrations. The amount of the surfactant adsorbed on the solid surface and the surface area per adsorbed molecule was estimated on the three different drug models used in this study.

4.2 Experimental

4.2.1 Materials

Adsorbents: Potassium chloride (BDH analar) of average particle size of 250–355 μm. It was heated at 500°C for four hours to purify its surfaces from any organic residue. The material was kept in a desiccator for use. The specific surface area of the powder, calculated by BET method, was 0.0736 m^2/g.

Anhydrous β–estradiol (crystalline) (Sigma) was dried in a vacuum oven for 24 hours and kept in a dark bottle, for use, in a desiccator over silica gel. The specific surface area was 3.14 m^2/g.

Crystalline 5–aminosalicylic acid (Sigma) approximately 99%. Its BET surface area was 1.69 m^2/g. It was used as supplied.

Adsorbate: Anhydrous α–monoolein (Sigma grade) approx. 90% is stated to be the α–isomer and the balance is β–isomer. It was used without further purification.

Solvent: n–Heptane (F.S.A. Laboratory) was double distilled.

Solution of Surfactant

A solution of α–monoolein, in n–heptane, at concentrations of 2.62×10^{-4} and

5.27 x 10^{-4} mol/l for KCl adsorption studies and at concentration of 6.26 x 10^{-4} and 7.51 x 10^{-4} mol/l for the adsorption studies on β–estradiol was used; the surfactant solution at a concentration of 7.95 x 10^{-4} mol/l was used for the adsorption studies on 5–aminosalicylic acid.

4.2.2 Set up of the Nitrogen Dry Box

A nitrogen dry chamber was set up by connecting a box to purified nitrogen gas stream from one side and to a water pump from the other side. The water pump was used to evacuate the chamber and to suck off the excess nitrogen gas throughout the box. The nitrogen gas was purified by passing through a set of jars containing respectively a solution of KOH (50%), Pyrogallol (20%) in 50% KOH solution, ammonium metavanedate solution reduced by nascent hydrogen delivered by adding metallic zinc pellets and hydrochloric acid till the solution became blue coloured, and finally bubbled through jars containing concentrated sulphuric acid. A set of empty jars was connected to the system as traps for safety to avoid any mixing of the previously mentioned solutions with sulphuric acid or to be sucked inside the box by any back pressure. The nitrogen atmosphere inside the box was kept dry by the aid of phosphorous pentaoxide.

4.2.3 Adsorption Procedure

All glassware used were cleaned with permanganic acid followed by copious rinsing with tap water and double distilled water. Some of the glassware was rinsed with distilled Analar acetone to avoid the step of drying the wet glassware at 60°C in the electrically heated clean oven. The hot glassware was cooled down in a desiccator over silica gel and all the tips were covered with tin foil and used within a few hours.

For each adsorbent, six clean dry vaccine bottles (30 cm^3 capacity) were loaded

with different known weights of the adsorbent i.e. 1.0 - 6.6 gram of potassium chloride 0.1 - 0.7 g of β-estradiol and 0.2 - 1.0 g of 5-amino-salicylic acid. A volume of 15 ml of the surfactant solution (adsorbate) were then pipetted into each bottle. The volume of adsorbate solution used for 5-aminosalicylic acid was 17 ml for each bottle. The addition of the surfactant solution to the adsorbent was carried out inside the nitrogen dry box. The bottles were then securely sealed with tap-top seal with Teflon-faced rubber septum. The bottles were taken out of the dry nitrogen box to be tumbled mechanically at a speed of 80 rpm for 15-20 hours to ensure that adsorption equilibrium was attained. The bottles were then centrifuged for 30 minutes to allow the solid particles to settle completely and using a syringe the supernatant solutions were transferred into 5 ml clean glass vials which were tightly stoppered (Teflon caps).

4.2.4 Analysis and Calculation

The surfactant concentrations were determined after adsorption by measuring the surface pressure-area of the respective monolayers formed on the water surface of the automated film balance of Langmuir type with temperature control.

The surfactant solutions in n-heptane were applied on the water surface of the Lauda-balance by means of Hamilton microsyrings (100 μl capacity) with an accuracy of $\pm$ 0.05 μl. After evaporation of the solvent (2 min), the surfactant molecules were compressed to form a monolayer at the maximum speed of the moving barrier, and a temperature of 25 $\pm$ 0.1^{o}C. The microsyringe, after each delivery of a particular test solution, was thoroughly cleaned and rinsed with the next test solution that was to be spread.

The monolayer area was determined by extrapolation of the linear part of the

curves to zero surface pressure. The number of molecules of α-monoolein present in the monolayer in each case was calculated from the calibration curve which relates the number of molecules with monolayer's area (Fig. 2.6 Chapter II).

The equilibrium concentration of α-monoolein solution (C_e) (after adsorption) was calculated from the expression.

$$C_e \text{ mol/l} = \frac{\text{No. mol. on water surface of packed monolayer x 1000}}{\text{Avaogadro's No. x vol. spread (cm}^3\text{)}}$$

Then

$C_i - C_e$ = amount of α-monoolein adsorbed onto the adsorbent used.

where C_i = Initial concentration of α-monoolein (before adsorption)

C_e = Equilibrium concentration of α-monoolein in the supernatant solution (after adsorption)

Then,

The adsorption density of surfactant (μmol/m^2)

$$= \frac{\dfrac{(C_i - C_e) \times 10^6}{\text{vol. used (l)}}}{\text{Area of adsorbent (m}^2\text{)}}$$

and,

Area per adsorbed molecule of surfactant (Å^2)

$$= \frac{\text{Area of solid substrate A}^2\text{/gram (solid)}}{\text{No. of molecules adsorbed/gram (solid)}}$$

4.3 Results

4.3.1 Adsorption of Glyceryl Monooleate on Potassium Chloride Crystals

Typical data of the adsorption of surfactant of initial concentrations 2.62 x 10^{-4} and 5.27 x 10^{-4} mole/l are given in Tables 4.1 and 4.2 respectively. The number

of molecules at the packed monolayers were obtained from the calibration curve (Fig. 2.6 Chapter II).

The data include the weight of KCl powder corresponding to certain surface area, the equilibrium concentrations, the percentage difference between the initial and the equilibrium concentrations due to adsorption, the adsorption density of α-monoolein on the drug surface and the molecular area of the adsorbed molecules.

Table 4.1 Adsorption of α–monoolein onto KCl (initial conc. 2.62×10^{-4} mole/l)

Wt. of KCl (g)	Equilibrum conc. Ce (μmol/ml)	% of conc. difference before and after adsorption	Adsorption density μmol/m^2	Molecular area of adsorbed molecules ($Å^2$)
1.73025	0.259	1.1 -	0.23 -	706.4
2.11376	0.254	3.0 -	1.16 -	143.5
3.31590	0.211	19.5	3.19	51.9
3.32608	0.243	7.2	1.35	123.2
3.66672	0.239	8.8	1.22	135.9
6.55047	0.229	12.6	0.99	166.9
Standard deviation (σ_{n-1})				48.6
Mean ($\bar{x}$)				119.6
Number of data (n)				4.0

Table 4.2 Adsorption of α-monoolein on KCl (initial conc. 5.27×10^{-4} mole/l)

Wt. of KCl (g)	Equilibrum conc. Ce (μmol/ml)	% of conc. difference before and after adsorption	Adsorption density μmol/m^2	Molecular area of adsorbed molecules ($\AA^2$)
1.95807	0.508	3.6 -	2.23 -	93.8
4.72829	0.478	9.3	2.02	81.9
3.64049	0.483	8.3	2.63	63.1
1.72364	0.509	3.4 -	2.01 -	82.6
1.07667	0.525	0.4 -	1.32 -	125.3
2.74846	0.469	11.0	4.23	39.3
Standard deviation (σ_{n-1})				21.3
Mean ($\bar{x}$)				61.4
Number of data (n)				3.0

4.3.2 Adsorption of Glyceryl Monooleate on β-Estradiol Crystals

The initial concentration of the surfactant solution of the two sets of data given in Table 4.3 and 4.4 were 6.26×10^{-4} and 7.51×10^{-4} mol/l respectively. The number of molecules at the packed monolayer of each isotherm was calculated from the calibration curve.

Table 4.3 Adsorption of α-monoolein (initial conc. 6.26×10^{-4} mol/l) onto β-estradiol

Weight of β-estradiol (g)	Equilibrum conc. Ce (μmol/ml)	% of conc. difference before and after adsorption	Adsorption density μmol/m^2	Molecular area of adsorbed molecules ($\AA^2$)
0.40167	0.557	11.0	0.78	208.5
0.13888	0.569	9.0	1.93	86.9
0.20814	0.545	12.9	1.97	84.1
0.67114	0.521	16.8	0.75	217.2
0.31336	0.581	7.2	0.70	236.9
0.90436	0.502	19.8	0.66	248.2
Standard deviation (σ_{n-1})				74.8
Mean ($\bar{x}$)				180.3
Number of data (n)				6.0

Table 4.4 Adsorption of α-monoolein (initial conc. 7.51×10^{-4} mol/l) onto β-estradiol

Weight of β-estradiol (g)	Equilibrum conc. Ce (μmol/ml)	% of conc. difference before and after adsorption	Adsorption density μmol/m^2	Molecular area of adsorbed molecules ($Å^2$)
0.18696	0.678	9.7	1.81	91.4
0.62201	0.642	14.5	0.85	193.0
0.17745	0.690	8.1	1.64	102.2
0.14977	0.702	6.5	1.62	102.2
0.20831	0.666	11.3	1.86	89.8
0.53125	0.650	13.4	0.91	186.1
Standard deviation (σ_{n-1})				48.4
Mean ($\bar{x}$)				127.4
Number of data (n)				6.0

4.3.3 Adsorption of α-Monoolein on 5-Aminosalicylic Acid

The adsorption of α-monoolein surfactant of initial concentration of 7.95×10^{-4} mol/l on different weights of the adsorbent was studied and typical data are given in Table 4.5.

Table 4.5 Adsorption of α-monoolein (initial conc. 7.95×10^{-4} mol/l) onto 5-aminosalicylic acid

Weight of acid (g)	Equilibrum conc. Ce (μmol/ml)	% of conc. difference before and after adsorption	Adsorption density μmol/m^2	Molecular area of adsorbed molecules ($Å^2$)
0.5281	0.699	12.0	1.83	90.7
0.42590	0.708	10.9	2.01	82.6
0.22431	0.772	2.9	1.12	148.2
0.36090	0.727	8.5	1.81	91.7
0.31047	0.763	4.0	1.13	146.9
0.99480	0.672	15.5	1.26	131.7
Standard deviation (σ_{n-1})			22.1	
Mean ($\bar{x}$)			99.2	
Number of data (n)			4.0	

4.4 Discussion

The equilibrium adsorption density of glyceryl monooleate on potassium chloride crystals was studied as a function of its equilibrium concentration in n-heptane. From the two sets of data given in Table 4.1 and 4.2, it is obvious that the adsorption density increased in the higher concentration of α-monoolein. It exhibited a maximum value of 3.2 and 4.2 μmol/m^2 for the two sets of experiment respectively.

The isotherm of α-monoolein is classified as S-curve because of its initial slope[5] and shape. This may illustrate that higher adsorption density was obtained when relatively higher concentration was used. The more solute there is already adsorbed, the easier it is for additional amounts to become fixed[5]. This implies a side-by-side association between adsorbed molecules, helping to hold them to the surface. This has been called "co-operative adsorption"[14].

From Table 4.1 and 4.2, the mean of the molecular area in the lower concentration 119.5 $\dot{A}^2$ of the set, is about twice the value in the relatively higher concentration 61.4 $\dot{A}^2$ shown in Table 4.2. It is obvious that the molecular area of the adsorbed molecules is larger than that obtained from monolayer measurements by compression on water surface which had a mean value of 46.1 $\dot{A}^2$ (Chapter II). This may indicate that using such low concentrations of surfactant, the monolayer formed may not be close-packed on the solid substrate. In such case, various configurations of the surfactant may be possible. One hydroxyl group might be

adsorbed on the solid substrate while the hydrocarbon tail of the molecule is tilted in a horizontal position to the solid surface. The other case is that the two glyceryl groups may be oriented towards the solid surface while the hydrocarbon chain lies flat on the crystal surface. In both cases the molecular area could be much larger than that obtained from the compressed monolayer.

The mean values of the molecular area of α–monoolein adsorbed on β–estradiol were 180.3 and 127.4 $\dot{A}^2$/molecule. This indicates that on β–estradiol the adsorbed molecule is in a tilted or flat configuration to the substrate surface. In such a case the molecular area will be much larger than the case of vertical orientation, the latter provided a surface area/molecule of 46.1 $\dot{A}^2$.

Rashid[13] studied the adsorption of α–monoolein on β–estradiol with surface area of 8.5 m^2/g. The molecular area of the adsorbed molecules reported from his study was 53.25 and 61.35 $\dot{A}^2$/molecule and adsorption density of about 3.12×10^{-3} $\mu mol/m^2$. These values are relatively smaller than the values obtained in this study as shown in Tables 4.3 and 4.4. The surface area of the solid substrate (β–estradiol) and the initial concentration of the surfactant used in this study were much different from those reported by Rashid which were 8.5 m^2/g and 1.68×10^{-4} – 20.08×10^{-4} mol/l respectively.

The adsorption of α–monoolein on 5–aminosalicylic acid was carried out to check the general application of this technique. 5–Aminosalicylic acid provides a larger surface area than KCl but smaller than β–estradiol. The maximum adsorption density obtained from the single initial concentration used (7.95×10^{-4} mol/l) was 2.01 $\mu mol/m^2$. The mean value of the molecular area of the adsorbed molecules

was 99.2 Å²/molecule. This value confirms the possibility of a tilted configuration of the adsorbed molecules on this solid substrate.

Possible orientations of glyceryl monooleate on the solid substrates which could be responsible for the wide variation of the observed molecular areas are represented in the following diagram of Fig. 4.2. The molecule may tilt around the double bond of the hydrocarbon chain.

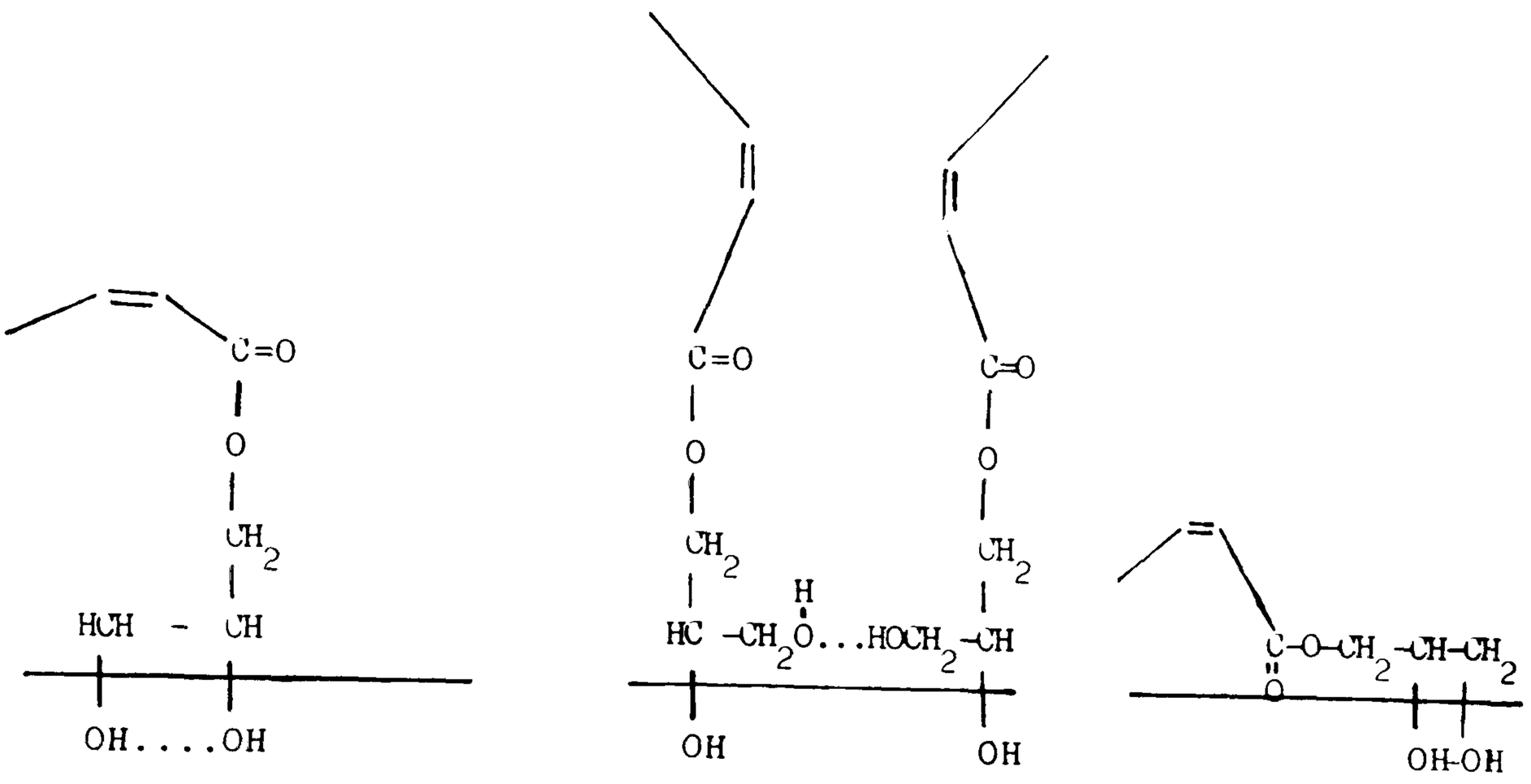

(a) (b) (c)

Fig. 4.2 Possible orientation of α–monoolein on solid substrate.

(a) The two glyceryl groups are adsorbed to the solid substrate while the hydrocarbon chain is in tilted position to the substrate surface. The two adsorbed glyceryl groups may associate by hydrogen bonding.

(b) Only one glyceryl group is oriented toward the substrate while the other dipole hydroxyl group may associate by hydrogen bonding with another molecule.

(c) The molecule is less oriented and all the polar groups lie flat independently on the surface.

4.5 Conclusion

The results of adsorption densities and area per adsorbed molecules are quite erratic and this can be attributed to the difficulties and sensitivity of the technique. It works best for a large surface area (an area of some 0.5 m^2/g) and high adsorption in order that the uptake should produce a significant measurable change in the concentration of the surfactant solution. Materials with relatively low surface areas and low adsorption push the technique to its limits. It is not possible to know the degree of adsorption in advance but it turned out that we had a) large adsorption combined with small surface area (potassium chloride) b) small adsorption combined with large surface area (β–estradiol and 5–aminosalicylic acid). Neither of these was ideal. Also there is some possibility of solvent evaporation during the measurements. These errors would be magnified when the values of the equilibrium concentrations tested for each set of data were very close to those of the starting concentrations and a measured concentration change of > 5% is clearly desirable and was used to select out measurements quoted in the Tables 4.1–4.5. From the results obtained it is quite clear that using such very low concentrations of surfactant, the adsorption process on the three drug surfaces formed a template layer of surfactant on each drug surface.

This adsorbed layer will be activated with boron trifluoride diethyletherate catalyst (cationic initiator) which will initiate a cationically polymerizable monomer to polymerize and provide encapsulation of drug particles by a polymer envelope.

4.6 References

1. M.J. Rosen and H.A. Goldsmith "Systematic Analysis of Surface-Active Agents". Wiley-Interscience, New York, 2nd edn. (1972)
2. I, Langmuir, J. Amer. Chem. Soc., 39, 1848 (1917)
3. E. Hutchinson, Trans. Faraday Soc., 43, 439 (1947)
4. D.J. Crisp, J. Colloid. Sci., 11, 356 (1956)
5. C.H. Giles, T.H. MacEwan, S.N. Nakhwa, and D. Smith, J. Chem. Soc. 3, 3973 (1960)
6. S. Stattberg-Stenhagen and E. Stenhagen, J. Biol. Chem., 165, 599 (1946); Acta Chem. Scand., 3, 1035 (1949)
7. E. Stenhagen in "Determination of Organic Structure by Physical Methods", E. Brande and F.C. Nachod, eds., Academic Press, New York, Chapt. 8. 1955
8. A.T. Florence and D. Attwood, "Physiochemical Principles of Pharmacy", 2nd edn., Macmillan Press, London, 1988
9. J. J. Schaer, L. Redarn and E. Doelker, Acta Pharm. Technol. 34, 32 (1988)
10. K. Thoma, H. Lieb, Pharm. Acta Helv., 60 98 (1985)
11. J. McCinity and J-L Lach, J. Pharm. Sci., 65, 896 (1978)
12. N.B. Graham, A. Rashid and K.P. Rao, UK Patent 2112730 B (1985)
13. "Some Aspects of Surface Chemistry, Microencapsulation and In Vitro Evaluation of β-estradiol from an Injectable Formulation" MSc Thesis (1980) by A. Rashid, University of Strathclyde
14. West, Carroll and Whitcomb, J. Phys. Chem., 56, 1054 (1952)

CHAPTER V

Microencapsulation by Surface Polymerization

Chapter V

Microencapsulation by Surface Polymerization

5.1 Introduction

Graham reported that the development of a useful therapy involves the combination of an active agent and a delivery system. The pharmaceutical industry has been much more concerned about the development of new chemical entities than about novel delivery systems but nevertheless these latter have become increasingly important over the last thirty years and have progressed from instant to constant delivery and now these efforts are directed towards programmed delivery with an awareness of chromobiology.

If a drug is given as an instant delivery tablet taken four times a day orally, the normal result would be plasma levels similar to those shown in Fig. 5.1

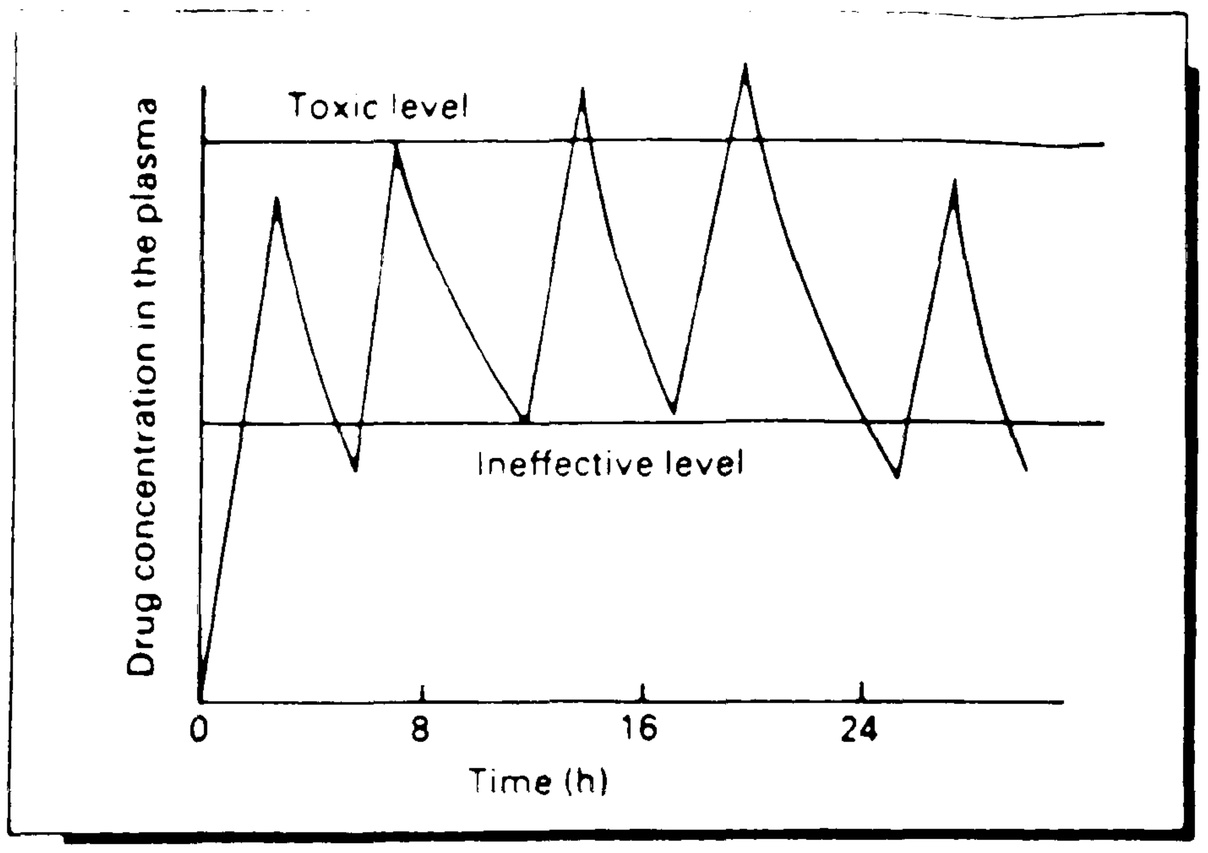

Fig. 5.1 The fluctuations in plasma levels which can result from taking instant delivery pills four times daily

Peaks and troughs of the plasma levels will be obtained and the result may involve either temporary overdosing with attendant side-effects or underdosing with attendant lack of protection. Pharmaceutical uses of microencapsulation range from the separation of mutually reactive compounds to the controlled rate of delivery of drugs for many purposes including birth control to cancer treatment. It has long been the objective of drug delivery formulators to attain control of the constancy and the length of the drug delivery. In general terms there are four techniques for attaining such objectives. The first is the incorporation of the active agent in a matrix of a variety of excipients which may or may not be polymeric. This would provide delayed but not constant rates of release of the active agents. The second is to provide a matrix which dissolves or degrades at a predictable rate. This can provide the essentially instant delivery of many conventional tablet or the prolonged sustained release of a biodegradable implant such as Zoladex^{TM}. The third is the use of swelling hydrogels which by a complex mechanism can provide an essentially constant rate of release as in Propess^{TM}. The fourth is the main subject of this chapter and involves the use of thin layers around a central reservoir of the agent[1]. Such systems are subject to the well known Fickian Diffusion Laws and would be expected to provide constant rates of release as long as the reservoir enclosed within the membrane contains solid undissolved drug which can maintain the saturated solution in the interior. Such system can provide constant release and can be mathematically modelled. This chapter describes a new method for the encapsulation of crystals by surface polymerization which can provide very thin rate-controlling layers rather than the more commonly used coating techniques. There are a number of such techniques known and some are used commercially. Interfacial polymerization at liquid-liquid[2,3], polymerization of liposomes[4-6] and

the formation of admicelles followed by adsolubilization of monomers into admicelles and then polymerization of the monomers *in situ* constitutes a three step process to construct a thin film on a solid substrate[7,8] via a low energy process have been reported. The encapsulation of solids by direct polymerization was first studied by Graham[9] and Rashid[10]. The thinnest rate controlling layer on a solid surface would be a monolayer. This and thicker layers could in principle be obtained by the process shown in Fig. 5.2.

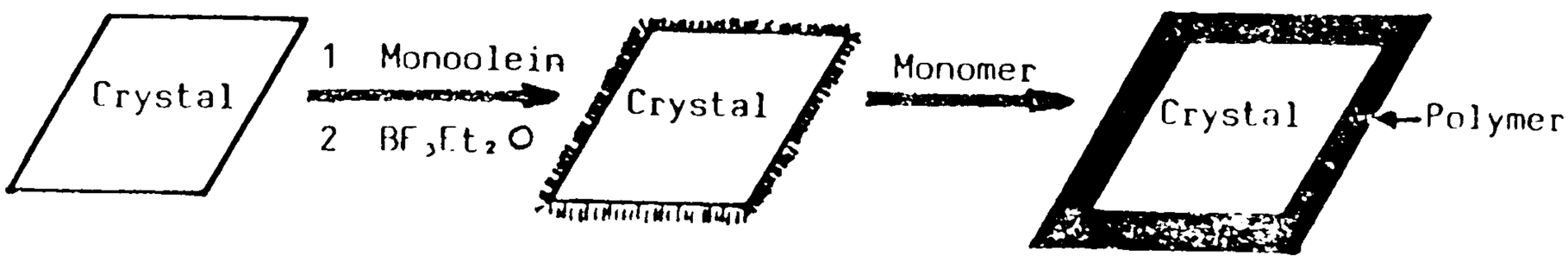

Fig. 5.2 Schematic presentation of the encapsulation process

The first step of this proposed technique involves the adsorption of a surfactant (α-monoolein) from solution onto the crystalline solid drug, as described in Chapter IV. As α-monoolein is polar and contain two alcoholic groups which can interact with many catalyst species and accordingly its adsorbed layer may be able to complex an appropriate catalyst from solution to form highly concentrated layers which in turn should be capable of polymerizing an appropriate monomer in the solution phase to produce the rate-controlling layer.

Cationic[11] polymerization was the method of choice as it proceeds rapidly at ambient temperature. Four effective monomers were selected: styrene, 3,4-dihydro-2H-pyran -2-methyl (3,4-dihydro-2H-pyran-2-carboxylate), 2,3-epoxypropyl methacrylate and bisphenol-A diglycidyl ether (Epikote 828). The polymerization

process was initiated by borontrifluoride diethyl etherate catalyst[12-14]. The polymerization was carried out in n-heptane solvent which was a critical choice to act as a non-solvent for the core materials and a reasonable solvency for the catalyst and monomers and a moderate solvent for the surfactant. It was also important to be a non-solvent for the formed polymer layers.

The microencapsulation technique used in this study, which as described based on interfacial cationic addition polymerization, is suitable for encapsulating almost any particle size of the required solid materials. The polymerization was carried out in an entirely non-aqueous condition by first formation of a dispersion of crystals with a template layer of catalyst on the crystal surface then subsequently adsorbing and polymerizing the suitable monomer.

5.2 Experimental

5.2.1 Materials

Surfactant: α-monoolein, as described in Chapter II used without further purification.

Solvent: n-Heptane, as described in Chapter II

Core Materials:

Potassium chloride

Three different samples of potassium chloride were used in this study.

1. KCl of average particle size 250-355 μm and of measured BET surface area 0.0735 m^2/g, as described in Chapter III.

   Discs of KCl (mentioned above) of 1 cm diameter and 0.1 cm thickness

were prepared by fine grinding of KCl and compressing it into discs. These were used as core materials which were encapsulated and studied.

2. A single crystal of KCl was grown from which crystals were cut to different sizes which provided smooth substrates for surface polymerization. These crystals were encapsulated and studied.

5.2.2 Method of Single Crystal Growth

A super saturated solution of KCl, in distilled water, was prepared at 60°C. This solution was filtered, when its temperature was about 40–50°C, into a glass jar. The jar was then suspended in an automatically temperature controlled water bath (42°C). A lid holding a stirrer in which a glass bar stirrer, carrying a KCl crystal seed was attached, was then put on the top of the jar. By this, the KCl seed was kept suspended and rotating in a homogeneous saturated KCl solution. The seed was gradually growing forming a clear single crystal as KCl deposited from the solution onto the seed. The solution was kept saturated by gradual evaporation through a small hole in the lid.

3. KCl (Alfred Benzon–Copenhagen) of two chosen average particle sizes, 500–600 and 710–800 μm were treated in the same way as KCl (250–355 μm), Chapter III

   - β–Estradiol of BET surface area 3.14 m^2/g, as described in Chapter II.
   - 5–Aminosalicylic acid of measured BET surface area 1.69 m^2/g as described in Chapter II.

Catalyst Borontrifluoride diethyletherate complex $BF_3(C_2H_5)_2O$ purified redistilled and packaged under nitrogen in sure/seal bottle by Aldrich density 1.13 g/ml.

Monomers: Styrene (Fisons plc), density at 20°C is 0.905 g/ml was stabilized with 10-15 ppm tert-butylcatechol. It was treated by washing three times with 10% aqueous NaOH solution to remove the inhibitor then washed with distilled wter, dried over anhydrous $CaCl_2$ overnight, distilled under vacuum and kept in the fridge for use.

- 3,4-Dihydro-2H-pyran-2-methyl-(3,4-dihydro-2H-pyran-2-carboxylate) abbreviated to "C1 monomer" (Degussa) and specified as Q.C.12 (1) C1 of the structure:

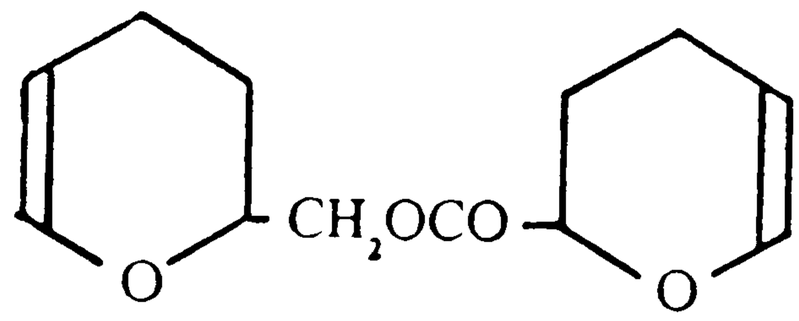

C1 Monomer

and its density at 20°C is 1.1258 g/ml. It was used without further purification.

- 2,3-epoxypropyl methacrylate or glycidyl methacrylate (GMA), (Polyscience) of structural formula $CH_2-CH(\backslash O /)-CH_2-OCOC(CH_3) = CH_2$. It was stabilized with 50 ppm hydroquinone, had a specified purity of 97.5% and the dimer impurity was < 2.5%. The compound was treated by passing through a short column of natural alumina (20 g to a 100 g of the monomer) under normal pressure at room temperature. The product had a density of 1.042 g/ml and 20°C and was kept in the freezer for use.

- Epikote 828 is an unmodified liquid bisphenol A-epichlorohydrin epoxide resin or (bisphenol-A diglycidyl ether) of medium viscosity (Shell). Density

at 25°C is 1.16 g/ml. It was used as supplied. The structural formula of Epikote 828 is

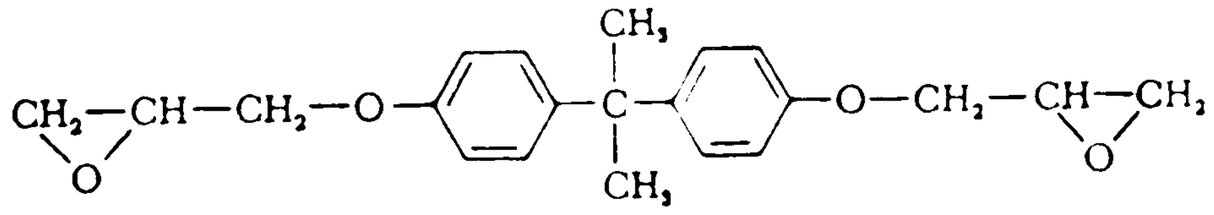

5.2.3 Preparation of Solutions

Solutions of surfactant

Stock solutions of α–monoolein in n–heptane were prepared at concentrations of 4.74×10^{-4}, 8.15×10^{-4} and 2.45×10^{-3} mol/l for adsorption on KCl, β–estradiol and 5–aminosalicylic acid, respectively.

Catalyst solution

Solutions of the catalyst of concentration 0.01M in n–heptane were prepared by tumbling the components (25 μl BF_3 complex + 20 ml n–heptane) in sealed bottles under nitrogen at room temperature for two hours. The catalyst has low solubility in n–heptane and if its concentration in the solvent is much higher than 0.01M, it forms two separate layers, the upper layer is dissolved catalyst in n–heptane and the lower is the excess catalyst.

Solutions of Monomers

Solutions of Styrene

The styrene solutions in n–heptane were prepared under nitrogen in sealed bottles (30 ml capacity), by dissolving 0.1–0.3 ml of styrene in 25 ml n–heptane giving concentrations of 3.62×10^{-3} - 10.86×10^{-3} g/ml. A volume of 20–25 ml of these solutions were injected into each bottle containing the drug to be encapsulated.

Solutions of C1 monomer

The solutions of C1 monomer in n–heptane were prepared as mentioned above by dissolving 0.1–0.15 ml of C1 in 30 ml of n–heptane. The concentrations

obtained were $3.75 \times 10^{-3} - 5.65 \times 10^{-3}$ g/ml. A volume of 15 ml of the solutions were used for each encapsulation of KCl, but 20–25 ml were used to encapsulate β–estradiol and 5–aminosalicylic acid.

Solution of GMA monomer

The GMA monomer solutions were prepared at concentration of 6.25×10^{-3} g/ml by dissolving 0.3 ml GMA in 50 ml n–heptane. Volumes of 20 ml of the solution were injected to each bottle containing the drug to be encapsulated.

Solution of Epikote 828 monomer

The Epikote 828 solution was prepared at a concentration of 5.91×10^{-3} g/ml and 15 ml of that solution was used for each encapsulation of KCl and β–estradiol. Epikote 828 is a viscous liquid and only slightly soluble in n–heptane. The concentration required was obtained by tumbling a known weight of the monomer (0.928 g) in 25 ml of n–heptane for 4 hours under nitrogen, in sealed bottles. The concentration was determined from the weight of the undissolved monomer and also from the soluble part by evaporating the solvent.

5.2.4 Adsorption of α–Monoolein Surfactant onto Crystal Surfaces and Formation of the Activited Template Layer

For each drug (core material), a set of vaccine bottles (30 ml capacity) was loaded with a known weight of the required drug powder. The bottles were then taken into the dry box which was first evacuated and flushed with oxygen–free dry nitrogen gas (as described in Chapter IV, seciton 4.2.2), where 25 ml of α–monoolein solution of the required concentration were added to each bottle. The bottles were sealed and taken out to be mechanically tumbled for 15 hours. After adsorption, the bottles were taken into the dry box where the supernatant solution was sucked off (the bottles were centrifuged to allow the particles to settle in case of β–estradiol and 5–aminosalicylic acid, before the supernatant solutions

were sucked off). The catalyst solution was injected into the bottles in a nitrogen atmosphere and the bottles were tumbled for 2 hours. Again, the supernatant solutions were sucked off, referred to subsequently as activated core material. There were no analytical techniques developed to determine the adsorption of the catalyst on the crystals surfaces. Its presence or absence was deduced from the ability of the treated crystals to induce polymerization. The surfactant adsorption step was excluded in some experiments.

5.2.5 Encapsulation of the Core Materials by Surface Polymerization of Monomers

The required volume of each monomer solution (known concentration) was injected onto the activated core materials (KCl, β–estradiol and 5–aminosalicylic acid), in the vaccine bottles and were tumbled for a fixed period of 3 hours. The encapsulated particles were centrifuged, whenever required, and the supernatant solution was removed and sometimes retained for further study. The particles were washed with n–heptane (to remove any monomer residue) recentrifuged and the supernatant was discarded. Finally the encapsulated particles were dried in a vacuum over for 24 hours.

5.2.6 Encapsulation of the Core Material at Low Temperature

Potassium chloride (250–355 μm) was encapsulated at −12°C and 0°C using styrene monomer. The same procedure described above was applied except that tumbling the sample bottles to achieve adsorption of surfactant, activation and polymerization was carried out inside a cold cabinet.

5.2.7 Encapsulation of the Core Materials without Adsorbing a Surfactant Layer onto Their Surfaces

Encapsulation of the drugs was carried out with the monomers, without adsorption of surfactant, to investigate if the surfactant is essential in the encapsulation

process. In this case the catalyst solution was added directly to the drug powder, tumbled for two hours and the supernatant was sucked off as described previously and followed by injecting the required monomer solution and the procedure was completed as described previously.

5.3 Results

5.3.1 Encapsulation of Potassium Chloride with Polystyrene

- KCl of average particle size 250-300 μm was encapsulated with polystyrene at three different temperatures. The data are given in Tables 1-3.

Table 5.1 Encapsulation of KCl using styrene (conc. 10.86×10^{-3} g/ml) at -12°C

Weight of KCl (g)	Weight of Polymer (g)	Weight of Polymer per gram KCl (g)	Polymer %
3.18628	0.12703	0.0399	3.83
3.98372	0.16142	0.0405	3.89
4.26815	0.14635	0.0343	3.31
4.28634	0.16894	0.0394	3.79
4.54309	0.17239	0.0379	3.65
4.59991	0.17682	0.0384	3.70
Standard deviation (σ_{n-1})		2.2×10^{-3}	0.21
Mean ($\bar{x}$)		0.0384	3.69
Number of data (n)		6	6

Table 5.2 : Encapsulation of KCl using styrene (conc. 10.86×10^{-3} g/ml) at 0°C

Weight of KCl (g)	Weight of Polymer (g)	Weight of Polymer per gram KCl (g)	Polymer %
3.52369	0.04247	0.01205	1.19
4.26946	0.05245	0.01228	1.21
5.09907	0.06928	0.01359	1.34
5.18757	0.07128	0.01374	1.35
5.35433	0.08536	0.01594	1.57
6.42045	0.10729	0.01671	1.64
Standard deviation (σ_{n-1})	1.90×10^{-3}	0.18	
Mean ($\bar{x}$)	0.01405	1.38	
Number of data (n)	6.0	6.0	

Table 5.3 Encapsulation of KCl using styrene (conc. 3.62×10^{-3} g/ml) at room temperature

Weight of KCl (g)	Weight of Polymer (g) x 10^3	Weight of Polymer gram KCl (g) x 10^3	Polymer %
3.99959	4.52	1.13	0.11
3.99980	4.08	1.02	0.10
4.00008	5.18	1.29	0.13
4.00018	4.95	1.24	0.12
4.00057	5.68	1.42	0.14
4.00058	5.65	1.41	0.14
Standard deviation (σ_{n-1})		1.6×10^{-4}	0.016
Mean ($\bar{x}$)		1.25×10^{-3}	0.12
Number of data (n)		6.0	6.0

- KCl of average particle size of 500–600 μm was encapsulated with polystyrene without surfactant adsorption onto the particles. The encapsulation was carried out at room temperature and data are given in Table 5.4.

Table 5.4 : Encapsulation of KCl (500–600 μm) using styrene (conc. 3.62×10^{-3} g/ml), no surfactant, at room temperature

Weight of KCl (g)	Weight of Polymer (g) x 10^3	Weight of Polymer gram KCl (g) x 10^4	Polymer %
4.10923	3.81	9.3	0.09
4.70425	3.64	7.7	0.08
4.99208	3.87	7.7	0.08
5.08235	4.50	8.8	0.09
5.28929	7.91	14.9	0.15
5.53787	4.92	8.9	0.09
Standard deviation (σ_{n-1})		2.7×10^{-4}	0.027
Mean ($\bar{x}$)		9.6×10^{-4}	0.09
Number of data (n)		6.0	6.0

5.3.2 Encapsulation of Potassium Chloride with C1 Polymer

Three different particle sizes of KCl were encapsulated with C1 polymer at room temperature. The data are given in Tables 5.5 - 5.7. Table 8 presents the data of KCl encapsulated without surfactant adsorption.

Table 5.5 Encapsulation of KCl (250–355 μm) using C1 monomer (concentration 3.75 x 10^{-3} g/ml)

Weight of KCl (g)	Weight of Polymer (g)	Weight of Polymer gram KCl (g) x 10^3	Polymer %
3.99731	0.02099	5.25	0.52
3.99883	0.02259	5.65	0.56
3.99994	0.02489	6.22	0.62
4.00004	0.04012	10.03	0.99
4.00014	0.02829	7.07	0.70
4.00019	0.03218	8.04	0.80
4.00029	0.03696	9.24	0.91
4.00035	0.03927	9.82	0.97
Standard deviation (σ_{n-1})		1.90×10^{-3}	0.18
Mean ($\bar{x}$)		7.66×10^{-3}	0.76
Number of data (n)		8.0	8.0

Table 5.6 Encapsulation of KCl (500–600 μm) using C1 monomer (conc. 3.75 x 10^{-3} g/ml)

Weight of KCl (g)	Weight of Polymer (g)	Weight of Polymer gram KCl (g) x 10^3	Polymer %
4.91034	0.01266	2.58	0.26
5.11056	0.01281	2.51	0.25
5.57643	0.01478	2.65	0.26
5.78900	0.01411	2.44	0.24
6.74162	0.01439	2.13	0.21
7.13018	0.01562	2.19	0.22
Standard deviation (σ_{n-1})		2.12×10^{-4}	0.02
Mean ($\bar{x}$)		2.42×10^{-3}	0.24
Number of data (n)		6.0	6.0

Table 5.7 Encapsulation of KCl (710–800 μm) using C1 monomer (conc. 3.75×10^{-3} g/ml)

Weight of KCl (g)	Weight of Polymer (g)	Weight of Polymer gram KCl (g) $\times 10^3$	Polymer %
5.12917	0.01484	2.89	0.29
5.46500	0.01380	2.52	0.25
5.80356	0.01301	2.24	0.22
6.07886	0.01307	2.15	0.21
6.11156	0.01129	1.85	0.18
7.00623	0.01418	2.02	0.20
Standard deviation (σ_{n-1})		3.7×10^{-4}	0.04
Mean ($\bar{x}$)		2.27×10^{-3}	0.22
Number of data (n)		6.0	6.0

Table 5.8 Encapsulation of KCl (500–600 μm) using C1 monomer (conc. 3.75×10^3 g/ml) without surfactant

Weight of KCl (g)	Weight of Polymer (g)	Weight of Polymer gram KCl (g) $\times 10^3$	Polymer %
4.58231	0.01120	2.44	0.24
5.10342	0.01109	2.17	0.22
5.53787	0.01140	2.06	0.20
5.88706	0.01195	2.03	0.20
6.94185	0.01219	1.76	0.17
7.12340	0.01241	1.74	0.17
Standard deviation (σ_{n-1})		2.63×10^{-4}	0.028
Mean ($\bar{x}$)		2.03×10^{-3}	0.20
Number of data (n)		6.0	6.0

5.3.3 Encapsulation of Potassium Chloride with GMA Polymer

– KCl (250–355 μm) was encapsulated with GMA polymer at room temperature. The encapsulation of KCl (500–600 μm) was carried out without adsorbing surfactant layer onto the core particles. Data are presented in Table 5.9 and 5.10 respectively.

Table 5.9 Encapsulation of KCl (250–355 μm) with GMA polymer (monomer conc. 6.95×10^{-3} g/ml)

Weight of KCl (g)	Weight of Polymer (g)	Weight of Polymer per gram KCl (g)	Polymer %
3.99963	0.05524	0.0138	1.36
3.99973	0.07910	0.0197	1.94
4.00083	0.10264	0.0256	2.50
4.00461	0.07469	0.0186	1.83
4.00589	0.10433	0.0260	2.54
4.00718	0.0556	0.0139	1.37
Standard deviation (σ_{n-1})		5.37×10^{-3}	0.52
Mean ($\bar{x}$)		0.0196	1.92
Number of data		6.0	6.0

Table 5.10 Encapsulation of KCl (500–600 μm) with GMA polymer (monomer conc. 6.95×10^{-3} g/ml), no surfactant

Weight of KCl (g)	Weight of Polymer (g)	Weight of Polymer per gram KCl (g)	Polymer %
3.53620	0.04652	0.0131	1.30
4.26715	0.04895	0.0115	1.31
4.87958	0.07537	0.0154	1.52
4.96725	0.05134	0.0103	1.02
5.04832	0.07986	0.0158	1.56
5.32491	0.05968	0.0112	1.11
Standard deviation (σ_{n-1})		2.29×10^{-3}	0.23
Mean ($\bar{x}$)		0.0129	1.27
Number of data		6.0	6.0

5.3.4 Encapsulation of Potassium Chloride with Epikote 828 Polymer

KCl (250–355 μm) was encapsulated with Epikote 828 polymer at room temperature. The encapsulation was carried out onto KCl (710–800 μm) without preadsorption of surfactant (α–monoolein) onto the particles. Typical data are given in Tables 5.11 and 5.12.

Table 5.11 Encapsulation of KCl (250–355 μm) with Epikote 828 polymer (monomer conc. 5.91 x 10^{-3} g/ml)

Weight of KCl (g)	Weight of Polymer (g)	Weight of Polymer per gram KCl (g)	Polymer %
3.07350	0.04886	0.016	1.56
3.94242	0.05638	0.014	1.41
4.00024	0.07357	0.018	1.81
4.00030	0.07118	0.018	1.75
4.00050	0.05350	0.013	1.32
4.00098	0.05305	0.013	1.31
4.00170	0.04821	0.012	1.19
4.16846	0.06669	0.016	1.57
Standard deviation (σ_{n-1})		2.3×10^{-3}	0.22
Mean ($\bar{x}$)		0.015	1.49
Number of data (n)		8.0	8.0

Table 5.12 Encapsulation of KCl (710 – 800 μm) with Epikote 828 polymer (monomer conc. 5.91 x 10^{-3} g/ml), no surfactant

Weight of KCl (g)	Weight of Polymer (g)	Weight of Polymer per gram KCl (g)	Polymer %
3.76890	0.02015	5.35	0.53
4.56921	0.02501	5.47	0.54
4.96800	0.02820	5.68	0.56
5.32518	0.02612	4.90	0.49
6.41050	0.03766	5.87	0.58
6.49271	0.02465	3.79	0.39
Standard deviation (σ_{n-1})		7.5×10^{-4}	0.068
Mean ($\bar{x}$)		5.20×10^{-3}	0.51
Number of data (n)		6.0	6.0

5.3.5 Encapsulation of β–Estradiol with Polystyrene

Encapsulation of β–estradiol was performed at room temperature. The data are given in Table 5.13.

Table 5.13 Encapsulation of β–estradiol with polystyrene (monomer conc. 10.86×10^{-3} g/ml)

Weight of β-estradiol (g)	Weight of Polymer (g)	Weight of Polymer per gram β-estradiol (g)	Polymer %
0.30114	0.02729	0.0906	8.31
0.34130	0.03972	0.1164	10.42
0.34914	0.04466	0.1279	11.34
0.35666	0.03778	0.1059	9.58
0.39842	0.03903	0.0979	8.92
0.44306	0.04564	0.1030	9.34
Standard deviation (σ_{n-1})		0.0134	1.08
Mean ($\bar{x}$)		0.1069	9.65
Number of data (n)		6.0	6.0

5.3.6 Encapsulation of β–Estradiol with C1 Polymer

The encapsulation was carried out at room temperature with and without adsorption of α–monoolein surfactant into crystal surfaces. Data are presented in Tables 5.14 and 5.15 respectively.

Table 5.14 Encapsulation of β–estradiol with C1 polymers (monomer conc. 3.75×10^{-3} g/ml)

Weight of β-estradiol (g)	Weight of Polymer (g)	Weight of Polymer per gram β-estradiol (g)	Polymer %
0.23655	0.05107	0.2159	17.76
0.24820	0.04210	0.1692	14.50
0.28000	0.04490	0.1603	13.82
0.29485	0.03600	0.1221	10.88
0.32749	0.05416	0.1654	14.19
0.33352	0.05278	0.1582	13.66
0.33385	0.05067	0.1518	13.18
0.37482	0.05711	0.1523	13.22
Standard deviation (σ_{n-1})		0.0261	1.91
Mean ($\bar{x}$)		0.1619	13.90
Number of data (n)		8.0	8.0

Table 5.15 Encapsulation of β-estradiol with C1 polymer (monomer conc. 5.63 x 10^{-3} g/ml)

Weight of β-estradiol (g)	Weight of Polymer (g)	Weight of Polymer per gram β-estradiol (g)	Polymer %
0.23814	0.03055	0.128	11.37
0.29058	0.03298	0.113	10.19
0.37865	0.04813	0.127	11.28
0.40219	0.05128	0.127	11.31
0.59859	0.08298	0.139	12.17
0.66398	0.10182	0.153	13.29
Standard deviation (σ_{n-1})		0.013	1.04
mean ($\bar{x}$)		0.131	11.60
Number of data (n)		6.0	6.0

5.3.7 Encapsulation of β-estradiol with GMA polymer

Encapsulation was performed at room temperature and data obtained are given in Table 5.16.

Table 5.16 Encapsulation of β-estradiol with GMA polymer (monomer conc. 6.95 x 10^{-3} g/ml)

Weight of β-estradiol (g)	Weight of Polymer (g)	Weight of Polymer per gram β-estradiol (g)	Polymer %
0.14546	0.05766	0.396	28.39
0.17317	0.07510	0.434	30.25
0.19452	0.07911	0.407	28.91
0.20218	0.05952	0.294	22.74
0.30043	0.09008	0.299	23.07
0.33468	0.12130	0.362	26.60
Standard deviation (σ_{n-1})		0.058	3.14
Mean ($\bar{x}$)		0.365	26.66
Number of data (n)		6.0	6.0

5.3.8 Encapsulation of β-Estradiol with Epikote 828 Polymer

Encapsulation was performed at room temperature and data are given in Table 5.17.

Table 5.17 Encapsulation of β-estradiol with Epikote polymer (monomer conc. 5.91 x 10^{-3} g/ml)

Weight of β-estradiol (g)	Weight of Polymer (g)	Weight of Polymer per gram β-estradiol (g)	Polymer %
0.33010	0.04230	0.128	11.36
0.35040	0.05792	0.165	14.18
0.38892	0.0476	0.122	10.90
0.39050	0.0497	0.127	11.29
0.44445	0.06595	0.148	12.92
Standard deviation (σ_{n-1})		0.018	1.38
Mean ($\bar{x}$)		0.138	12.13
Number of data (n)		5.0	5.0

5.3.9 Encapsulation of 5-Aminosalicylc Acid with C1 Polymer

Encapsulation with and without pre-adsorption of the surfactant onto the crystals. The encapsulation was carried out at room temperature and data are given in Tables 5.18 and 5.19 respectively.

Table 5.18 Encapsulation of 5-aminosalicylic acid with C1 polymer (monomer conc. 5.63 x 10^{-3} g/ml)

Weight of acid powder (g)	Weight of Polymer (g)	Weight of Polymer per gram of acid (g)	Polymer %
0.22431	0.03262	0.145	12.70
0.31047	0.03945	0.127	11.27
0.36090	0.03779	0.107	9.48
0.42590	0.04871	0.114	10.26
0.52081	0.05371	0.103	9.35
0.99480	0.10871	0.109	9.85
Standard deviation (σ_{n-1})		0.016	1.29
Mean ($\bar{x}$)		0.117	10.48
Number of data (n)		6.0	6.0

Table 5.19 Encapsulation of 5-aminosalicylic acid with C1 polymer (monomer conc. 5.63 x 10^{-3} g/ml), no surfactant

Weight of acid powder (g)	Weight of Polymer (g)	Weight of Polymer per gram of acid (g)	Polymer %
0.52381	0.071932	0.137	12.07
0.58235	0.08052	0.138	12.15
0.79250	0.09250	0.118	10.57
0.82742	0.09327	0.113	10.13
0.95013	0.12773	0.134	11.85
1.17870	0.13052	0.111	9.96
Standard deviation (σ_{n-1})		0.012	1.01
Mean ($\bar{x}$)		0.125	11.12
Number of data (n)		6.0	6.0

5.3.10 Encapsulation of 5-Aminosalicylic Acid wtih GMA Polymer

Encapsulation was performed at room temperature and typical data are given in Table 5.20.

Table 5.20 : Encapsulation of 5-aminosalicylic acid with GMA polymer (monomer conc. 6.25×10^{-3} g/ml)

Weight of acid powder (g)	Weight of Polymer (g)	Weight of Polymer per gram of acid (g)	Polymer %
0.31638	0.03521	0.111	10.01
0.35065	0.07586	0.216	17.80
0.36073	0.06855	0.122	10.90
0.36104	0.0491	0.136	11.97
0.44139	0.0415	0.096	8.59
0.45567	0.08702	0.191	16.00
Standard deviation (σ_{n-1})		0.048	3.59
Mean ($\bar{x}$)		0.145	12.54
Number of data (n)		6.0	6.0

5.4 Discussion

The main goal of using the technique described therein was to achieve individual microencapsulation of each particle of the three biologically active drugs chosen for this study in a polymer membrane of minimum thickness which would control their release.

The microencapsulation was achieved by cationic polymerization initiated by addition of a proton and polymerized by a carbonium ion addition process. The mechanism can be speculated as follows:

Activation of the drug surface by boron trifluoride diethyl etherate complex

The activation step can be speculated in two ways concerning the condition of the drug surface:

1. In presence of α-monoolein

Though it is possible to propose the partial ionization of born trifluoride etherate as below

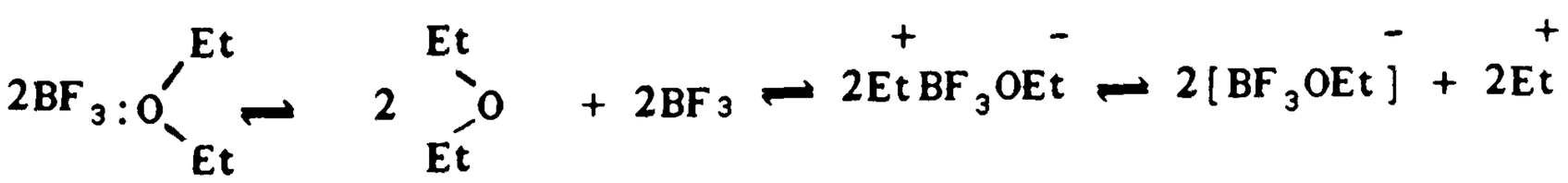

it is very improbable and, in the presence of the hydroxyls of α-monoolein, the following mechanism involving one or both of the hydroxyls to generate the proton for initiation is likely.

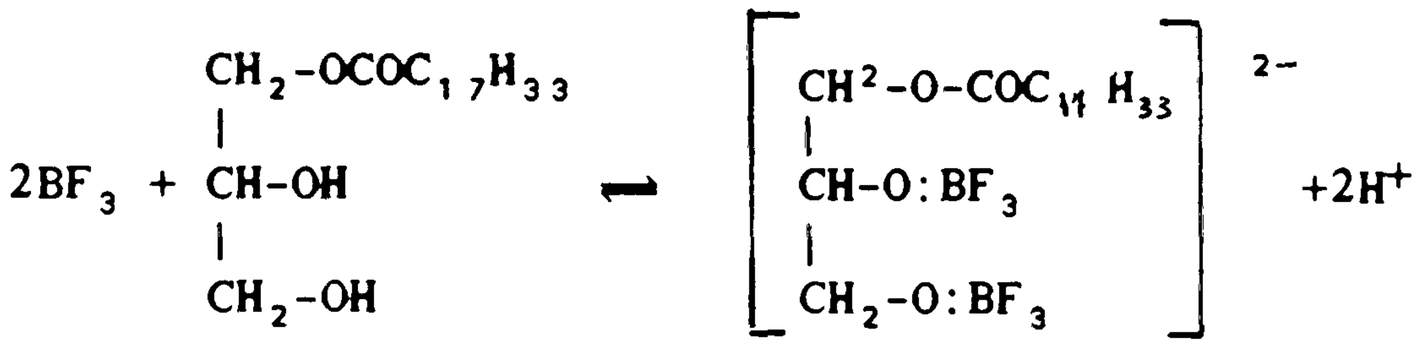

The proton will itself become solvated by the hydroxyls or ether present. In the system as used it is probable that trace amounts of residual water are present which may themselves interact with boron trifluoride to form protons as shown below.

2. <u>In absence of α-monoolein</u>

It is likely that in the presence of trace quantities of water

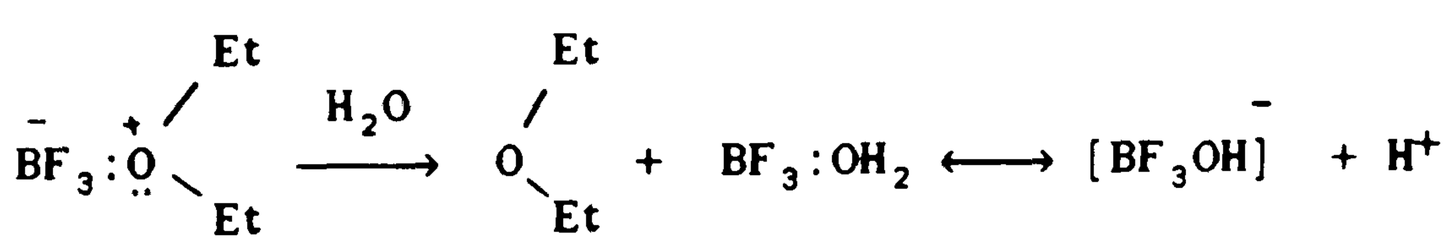

boron trifluoride etherate can form the two acids $[BF_3OEt]H^+$ and $[BF_3OH]H^+$, both of which can provide a source of protons for polymerization initiation.

<u>Initiation of monomers</u>

Representation of the various polymerization processes most likely to be involved are given below

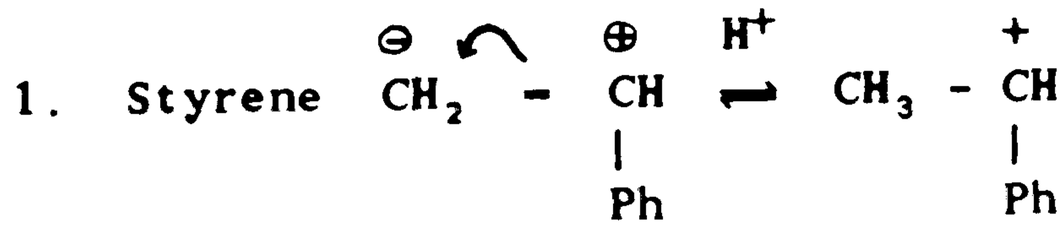

2. Cl monomer

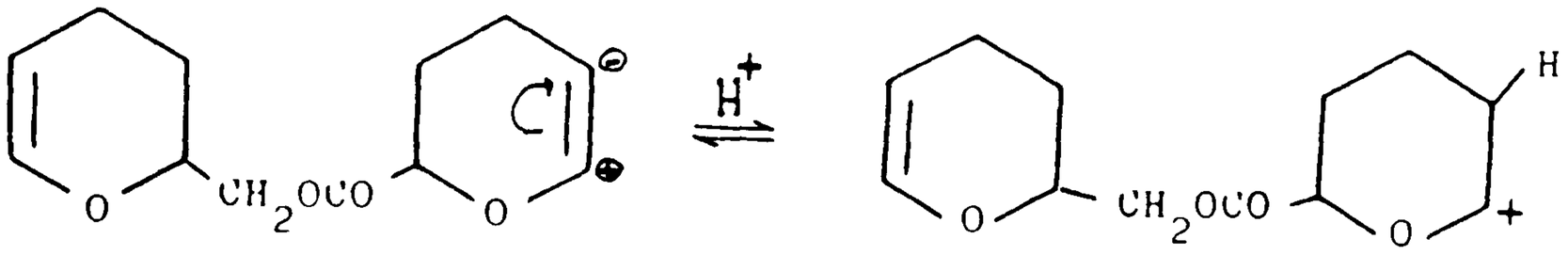

3. GMA monomer

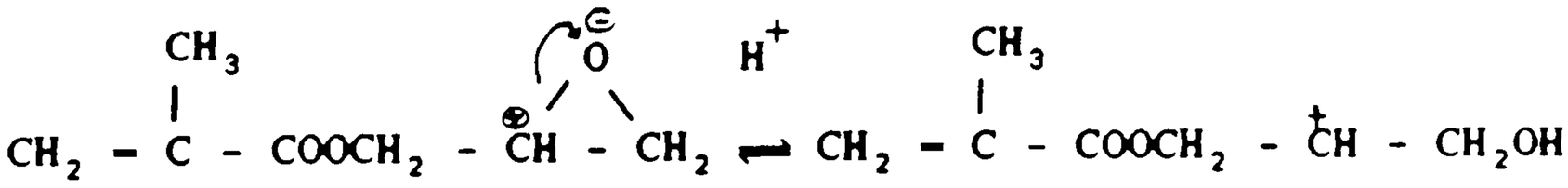

4. Epikote 828

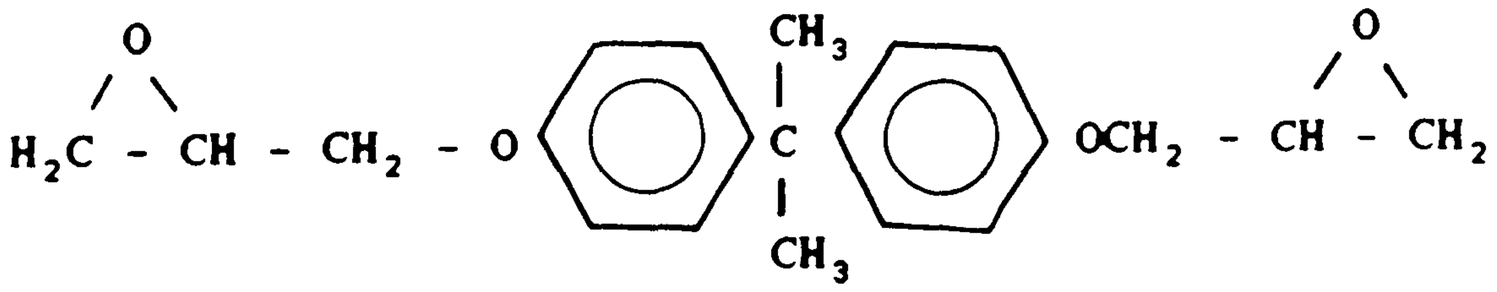

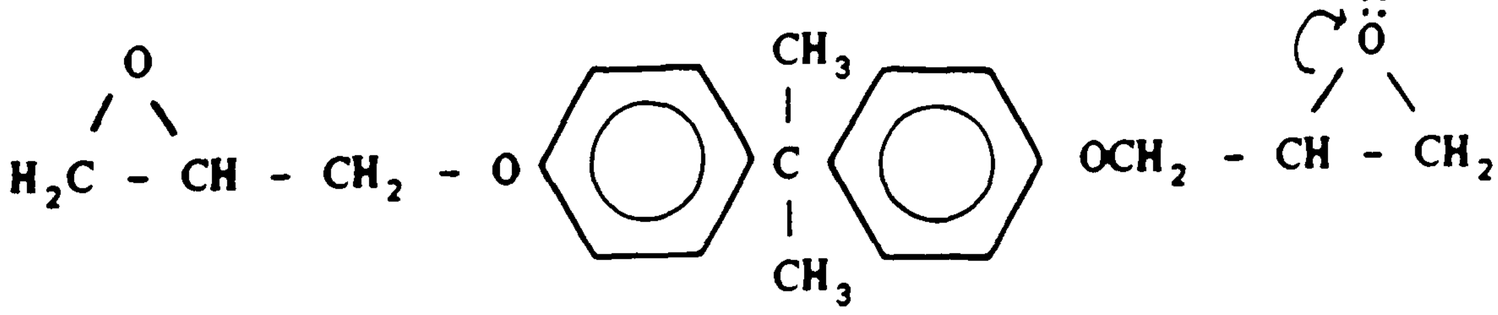

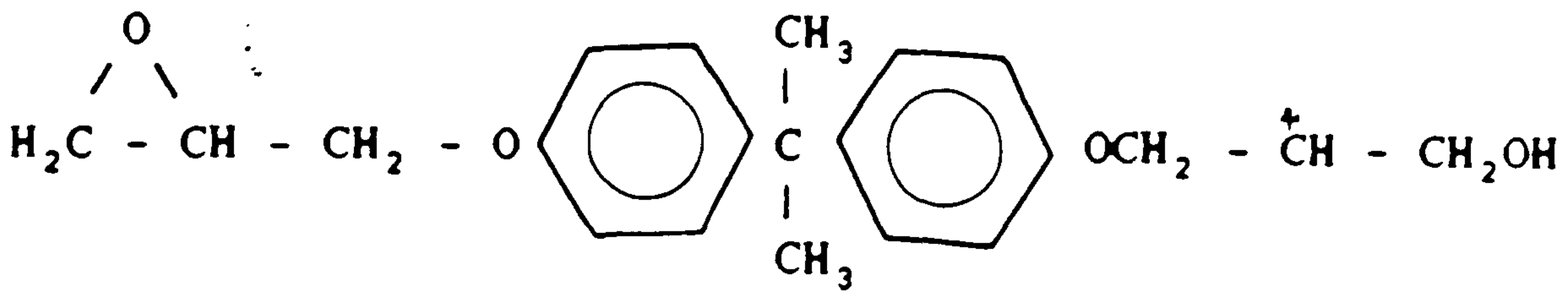

Propagation

Styrene

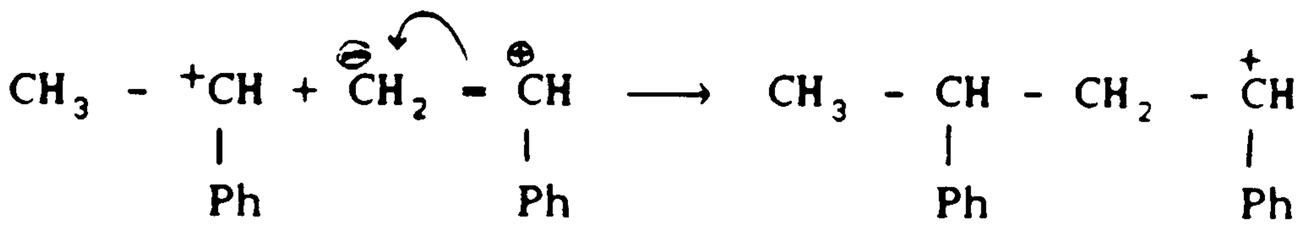

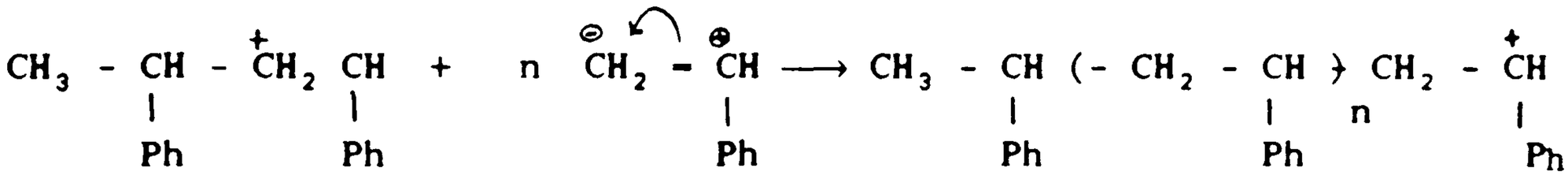

C1:

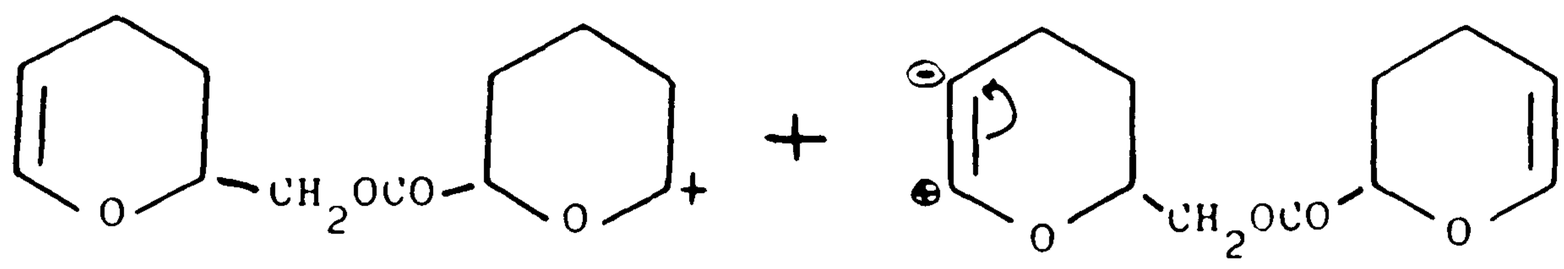

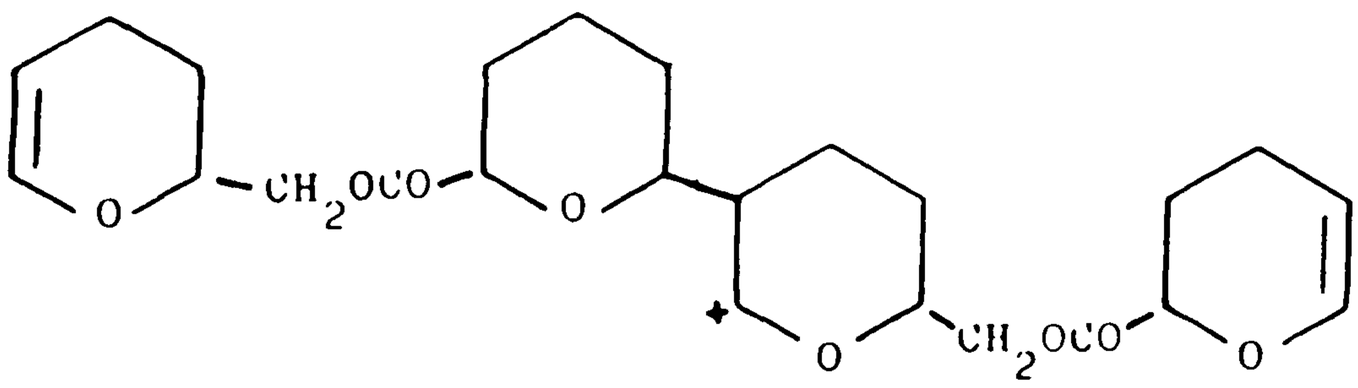

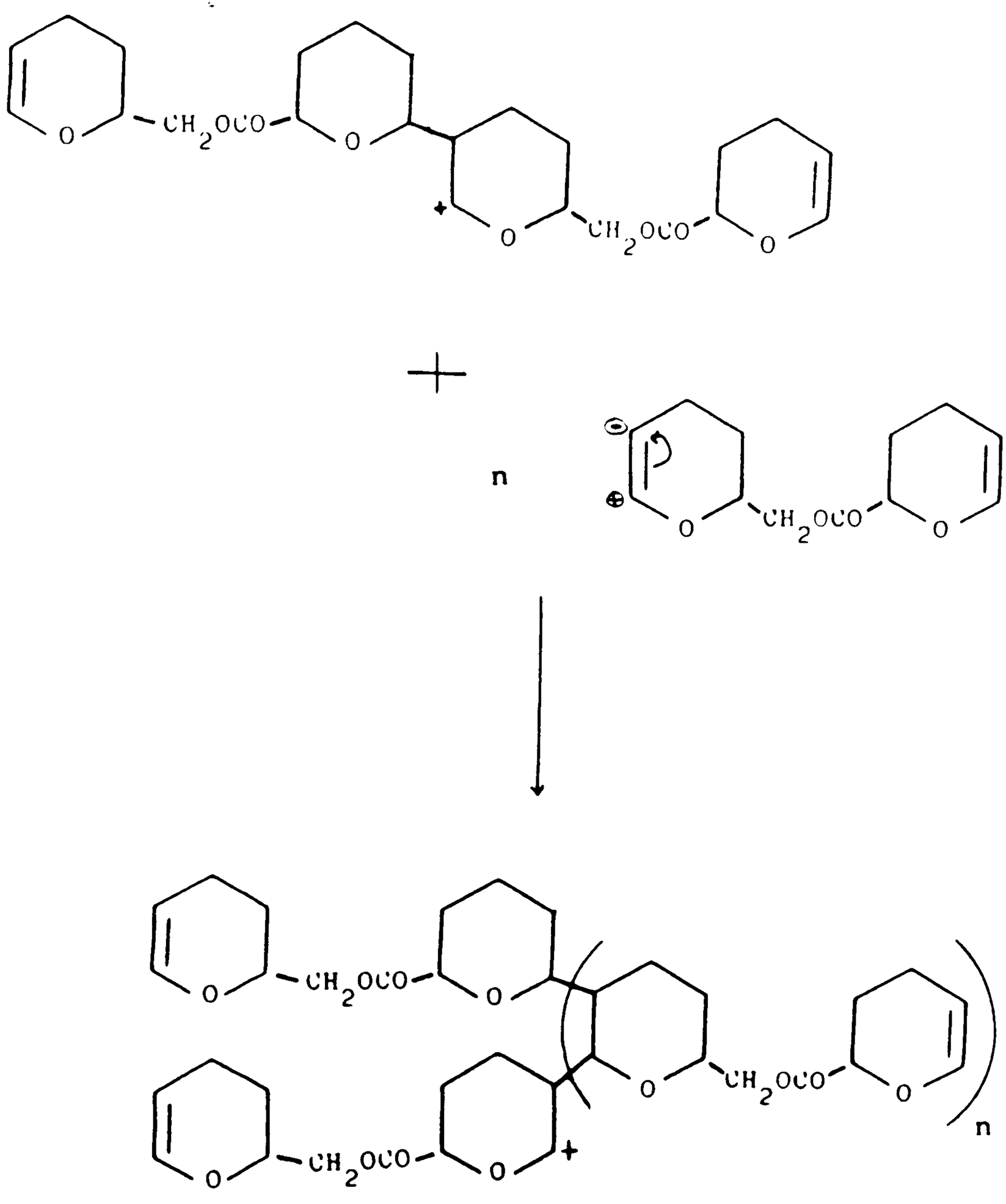

Polymerization is represented here as involving only one double bond and gives a linear polymer. This is for simplicity of representation and is most unlikely. Both double bonds will polymerize to produce a crosslinked polymer.

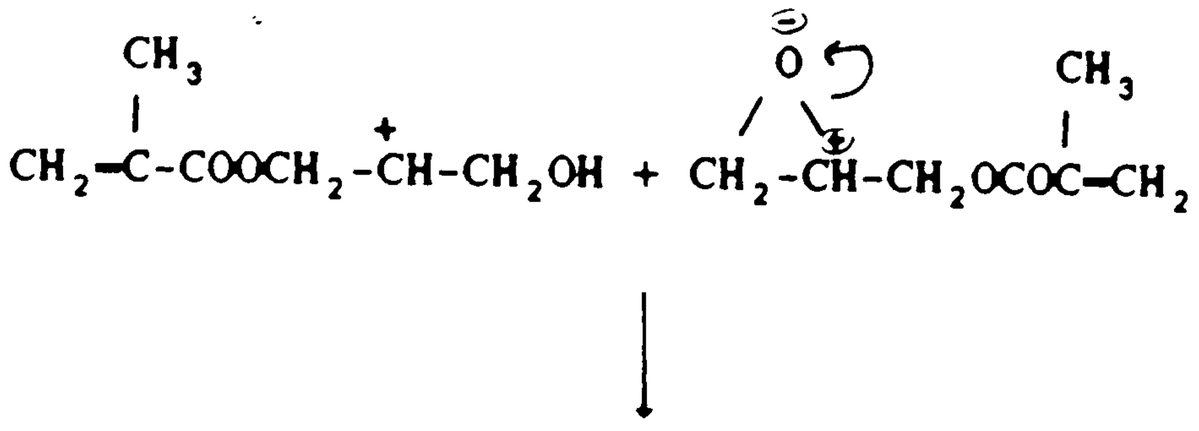

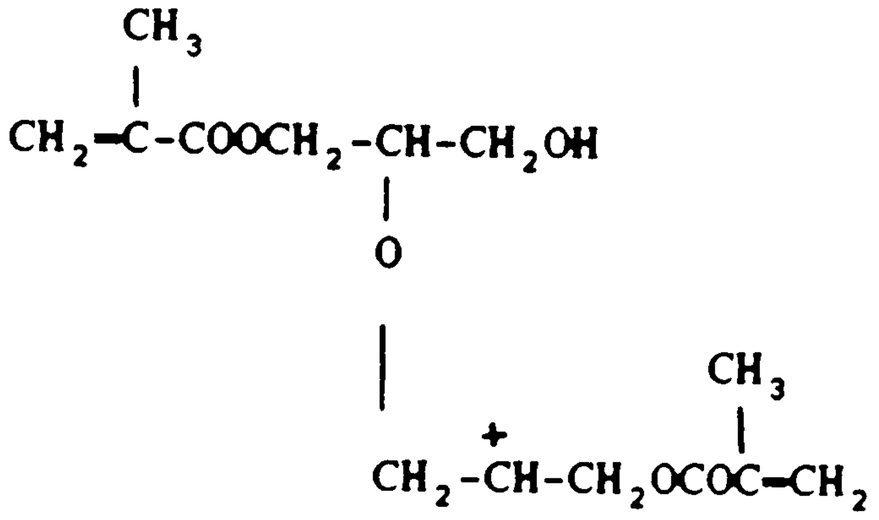

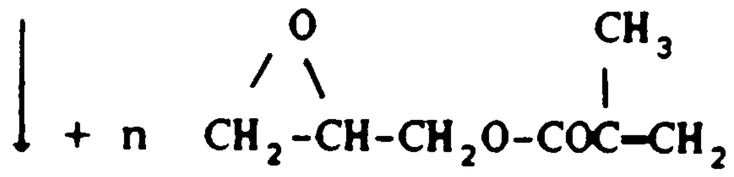

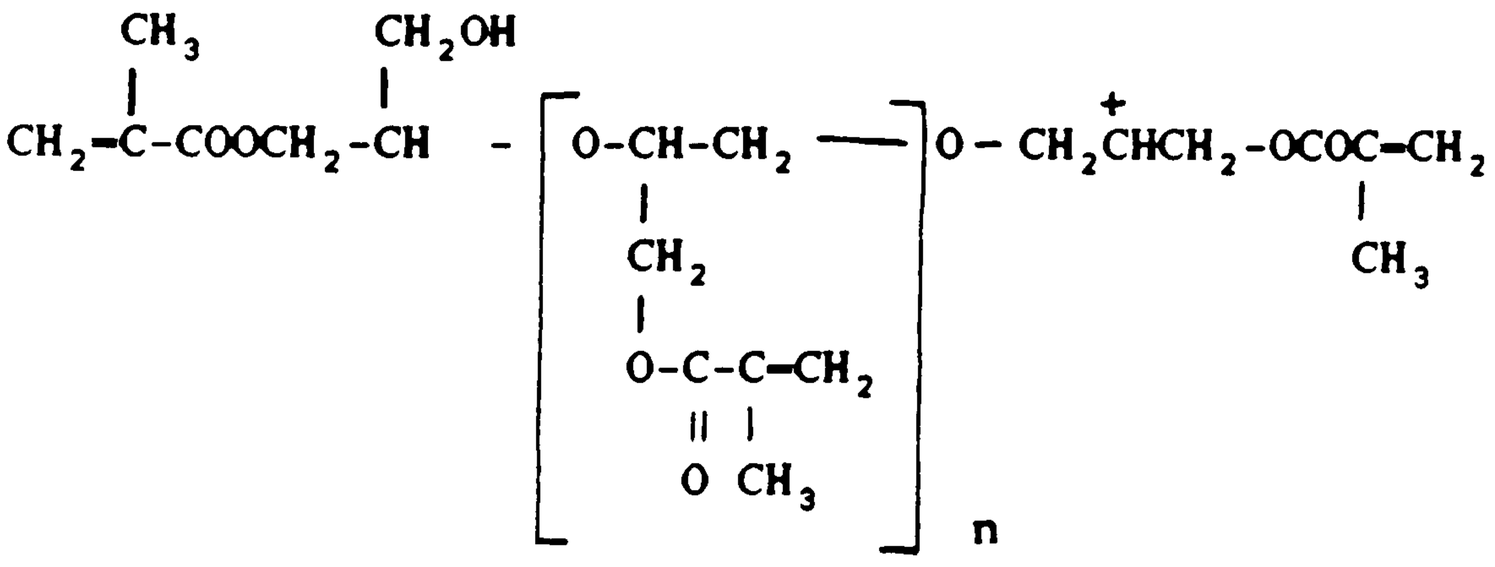

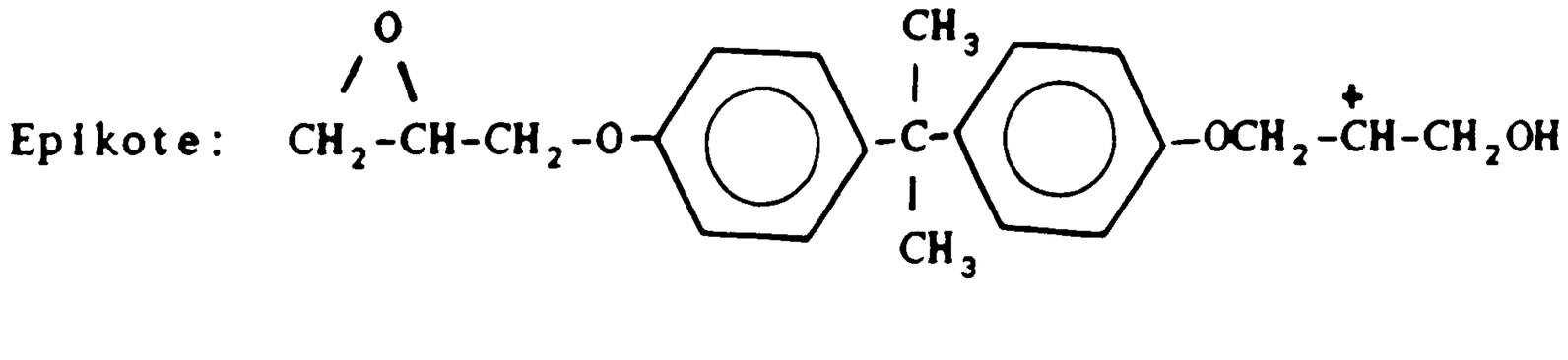

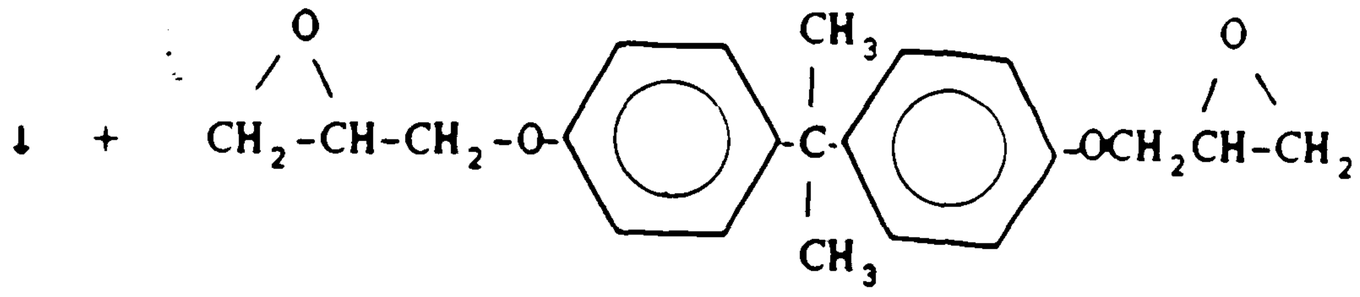

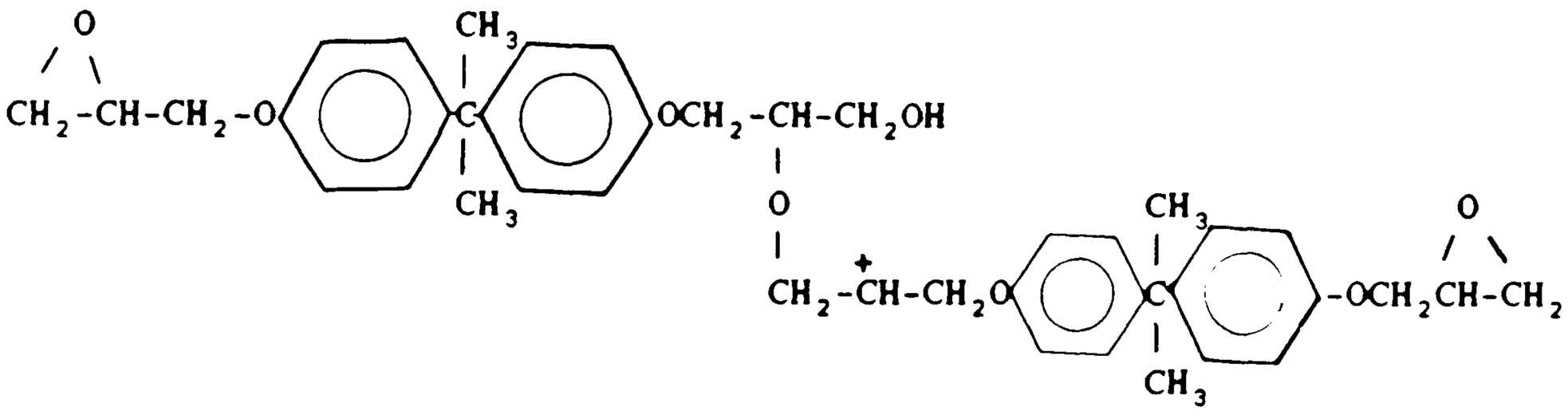

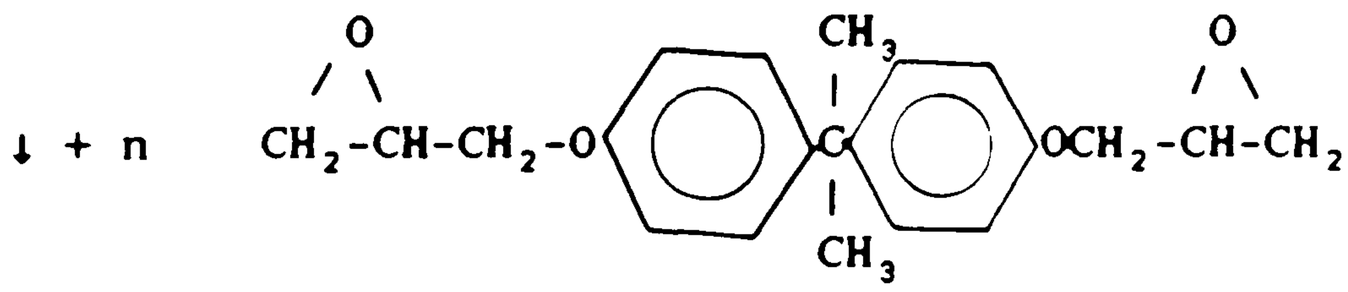

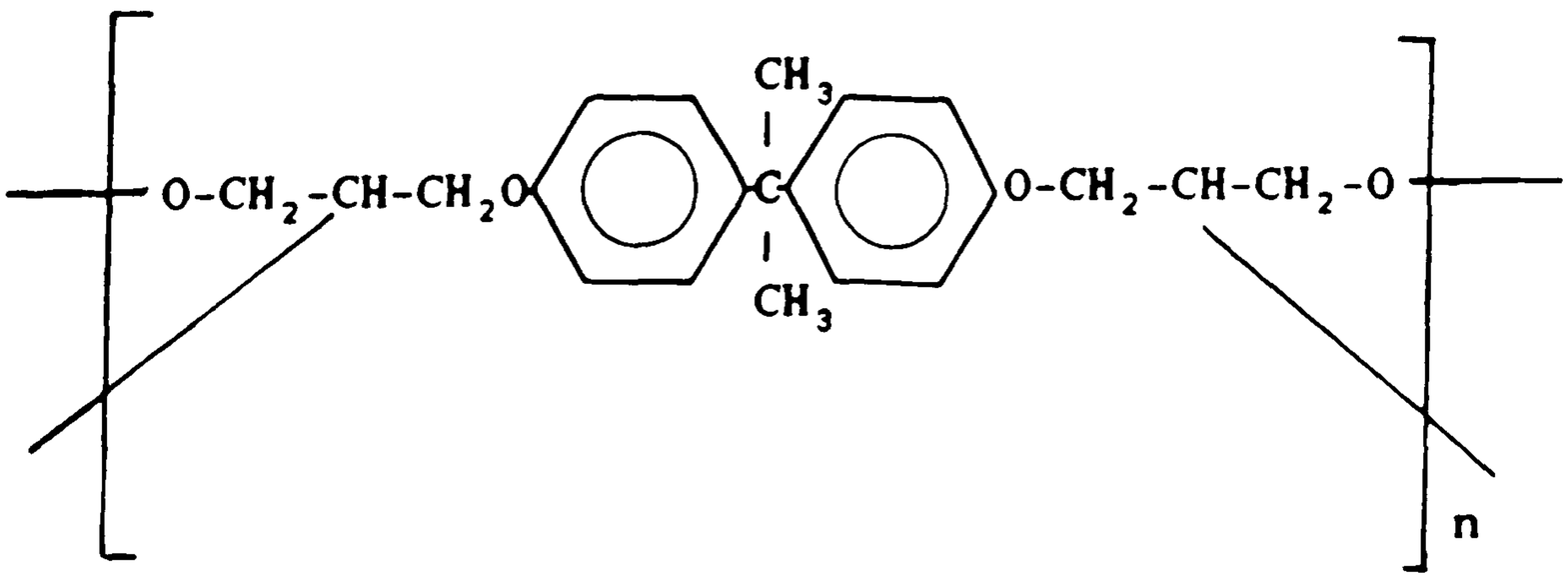
n

The two epoxy groups will polymerize to give a crosslinked polymer.

Termination

Termination probably took place by usual mechanism of elimination of H^+ or carbon cation or by transfer to monomer which would effectively start a new chain.

The counter ions $[BF_3OEt]^-$ and $[BF_3OH]^-$ can not form a co–ordinate bond with the carbonium ion, and proton abstraction from the latter could be the operative termination.

The transfer to monomer, elimination of a proton to a base, ether or α–monoolein would give a terminal double bond.

The yield of different polymers obtained on the different drugs were calculated gravimetrically from the weight difference of the drug powder before and after encapsulation.

From Tables 5.1–5.4 the standard deviation (σ_{n-1}) of the weight of polystyrene per gram KCl and that of the polymer percentage show a good correlation between the surface polymerization on the crystals and the weight of KCl used in each case.

The arithmetic mean ($\bar{x}$) of each set of data in the above mentioned tables shows a marked dependence of the polymer percentage on the temperature at which microencapsulation was carried out and also on the particle size of the core

material. For KCl of the same particle size (250–355), as the microencapsulation process decreases, the $\bar{x}$ of the polymer percentage increases. This is logical for styrene monomer which is well known to polymerize more rapidly cationically at lower temperatures. The mean values ($\bar{x}$) of the polystyrene % polymerized at −12°C, 0°C and room temperature are 3.69, 1.38 and 0.12 respectively.

Increasing the particle size from 250 to 500 μm decreased the $\bar{x}$ value of the polymer % from 0.12 to 0.09 due to the decrease in surface area. This also was observed with C1 polymer using KCl of different particle sizes. The polymer % was on the average 0.76, 0.24 and 0.2 for the particle sizes 250, 500 and 710 mm respectively.

The C1 polymer is useful for microencapsulation because it is crosslinked and potentially biodegradable whereas polystyrene is potentially useful to encapsulate pharmaceutical drugs to control their release because it is chemically inert.

GMA polymer was used, in part, for encapsulation in this study because it provides a rubbery coating to avoid osmotic rupture of the capsule as was noticed with polystyrene. The polymer yield was more than that obtained from polystyrene and C1 polymer coating. The polymer % averaged 1.92 and 1.27 for KCl of particle size 250 and 500 μm, respectively.

Epikote 828 coating provided yield % values of 1.49 and 0.51 for KCl of the average particle sizes 250 and 710 μm respectively, with a good correlation between the surface area and the polymer yield.

β–Estradiol was encapsulated using the four previously mentioned polymers. A marked increase of the polymer yield in each case was observed from the data presented in Tables 5.13–5.17. The increase in yield is attributed to the larger surface area provided by β–estradiol (3.14 m^2/g) compared to 0.073 m^2/g for KCl of particle size 250–355μm. The mean values of yield % on β–estradiol coated with polystyrene, Cl, GMA and Epikote polymers were 9.65, 13.9, 26.66 and 12.13 respectively.

For 5–Aminosalicylic acid encapsulated with C1 and GMA polymers, the polymer yields were higher than in case of KCl but lower than those with β–estradiol. This is because the surface area of 5–aminosalicylic acid (1.69 m^2/g) is larger than that of KCl but smaller than that of β–estradiol. The average polymer % was 10.48, 11.12 and 12.54 for C1 polymer, C1 polymer without surfactant and GMA polymer, respectively. It was observed that the particles of 5–aminosalicylic acid were coagulating together, forming balls of many crystals adhered together in the reaction medium during the encapsulation process. In such case the actual surface area of the core used was not totally exposed to the reaction medium. This would result in a lower yield than what would be expected.

Evaluation of the nature of the different coatings of the different core materials will be discussed in the following chapters.

5.5 References

1. Graham, N.B., Amer, L.I. and (in part) Rashid, A. "Surface polymerization as an encapsulation technique", International Symposium on Microencapsulation, Glagow, April (1990)
2. Jay, A.W.I., Edwards, M.A., Can. J. Physiol. Pharm., 46, 731, (1968)
3. Balla, K., Vasudenuan, P. J. Pharm. Sci., 71, 960, (1982)
4. Hub, H.H., Hupfer, B., Koch, H. and Ringsdorf, H. J. Macromol. Sci., Chem. A15, 701 (1981)
5. Bader, H. and Ringsdorf, H. J. Polym. Sci., 20, 1623-1628 (1982)
6. Ringsdorf, H., Schlarb, B. and Venzmer, J. Angew. Chem. Int. Ed. Engl. 27, 113-158 (1988)
7. Wu, J., Harwell, J.H. and O'Rear, E.A., Langmuir, 3, 531-537 (1987)
8. Wu, J., Harwell, J.H. & O'Rear, E.A., J. Phys. Chem., 91, 623-634, (1987)
9. Graham, N.B., Rashid, A. and Reo, K.P., UK Patent 2112730B (1985)
10. "Some aspects of surface chemistry, microencapsulation and In vitro evaluation of β-estradiol from an injectable formulation" MSc Thesis by Abdul Rashid, University of Strathclyde (1980)
11. The Chemistry of Cationic Polymerization, Plesch, P.H., (1963)
12. Schildknecht, C.E., Zoss, A.O. and Grosser, F., Industrial Engineering Chem., 41, No. 12 (1949)
13. Kennedy, J.P., J. Polym. Sci., 38, No. 133 (1959)
14. Coombes, J.D. and Eley, D.D., J. Chem. Soc. Part III, 3700-3707 (1957)
15. Graham, N.B., International Symposium on cationic polymerisation, Rouen, Sept., 1973, C13
16. Graham, N.B., 9th International Symposium on controlled release of bioactive materials, Florida, (16-20), July (1982).

CHAPTER VI

Chemistry and Characterization of the Polymer Membranes

Chapter VI

Chemistry and Characterization of the Polymer Membranes

6.1 Introduction

A very wide range of analytical techniques can be used to characterize polymeric materials. Many of these are basically similar to those used in the analysis of low-molecular weight organic compounds providing appropriate modification can be made to ensure solubility or availability of sites for reaction. Functional group and elemental analyses are generally applicable to polymers as are many other standard analytical techniques[1]. The degradation of polymers provides additional methods of analysis. Mass spectrometry[2] allows the structure of low-molecular weight species to be inferred, and coupled with gas chromatography[3], it provides information about the number, nature and amounts of the components present. Infrared (IR) spectroscopy is one of the most informative techniques in the study of the chemical and physical nature of polymers. In many polymer applications and particularly in the case of organic films, it is important to devise methods[4-7] which enable the infrared spectrum of the surface to be determined without interference from the bulk of the sample. Raman and nuclear magnetic resonance (NMR) are also common spectroscopic techniques used in polymer characterization. All of these techniques can distinguish specific chemical groups in a complex system. Raman may be used on small particles and inclusions much more easily than IR, but IR and in particular FTIR has advantages[8-9] of sensitivity precision and superior data collection which enable the average of multiple scans to be made and to manipulate the spectral data as required. NMR also gives local information, on a very fine scale, about the environment of the atoms investigated. The molecular weight distribution of the polymer is an

important characteristic to be determined, unless the material is a thermoset or elastomer with infinite molecular weight. The molecular weight distribution can be determined by a range of solution methods of physical chemistry such as viscometry, osmometry, light scattering and size exclusion chromatography. Chemical and physical characterization[10-12] methods overlap in polymer fields, NMR of solid samples can determine the mobility of atoms in various regions and the orientation of molecules. Infrared and Raman are also sensitive to orientation and crystallinity of the sample. Differential scanning calorimetry (DSC) can be used to record the temperature and energies involved in processes such as crystallization, glass transition, melting, solid phase transitions, chemical reactions and degradations or vaporisations.

The purpose of this chapter is to present the of the different polymer layers which were formed on the surfaces of different drug powders.

Potassium chloride is a very water soluble drug which can be easily released leaving the empty shells of polymers which were subsequently analyzed. Soluble polymers can be analyzed by many more techniques than crosslinked ones.

6.2 Experimental

6.2.1 Polymer membranes (shells)

Potassium chloride encapsulated with the four polymers used in this study namely, polystyrene, C1, GMA and Epikote 828 polymers was totally released leaving the empty shells of the polymers. The shells were washed with plenty of distilled water and collected on a microfilter then transferred into a petri dish and were dried for 24 hours in a vacuum oven. The choice of the analyses of the

different polymers by different techniques was determined by their solubilities.

6.2.2 Techniques and Instruments

1. Gel permeation chromatography (GPC) technique was used to determine the molecular weights and the polydispersities of polystyrene shells formed at different temperatures for both soluble and insoluble fractions.. The GPC system used consisted of RHEODYNE injection valve, 4 x 35 cm, 10 μm PLGEL column (Polymer Labs.), and Waters Associates R401 Differential Refractometer as a detector..

Chloroform was used as a solvent for the polystyrene samples. Tetrahydrofuran (THF) was used as a solvent for polystyrene, samples which were formed in n-decane (reaction medium).

2. The IR absorption spectra of the four monomers (styrene, C1, GMA and Epikote 828) and those of their polymers (shells) were recorded using the Perkin Elmer 397 Infrared, and a Nicolet 20SXB, FTIR spectrophotometer.

The monomers were applied as a thin film between two KBr discs. The polymers shells were milled and dispersed in Nujol and a film was placed between two KBr discs and the spectrum was recorded.

3. The ^{1}H- and ^{13}C-NMR spectra of polystyrene shells formed at different temperatures and those of the soluble polystyrene samples were recorded using a Brucker WM-250 MHz and 62 MHz spectrophotometer, respectively.

Deuterated chloroform was used as a solvent for all the samples. The

^{1}H-NMR spectra of the total extract of polystyrene formed in n-decane was also recorded in $CDCl_3$ solvent.

4. Differential scanning calorimetry was carried out using a Dupont 910 DSC Module in conjunction with a Dupont 9900 computer/thermal analyser. Tested samples of C1 and Epikote polymers were heated at a rate of 10°C/min.

6.3 Results

6.3.1 GPC Analysis

Samples of polystyrene shells formed on KCl crystals at different temperatures and those formed in solutions (soluble polymers) were analyzed by the GPC and data are given in Table 6.1.

Solid polystyrene shells and the soluble polymer formed in n-decane reaction medium were analyzed by GPC using THF as a solvent. The results are given in Table 6.2.

Table 6.2 GPC analysis of polystyrene samples formed in n-decane

Polymer	M_n	M_w	M_z	M_v	M_w/M_n
Polystyrene shells	12.151×10^3	16.451×10^3	21.533×10^3	15.787×10^3	1.34
soluble polystyrene	4.133×10^3	6.979×10^3	10.37×10^3	6.546×10^3	1.69
total polystyrene extract	6.945×10^3	12.905×10^3	21.492×10^3	11.868×10^3	1.86

Table 6.1 GPC Analysis of polystyrene samples

Temperature °C	Solid Polystyrene Shells					Soluble polystyrene formed in the reaction medium				
	Mn	Mw	Mz	Mv	Mw/Mn	Mn	Mw	Mz	Mv	Mw/Mn
Room Temp.	9.099×10^3	1.238×10^4	1.674×10^4	1.187×10^4	1.36	The yield of soluble polymer was too small to be precipitated				
0	1.123×10^3	3.318×10^3	6.587×10^3	2.964×10^3	2.96	6.233×10^2	1.482×10^3	2.405×10^3	1.366×10^3	2.38
-12	1.310×10^3	3.993×10^3	7.617×10^3	3.583×10^3	3.05	1.300×10^3	2.244×10^3	3.060×10^3	2.132×10^3	1.73

6.3.2 The IR and FTIR Analysis

Infrared spectra of the monomers and their polymers, obtained after releasing KCl, were recorded and shown in Figs. 6.1–6.4.

6.3.3 NMR Analysis

Proton magnetic resonance of polystyrene shells formed at different temperatures (room temperature, 0°C and −12°C) and that of the total extract (solid and soluble polymer) were recorded. The ^{1}H-NMR of the soluble polymer formed at −12°C was also recorded. The ^{13}C-NMR spectra of polystyrene shells formed at zero and −12°C and that of the soluble polystyrene formed at −12°C were recorded. The spectra are shown in Figs. 6.5–6.8.

6.3.4 DSC Analysis

The differential thermal change of C1 and Epikote polymers are shown in Figs. 6.9 and 6.10, respectively.

6.4 Discussion

The GPC analysis indicated that polystyrene shells and the soluble polystyrene formed in the reaction medium were polydisperse as $Mn<Mw<Mz$ for each (Table 6.1). The molecular weights of the solid polystyrene samples formed on the drug surface were higher than those formed in solution at the three temperatures studied. This may indicate that the polymers formed on the surface came from a different process than those formed in solution i.e. it is not a polymer adsorption after a solution polymerization. It is very unusual that polystyrene shells formed at room temperature, to have higher molecular weight and lower polydispersity than thos formed at lower temperatures (0.0 and −12°C). This may be attributed to

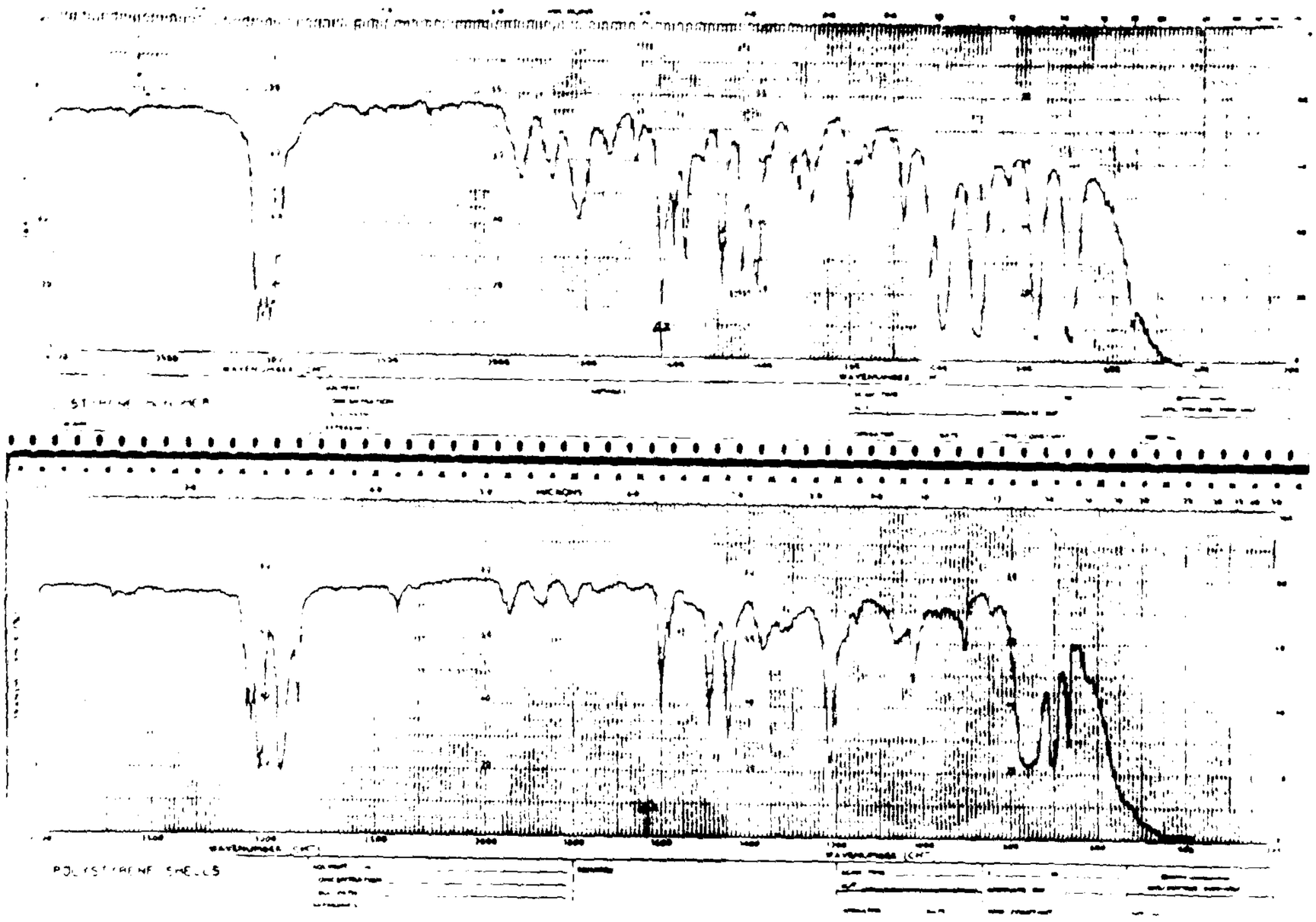

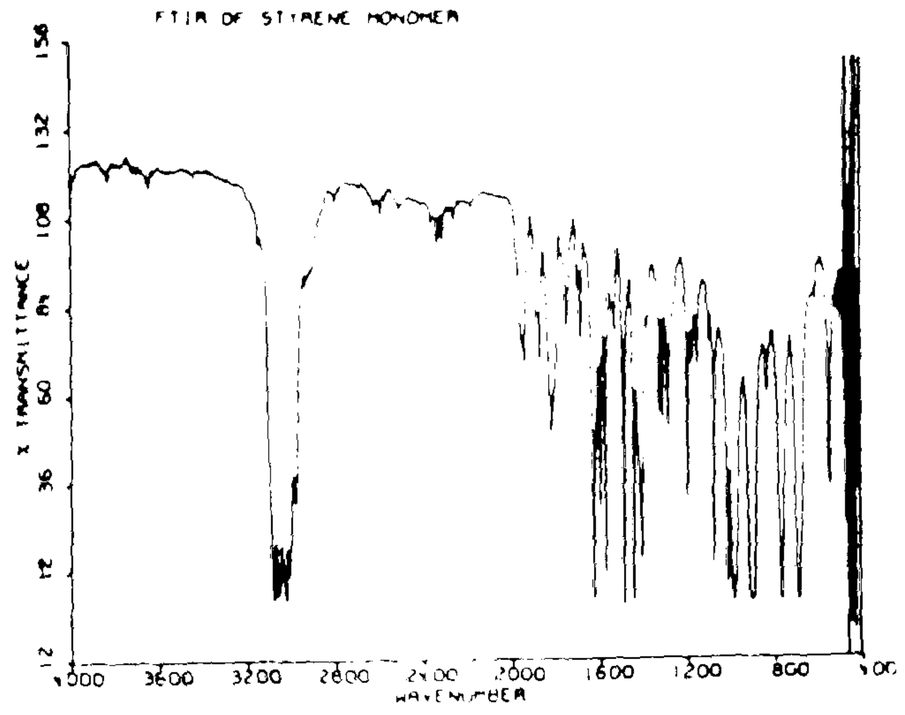

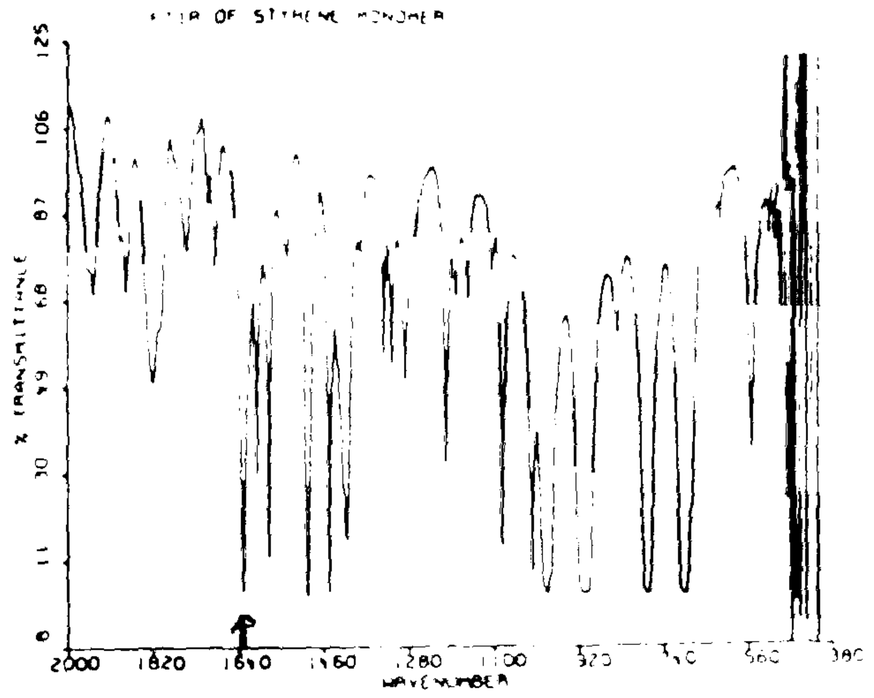

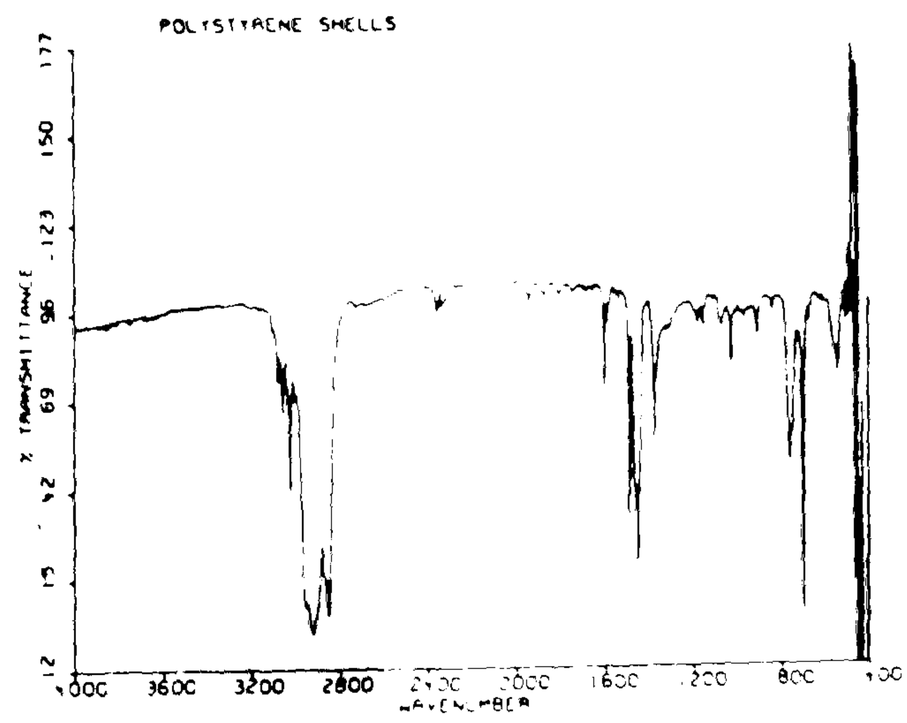

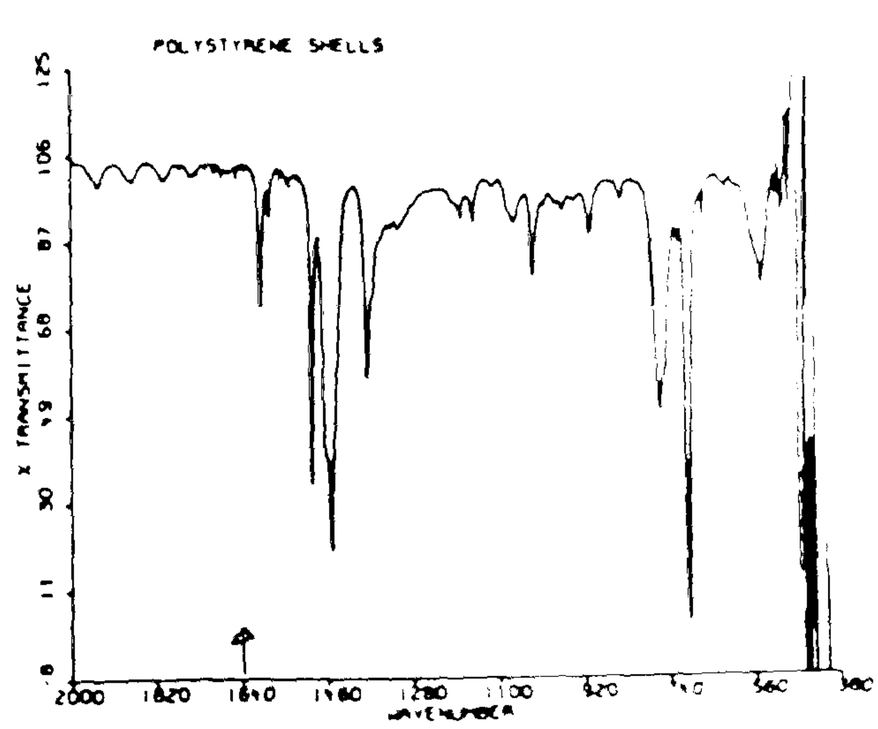

Fig. 6.1 IR and FTIR of styrene monomer and polystyrene shells

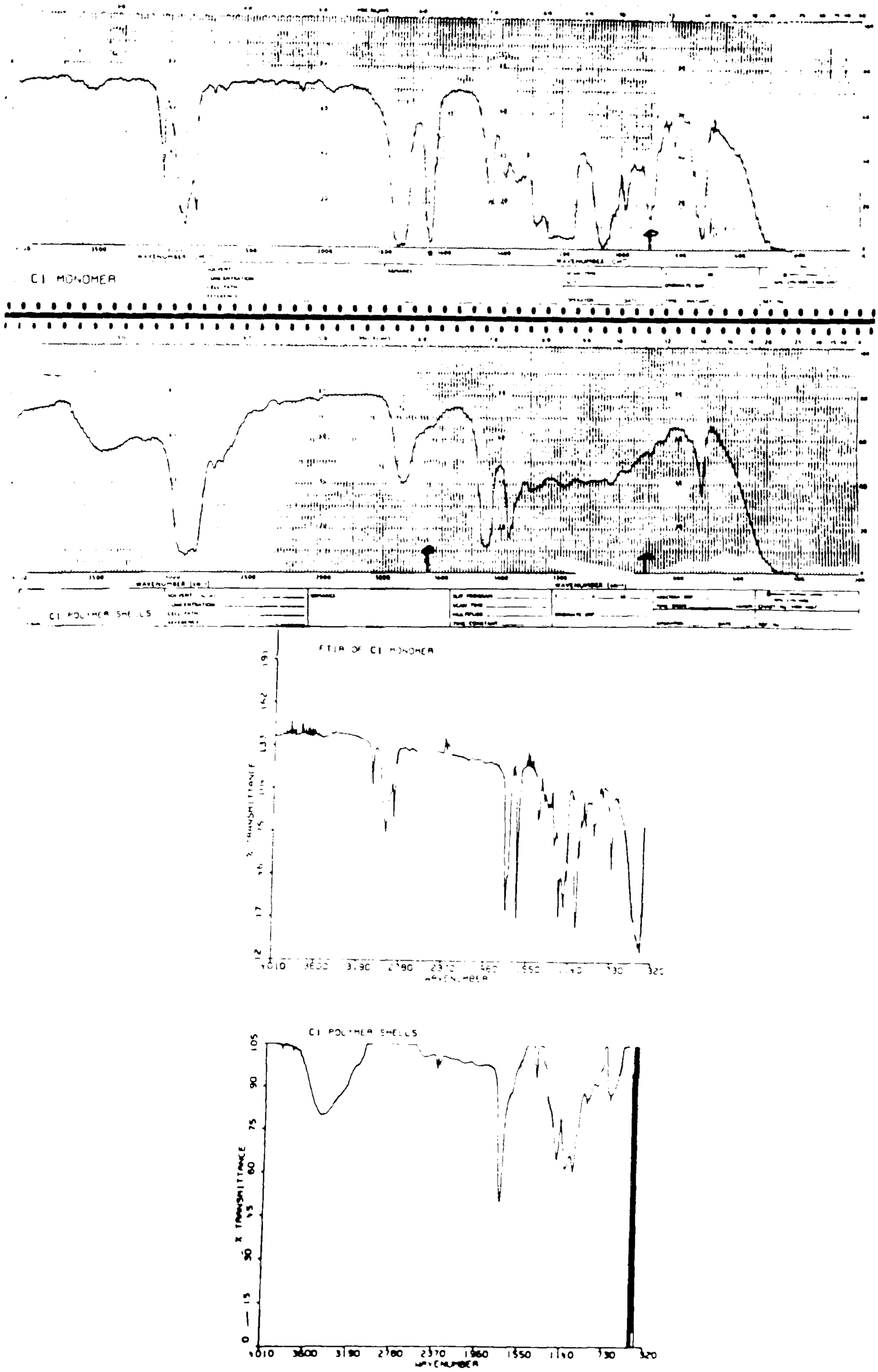

Fig. 6.2 IR and FTIR spectra of Cl monomer and Cl polymer shells

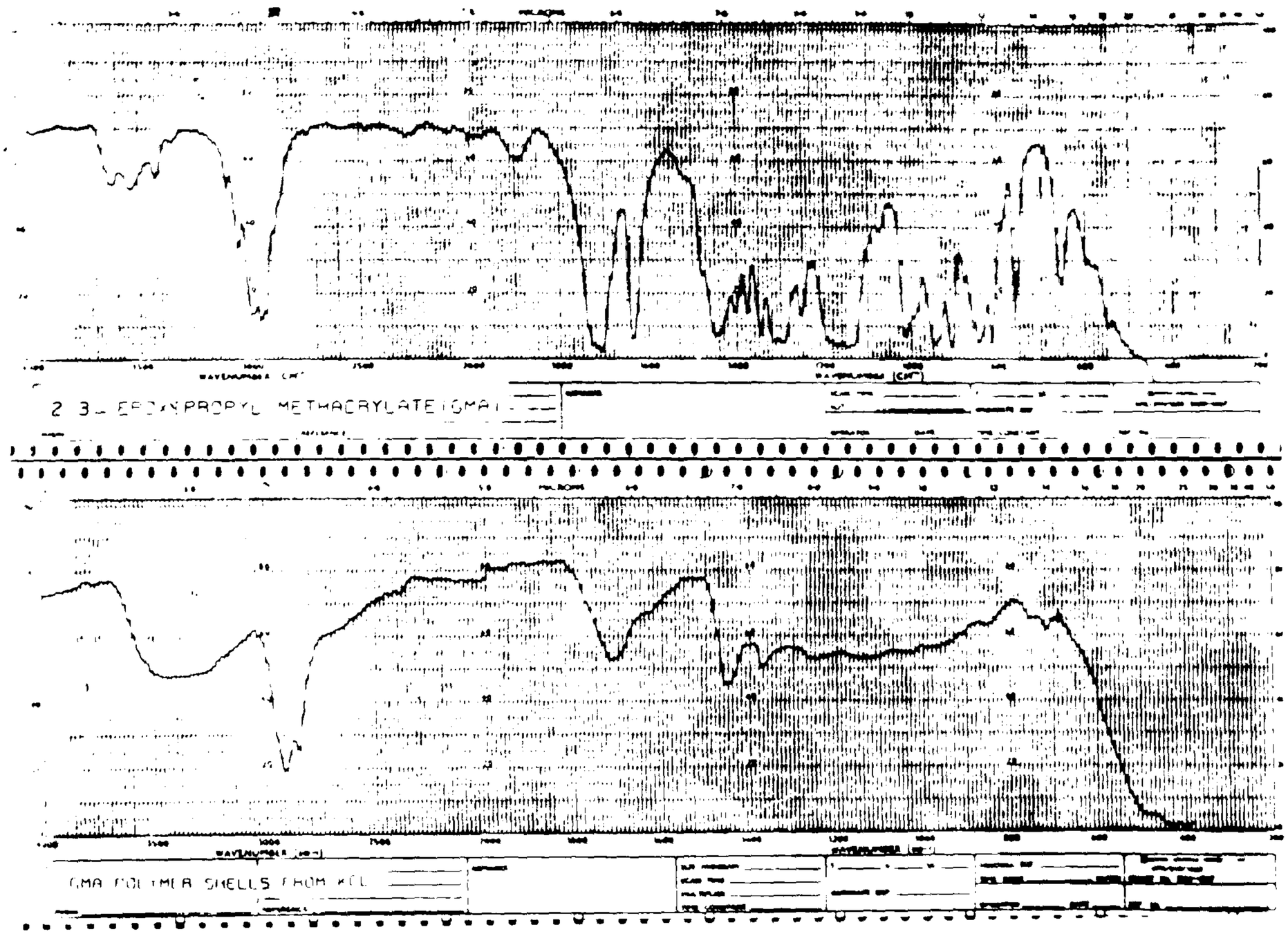

Fig. 6.3 IR and FTIR spectra of GMA monomer and GMA polymer shells

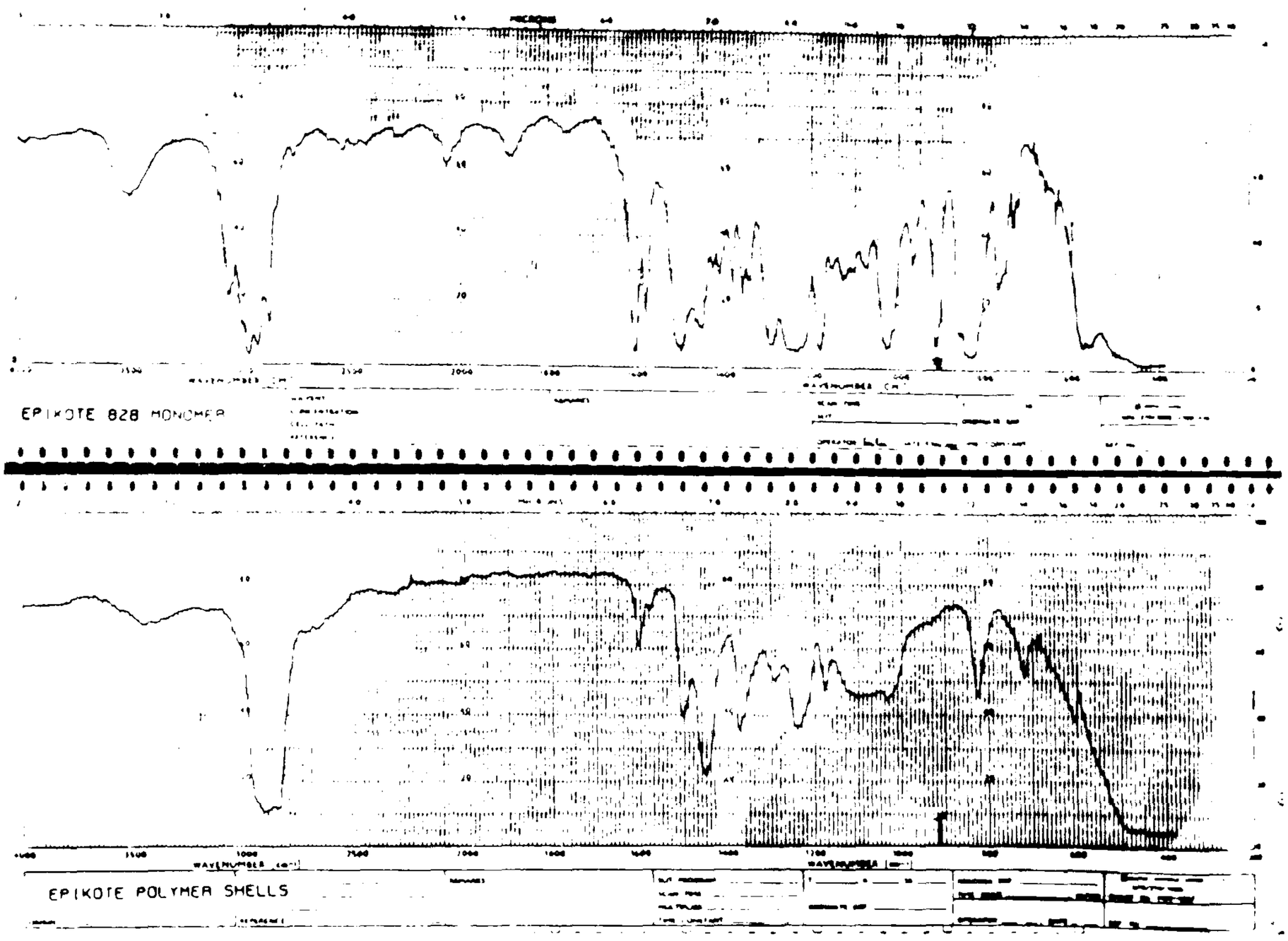

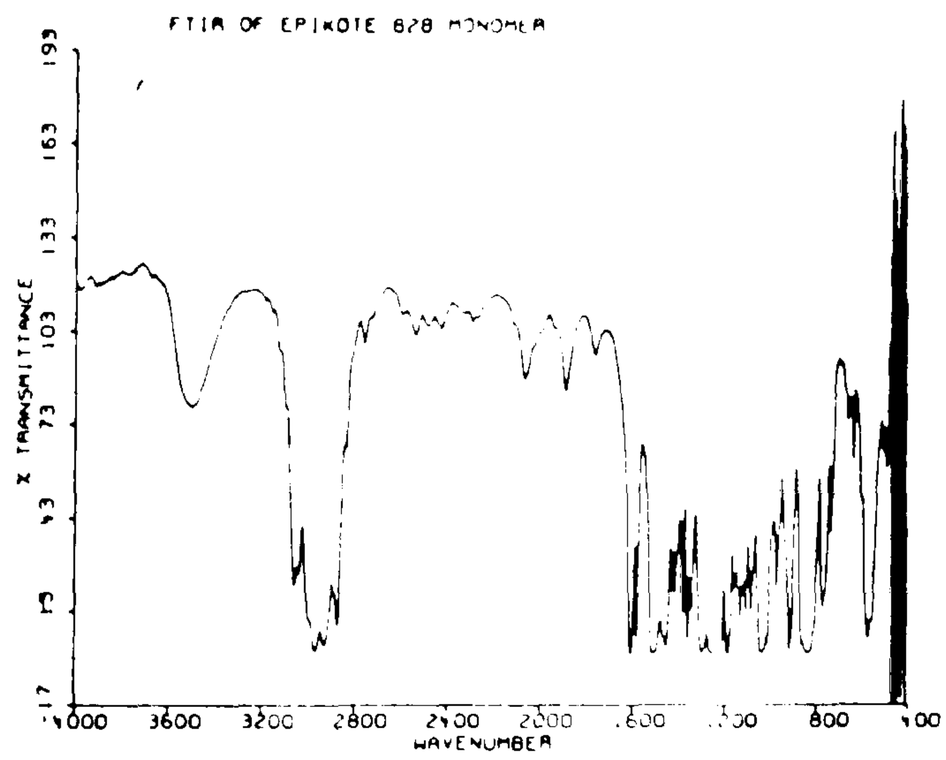

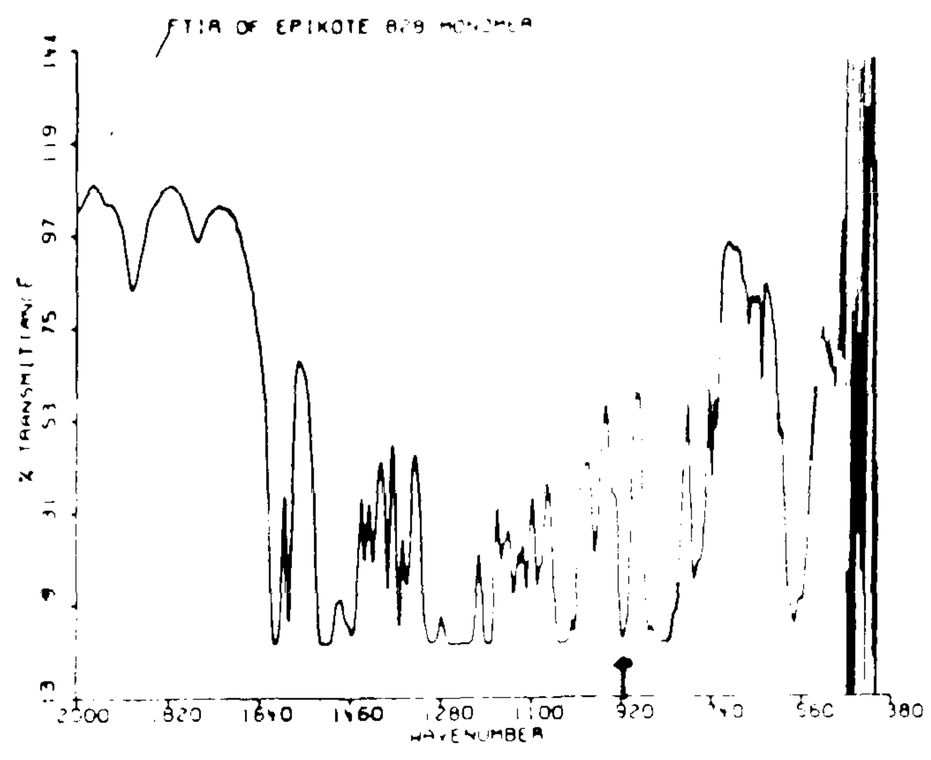

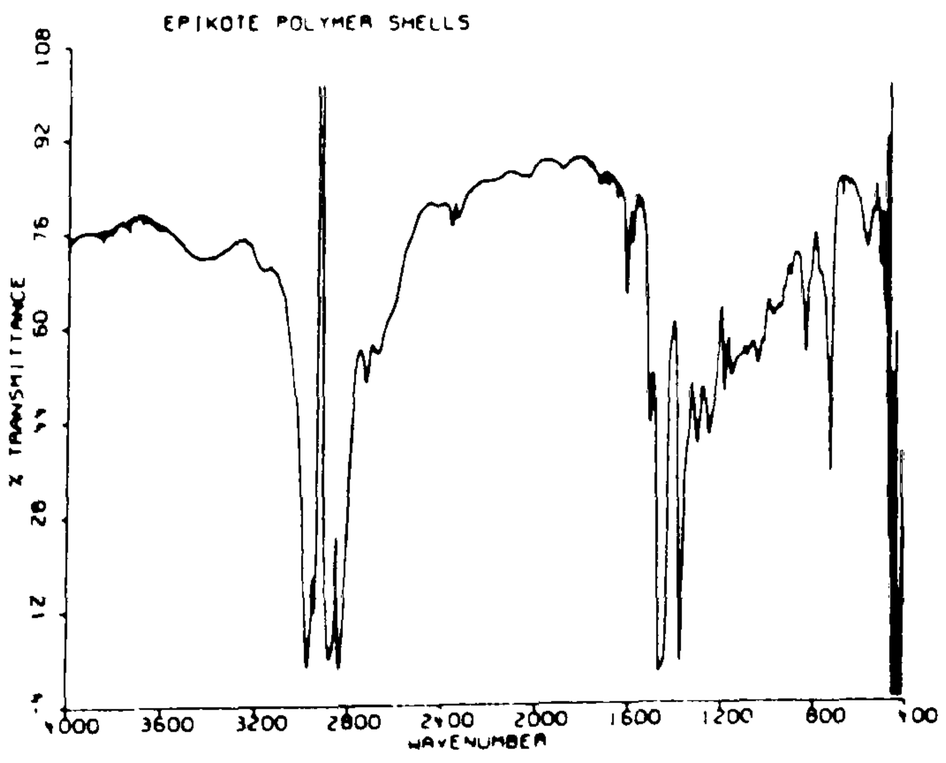

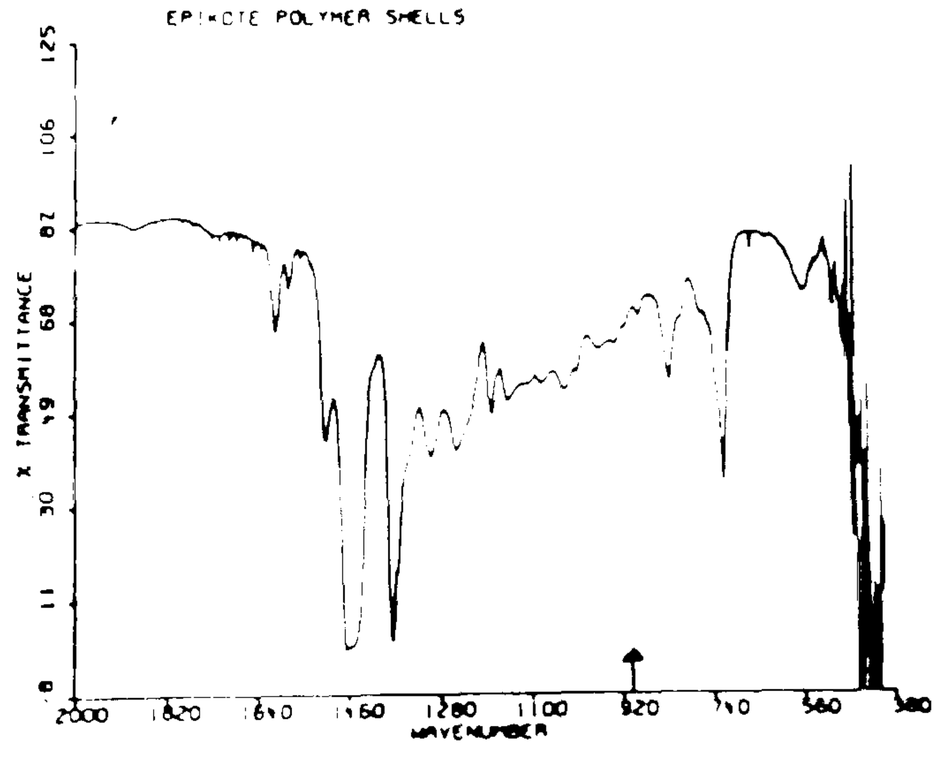

Fig. 6.4 IR and FTIR spectra of Epikote monomer and Epikote polymer shells

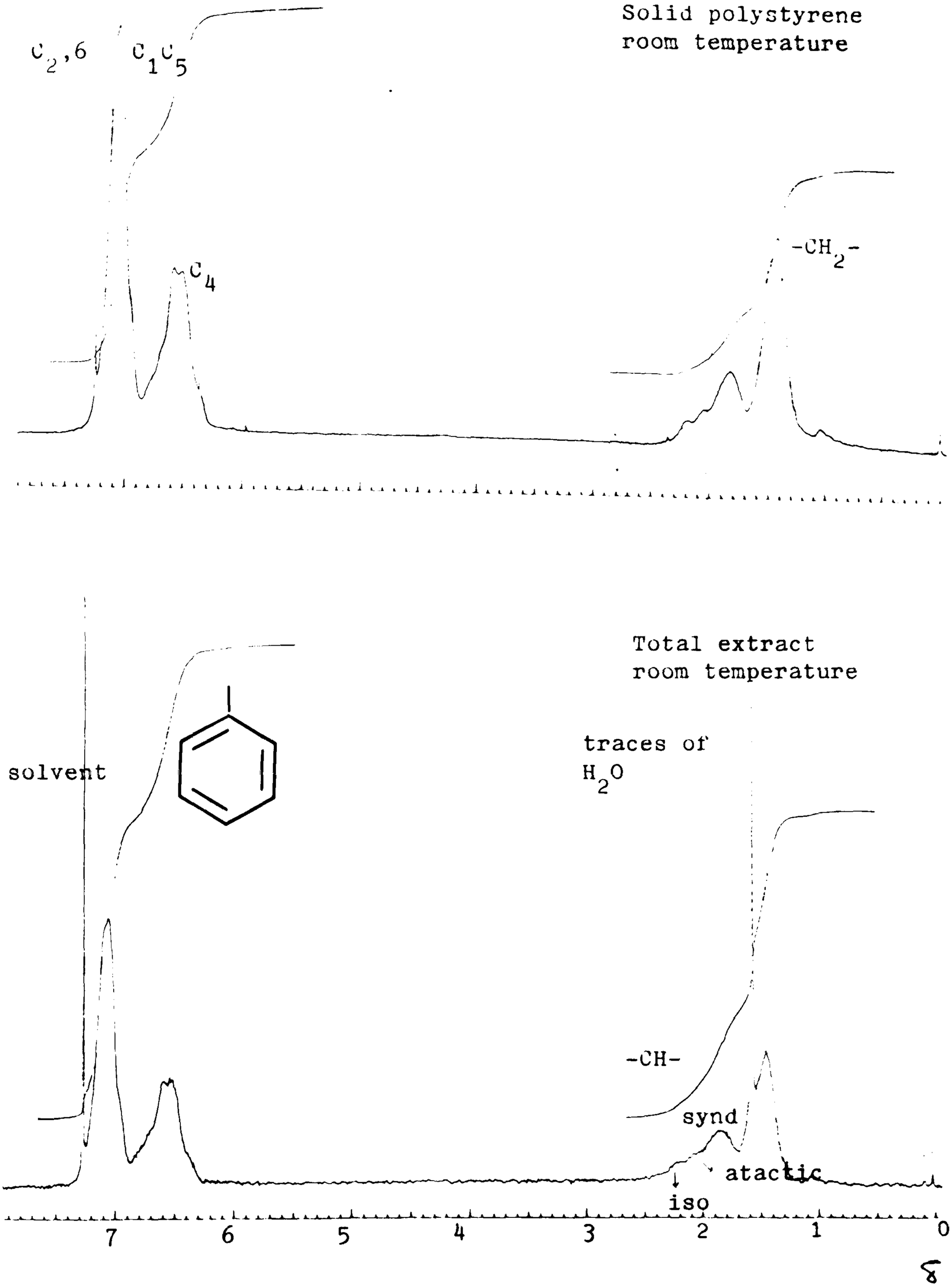

Fig. 6.5 H^1-NMR spectra of solid polystyrene shell and the total extract at room temperature

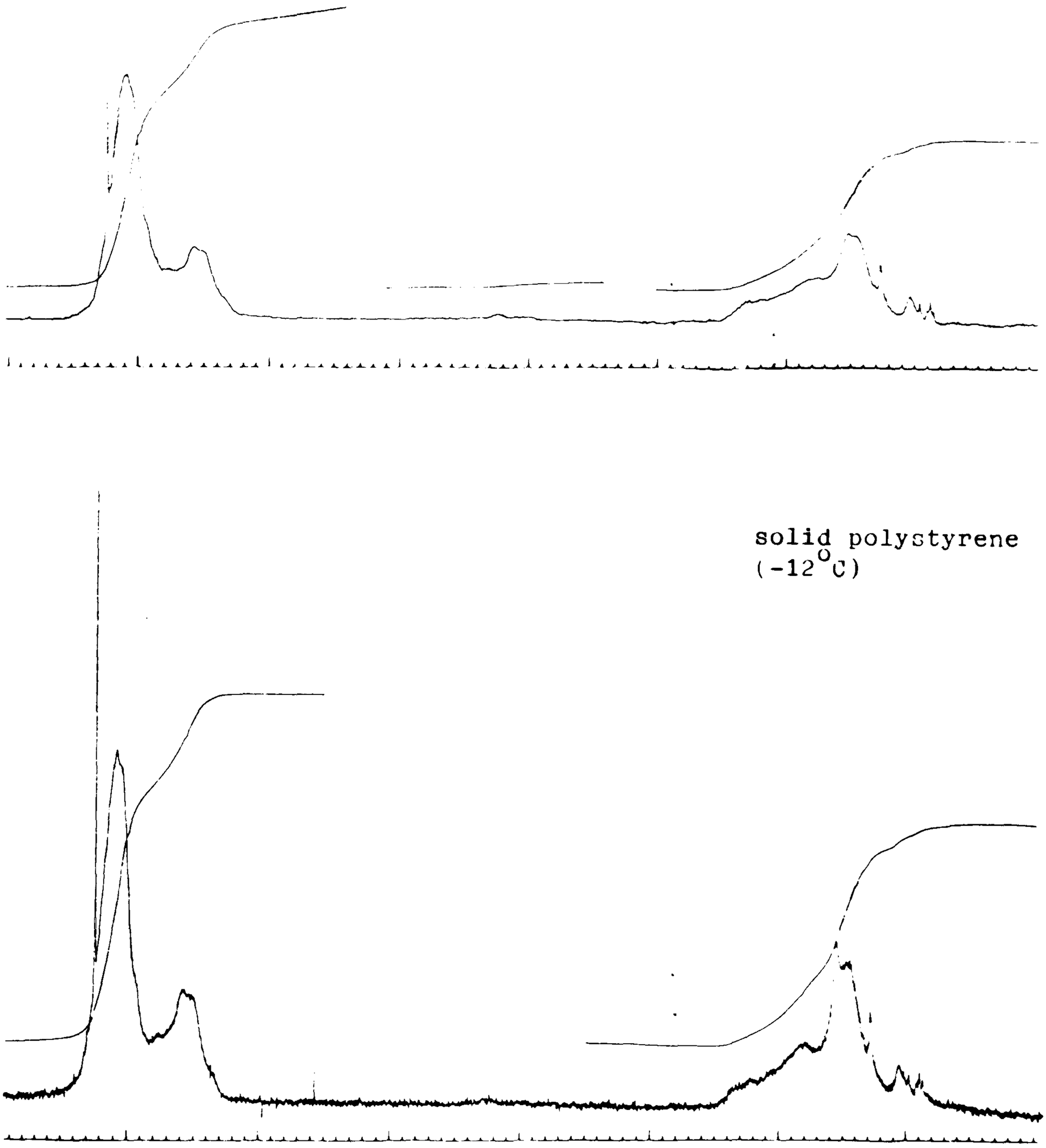

Fig. 6.6 H^1-NMR spectra of polystyrene shells found at 0°C and -12°C

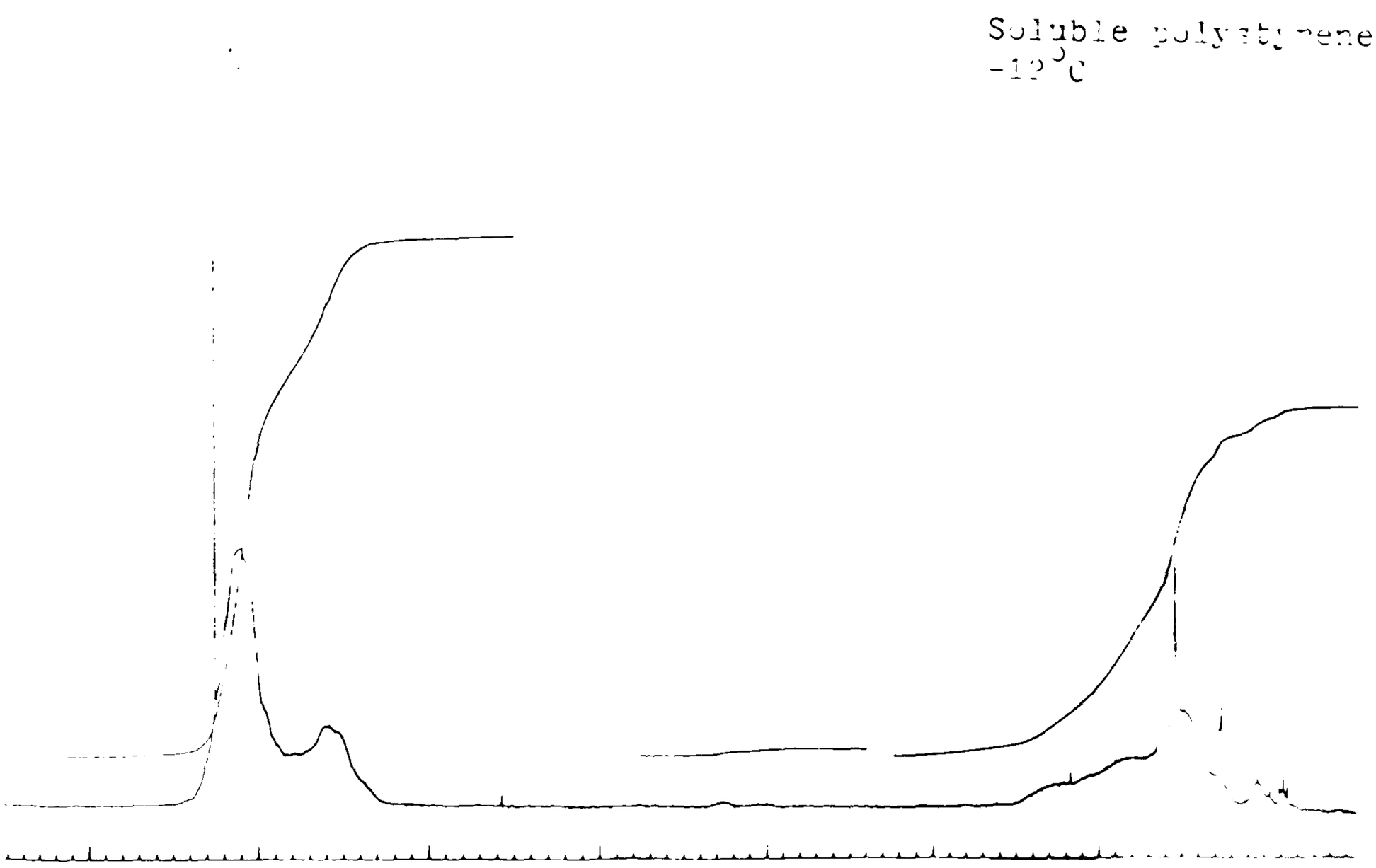

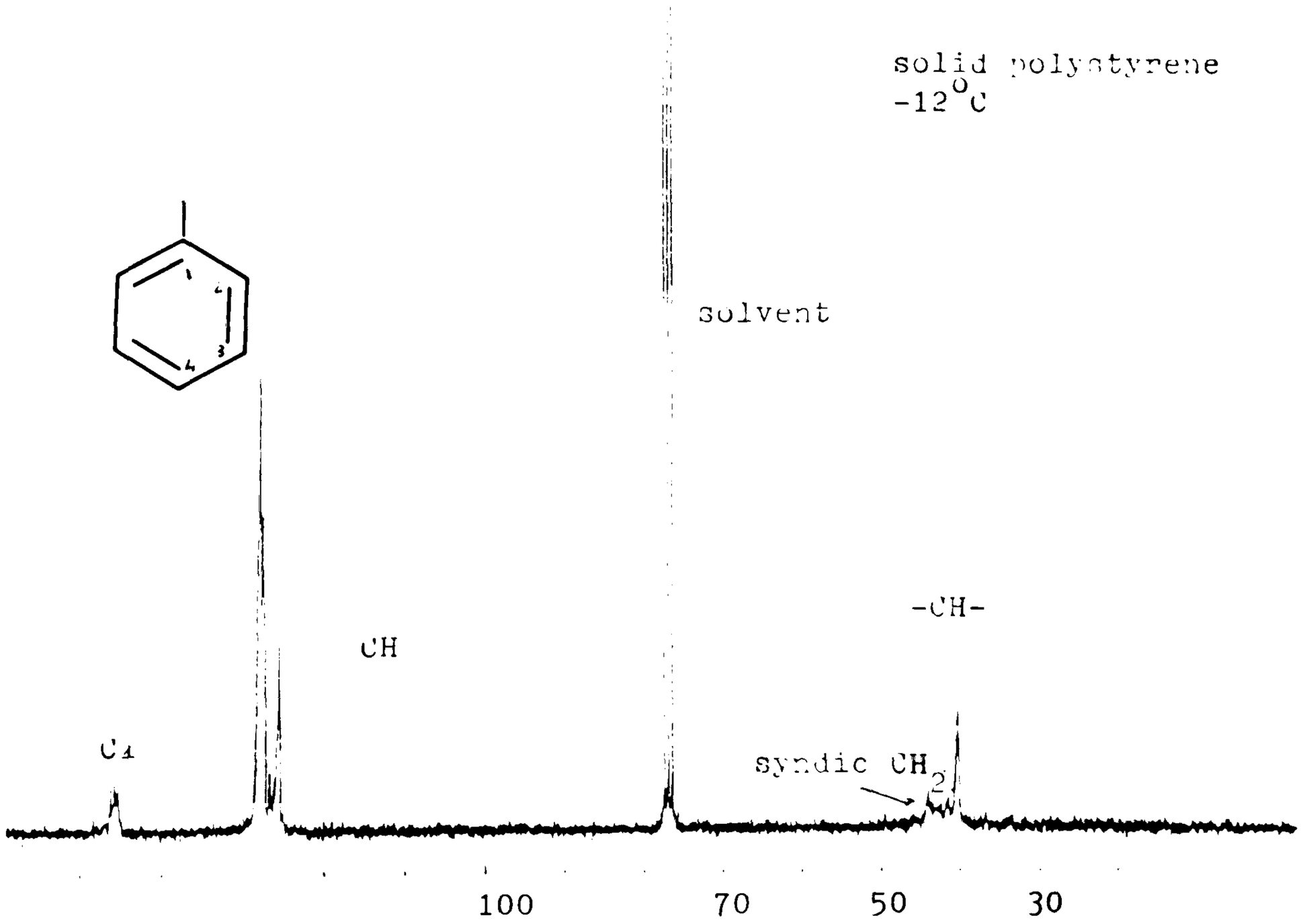

Fig. 6.7 H^1-NMR spectra of the soluble polystyrene (-12°C) and ^{13}C-NMR spectra of the solid polystyrene (-12°C)

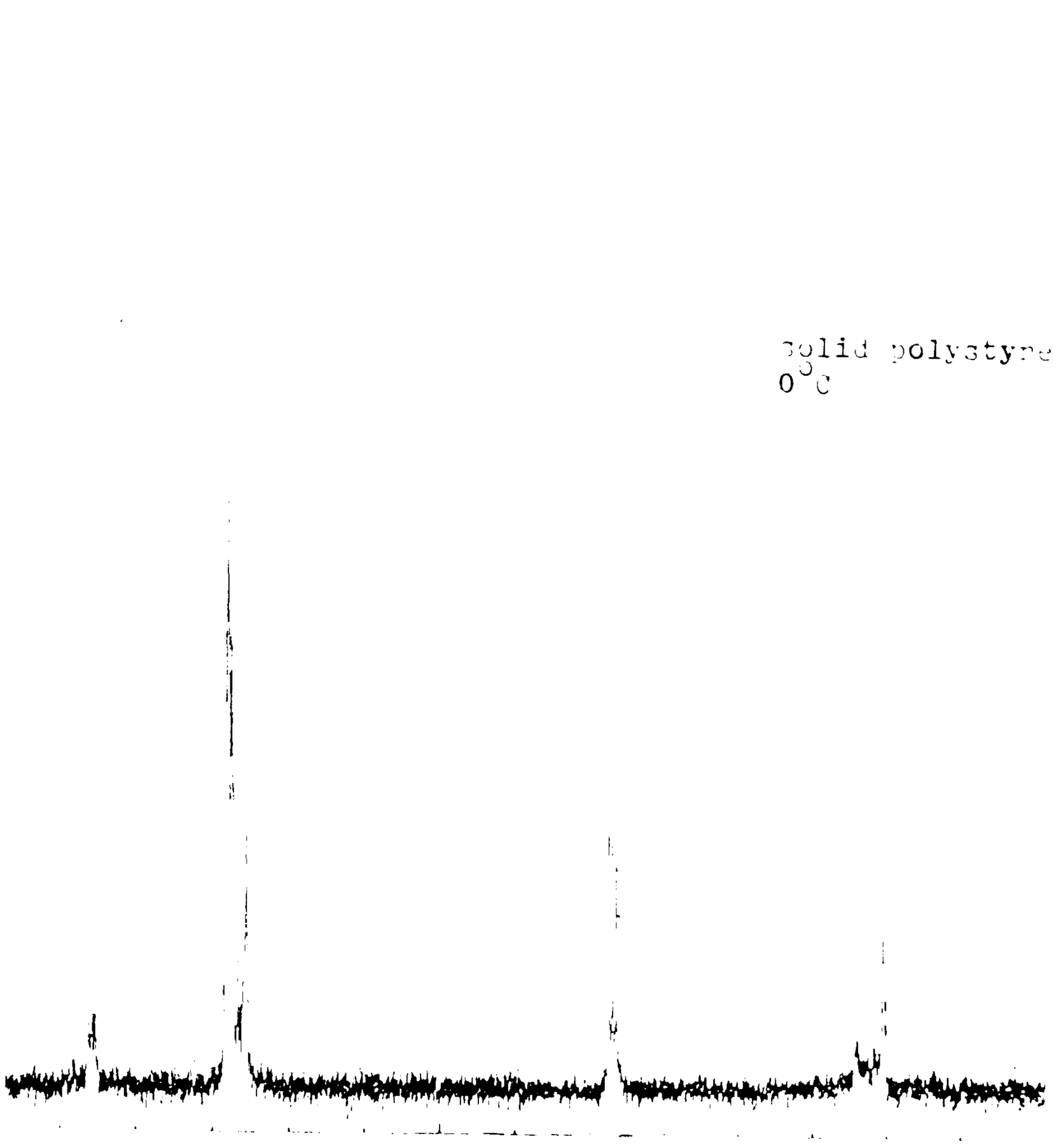

Fig. 6.8 ^{13}C-NMR spectra of the solid polystyrene (0°C) and of the soluble polystyrene (-12°C)

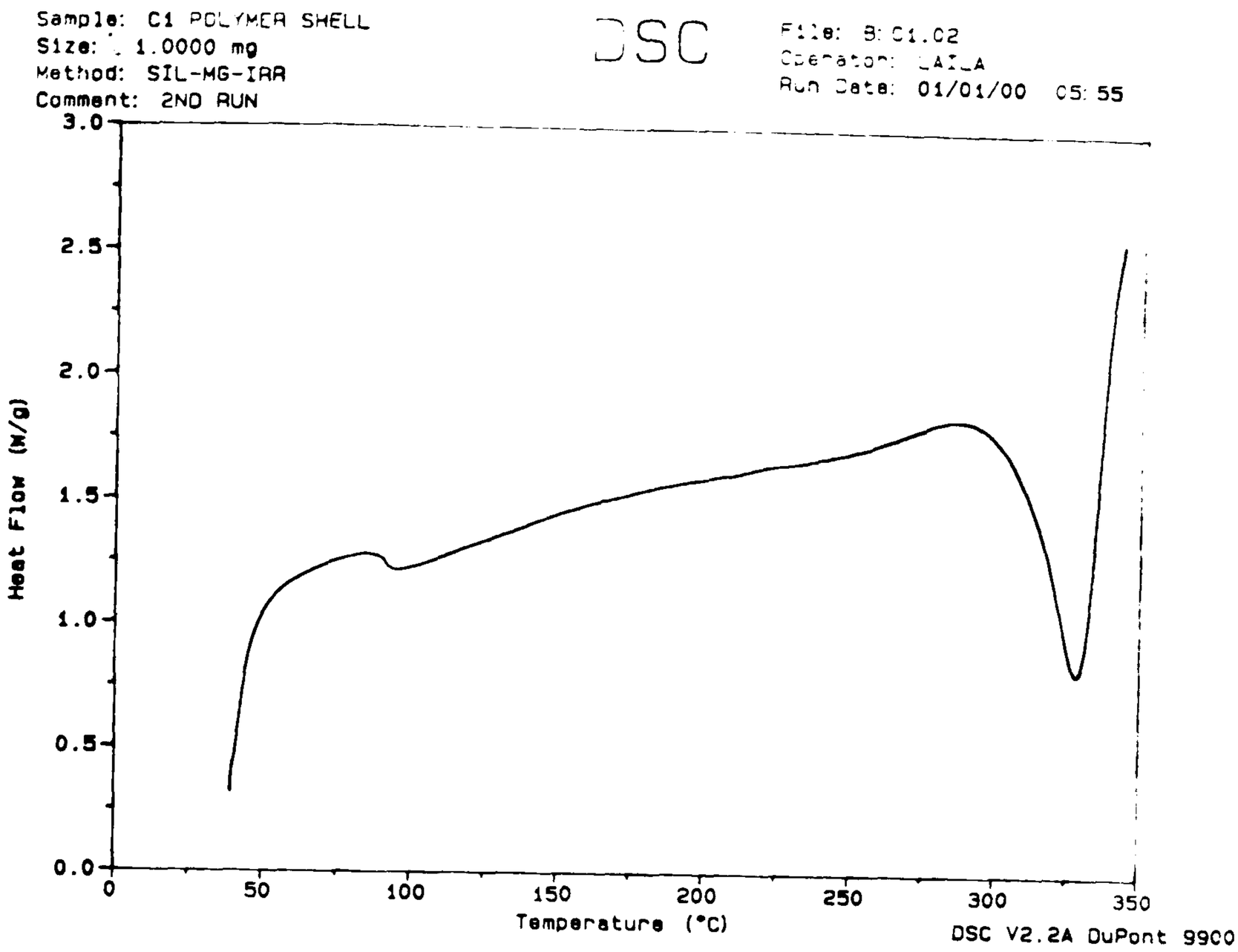

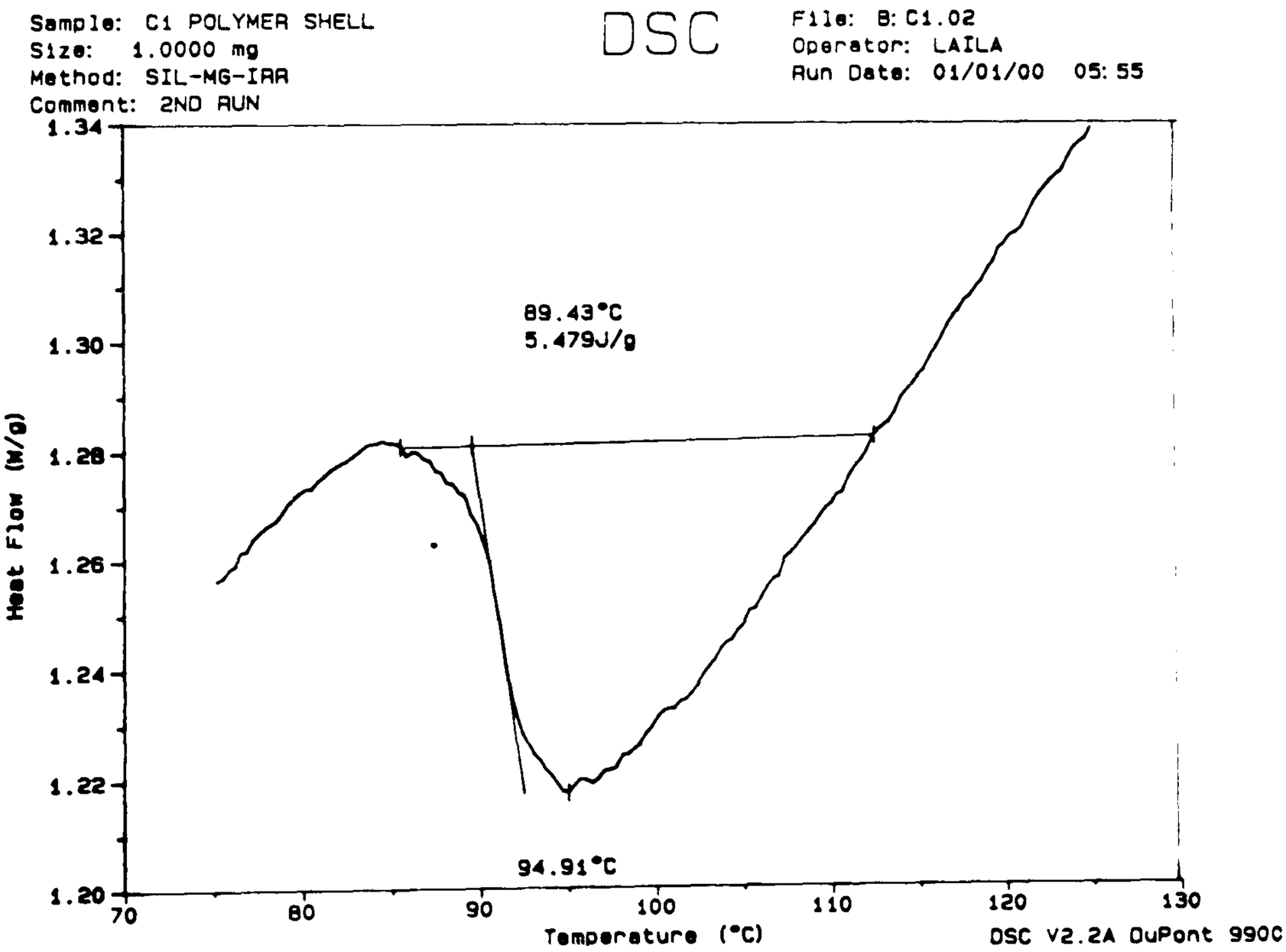

Fig. 6.9 The DSC curve of C1 polymer

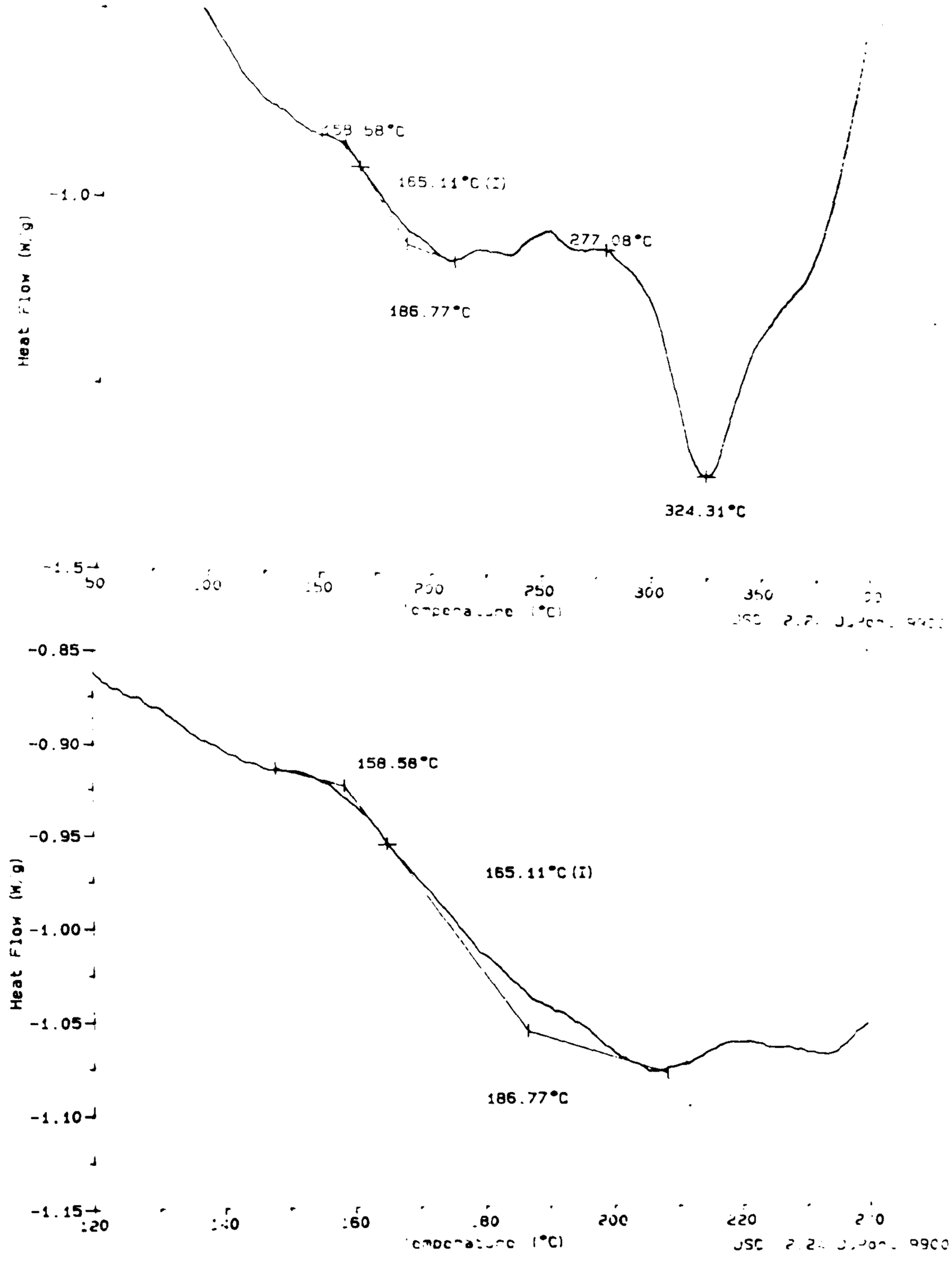

Fig. 6.10 DSC plot of Epikote polymer shells

the effect of temperature on the solubility of the surfactant, initiator and monomer and their adsorption on the drug surface. The dielectric properties of the drug surface and the reaction medium (n-heptane) are also functions of the reaction temperature. This may significantly decrease the polymerization rate.

The polydispersities of the polymers formed in solution are less than those formed on the crystals. This could be attributed to the fact that the soluble polymers were precipitated by ethanol. This process would eliminate the very small molecular weight species from precipitation as they could be soluble in n-heptane-ethanol mixture. This would improve the polydispersity of the precipitated polymers. The molecular weights of polystyrene shells are not very high so their mechanical properties are expected to be poor.

The IR spectra of styrene and polystyrene show that the C=C absorption band at 1630 cm^{-1} in the monomer disappeared in the polymer. It also shows the absorption of the saturated C-H below 3000 cm^{-1}. The spectrum of C1 polymer displayed broad bands compared to those of the monomer as shown in Fig. 6.2. This could be related to the segmental motion and internal rotation along the polymer chain which could be responsible for broadening the absorption peaks. However it is clear from the spectra that the C=C absorption at 1650 cm^{-1} in the monomer has disappeared in the polymer spectrum. This is confirmed also by the absence of the unsaturated = C-H peak above 3000 cm^{-1} from the polymer spectra.

The GMA and Epikote 828 monomers showed a characteristic band at about 915 cm^{-1} for the epoxy group. This band disappeared in the spectra of both

polymers. The peak at 1650 cm^{-1} representing the double bond in the GMA monomer disappeared in the polymer. The peak corresponding to the stretching unsaturated carbon-hydrogen bond (=C-H) which appeared above 3000 cm^{-1} in the monomer spectrum disappeared in the polymer spectrum. This confirmed that both the double bond and the epoxy group had polymerized. The possible interpretation of this observation is that GMA monomer underwent cyclic polymerization and gave additionally a degree of crosslinking instead of giving linear polymer with a functional double bond as was expected and discussed in Chapter V. The speculated structure of the formed polymer is

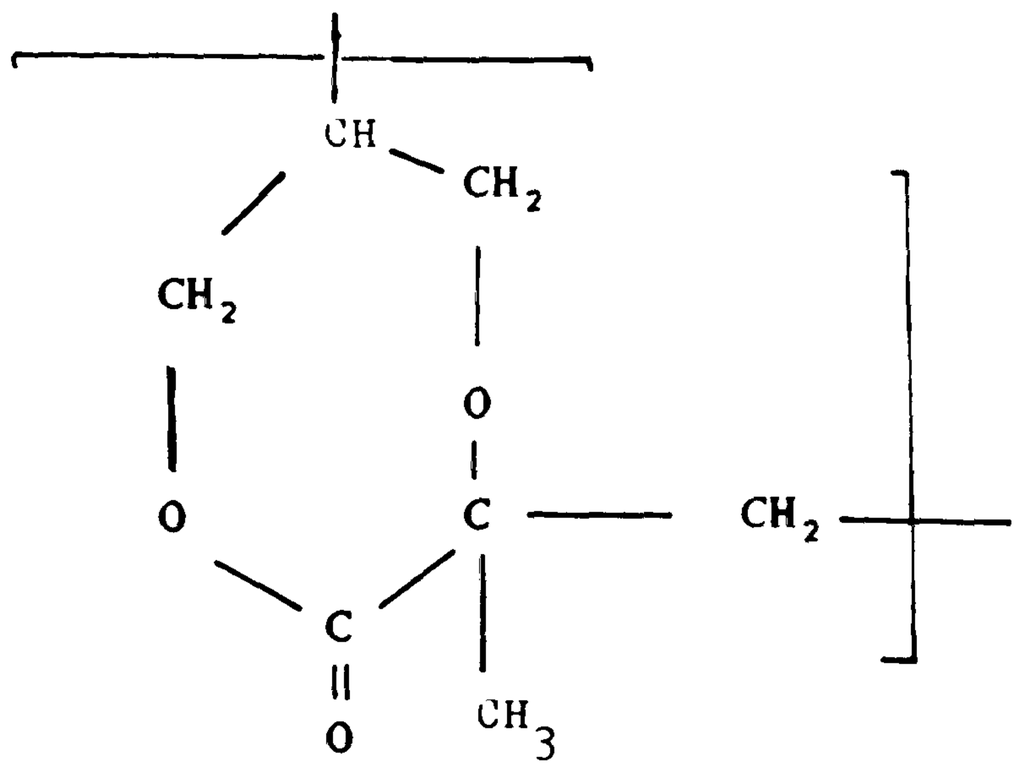

Speculated structure of GMA polymer

which is a seven membered ring. The solubility test indicated that the polymer is partially crosslinked but more investigation is necessary to confirm its chemical and physical properties.

The stereochemical configuration of polystyrene has been the subject of many

^{1}H-NMR investigations[13-17]. Detection and quantitative evaluation of configuration sequences are not easy for non-deuterated polystyrene because of the complexity due to proton coupling and the overlapping resonances. The ^{13}C-NMR analysis possibly provides a suitable means for studying the configurational sequences of polystyrene[18-19] as compared with ^{1}H-NMR. The complete proton decoupling ^{13}C-NMR spectra are rather simple because of the well discriminated chemical shifts over a wide range and hence the analysis of the spectra can be done easily. The ^{13}C-NMR analysis of polystyrene samples obtained in this study might, with hindsight, have produced better results, however, due to lack of enough sample for ^{13}C-NMR analysis, ^{1}H-NMR analysis was used instead.

Proton-NMR spectra of solid polystyrene which was formed on the surface of KCl crystals at the three different temperatures shown in Figs. 6.5-6.6 show slightly different profiles. The spectra indicate that the polymers contain different ratios of iso-, hetero-, and syndiotactic species in which the syndiotactic species seem to be predominant followed by the isotactic . This is clearer in the spectrum of the polystyrene sample formed at room temperature than the other two because their peak intensities are relatively low. The spectrum of the sample formed at -12°C shows some splitting in the peaks which may indicate a relatively higher ratio of the isotactic species. The total extract presented the same profile as the solid polymer but with lower intensity, this is because the solid polymer had a high percentage of the total extract. The soluble polymer (-12°C) did not present adequate information because of the low peak intensities. The low yield of samples made it difficult to improve the spectra.

The ^{13}C-NMR spectra of the aromatic region and of the methylene and methine carbons are shown in Figs. 6.7–6.8, each carbon peak was assigned[19] on the basis of the comparison of relative intensities. The peaks of C_2 and C_3 resonance overlap with each other. C_2 and C_3 carbons are slightly affected by the polymer stereochemistry. However the C_4 resonance shows a single peak and is hardly affected by the polymer structure. Carbon–4 is situated at the outermost part of the polymer chain.

The C1 resonance peak appear at the lowest field. The resonance split of the C1 peak which would indicate the tacticity is obscured in $CDCl_3$ solvent. This could be improved by choice of another solvent like deuterated dichlorobenzene but there was insufficient material to run further studies.

The ^{13}C NMR spectra of the methylene and methine carbons gave three small peaks; ($-CH_2-$) at a lower field and a sharp single peak (–CH–) at the upper field. The methine carbon is hardly affected by the polymer stereochemistry. The splitting of the methylene carbon resonance indicates the presence of the syndio–, iso–, and heterotactic species. The peak intensities are too low in $CDCl_3$ to indicate the percentage of each species. The aliphatic proton peaks separation would be better in an aromatic solvent[14] such as chlorobenzene. The other two ^{13}C-NMR spectra of the solid polystyrene (0°C) and the soluble polystyrene (–12°C) did not provide much information on the stereoregularity of the polymer. This is because of the low intensity of the peaks of the methylene carbon of the polymer backbone and also those of the aromatic C_1 carbon in $CDCl_3$ solvent.

The DSC plots were recorded for C1 and Epikote polymers. From Fig. 6.9, C1 polymer revealed two phase transitions, one at 94.91°C which is possibly the glass transition temperature (Tg) and the other at 328°C which is the degradation of the polymer. The DSC plot of the Epikote polymer in Fig. 6.10 revealed two main transitions, one at about 165°C which probably is a Tg and the other at 324.31°C which is the polymer degradation. The relatively high Tg of the C1 and Epikote polymers indicate the probability of low permeability of their membranes. This will be examined by the release studies of the drugs through their membranes in a following chapter.

6.5 References

1. Kline, G.M., ed., "Analytical Chemistry of Polymers", Interscience Publishers, New York, Part 1 (1959); Part II and III, (1962)
2. Wall, L.A., "Mass Spectrometry", Chap. VI in G.M. Kline, ed., Op. Cit., Part II, (1962)
3. Cassel, J.M. "Chromatography" Chap. x in G.M. Kline, ed., Op. Cit., Part II, (1962)
4. W.T.M. Johnson, Official Digest of the Oil and Colour Chemists' Association, 32, 1067 (1960)
5. Fahrenfort, J., Spectrochimica Acta, 17, 698 (1961)
6. Harrick, N.J., Phys. Rev. Letters, 4, 224 (1960)
7. Allara, D.L. and Swalen, J.D., J. Phys. Chem., 86, No. 14, 2700-2704 (1982)
8. Griffiths, P.R. and de Haseth, J.A. "Fourier Transform Infrared Spectrometry" A Wiley-Interscience Publication Vol. 83, (1986)
9. Ferraro, J.R. and Basile, L.J. "Fourier Transform Infrared Spectroscopy, Application to Chemical Analysis", Academic Press Inc., Vol. 4 (1985)
10. Cowie, J.M.G. "Polymers: Chemistry and Physics of Modern Materials", Intertext Books Publishers, (1973)
11. Billmeyer, F.W. Jr., "Textbook of Polymer Science", Chapter 4, Interscience Publishers (1962)
12. Clark, D.T. and Feast, W.J. "Polymer Surfaces", Chapter 15 and 16, A Wiley Interscience Publication, (1978)
13. Brownstein, S., Bywater, S. and Worsfold, D.J., J. Phys. Chem. 66, 2067 (1962)
14. Yoshino, T., Kyogoku, H., Komiyama, J. and Manabe, T., J. Chem. Phys.

38, 1026 (1963)

15. Bovey, F.A., Hood, F.P., Anderson, E.W. and Synder, L.C., J. Chem. Phys. 38, 3900 (1965)

16. Heatley, F. and Bovey, F.A., Macromolecules, 1, 301 (1968)

17. Segre, A.L., Ferruti, P., Toja, E. and Danusso, F., Macromolecules 2, 35 (1969)

18. Johnson, L.F., Heatley, F. and Bovey, F.A. Macromolecules, 3, No.2 175, (1970)

19. Inoue, Y., Nishioka, A. and Chujo, R., Die Mac. Chem., 156, 207 (1972)

CHAPTER VII

Morphology and Topography of the Polymer Membranes

Chapter VII

Morphology and Topography of the Polymer Membranes

7.1 Introduction

Chemical and physical characterization techniques are complementary to one another in the polymer field. Both techniques are needed to determine fully the morphology and the microstructure and to develop structure–property relationships. The morphology of a polymer is determined by a wide range of optical and electronic microscopy[1,2]. There are variations among microscopes in available resolution, magnification, contrast mechanism, the depth of focus and depth of field. Polarized light microscopy is an optical technique that enhances contrast in crystalline[3,4] materials. Phase contrast optical techniques enhance contrast between polymers that are transparent but which have different optical properties such as refractive index and thickness. Reflected light techniques reveal surface structure whereas observation of internal structure of thin polymer slices is possible by transmitted light. Combinations of these microscopy techniques provide images of the morphology of polymer[5,6] materials. Resolution and contrast are the key parameters in microscopy studies of the fine structure and morphology of polymers. Scanning and transmission electron microscopes provide detailed imaging, resolution and measurements. Transmission electron microscopy is analogous to optical microscopy except that a beam of electrons is used as the illuminating source. Resolution down to a few Angstroms is possible using normal accelerated voltages (70–120 KeV). Contrast is produced by electron density variations in the specimen. In contrast to transmission electron microscopy, scanning electron microscopy is used for examination of sample surfaces[7] and the beam is rastered across the sample. A summary of the experimental techniques currently available

to polymer microscopy analysis is reported by Hobbs[8] with the morphological descriptions related to preparation and examination of the samples. Review of rubber[9] microscopy and multiphase polymers[10] are also available. The use of various types of electron and optical microscopes have also been discussed in the literature[11].

The scope of this chapter is to provide important information on the topography and morphology of the polymer membranes encapsulating the drug particles and also to look at their properties after releasing their contents.

7.2 Experimental

7.2.1 Optical Microsocpy

The drug surface before and after encapsulation, the gradual release of the drug (KCl) through the different polymer shells and the dry shells were examined by Zetopan and Olympus VANOX microscopes by reflected and transmitted light. The samples were mounted onto a clean glass slide and in some cases covered with a thin glass slide. The surface of KCl crystal coated with polystyrene was examined by polarized optical microscopy between the crossed polarizer of a ME-Pol Kyowa microscope.

7.2.2 Scanning Electron Microscopy (SEM)

The samples to be examined were mounted onto aluminium stubs using double sided adhesive tape. The samples were then coated with gold by vacuum deposition.

The electron microscopes used were Philips Model PW 6700/10 and JEOL Model JSM-840A. The accelerated voltage employed was 15-25 KV and the

micrographs were recorded at the required magnifications from the image produced by collecting secondary electrons emitted from the excited surface.

7.2.3 Transmission Electron Micrsocopy (TEM)

Crystal surface of KCl before and after encapsulation process were coated with a film of carbon. The crystals were dissolved in distilled water and the carbon film holding a print of the crystal surface was washed many times to remove any traces of the KCl. The carbon films holding the surface print of the crystal and that of the polymer were mounted on a copper grid which was placed in the sample chamber microscope of Philips 400TE microscope.

7.3 Results

7.3.1 Potassium Chloride Encapsulated with Polystyrene

Fig. 7.1 shows the surface of KCl crystal before encapsulation (A) which reflects a smooth flat surface at magnification of 2500. The crystal was cut from a single grown crystal of KCl. The micrograph (B) show the surface of the KCl crystal after microencapsulation with polystyrene. It reflects the polystyrene layers on the surface of the crystal at 2500 magnification.

Fig. 7.2 is an optical polarized reflection image of the polystyrene layer on KCl crystal. It was taken between crossed polarizers of the ME-POL Kyowa microscope. The micrograph is of magnification 138 and shows surface irregularity which caused depolarization relfection, hence shows light in image.

Fig. 7.3 shows a single crystal of KCl coated with a thick layer of polystyrene in which the excess polystyrene formed in the reaction medium was deposited on the coated surface of the crystal. The encapsulation of only one single crystal was

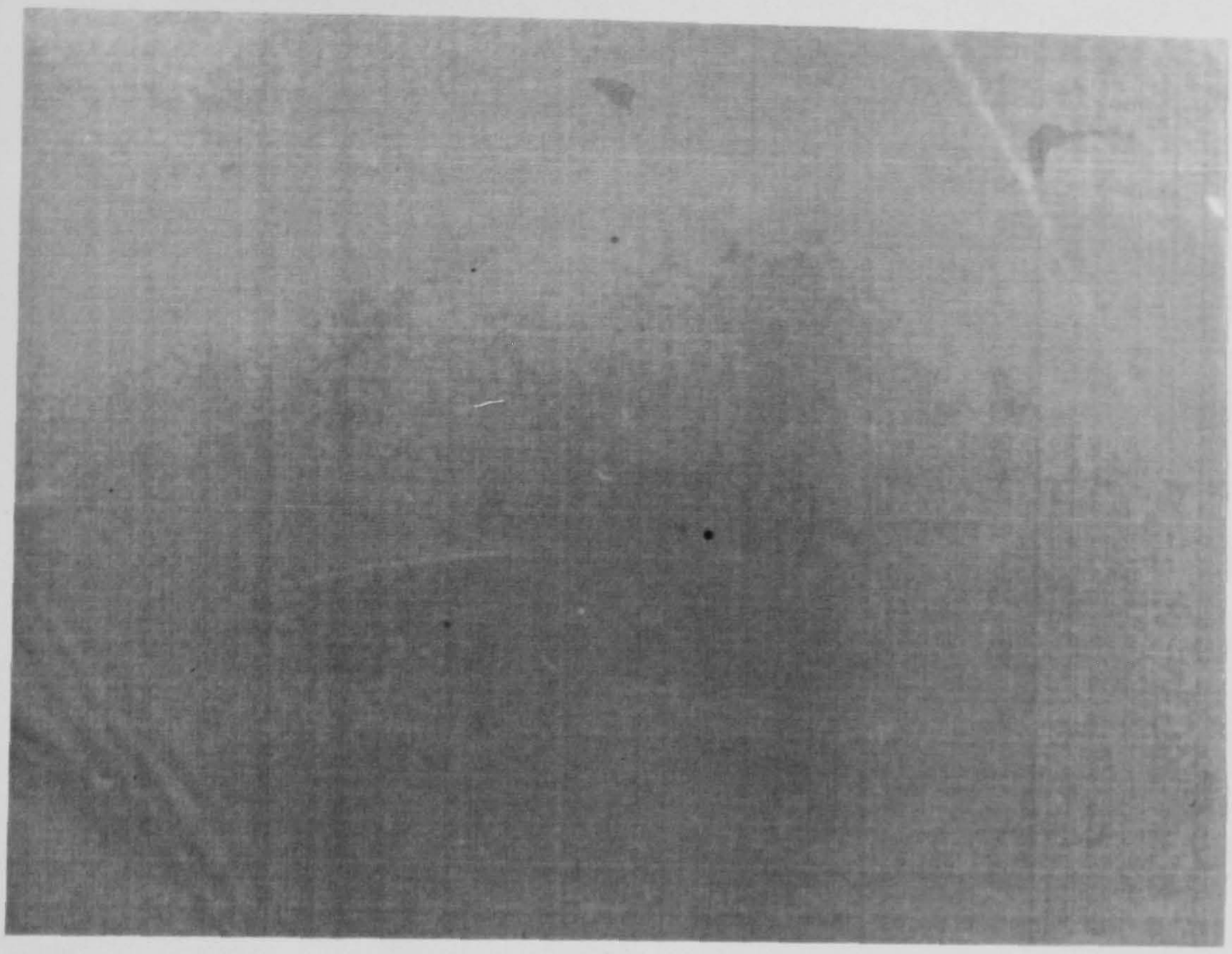

(A)

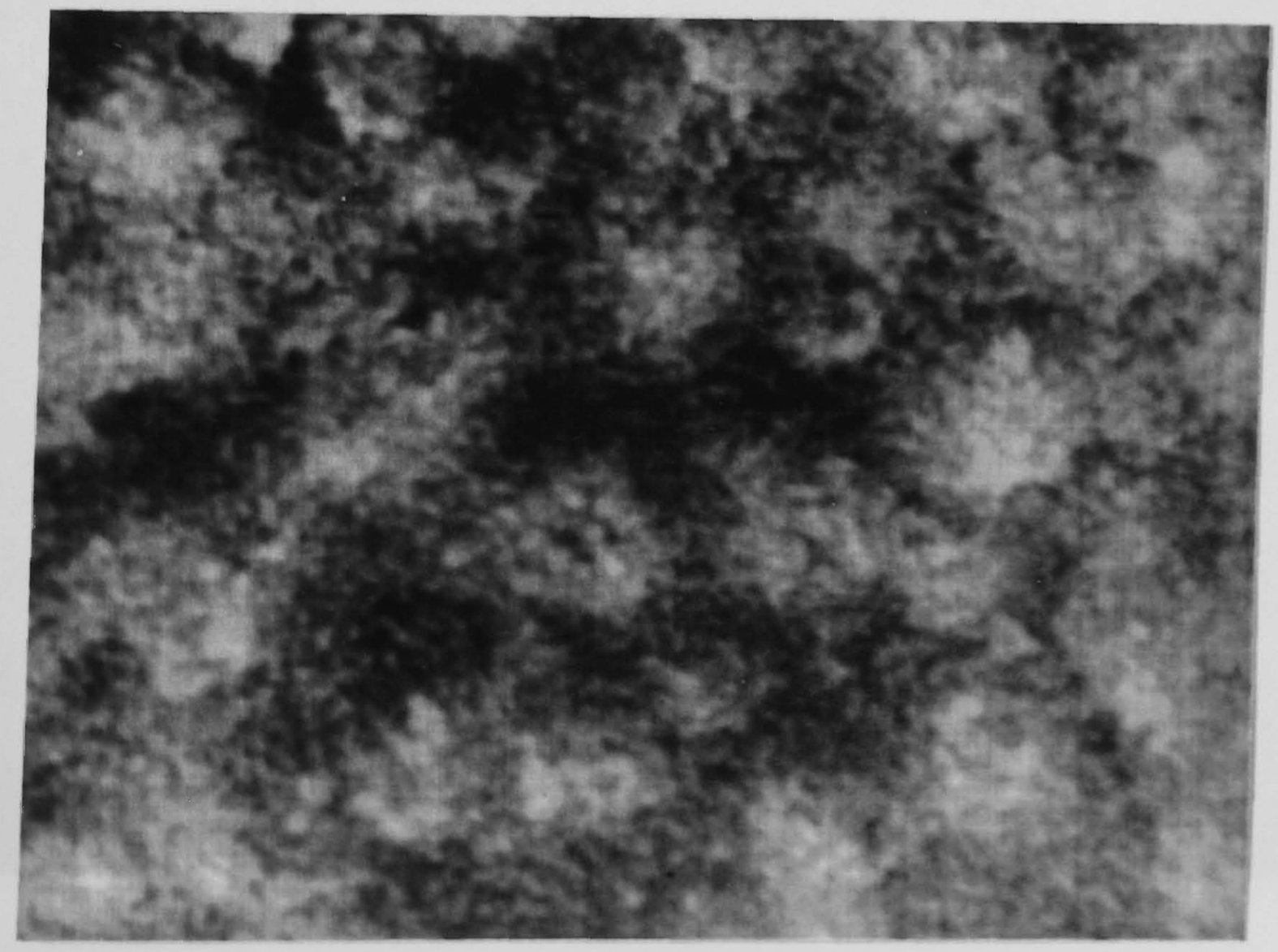

(B)

Fig. 7.1 (A) SEM micrograph of KCl crystal surface before encapsulation
(B) SEM micrograph of KCl crystal surface after encapsulation
The magnification is 2500 in both micrographs

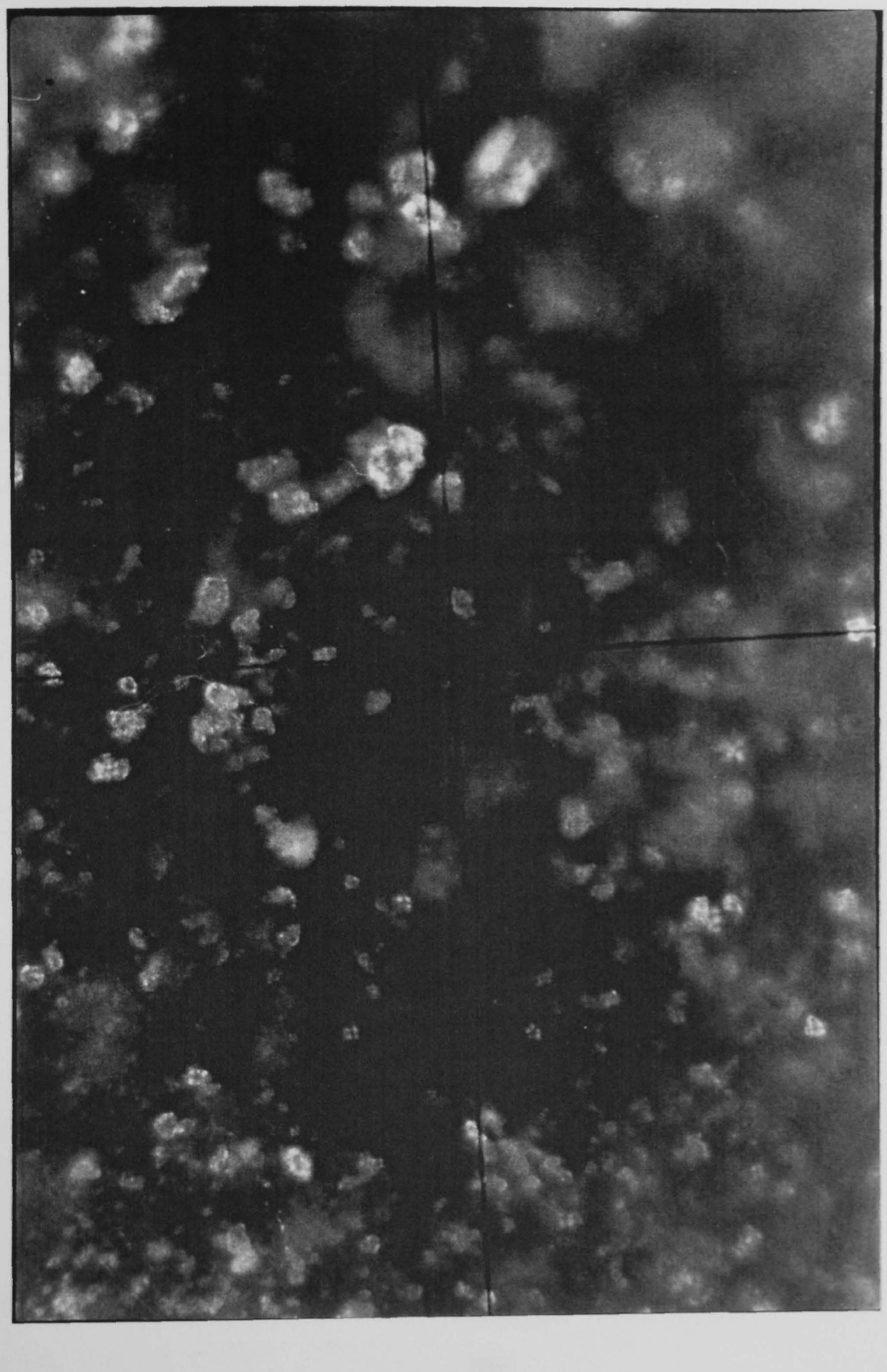

Fig. 7.2 Optical polarized micrograph of polystyrene shell on KCl surface magnification 138

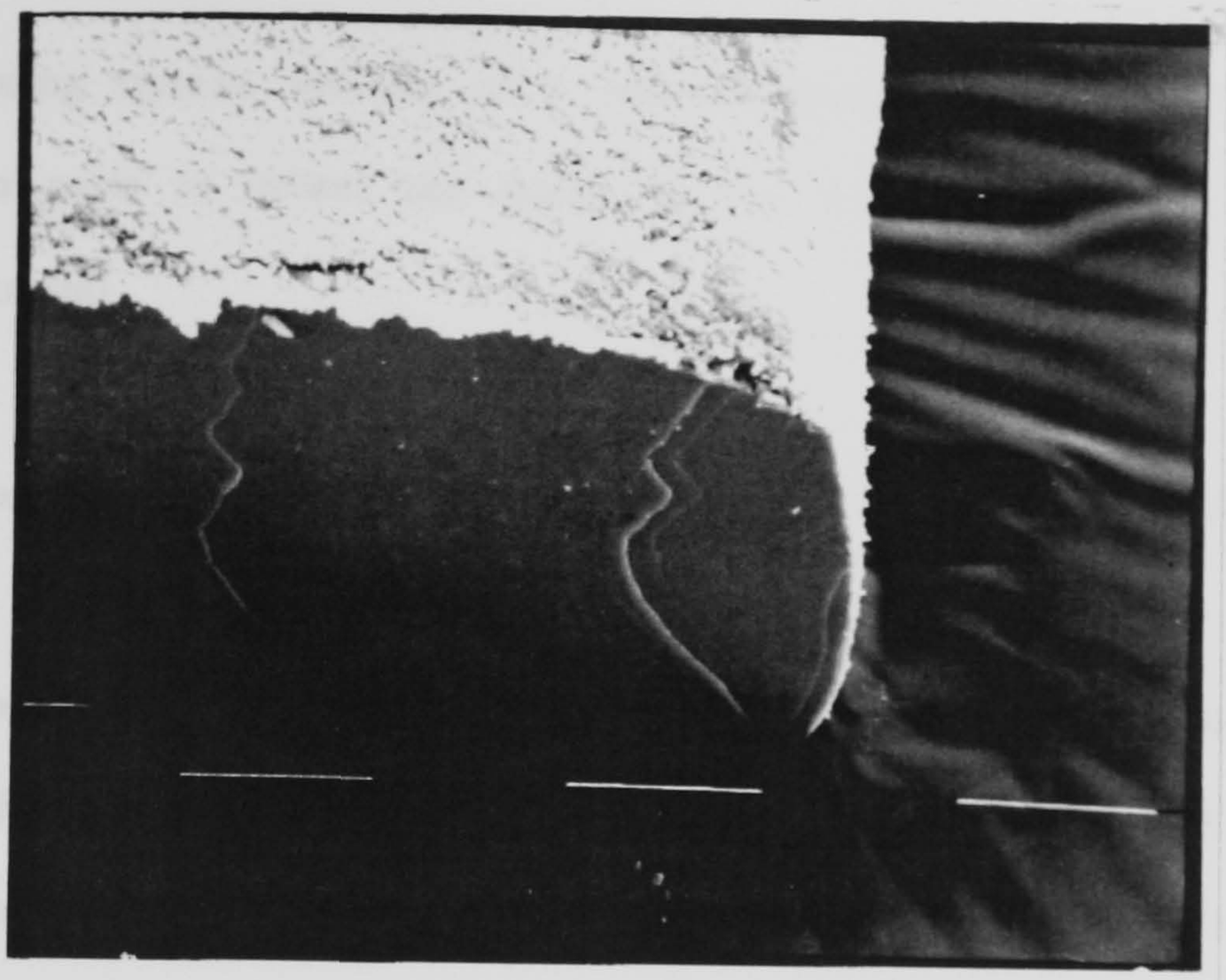

(A)

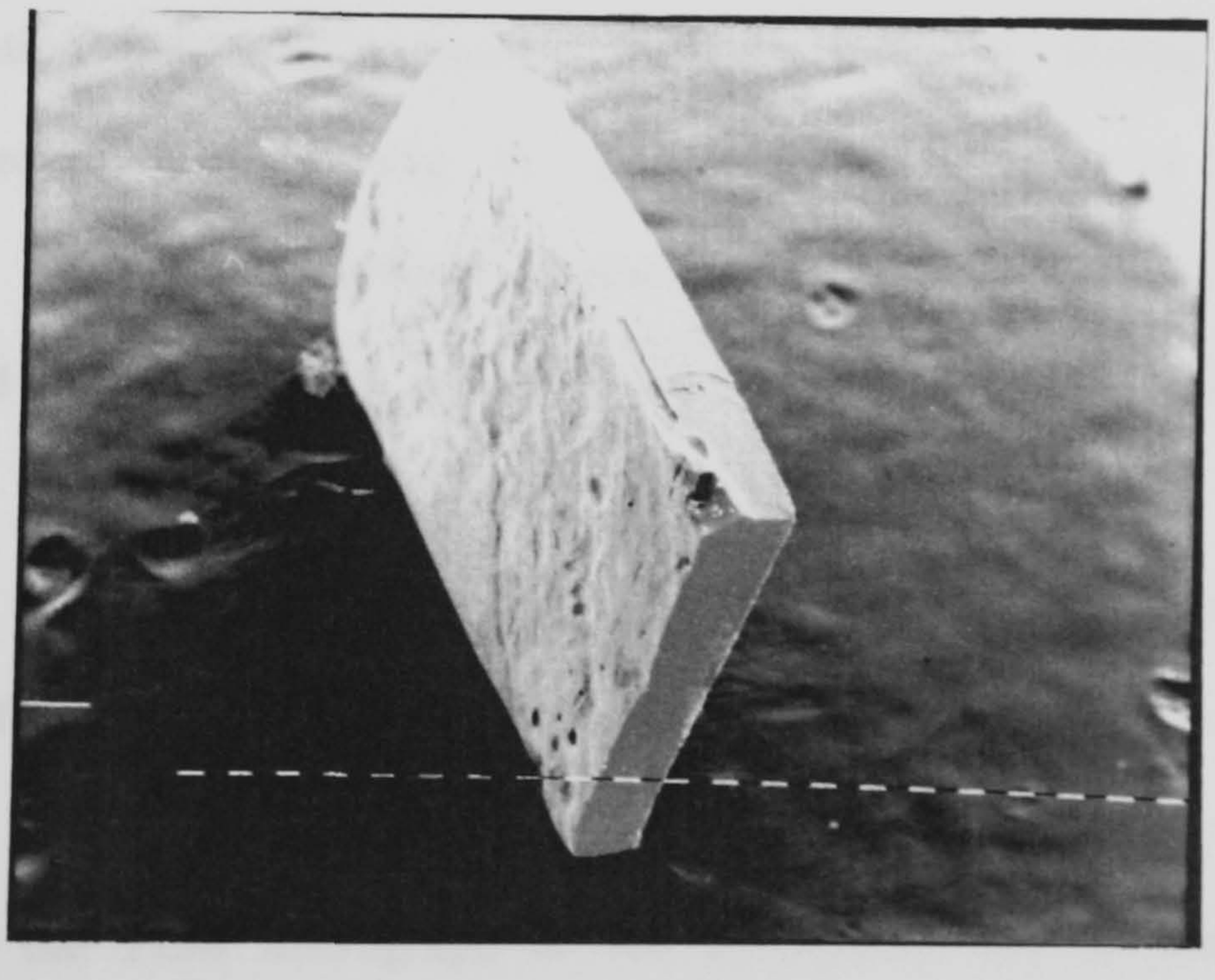

(B)

Fig. 7.3 SEM micrograph of KCl crystal coated with polystyrene. The scale marker = 100 μm
(A) shows the reflections of the coated surface and the uncoated crystal bulk.
(B) shows the thickness of the polymer layer

carried out using styrene solution of a concentration of 0.18 g/ml. The crystal was split into parts to reflect the image of the coated surface and the uncoated bulk of the crystal.

Fig. 7.4 shows the surfaces of compressed discs of KCl powder before and after encapsulation. In micrograph (A) it is clear that the surface of the uncoated crystal is smooth and the boundaries between the compressed particles are obvious. Micrograph (B) shows the morphology of the polymer layer formed on the disc surface by encapsulation. The boundaries between the particles are quite clear which indicates the polymer layer is too thin to hide them. In (C) it is clear that polystyrene is a brittle membrane as it is torn by handling the sample.

Fig. 7.5 shows TEM micrographs of the surface print of KCl crystal before and after encapsulation indicating a smooth flat surface before coating. The smooth surface disappeared after coating by polystyrene and shows a changed surface morphology. Dark black spheres appear on the surface which were due to a polymer formed in solution and deposited on the polystyrene film surface.

Fig. 7.6 shows the topography of polystyrene film on the surface of KCl crystal at different magnification. The polystyrene film appears to be porous.

Fig. 7.7 shows the TEM micrograph of the polystyrene film formed on the crystal surface and the electron diffraction of the polystyrene film presented by a ring pattern.

Fig. 7.8 shows the micrographs of polystyrene particles collected from the film

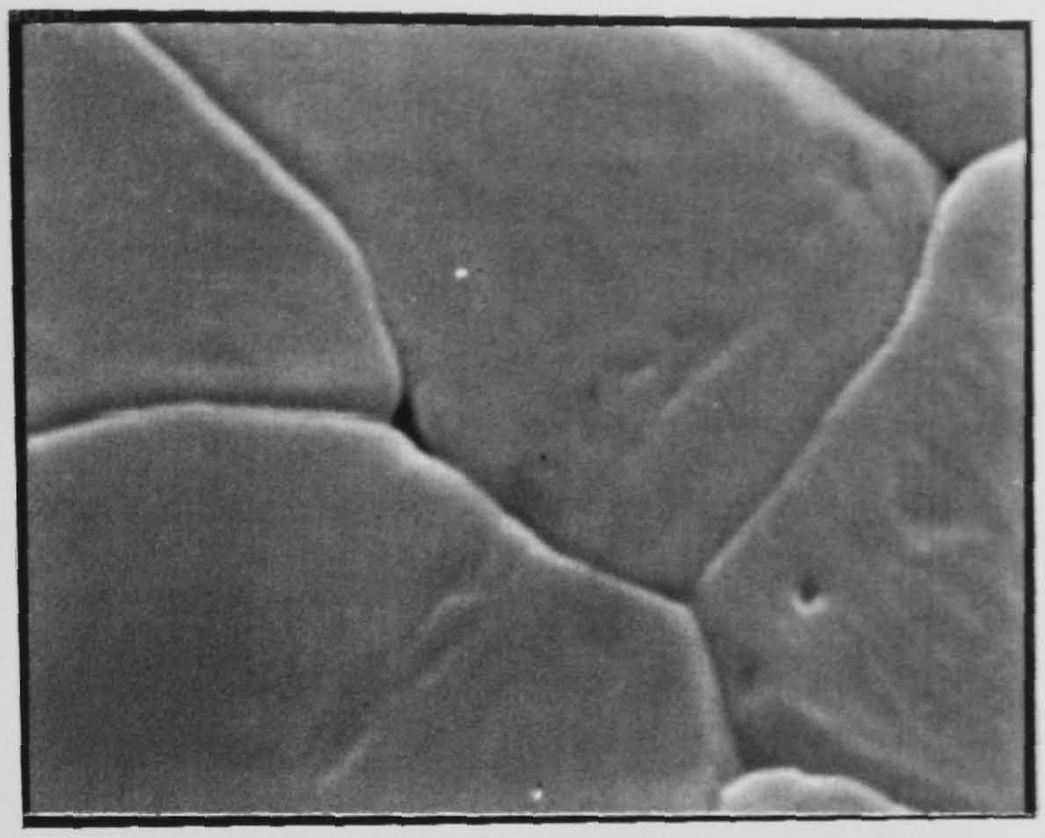

(A)

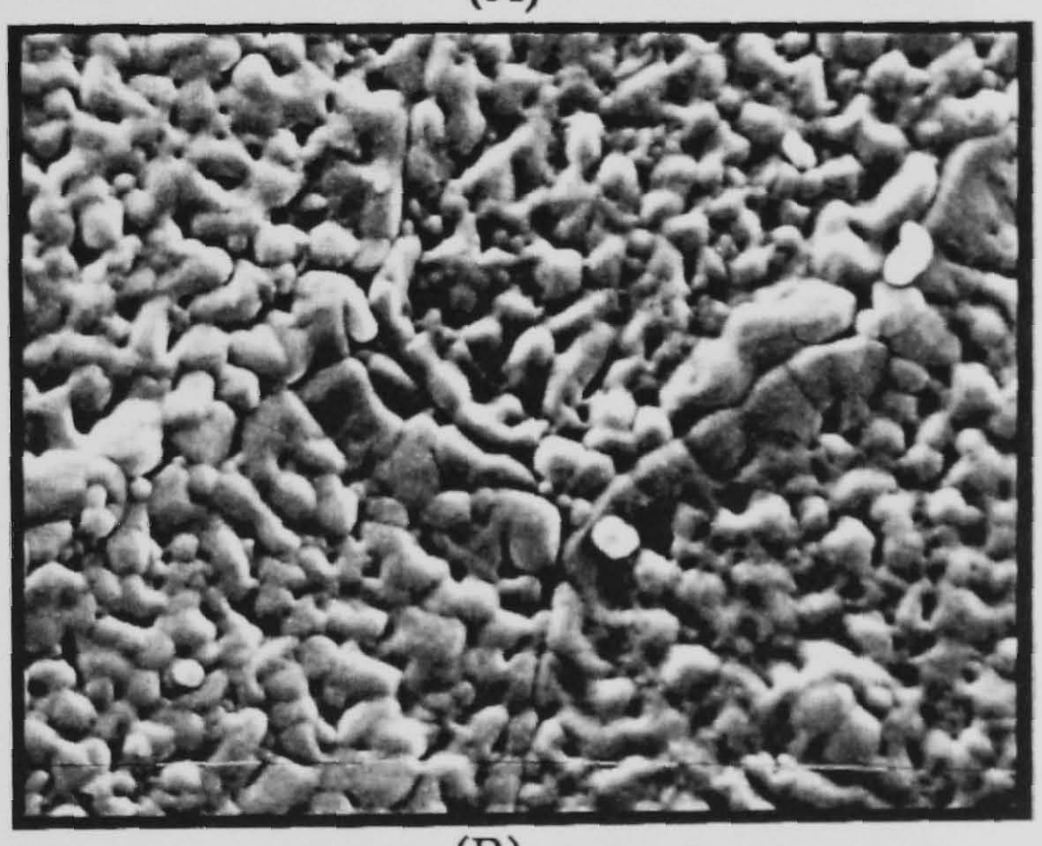

(B)

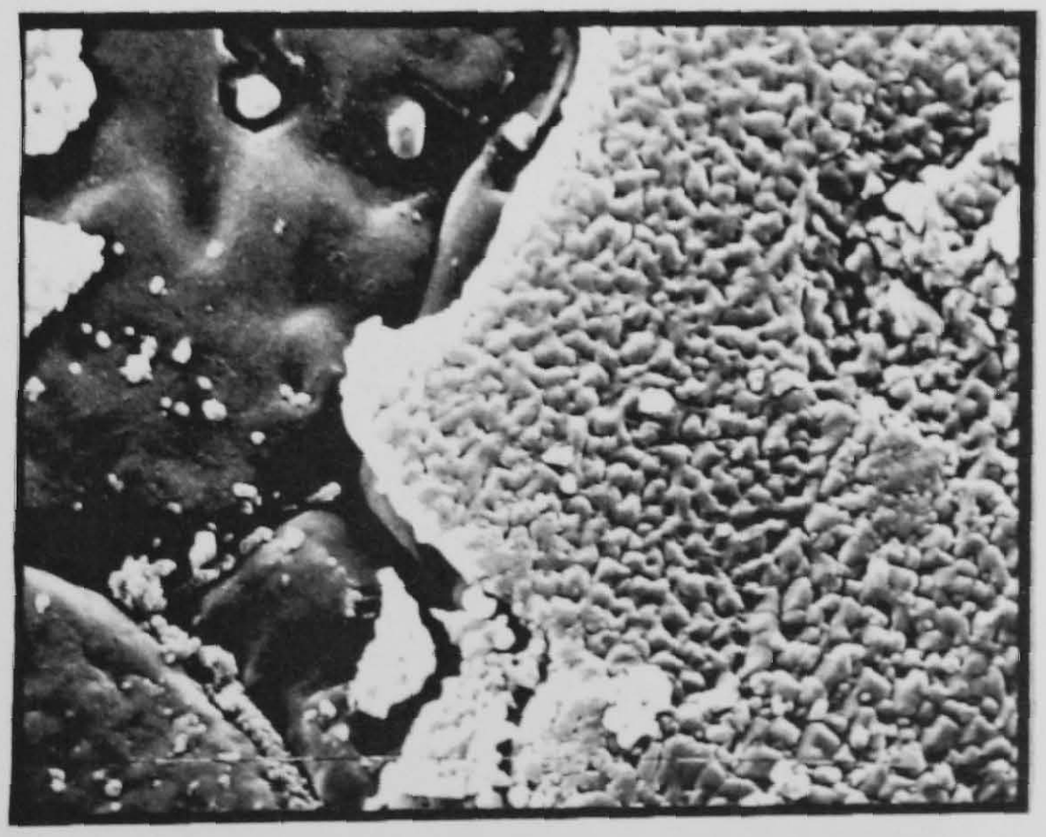

(C)

Fig. 7.4 (A) SEM micrograph of uncoated surface of KCl powder compressed disc, magnification 10,000
(B) SEM micrograph of the coated surface of KCl disc, magnification 10,000
(C) Micrograph of the disc surface underneath the torn polystyrene film, magnification 5000

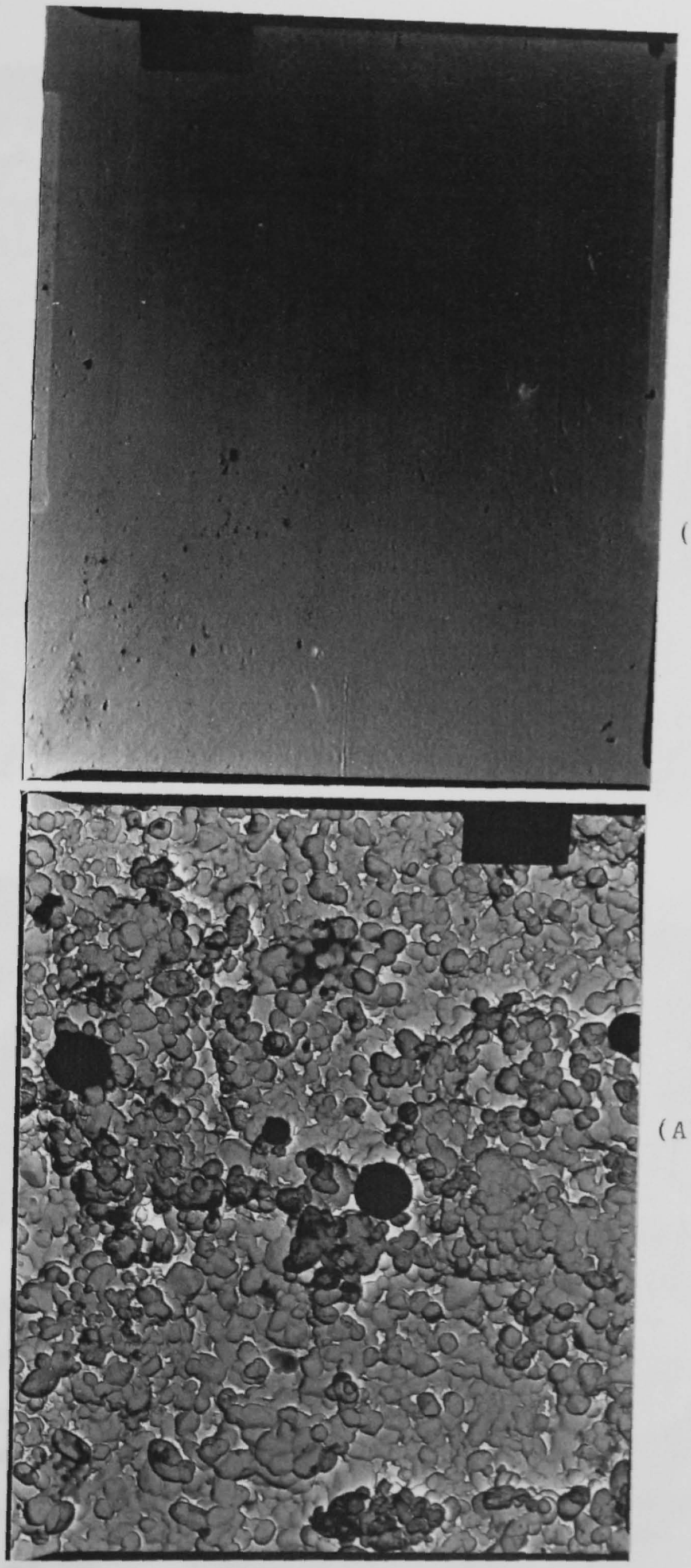

(B)

(A)

Fig. 7.5 (A) TEM micrograph of the surface feature of KCl crystal encapsulation, magnification 6000
(B) TEM micrograph of the topography of KCl crystal surfaced after encapsulation with polystyrene, magnification 6000

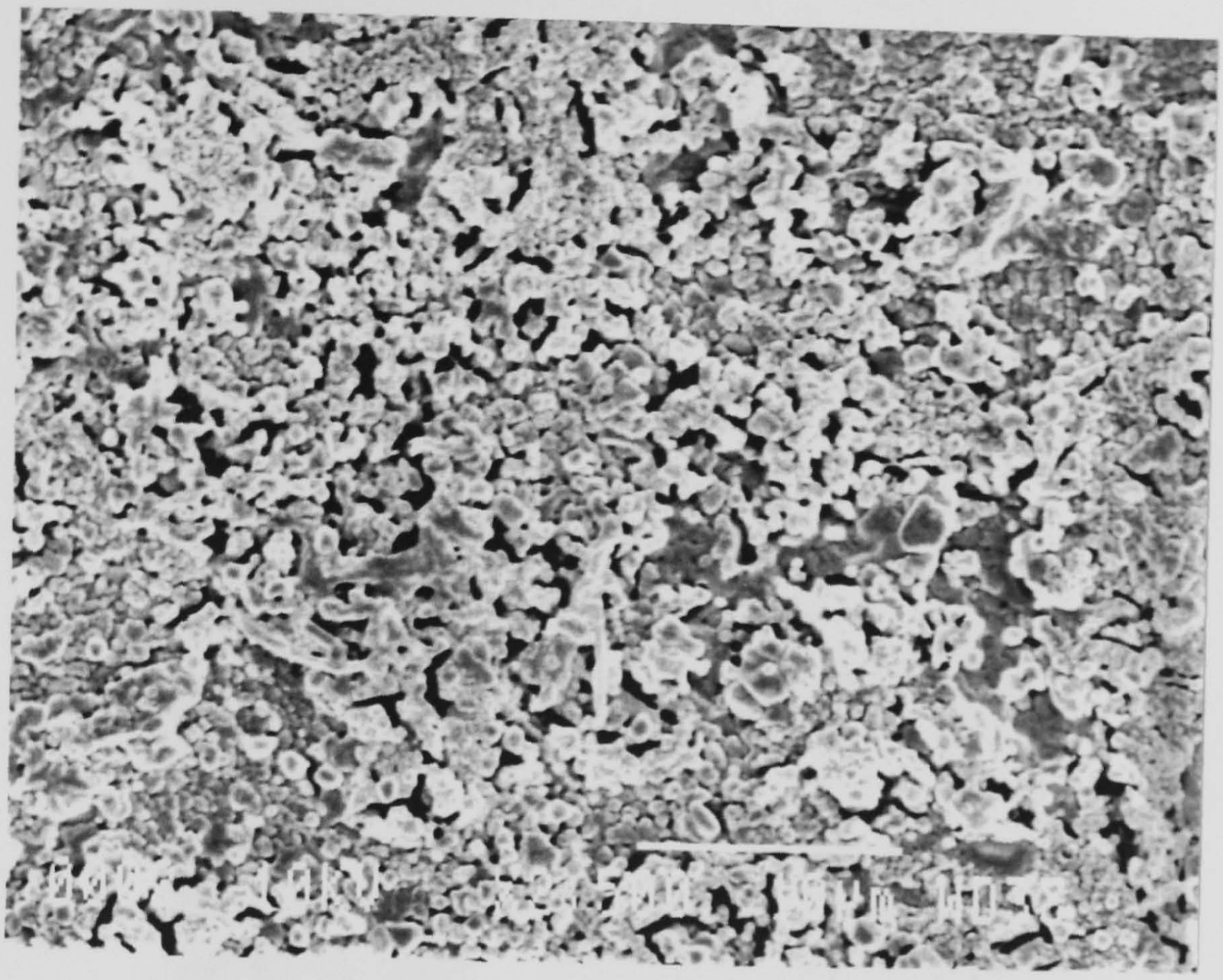

(A)

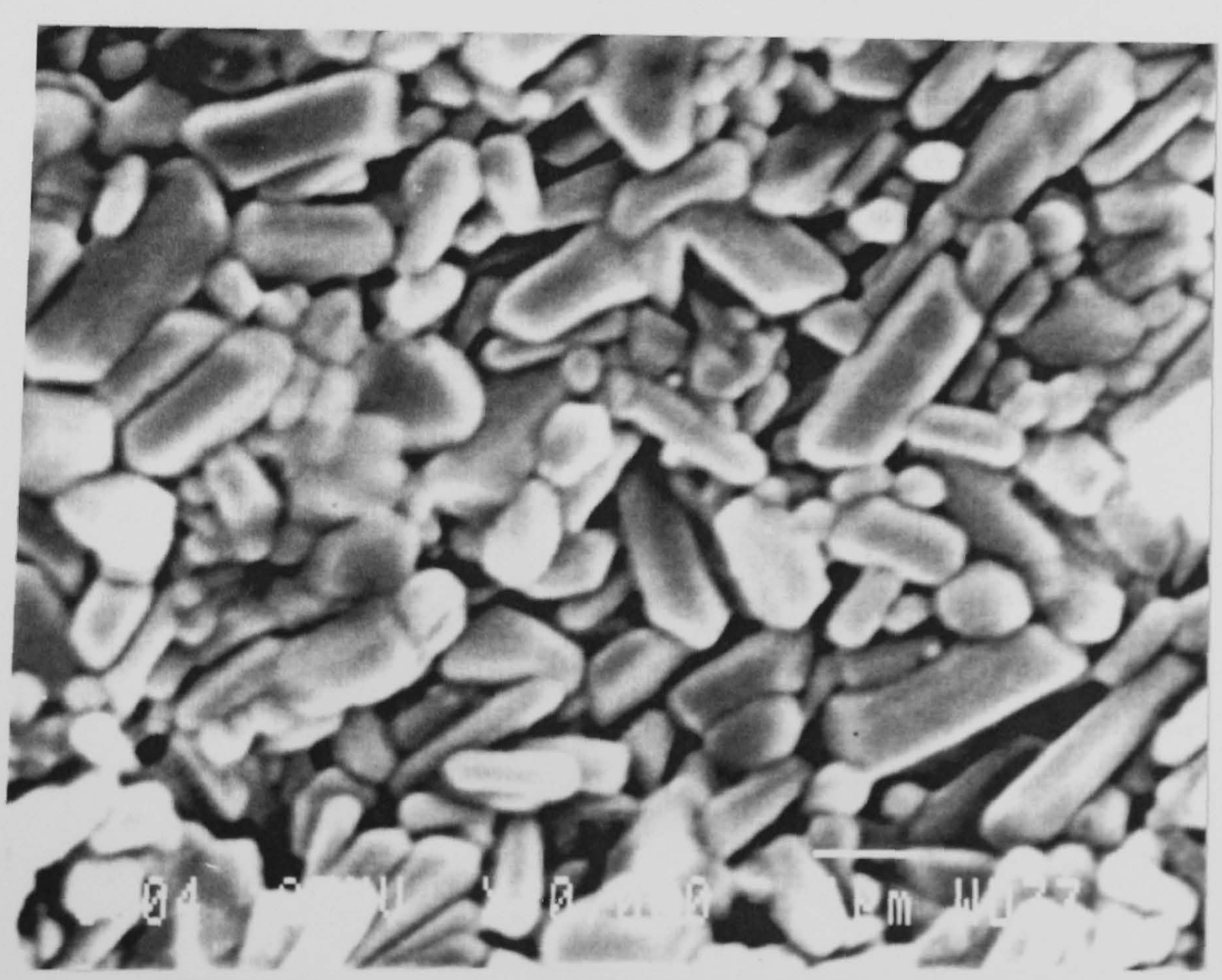

(B)

Fig. 7.6 SEM micrograph of a microporous polystyrene film encapsulating KCl crystal. The magnification in (A) and (B) is indicated in the scale marking.

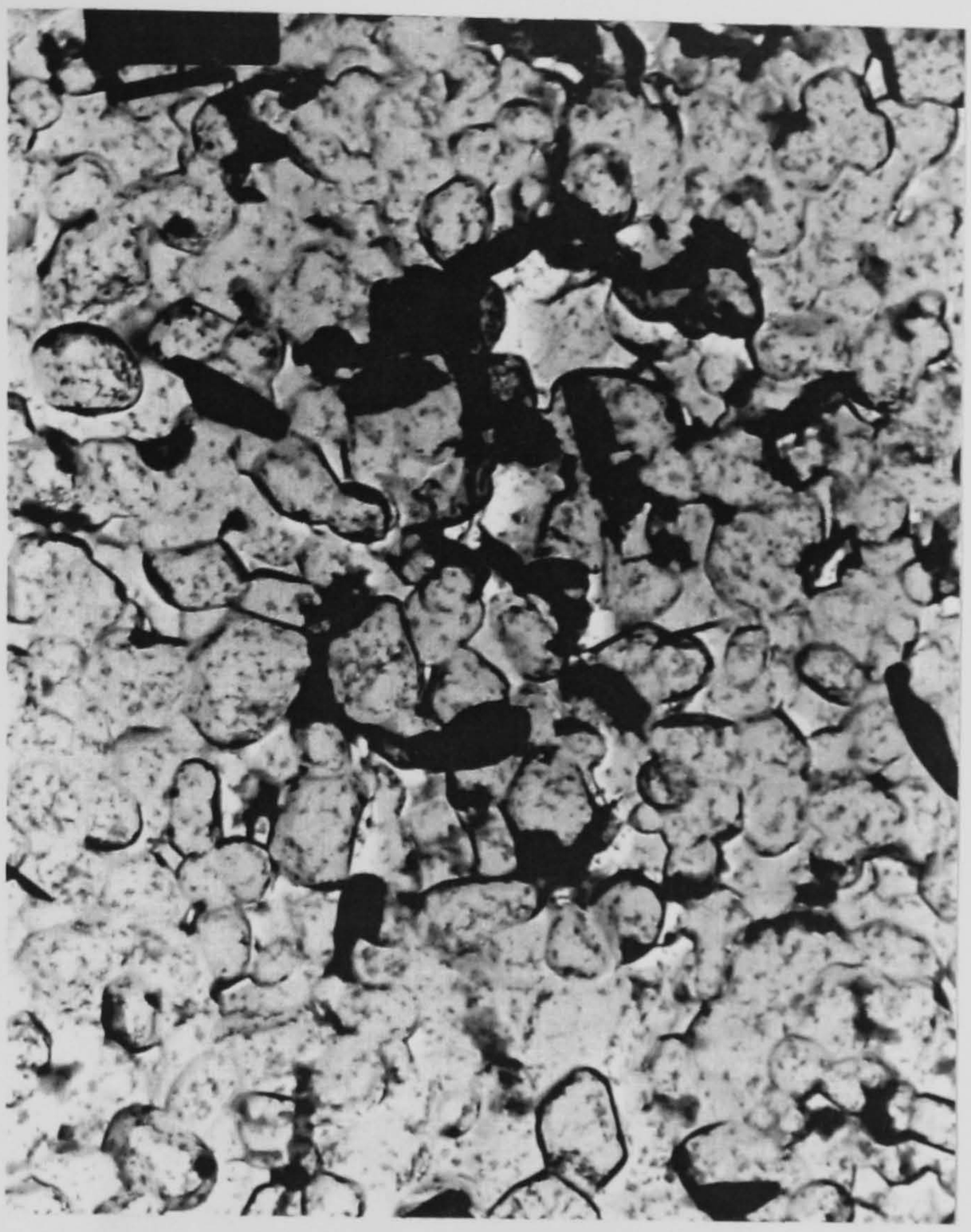

(A)

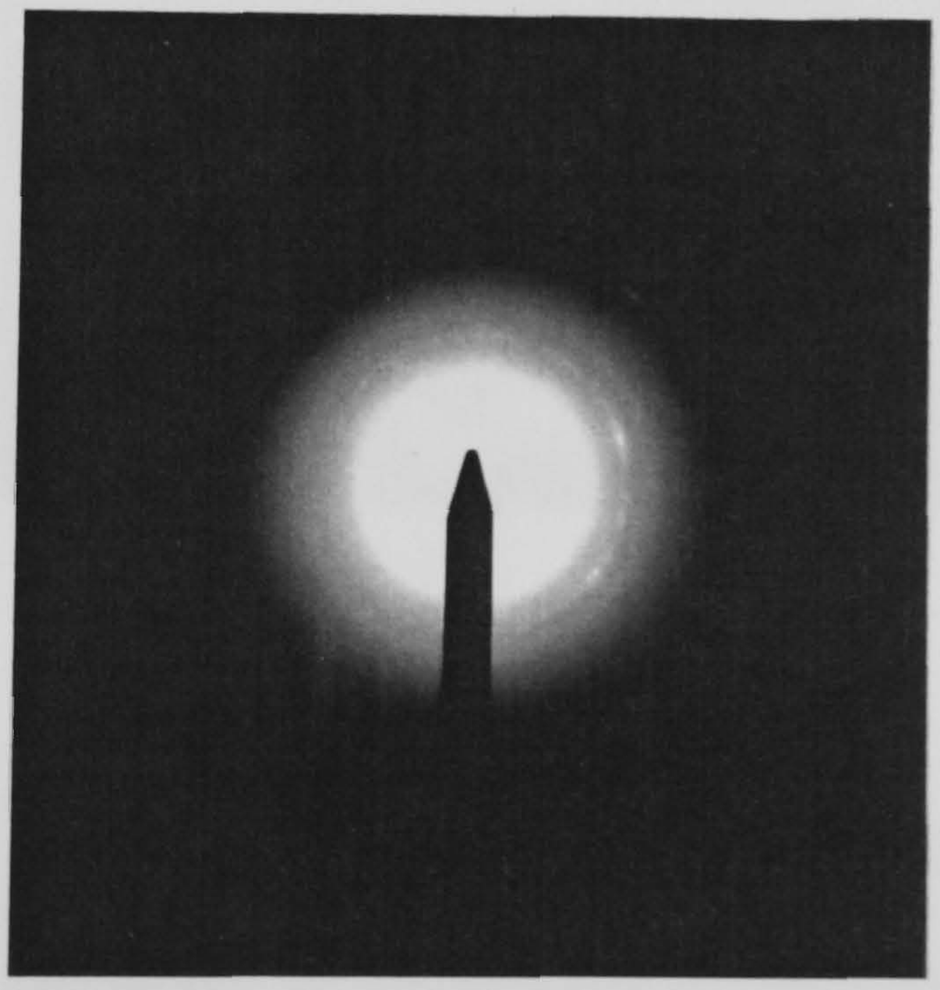

(B)

Fig. 7.7 (A) TEM micrograph of the polystyrene film topography on the KCl crystal surface, magnification is 3000
(B) Electron diffraction pattern of polystyrene film

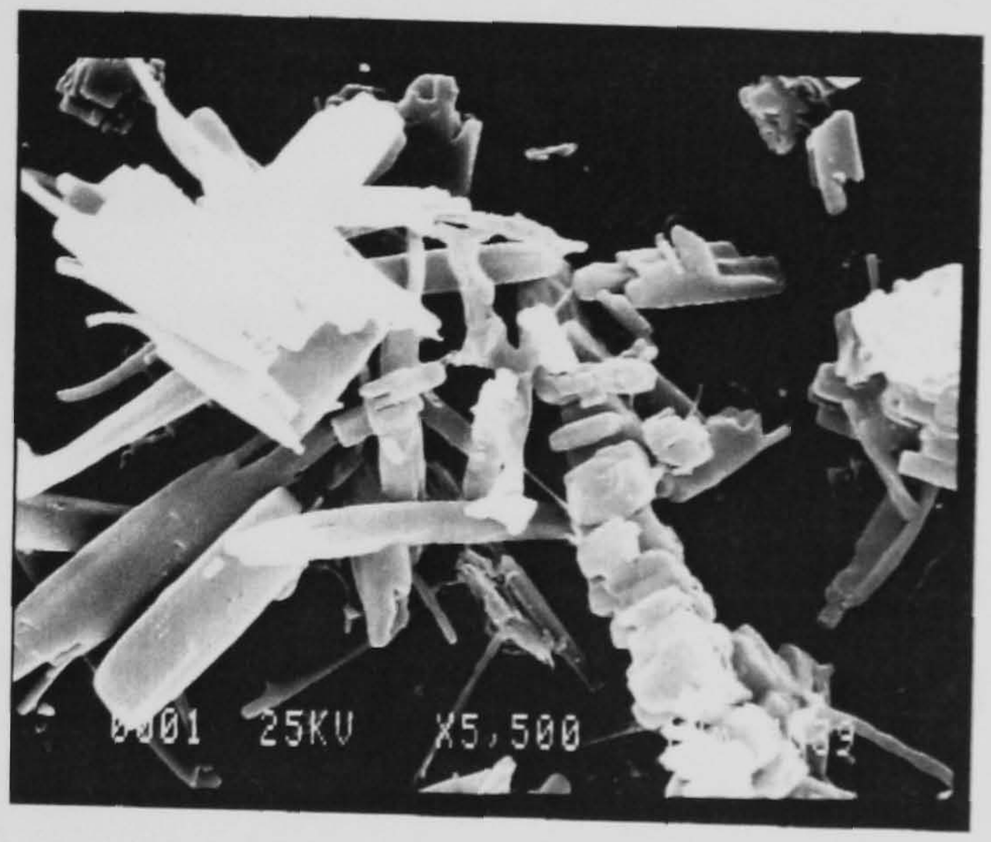

(A)

(B)

Fig. 7.8 (A) SEM micrograph of polystyrene particles formed on the surface.
(B) SEM micrograph of the precipitated polystyrene total extract (solid and soluble polystyrene). Magnification is given on the micrographs.

formed on the crystal surface and the particles of the precipitated polystyrene total extract of both the soluble polymer and solid polymer formed on the surface.

Fig. 7.9 shows two particles of KCl (250–355 μm) coated with polystyrene in micrograph (A) and the morphology of the polystyrene layer on the surface in micrograph (B) which indicates a microporous coating. Micrograph (C) shows the disintegrated shells of polystyrene obtained after KCl was released. Micrograph (D) shows an empty disintegrated shell which was encapsulating KCl particle and micrograph (E) is the surface morphology of the polystyrene shell shown in (D). It confirms the porous coating nature of the polystyrene membrane.

Fig. 7.10 shows the morphology of polystyrene film coating KCl particle. The encapsulation was carried out at −12°C and micrograph (A) indicates the formation of a microporous polystyrene membrane. Micrograph (B) shows the disintegrated shells obtained after all KCl has been released from the particles. Micrograph (C) shows the morphology of a polystyrene film formed without α–monoolein surfactant on the surface of 500 μm KCl particles. The polystyrene film has voids and seems to be porous.

7.3.2 Potassium Chloride Encapsulated with C1 Polymer

Fig. 7.11 shows the morphology of a C1 polymer membrane on the surface of a KCl particle (250 μm). The micrographs (A) and (B) indicate that a continuous film was obtained using the C1 polymer. Micrography (C) show the dry shells of C1 polymer obtained after the release of their contents. The C1 polymer shells show no signs of rupture or disintegration.

Fig. 7.12 shows that C1 polymer shells retain the shape of the original

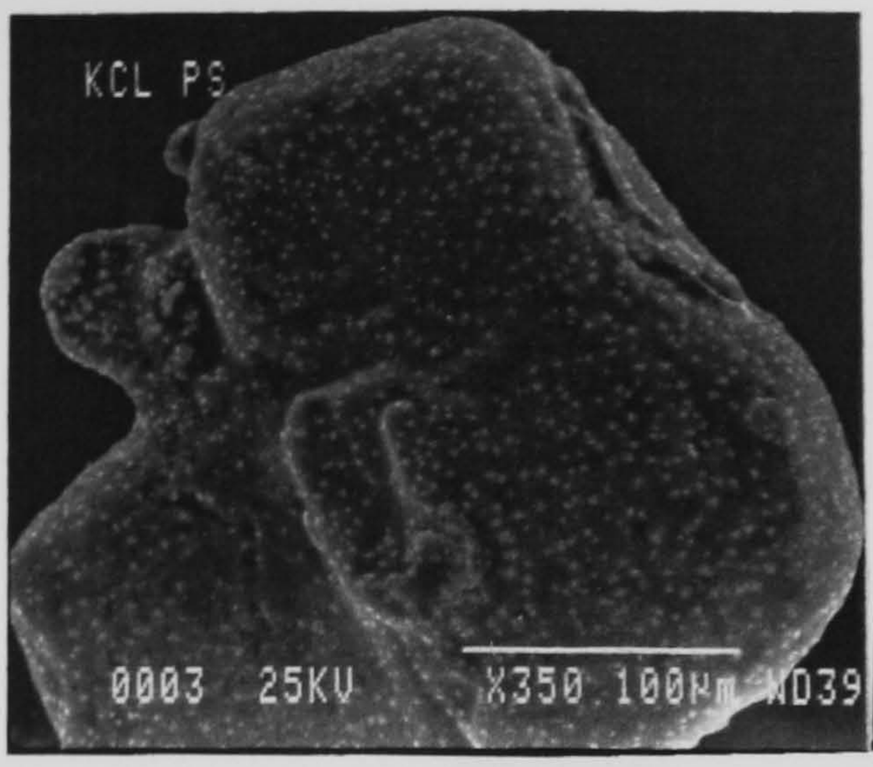

(A)

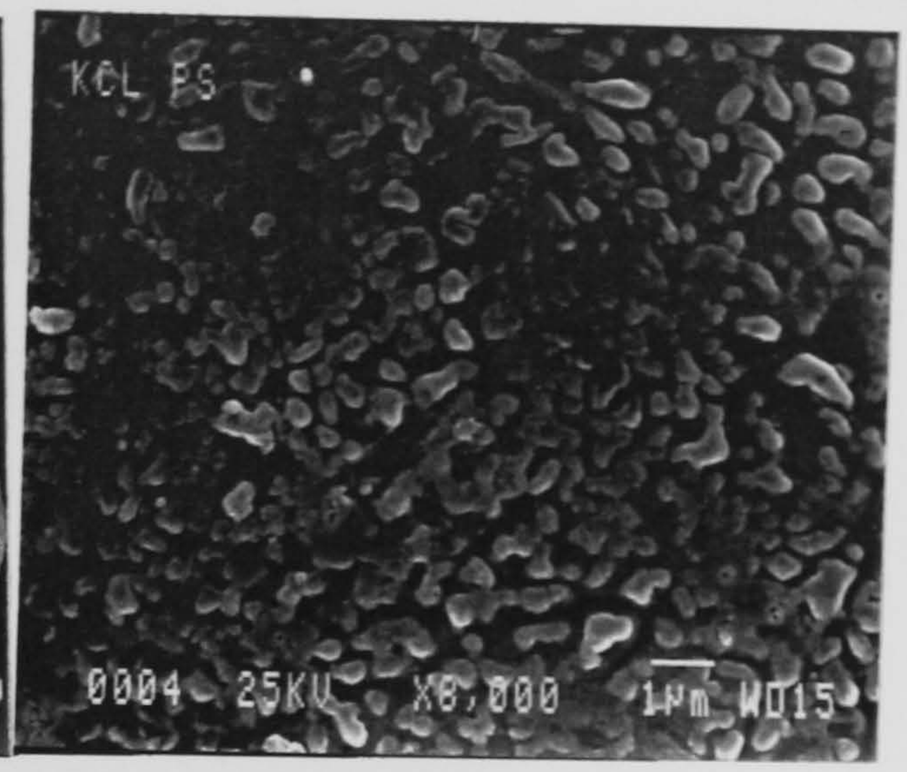

(B)

(C)

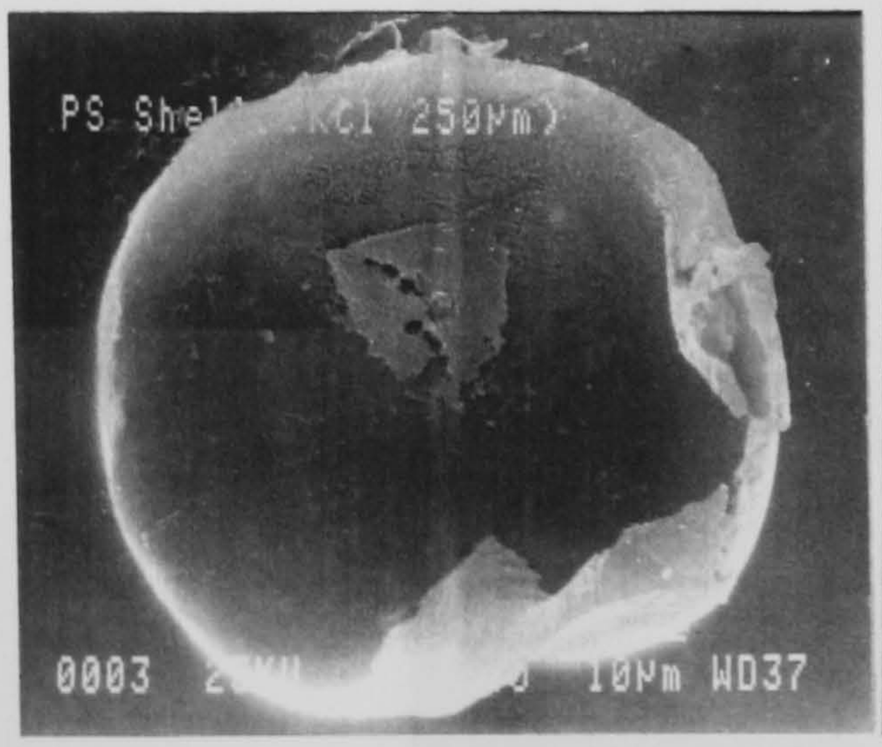

(D)

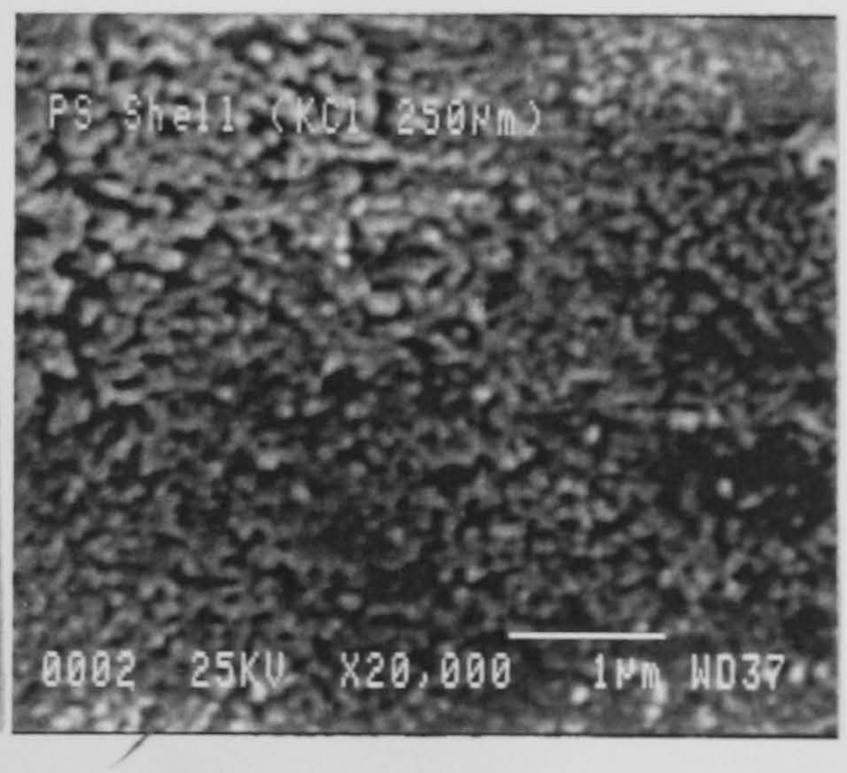

(E)

Fig. 7.9 (A) SEM micrograph of KCl particles coated with polystyrene.
(B) SEM micrograph of the surface morphology of polystyrene film on KCl particle surface.
(C) SEM micrograph of collected disintegrated polystyrene shells, KCl has been released.
(D) SEM micrograph of an empty shell of polystyrene, magnification 60.
(E) SEM micrograph of empty shell surface of polystyrene

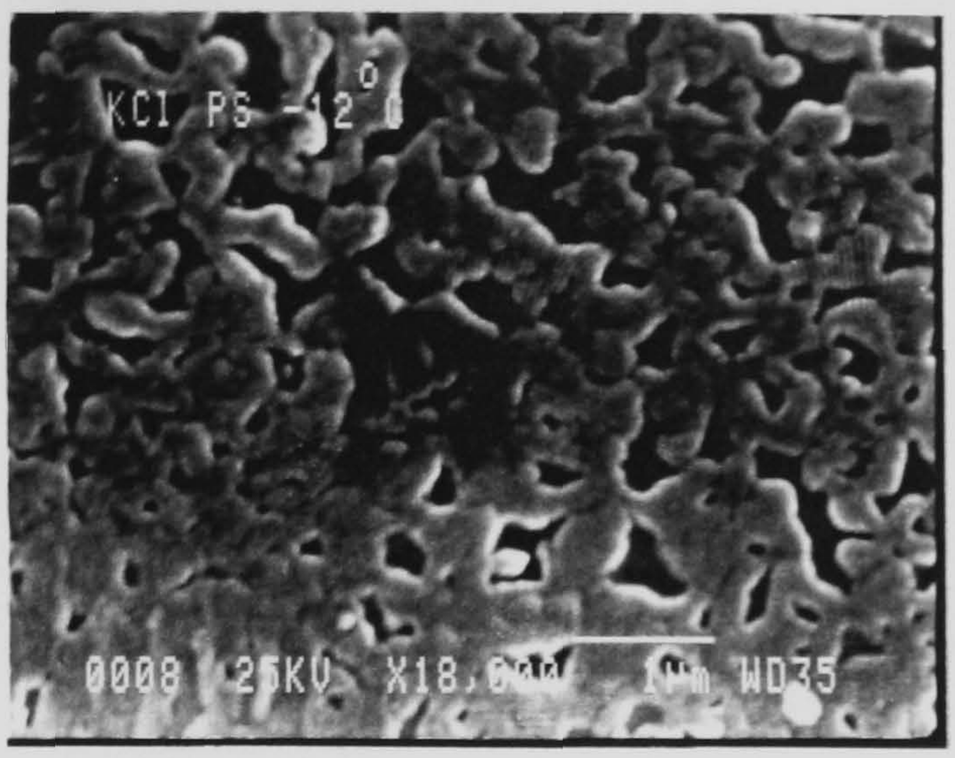

(A)

(B)

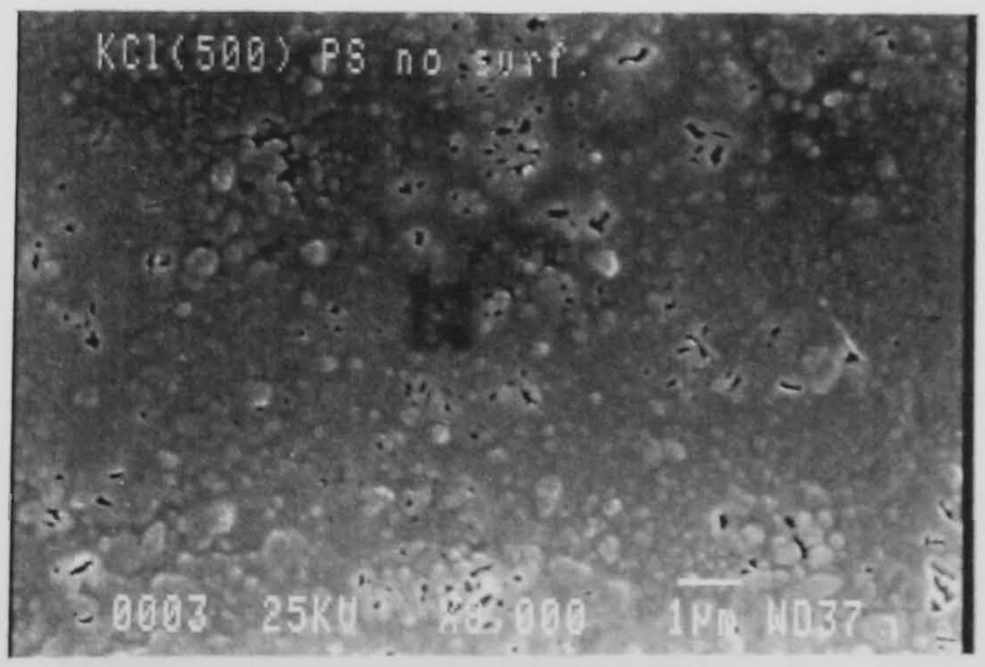

(C)

Fig. 7.10 (A) SEM micrograph of porous polystyrene film on KCL particle surface (encapsulated at (−12°C).
(B) SEM micrograph of the disintegrated shells after releasing KCl, magnification 60.
(C) SEM micrograph of polystyrene formed without surfactant on KCl particle (size 500 μm)

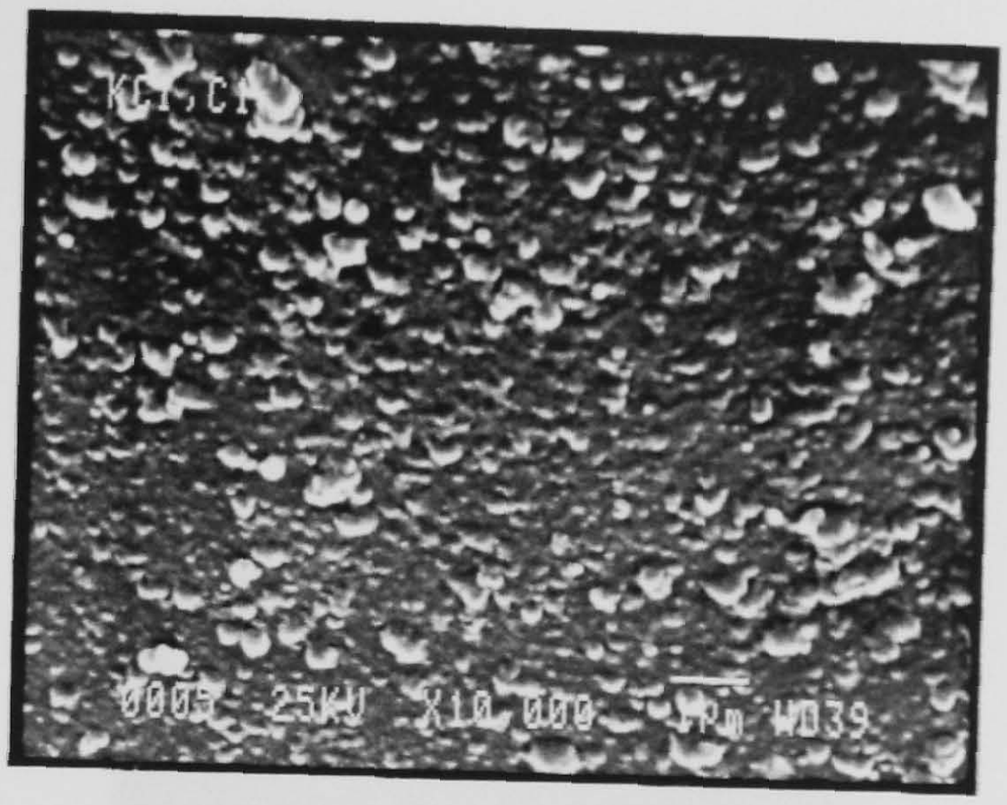

(A)

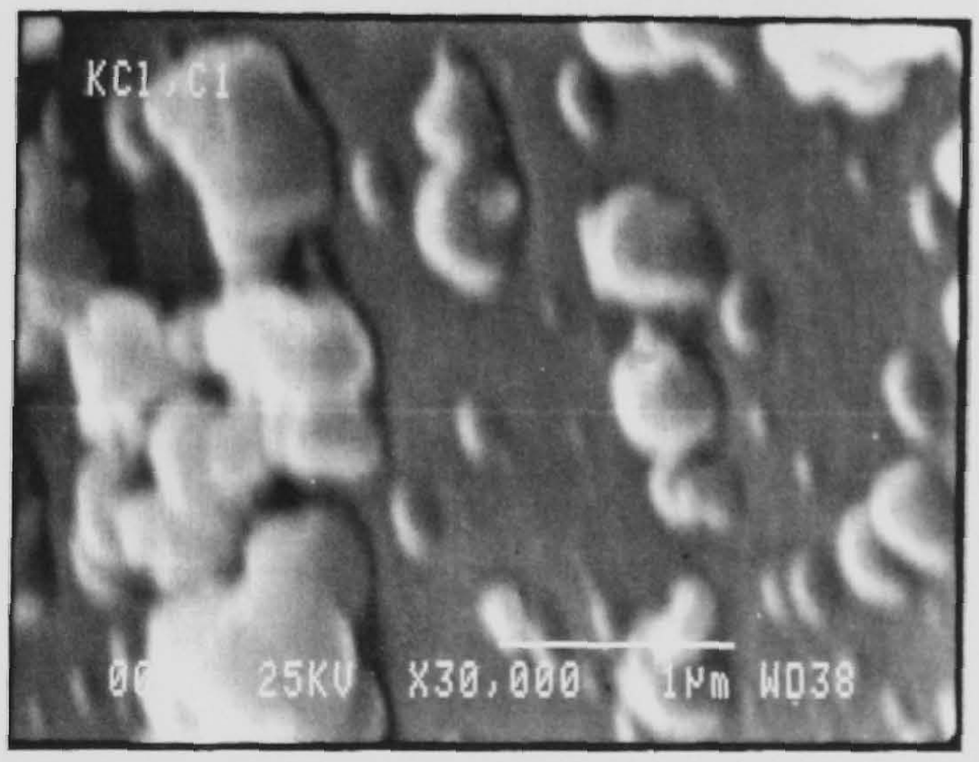

(B)

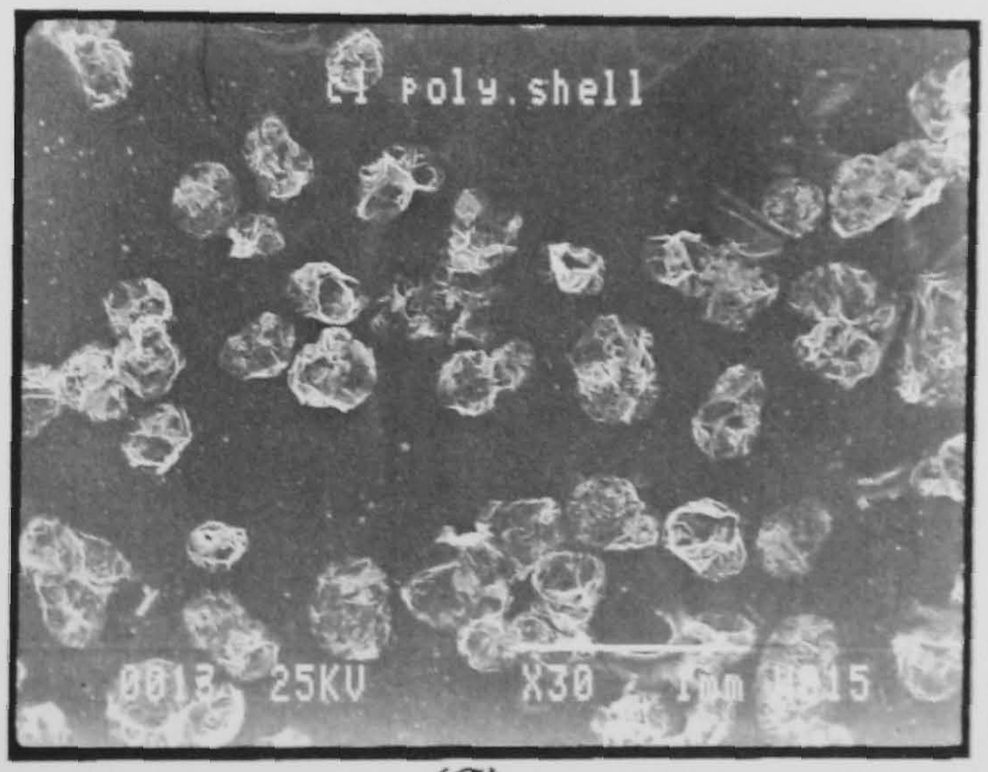

(C)

Fig. 7.11 (A) SEM micrograph of the morphology of Cl polymer membrane on the surface of KCl particle (250–355 μm).
(B) The same surface at higher magnification.
(C) SEM micrograph of the collected Cl polymer shells after release of KCl.

(A)

(B)

Fig. 7.12 (A) Cl polymer shells in water after KCl was released. The shells retained the original shape of KCl particles (250–355 μm).
(B) An optical micrograph of a dry shell of Cl polymer.

encapsulated particles.

7.3.3 Potassium Chloride Encapsulated with GMA Polymer

Fig. 7.13 (A) is a micrograph of KCl particle (500 μm) encapsulated with GMA polymer shell and (B) is the polymer shell left in water after the core particle has been released. Black rings are observed on the surface due to bubbles from the external phase caused by the pumping. Micrograph (C) shows GMA polymer shells suspended in water. It is obvious that they retain the shapes of KCl particles.

Fig. 7.14 shows the dry KCl particle (710 μm) encapsulated with GMA polymer shell. The progress of the dissolution of KCl inside the polymer shell is illustrated by the micrographs showing that the KCl particle inside the shell is getting smaller and the shell membrane has become more visible. Air bubbles appear as black rings on the surface and there is no signs of rupture or disintegration of the shell.

Fig. 7.15 A large number of GMA polymer shells appear in micrograph (A). Surface folding of the shells is observed as well as flocculation. This indicates the rubbery nature of the GMA polymer shells. Micrograph (B) illustrates the porous topography of the GMA membrane. Micrograph (C) is the polymer shell formed without surfactant on the surface of KCl (500 μm)

7.3.4 Potassium Chloride Encapsulated with Epikote Polymer

Fig. 7.16 shows the topography of Epikote polymer shell on the surface of KCl particle. It indicates a glassy continuous film coating. Polymer formed in solution and deposited on the shell surface is also observed (white particles)

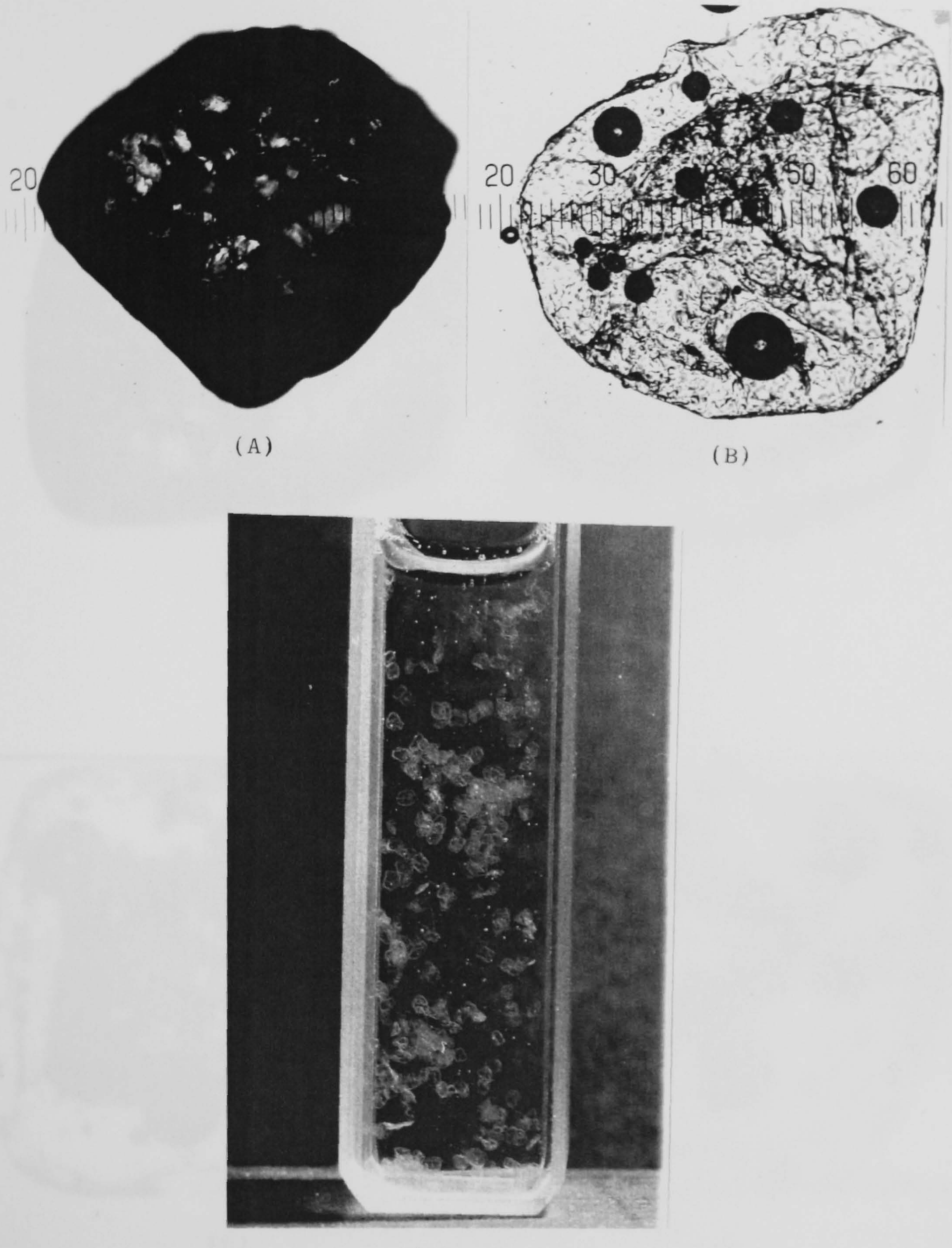

(A) (B)

(C)

Fig. 7.13 (A) Optical micrograph of KCl particles (500 μm) encapsulated in GMA polymer shell. (B) Optical micrograph of the shell left in water after the release of KCl particle. Air bubbles (black rings) are observed on the surface. (C) The shell suspended in water after releasing KCl particles. The shell retain the shape of the KCl encapsulated particles.

(A)

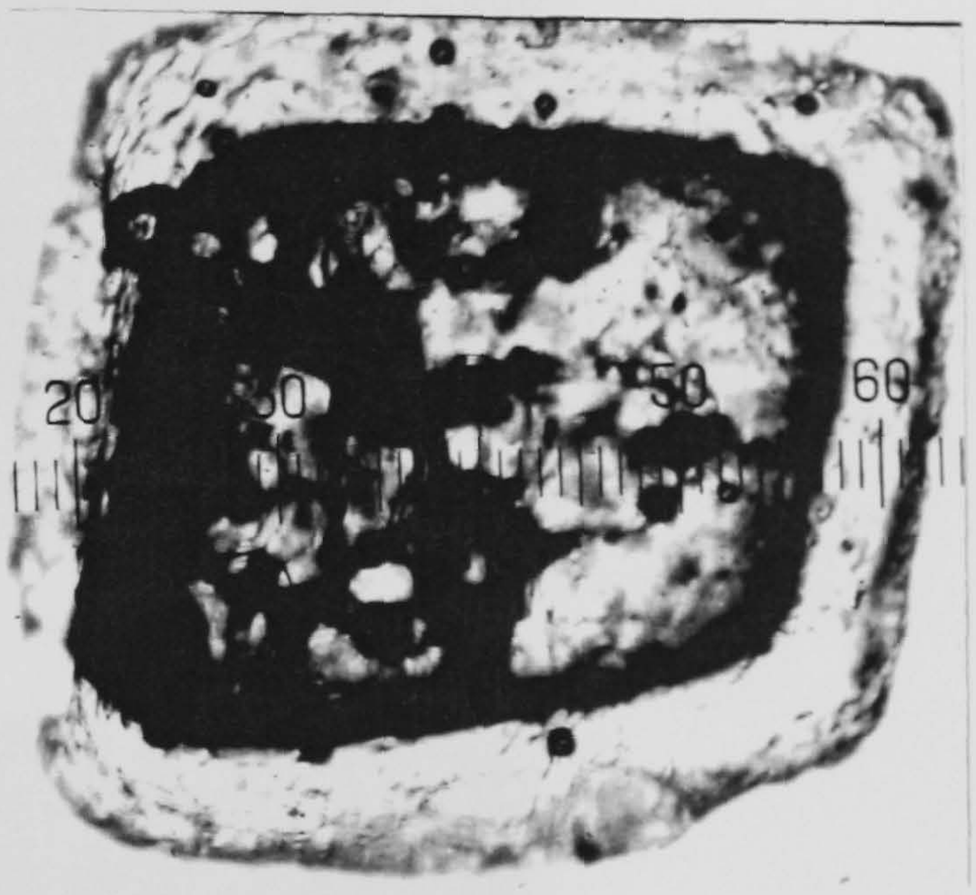

(B)

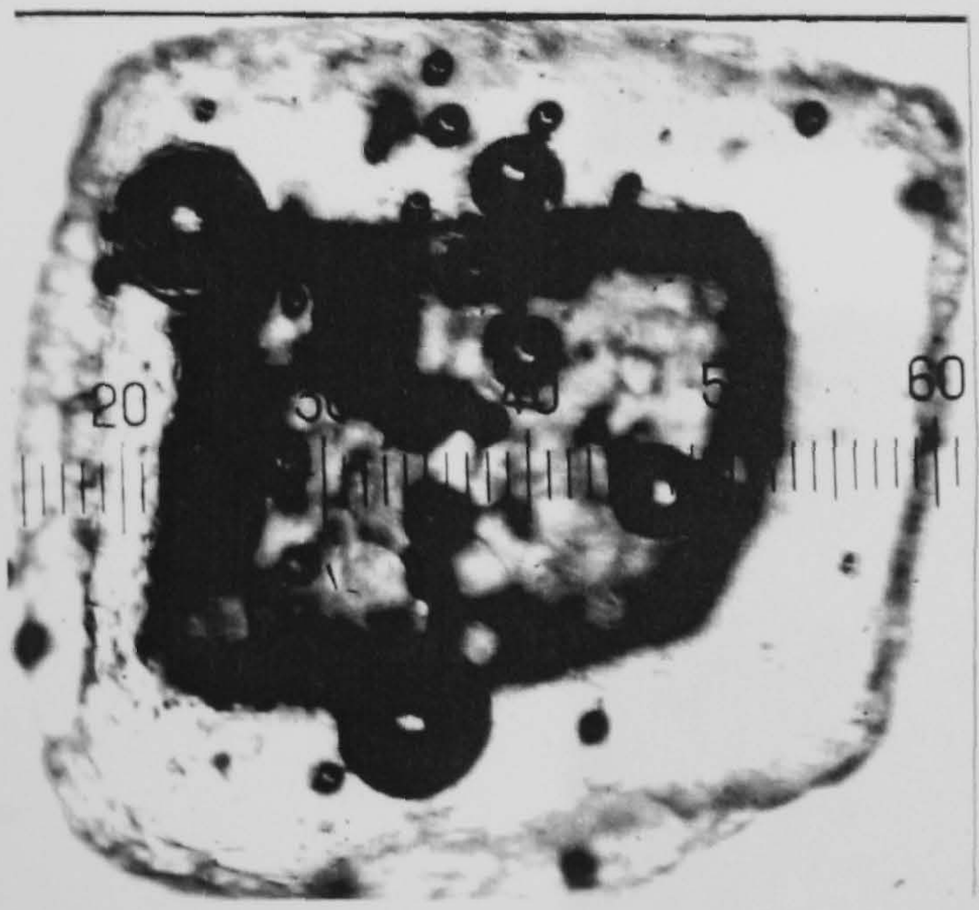

(C)

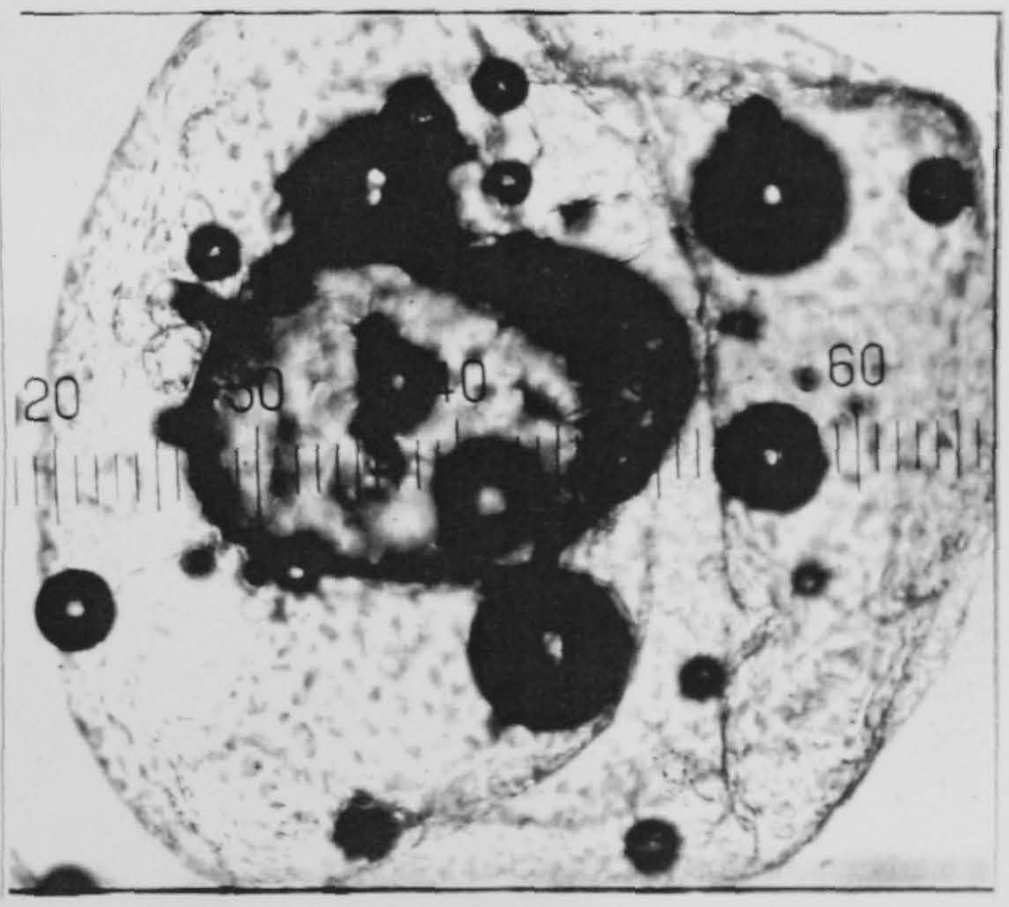

(D)

Fig. 7.14 An optical micrograph (A) of dry KCl particle (710 μm) encapsulated by GMA polymer shell. The micrographs (B), (C) and (D) illustrate the dissolvation progress of the core particle (KCl)

(A)

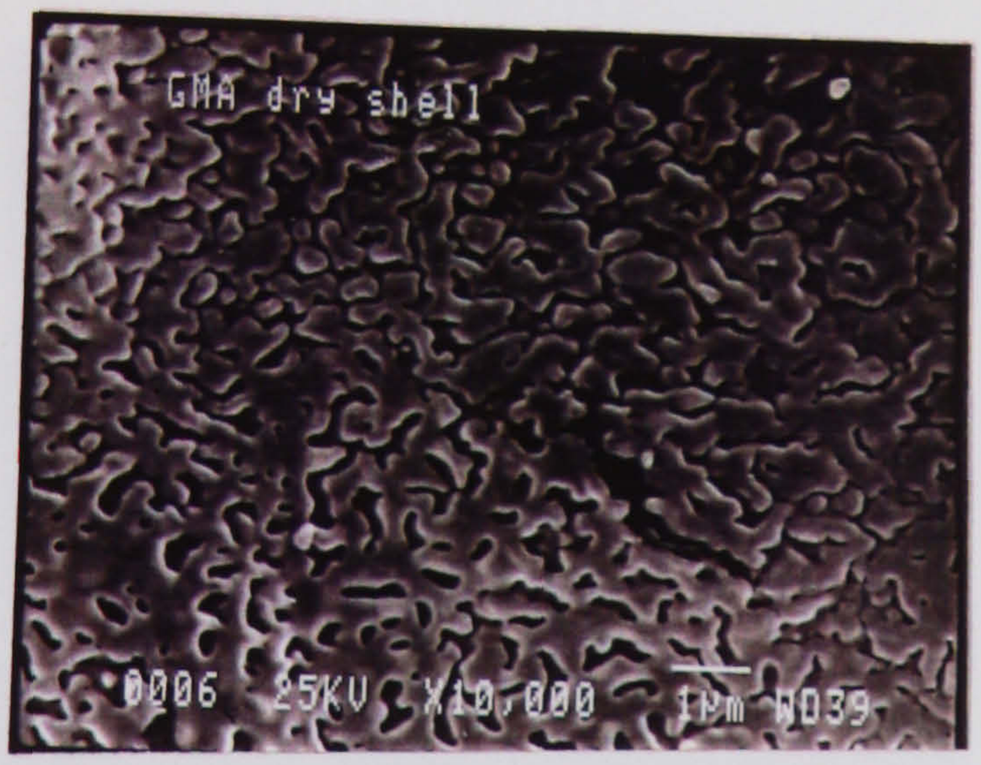

(B)

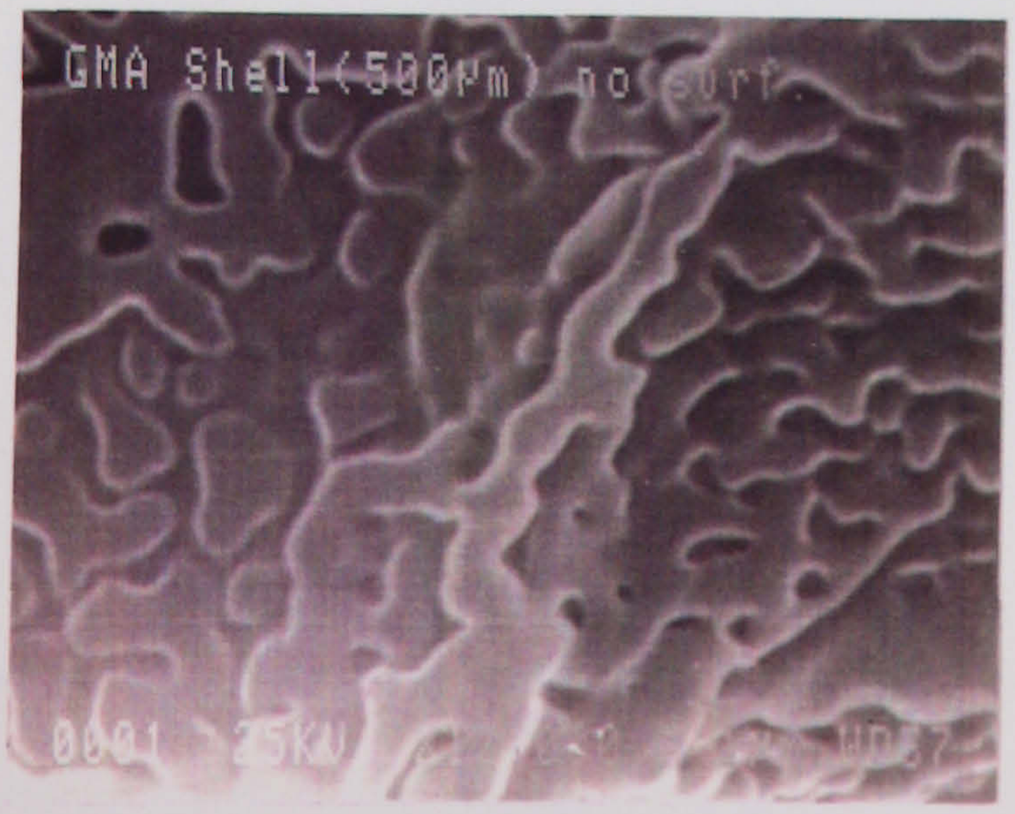

(C)

Fig. 7.15 SEM micrograph of a number of empty shells of GMA polymer. Surface folding and adhesion of the shells are observed. SEM micrographs (B) and (C) show the surface topography of GMS poly shells formed on KCl surface (250 μm) and that on KCl (500 μm withour surfactant) respectively.

(A)

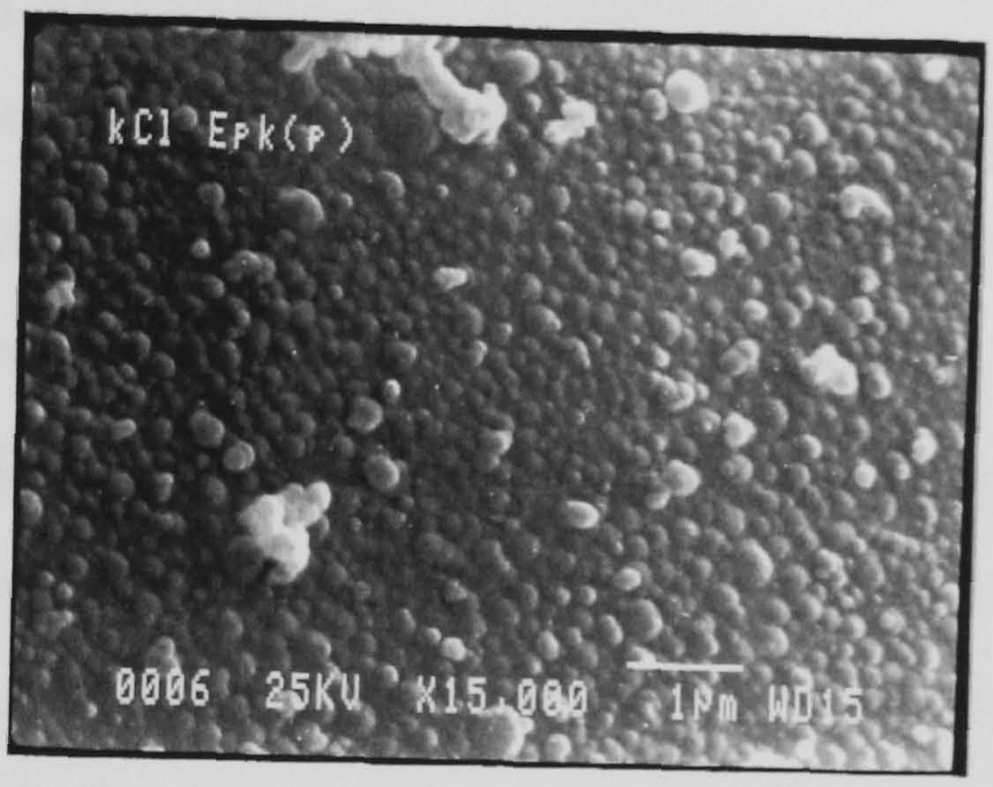

(B)

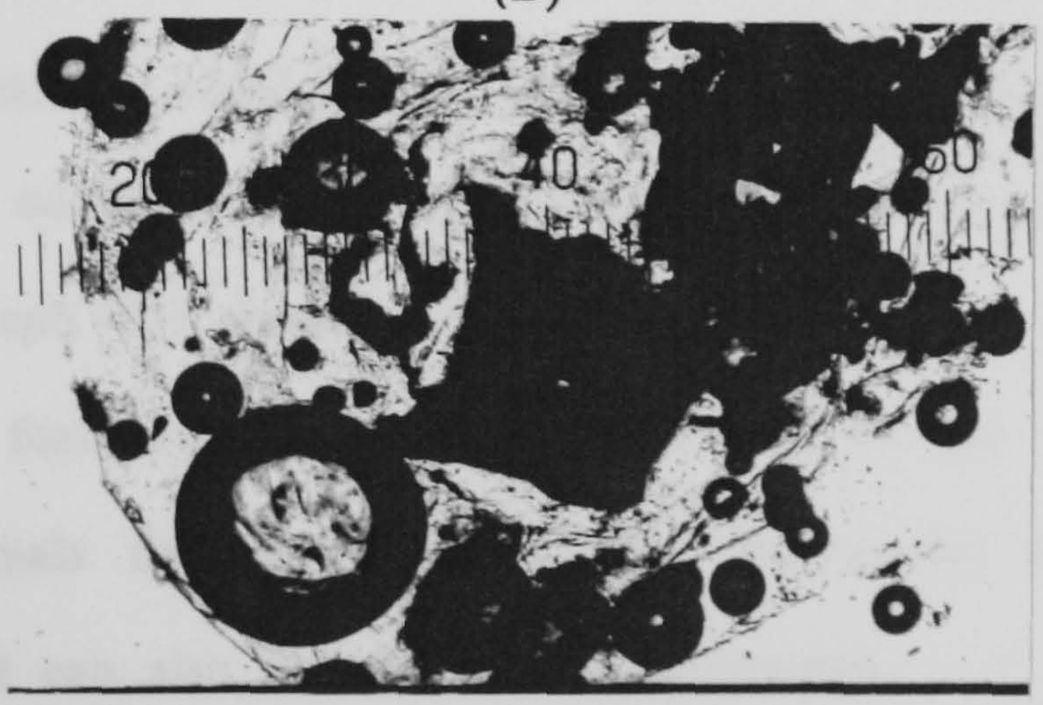

(C)

Fig. 7.16 SEM micrograph of the surface of Epikote polymer shell encapsulating KCl particle (A). It reveals continuous coating. In micrograph (B) polymer particles from solution deposited on the shell surface are observed (white particle). The optical micrograph (C) reveals the polymer shell as well as the deposited polymer on the shell surface during the dissolution of the core particle.

micrograph (B). This is confirmed also from the micrograph (C) showing the dissolution of KCl particle inside the Epikote shell observed in the micrograph with a dark thick part of the deposited polymer.

7.3.5 β–Estradiol Encapsulated with Polystyrene

Fig. 7.17 shows the nature and crystallographic structure of β–estradiol particles. It indicates a cohesive force between the particles which causes them to coagulate in lumps. The micrographs show also the morphology of the particles encapsulated with polystyrene.

7.3.6 β–Estradiol Encapuslated with C1 Polymer

Fig. 7.18 shows the crystals of β–estradiol coated with C1 polymer in micrograph (A). Micrographs (B) and (C) show the shells of C1 polymer encapsulating the crystals at sequential stages of the release period.

7.3.7 β–Estradiol Encapsulated with GMA and Epikote Polymers

Fig. 7.19 shows the β–estradiol crystals encapsulated with GMA polymer at different magnifications in micrographs (A) and (B), while micrograph (C) is the crystals coated with Epikote. Polymer deposited from solution can be seen.

7.3.8 5–Aminosalicylic Acid Encapsulated with C1 Polymers

Fig. 7.20 shows in micrograph (A) the encapsulated 5–aminosalicylic acid with C1 polymer. Micrograph (B) shows the polymer layer on the surface of a crystal, the excess polymer formed in solution and deposited on the crystal can be seen. Micrograph (C) reveals the polymer left after the partial release of the acid. The acid crystals left can also be seen in the micrograph.

7.3.9 Shell Membrane Thickness of C1 Polymer

The C1 polymer shell membrane can be observed from the micrograph given below which shows half of the polymer shell and indicates the very approximate membrane thickness.

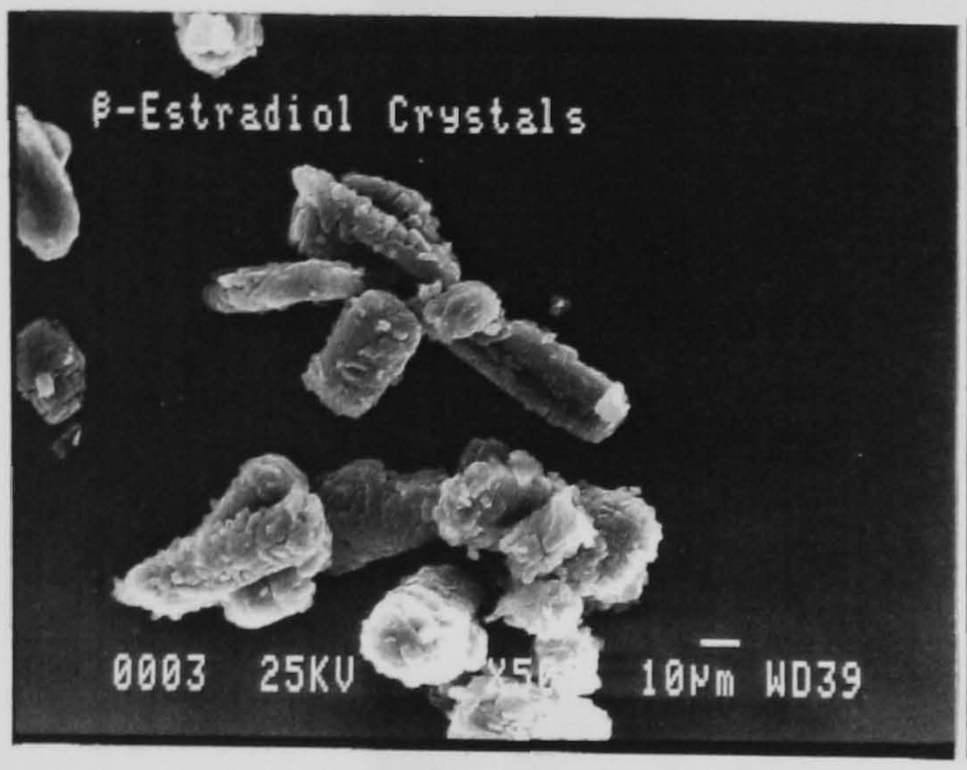

(A)

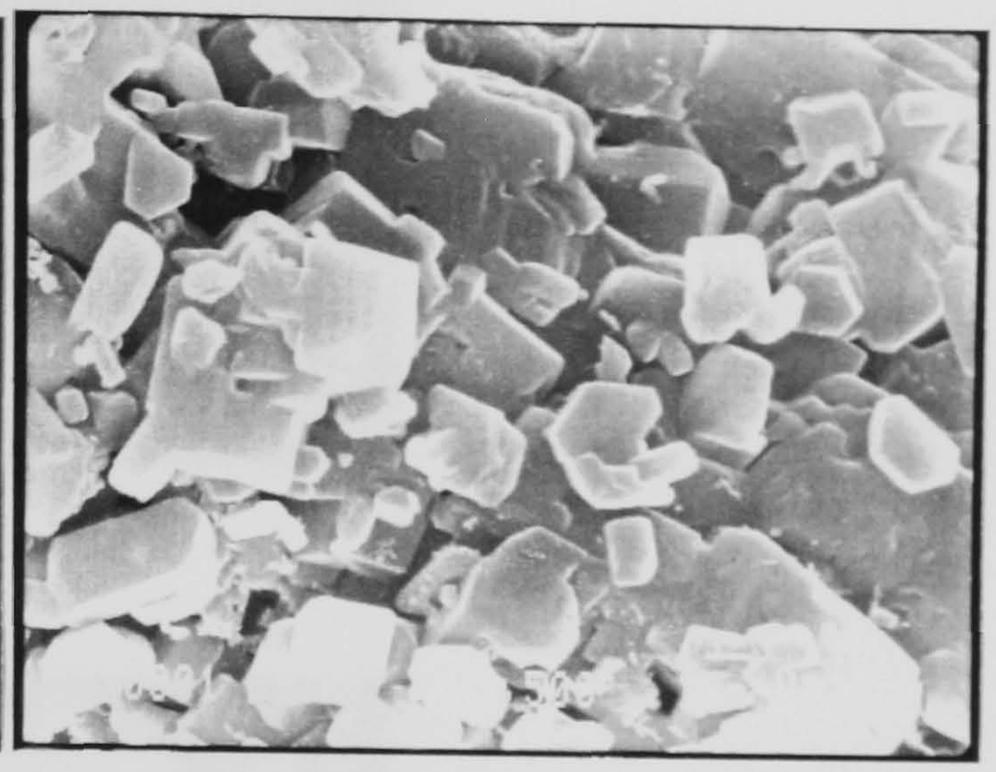

(B)

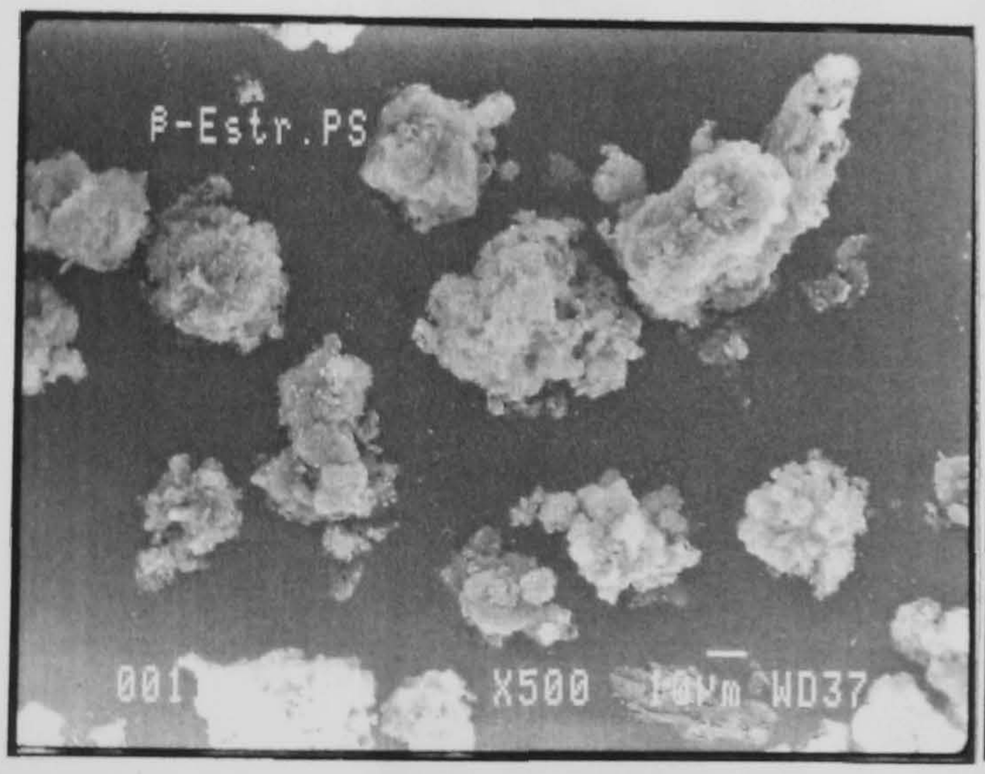

(C)

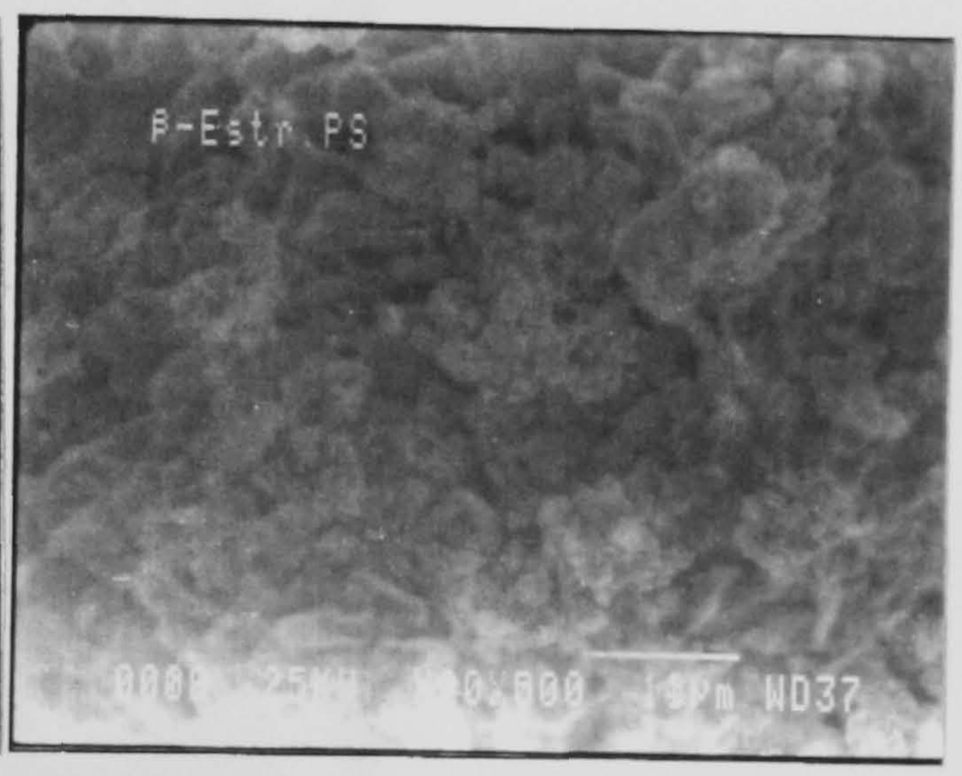

(D)

Fig. 7.17 SEM micrograph (A) and (B) for β–estradiol illustrate the flocculation of the particles and their crystallographic features. (C) and (D) are the SEM micrographs of β–estradiol encapsulated with polystyrene at different magnifications.

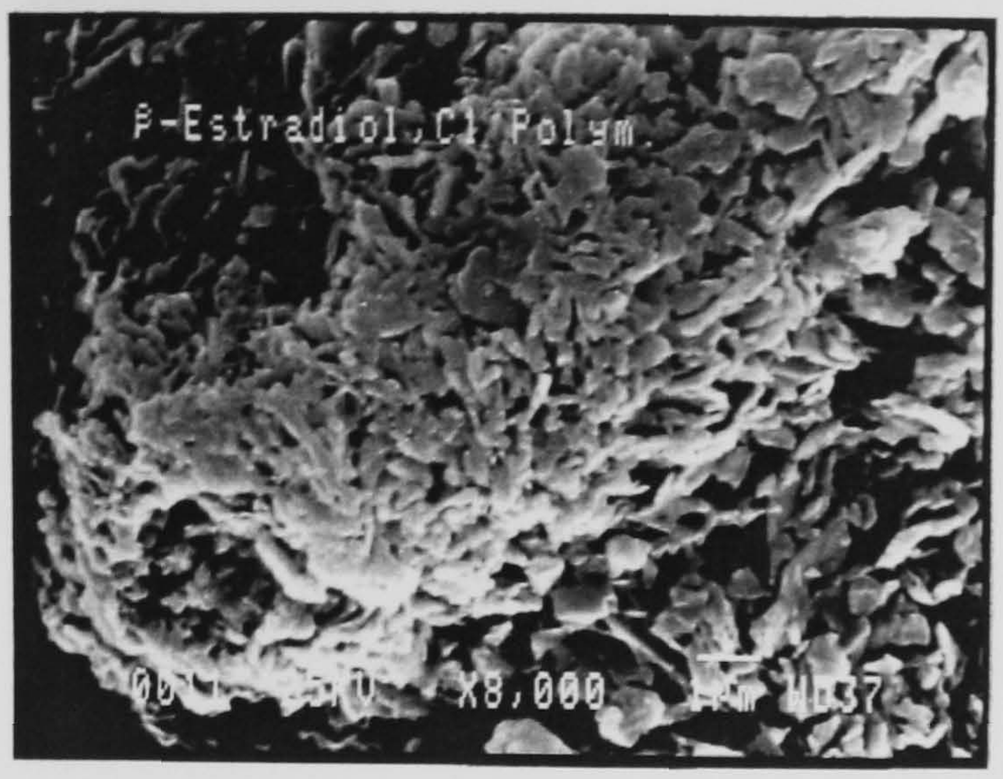

(A)

(B)

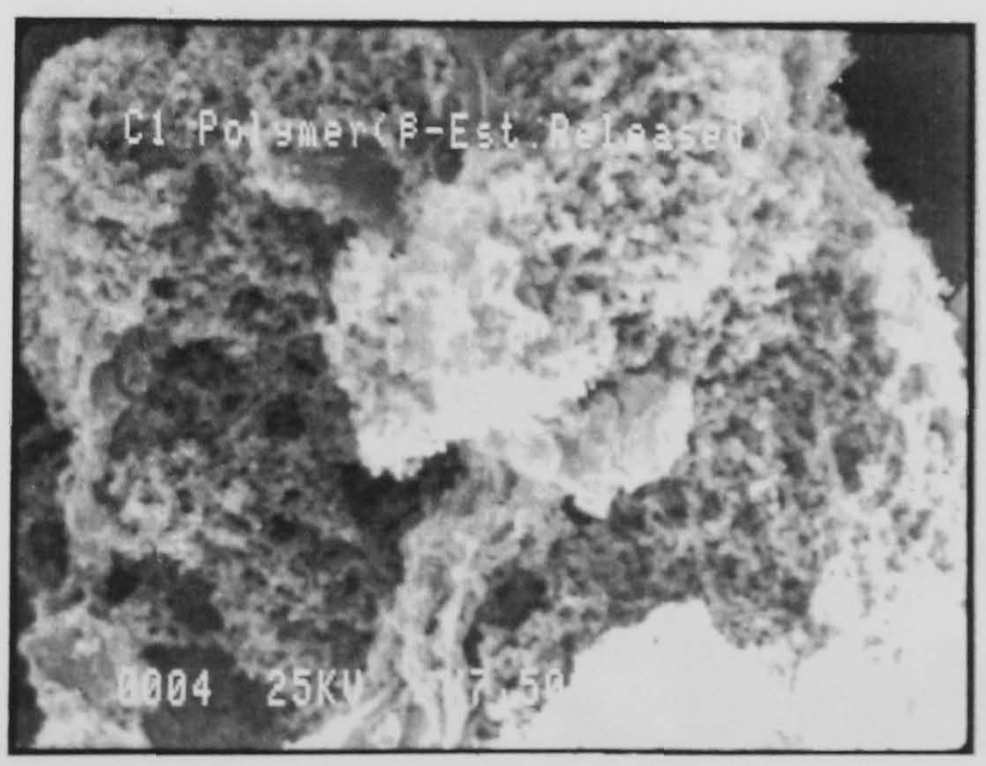

(C)

Fig. 7.18 SEM micrograph (A) of β–estradiol crystals encapsulated with Cl polymer shells. Micrograph (B) shows the shells after a partial release of β–estradiol crystals. In the micrograph (C), it is clear that most of the β–estradiol crystals have been released, but some can be still observed.

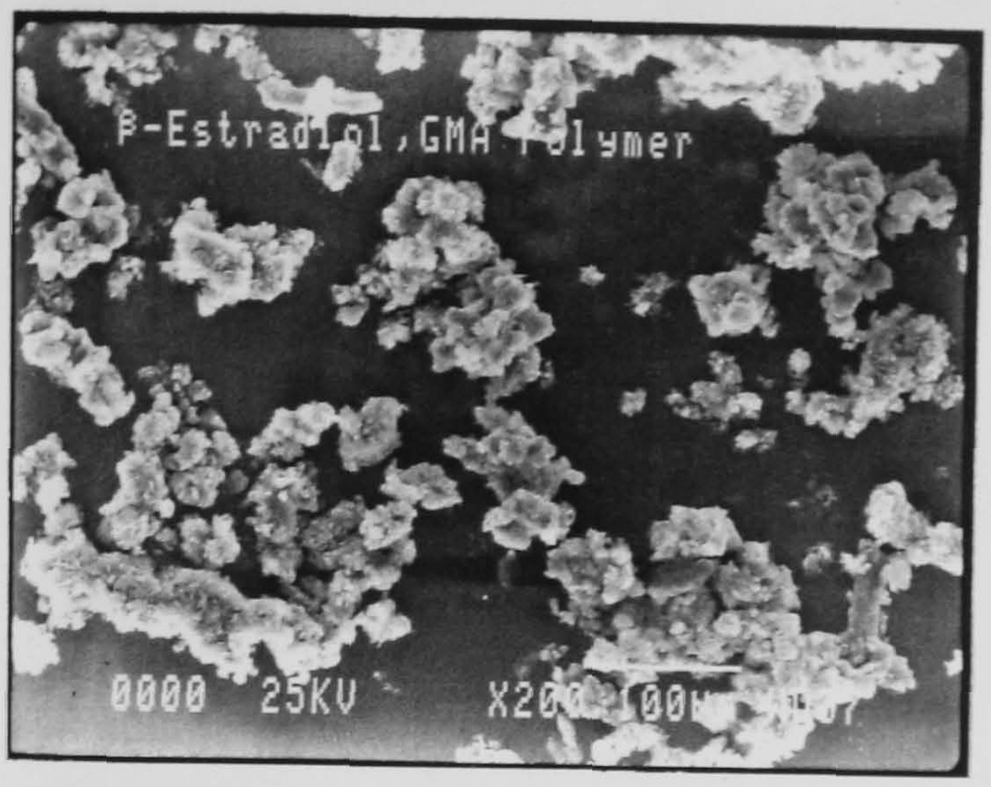

(A)

(B)

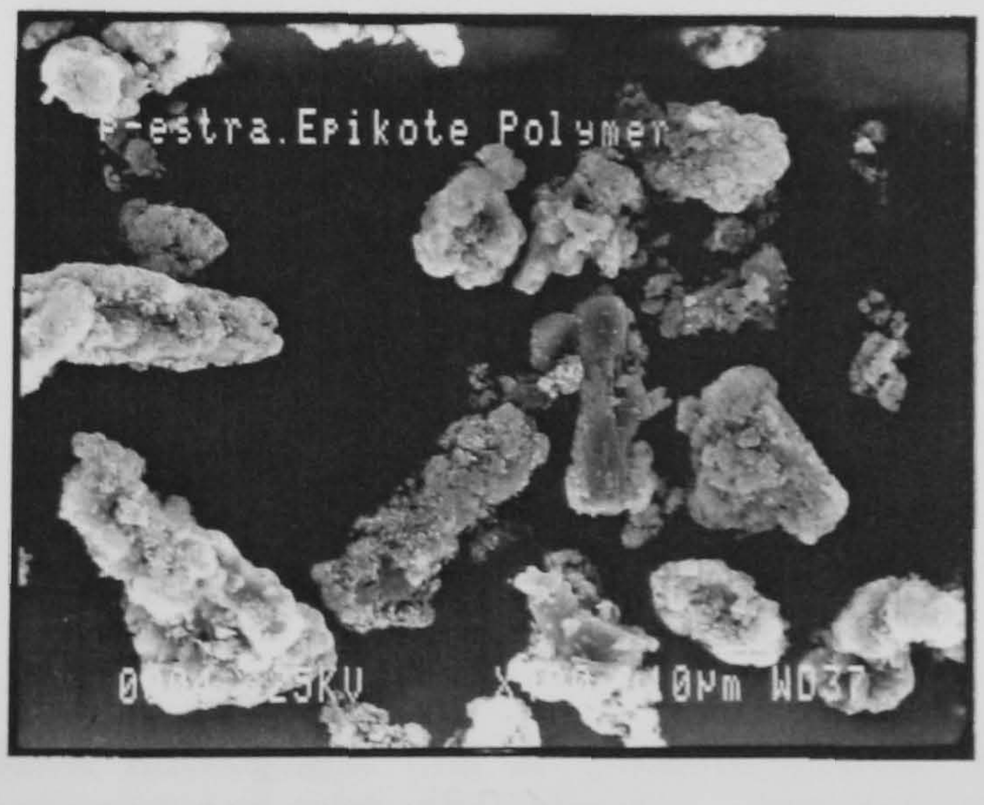

(C)

Fig. 7.19 SEM micrographs (A) and (B) show the encapsulated β–estradiol with GMA polymer at different magnification. SEM micrograph (C) shows the encapsulated crystals of β–estradiol with Epikote polymer. Deposited polymer from solution can be seen on the crystals surface.

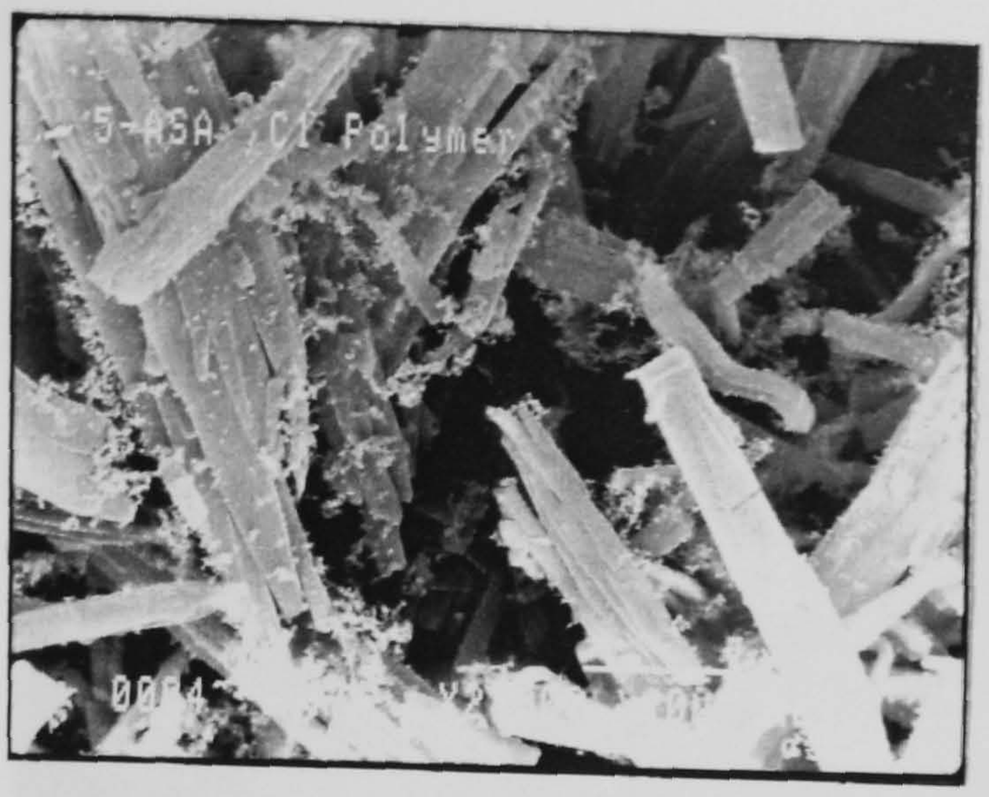

(A)

(B)

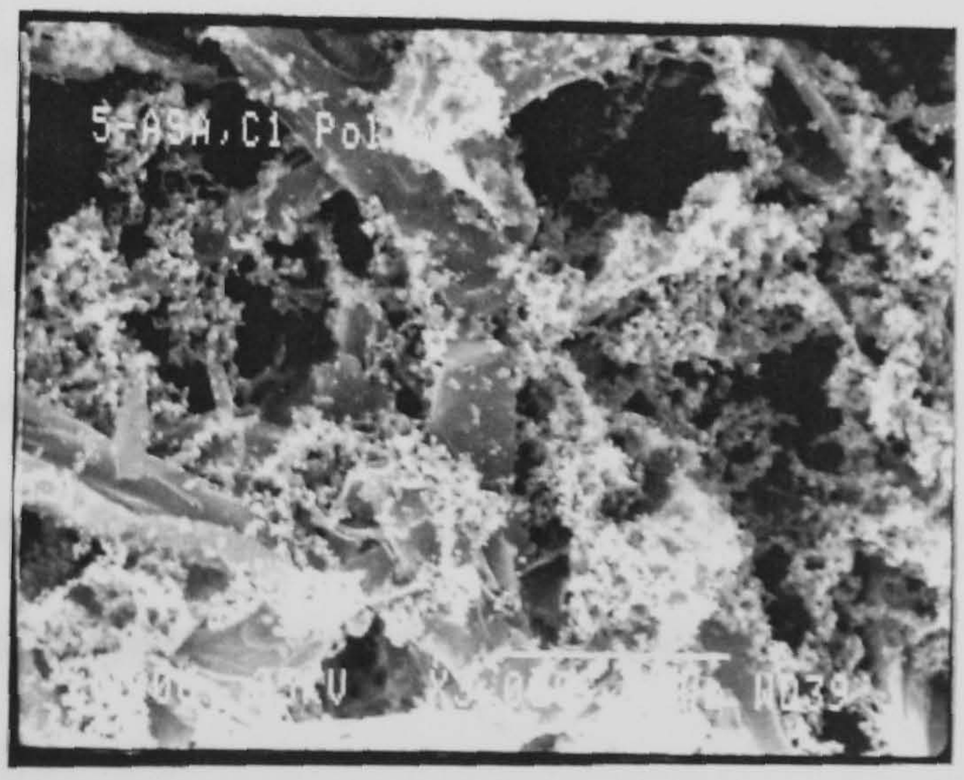

(C)

Fig. 7.20 SEM micrograph (A) of 5-aminosalicylic acid crystals encapsulated with Cl polymer. Micrograph (B) shows the polymer layer on the surface of the acid crystal and the deposited excess formed polymer. Micrograph (C) show the polymer left after a partial release of the acid.

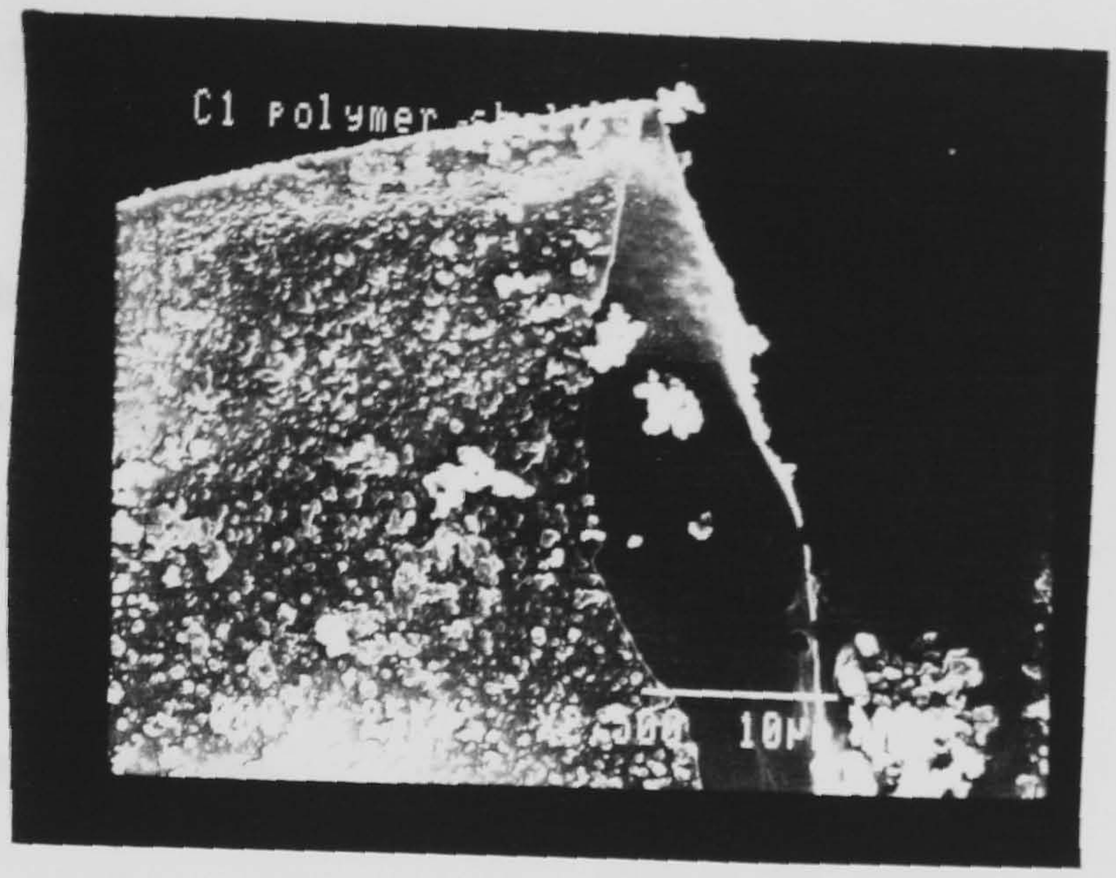

Fig. 7.21 SEM micrograph of an empty shell of C1 polymer. The shell was split into two parts, half of it is observed.

7.4 Discussion and Conclusion

The topographic study of the surface of the four polymers used for the microencapsulation revealed three different types of polymer films. These were, firstly a microporous glassy polystyrene membrane which disintegrated easily. This was the polystyrene membrane. Secondly a continuous smooth glassy membrane of low permeability obtained from C1 and Epikote polymers. The third was a microporous rubbery membrane obtained from GMA polymer. The membranes obtained from the four polymers on the crystal surfaces were very thin and they reproduced the underlying shape of the coated surfaces.

The polystyrene layer formed on the smooth surface of a KCl crystal had a very unusual regular rectangular solid structure possibly indicative of polystyrene crystals. It is difficult to see how this could have arisen unless the polymer has high tacticity. The presence of some degree of tacticity was confirmed by optical and TEM microscopy. The polymer film caused depolarized reflection to the

polarized optical light. The electron diffraction gave a sharp ring pattern for polystyrene shells in TEM micrograph which is characteristic for a semicrystalline material. This would imply that the polymer has a highly stereo-regular structure. Little evidence of this was obtained from IR and NMR analysis nevertheless it demands further investigation. The topography of the membranes indicated pore sizes of about 0.1–0.8 μm for polystyrene and of about 0.1–0.6 μm for GMA polymer membrane.

It is convenient that the polymeric shells were easily isolated by dissolving the core materials. This allowed the polymer shells formed on the drug crystals to be readily studied.

It was much easier to study the morphology and topography of the polymers encapsulated potassium chloride than in case of β-estradiol and 5-aminosalicylic acid because of their relatively small particle size. This problem was because the focussing required at very high magnification needed to observe the morphology of the membrane on the surface of a very small crystal was a difficult task to achieve. The flocculated particles mounted on top of each other made it difficult to focus the image of the surface at high magnification as the particle move from their position not being individually fixed on the stub. β-estradiol and 5-aminoslicylic acid were also significantly affected by the electron beam when focussed at high magnifications. These problems might be solved by compressing these drugs into discs to provide a fixed flat large surface to facilitate studying the morphology of the polymers..

The thickness of C1 polymer shell membrane observed from Fig. 7.21 indicates a

membrane thickness of less than 1 μm.

From the nature and morphology of the polymers observed in this study it is possible to select a certain polymer to combine with a particular drug for a specific application depending on the drug solubility and the polymer nature as rate controlling layer.

7.5 References

1. Linda C. Sawyer and David T. Grubb, "Polymer Microscopy", (Chapman and Hall, Cambridge), (1987).
2. Young, R.J., "Introduction to Polymers" (Chapman and Hall, London, 1981).
3. Geil, P.H., "Polymer Single Crystals" (Interscience, New York), (1963).
4. Grubb, D.T., in "Developments in Crystalline Polymer Materials - 1" (Applied Science, London), (1982).
5. Bassett, D.C. "Principles of Polymer Morphology" (Cambridge University Press, Cambridge), (1981).
6. Ward, I.M., Ed., "Structure and Properties of Oriented Polymers" (Applied Science, London), (1975).
7. Nixon, J.R., Matthews, B.R., Microencapsulation, vol. 3., Chapter 15 (173) edited by J. R. Nixon (Marcel Dekker, Inc.), (1976).
8. Hobbs, S.Y., J. Macromol. Sci., Rev. Macromol. Chem., C19(2), 221-225, (1980).
9. Kruse, J., Rubber Chem. Technol., 46, 653 (1973)
10. Thomas, D.A., J. Polym. Sci., Polym. Symp., 60, 189 (1977)
11. Wells, O.C., Scanning Electron Microscopy, McGraw-Hill, New York Chapt. 1-3 (1974).

CHAPTER VIII

In Vitro Release Study of Microencapsulated Particles

Chapter VIII

In Vitro Release Study of Microencapsulated Particles

8.1 Introduction

The area of sustained drug delivery was first studied by Lipowski[1]. His work involved coated pellets for the prolonged release of drugs which was presumably the stimulus for subsequent development of the coated particles approach to sustained drug delivery introduced in the early 1950's.

Small particles coated with a rate-controlling membrane have been called microcapsules. Sustained[2] release oral dosage can make the drug available to the body in amounts sufficient to produce and maintain the desired pharmacological response. The basic reasons for using sustained release medications are to decrease the frequency of taking the drug and to extend the drug's activity while maintaining a uniform plasma level to minimise any toxic[3] effects. Microcapsules can be placed into conventional dosage forms such as hard gelatin capsules or novel dosage forms tailored to fit the unique properties of microcapsules. The classical oral dosage forms are tablets. The goal of this investigation is to evaluate the *in situ* microencapsulation as a method to achieve a sustained release of three solid drug powders of different solubility in water (release medium). The influence of the different wall materials and the solubility of the drug on the rate and mechanism of release are discussed. The results obtained from this investigation could point the way to potentially useful microcapsule systems for particular therapies.

8.2 Experimental

8.2.1 *In Vitro* Release of Encapsulated Potassium Chloride

The release of potassium chloride through different polymer capsules was determined potentiometrically using a Philips chloride ion–selective electrode with a double junction reference electrode (Philips type RE3/DJ) containing 1 M KNO_3 electrolyte bridge.

Electrode Calibration

A stock solution of potassium chloride in deionized water was prepared from which four diluted known concentrations were prepared in the measuring range of the electrode $0.1-10^{-4}$ mol/l. The corresponding electrode potentials for these concentrations were recorded. The temperature of the solutions was automatically controlled to 37°C. A standard curve was constructed which was used to calculate the release rate of potassium chloride.

Assaying Procedure

A constant weight of the encapsulated KCl samples (0.6 g) was used for each release study. This weight was chosen to maintain the concentration during the release to less than 10% of the saturated solution and to be in the range of the electrode measurements and standard curve. The weighed particles of each sample were placed into a constant volume of deionized water (100 ml) where the electrodes were immersed in at an automatically temperature controlled bath set at 37 ± 0.5°C. The particles were agitated in the release medium by using a magnetic bar along with a magnetic stirrer. The increase in chloride ion concentration due to the release of potassium chloride as a function of time was obtained from the standard curve.

8.2.2 *In Vitro* Release of β–Estradiol

Release of β–estradiol through the different polymer capsules namely polystyrene,

C1 polymer, GMA and Epikote polymer was determined using Waters Associates high pressure liquid chromatography (HPLC) equipped with a variable wavelength u.v. detector set at 204 nm and at sensitivity of 0.1 AUFS. The HPLC was operated at ambient temperature. The column used was a Waters μ Bondapak™ C18 Radial Pak Cartridge. The mobile phase, acetonitrile/water (55:45 v/v) was pumped through the column at a rate of 2.0 ml/min. Samples of 200 μl were injected onto the column using a Waters Intelligent Sample Processor (WISP). Chromatograms of the β–estradiol peaks with their calculated areas and the amounts of β–estradiol were recorded on a chart recorder (Waters Data Module).

Calibration of the HPLC

A stock solution of β–estradiol in acetonitrile was prepared from which a set of dilute solutions of known concentrations was prepared. The standard solutions were injected into the column. The peak areas were plotted versus their concentrations. The standard calibration curve obtained was used to calibrate the HPLC using a standard solution freshly prepared whenever the apparatus was used to assay the unknown samples. As acetonitrile evaporates, the concentration of the standard solutions can change if not used at the time of their preparation. This was observed during plotting the standard curve from independent sets of standard solution of freshly and not freshly prepared ones. The independent freshly prepared standard sets gave matching calibration while the others did not. So the volume of samples was made up just before injecting them into the HPLC for assaying.

Release Procedure

An accurate weight of each encapsulated β–estradiol sample (0.07g) was placed in a glass tube made specially for the release analysis. The glass tube was connected from one side to a conical flask containing 500 ml of double distilled water that

was maintained at 37°C. The other side of the glass tube was connected to Millipore In-line filter holder (47 mm diameter) holding a microfilter membrane of pore size 0.8 μm.

The glass tube containing the sample, the conical flask (water sink) and most of the tubing used for connection were immersed in a water bath set at 37 ± 0.5°C. The rubber tubing used for connection was of a medical grade Silastic supplied by Dow Corning. The flow of water in one direction through the system was achieved by using a Gilson peristaltic pump at a rate of 10 ml per minute. The release medium was collected after different time intervals and its volume was measured. The release medium was replaced with fresh prewarmed 500 ml water. The collected volume was evaporated to dryness and the β-estradiol residue was dissolved in acetonitrile.

Assaying Procedure

After collecting a number of fractions, their volumes were made up to 10 ml volumetric flasks. The samples were assayed using the HPLC, after calibration with a freshly prepared standard solution of β-estradiol in acetonitrile and reading the result from the calibration curve. The amount of β-estradiol assayed in the injected 200 μl was obtained from the HPLC chromatogram chart from which the total amount of β-estradiol dissolved in acetonitrile was calculated and its concentration in the release medium was obtained.

Calculation from the chart:

Weight of β-estradiol in 200 μl injected = x

Weight/ml = x x 5 = μg/ml

Weight in the total volume of acetonitrile = x x 5 x (mls of MeCN)μg

= Y μg

$$\text{Concentration in } H_2O \text{ sink} = \frac{Y}{\text{Volume of } H_2O \text{ (500 ml)}}$$

The cumulative amounts of β–estradiol released were plotted versus time for the different wall materials.

8.2.3 *In vitro* Release of 5–Aminosalicylic Acid

The release of 5–aminosalicylic acid through C1 and GMA polymer shells was followed by utilising a Cecil Series 5000 Double Beam Scanning UV visible computing spectrophotometer at 297 nm wavelength.

Standard Curve

A stock solution of 5–aminosalicylic acid of a concentration of 100 μg/ml in double distilled water was prepared and a series of diluted standards was made up ranging between 5–40 μg/ml and their absorbance measured at 297 nm. A standard curve was constructed by plotting the concentration against absorbance. This standard curve was used to measure the concentration of the 5–aminosalicylic acid in the release medium and to calculate the amount released over periods of time.

Release Procedure

The release of 5–aminosalicylic acid through the C1 and GMA polymer was carried out in the same manner as described for the release of β–estradiol in section (8.2.2). A known weight of the encapsulated acid particles (0.05–0.055 g) was placed in the glass tube along with a 500 ml of prewarmed distilled water (37 ± 0.5°C) was used as a release medium.

Assay Procedure

Samples from the release medium were taken at different time intervals and their absorbances were measured spectrophotometrically at 297 nm. The concentrations were then calculated from the standard curve. The samples were returned back

to the release medium to maintain constant volume. The absorbance was measured using diluted solutions when the absorbance values exceeded that of the highest calibration standard. The diluted solutions were discarded and the concentrations of the release medium were calculated from their actual volume during the measurements. The discarded released amounts were taken into account in calculating the cumulative release.

The concentration of 5-aminosalicylic acid was not allowed to exceed 10% of the saturated solution concentration during the release. This was found to be 137 μg/ml. The amount of the acid released in the medium was calculated as follows:

$$\text{Concentration} = \frac{\text{Absorbance}}{\text{Slope}} \ \mu\text{g/ml}$$

$$\text{Amount released (Mt)} = \text{Concentration} \times \text{volume of release sink}$$

A plot of the fractional release versus time was constructed for the release of the acid through C1 and GMA microcapsules.

The dissolution rate of unmicroencapsulated particles was also plotted as a control experiment.

8.3 Results

8.3.1 *In Vitro* Release of Encapsulated Potassium Chloride

The *in vitro* release patterns of the preselected particle size 250, 500 and 710 μm of the encapsulated potassium chloride were studied and compared using the different wall materials. Fig. 8.1 illustrates the release patterns of potassium

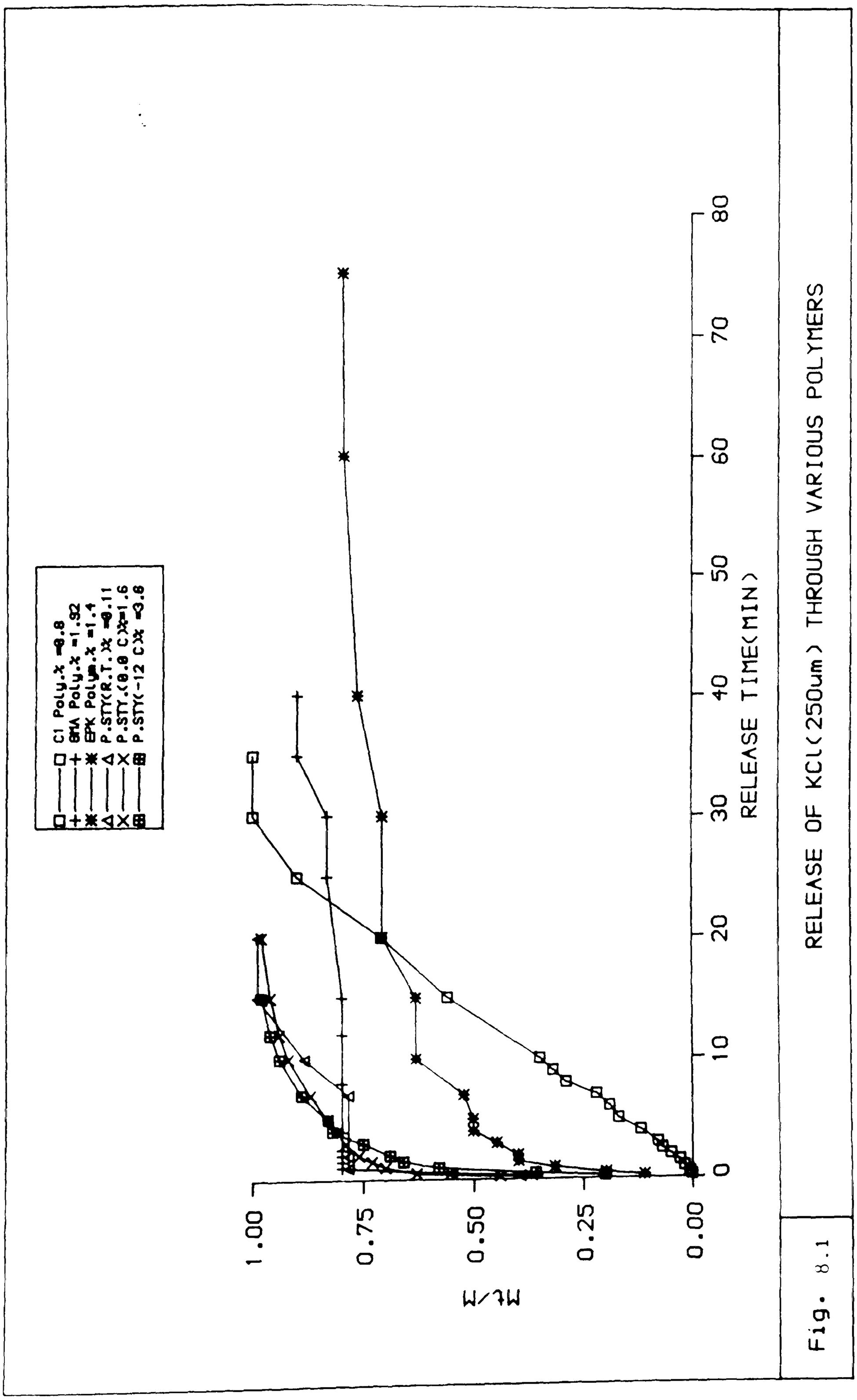
RELEASE OF KCl(250um) THROUGH VARIOUS POLYMERS
Mt/M
1.00
0.75
0.50
0.25
0.00
0
10
20
30
40
50
60
70
80
RELEASE TIME(MIN)
C1 Poly.x =0.8
EMA Poly.x =1.92
EMK Poly.x =1.4
P.STY(R.T.) x =0.11
P.STY.(0.0 C) x=1.6
P.STY(-12 C) x =3.8

Fig. 8.1

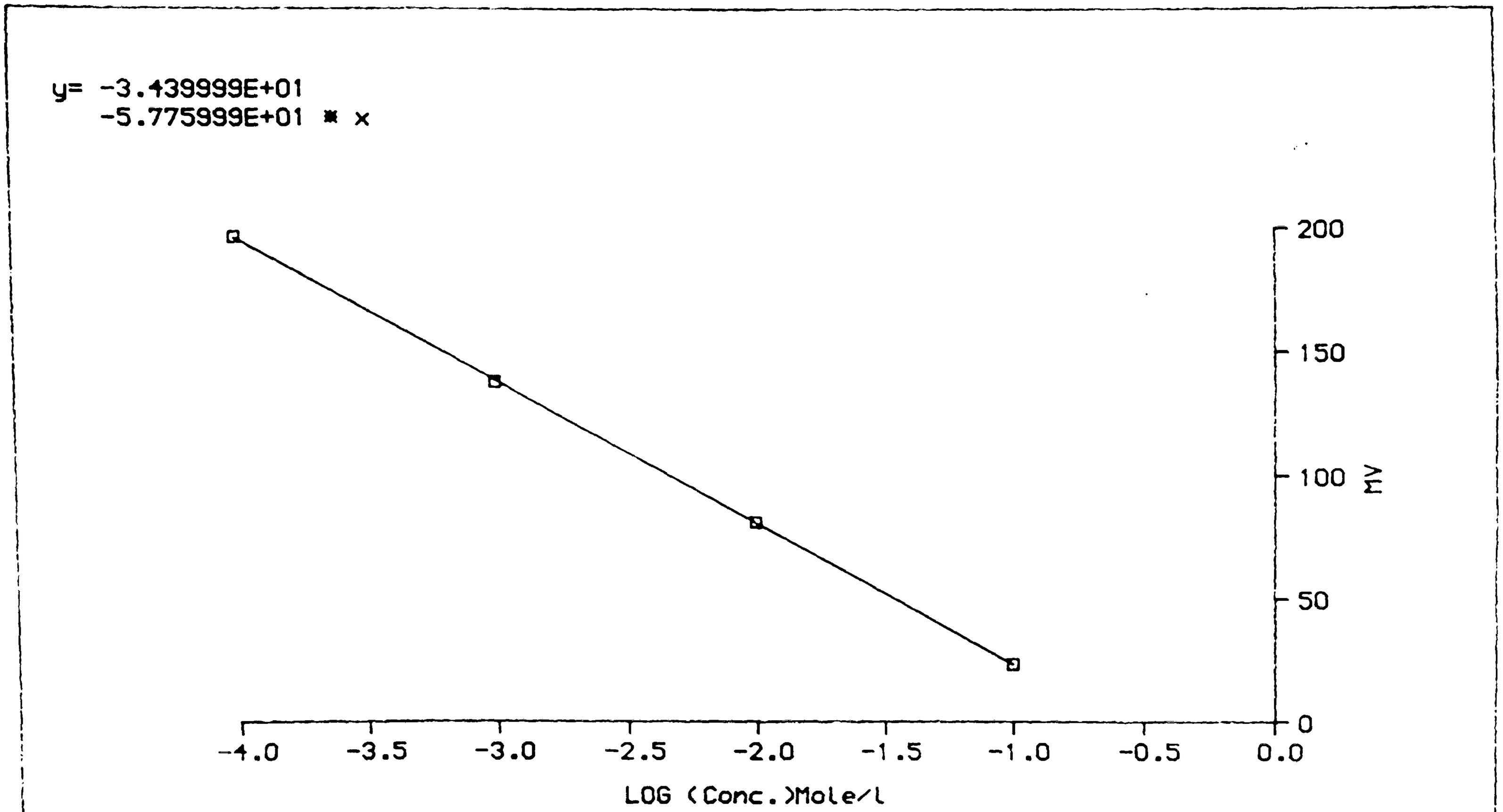

Fig.8.2 CALIBRATION CURVE OF Cl ION ELECTRODE

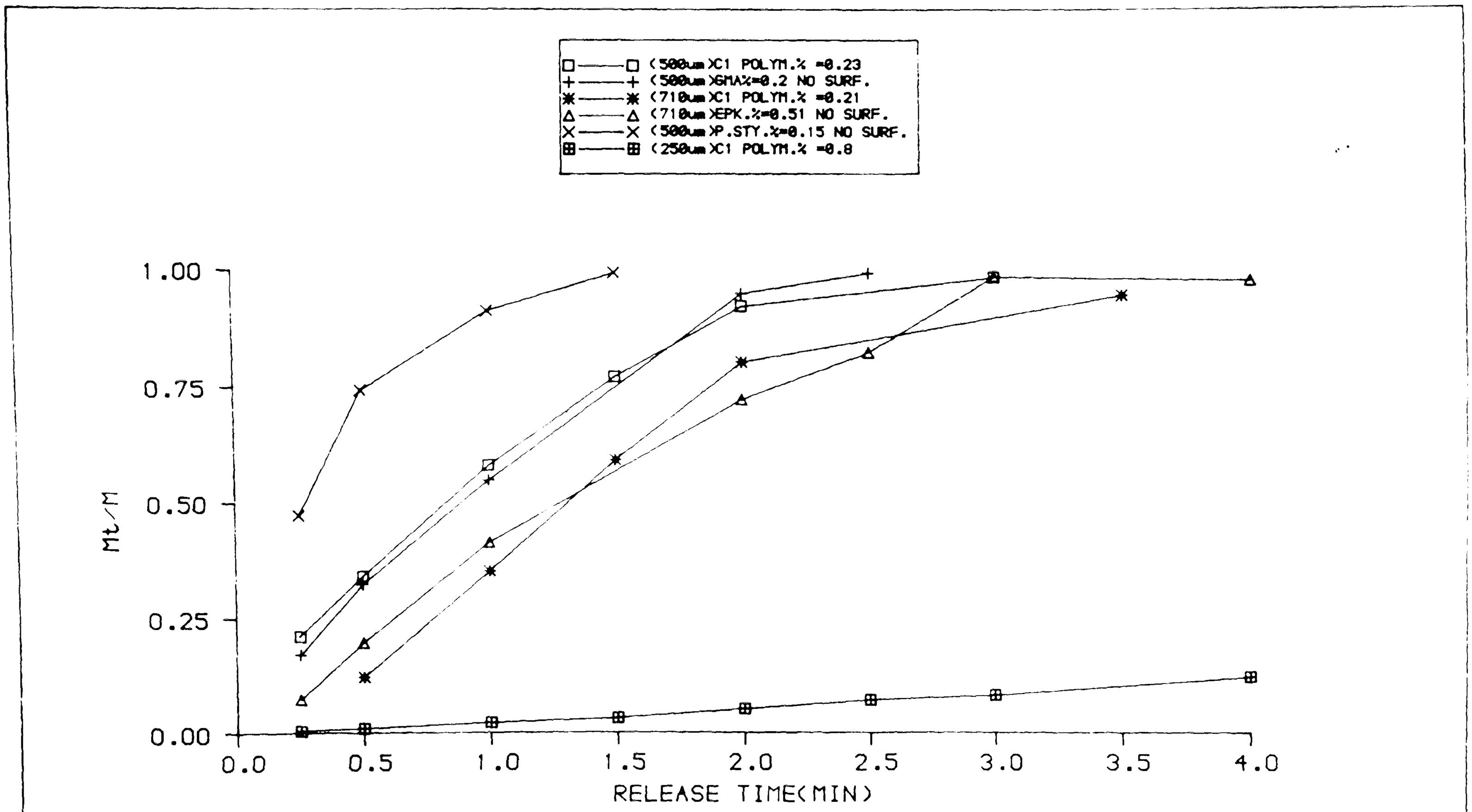

Fig. 8.3 RELEASE OF KCl(250 , 500 & 710um) THROUGH VARIOUS POLYMERS

chloride powder of particle size 250 μm through C1, GMA and Epikote 828 polymers. The release through three samples of polystyrene formed at three different temperatures (Room temperature, zero and $-12^{o}C$) are also presented.

Fig. 8.2 represents the standard curve of the chloride ion selective electrode which was used to estimate the drug release through the different membranes.

Fig. 8.3 shows the release of potassium chloride of the different particle sizes mentioned above from the four different polymers of styrene, C1, GMA and Epikote 828. Styrene, GMA and Epikote were polymerized directly on the activated surface of the drug without first adsorbing a template layer of surfactant on the drug surface.

Figure 8.4 shows the standard curve of the chloride ion electrode constructed previously which was used to calculate the drug released.

Permeability of C1 membrane

Since the release rate is proportional to the permeability of microcapsule wall, the C1 polymer provided a membrane coating of lower permeability than the other polymers on KCl (250 μm particle size) as shown in Figs. 8.1 and 8.3.

The permeability of the C1 membrane was estimated from the release rate calculated from the slope of the fractional release/time plot given in Fig. 8.5, and the membrane thickness. The membrane thickness was calculated from the area and the volume of the microcapsules. The volume of the membrane was calculated from its weight on the particles (0.8% w/w) and its density (0.94 g/cm^{3}) which was measured by TECHNE density gradient column. The liquid system used for the column in this case was (zinc chloride–ethanol–water).

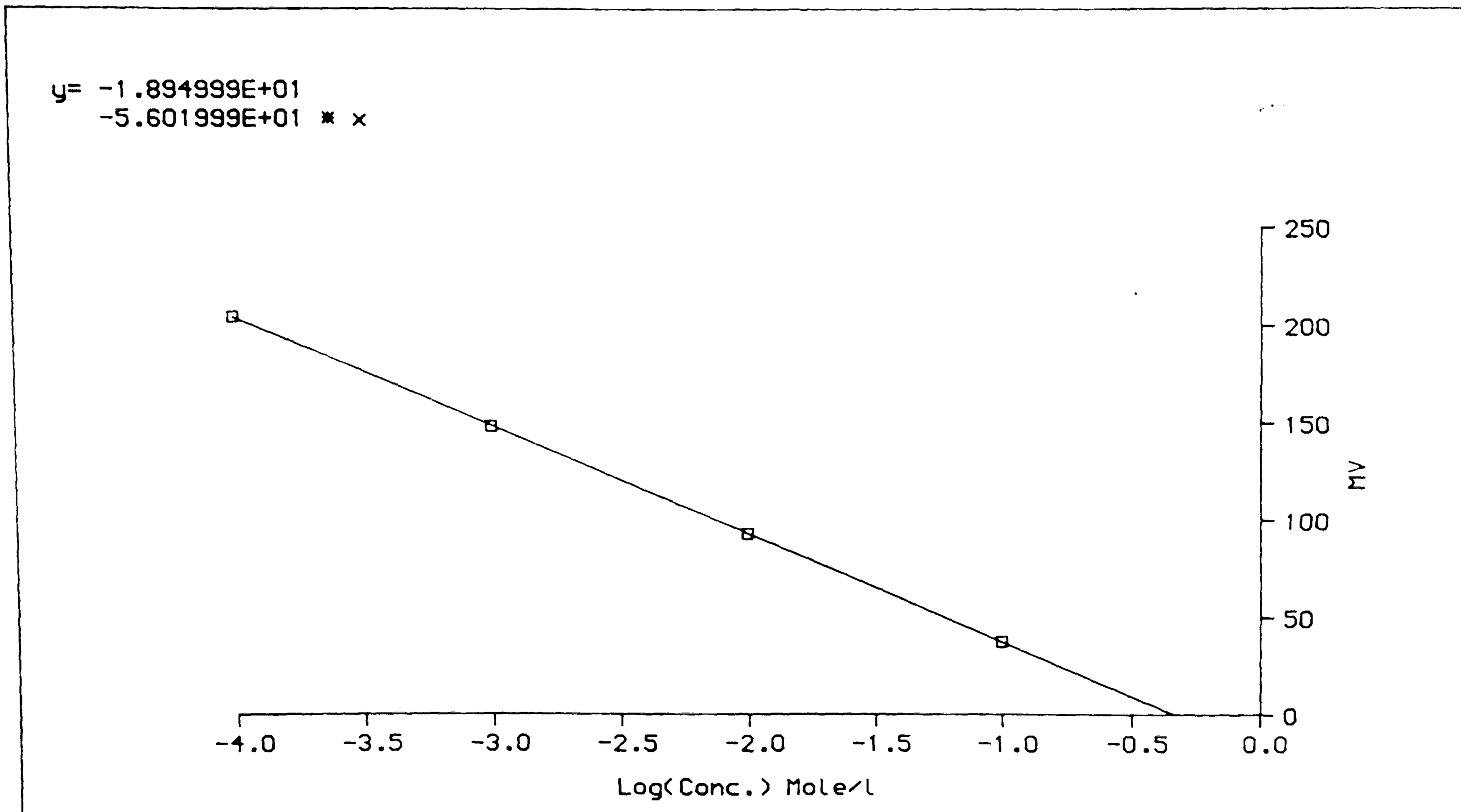

Fig. 8.4 CALIBRATION CURVE OF Cl ION ELECTRODE

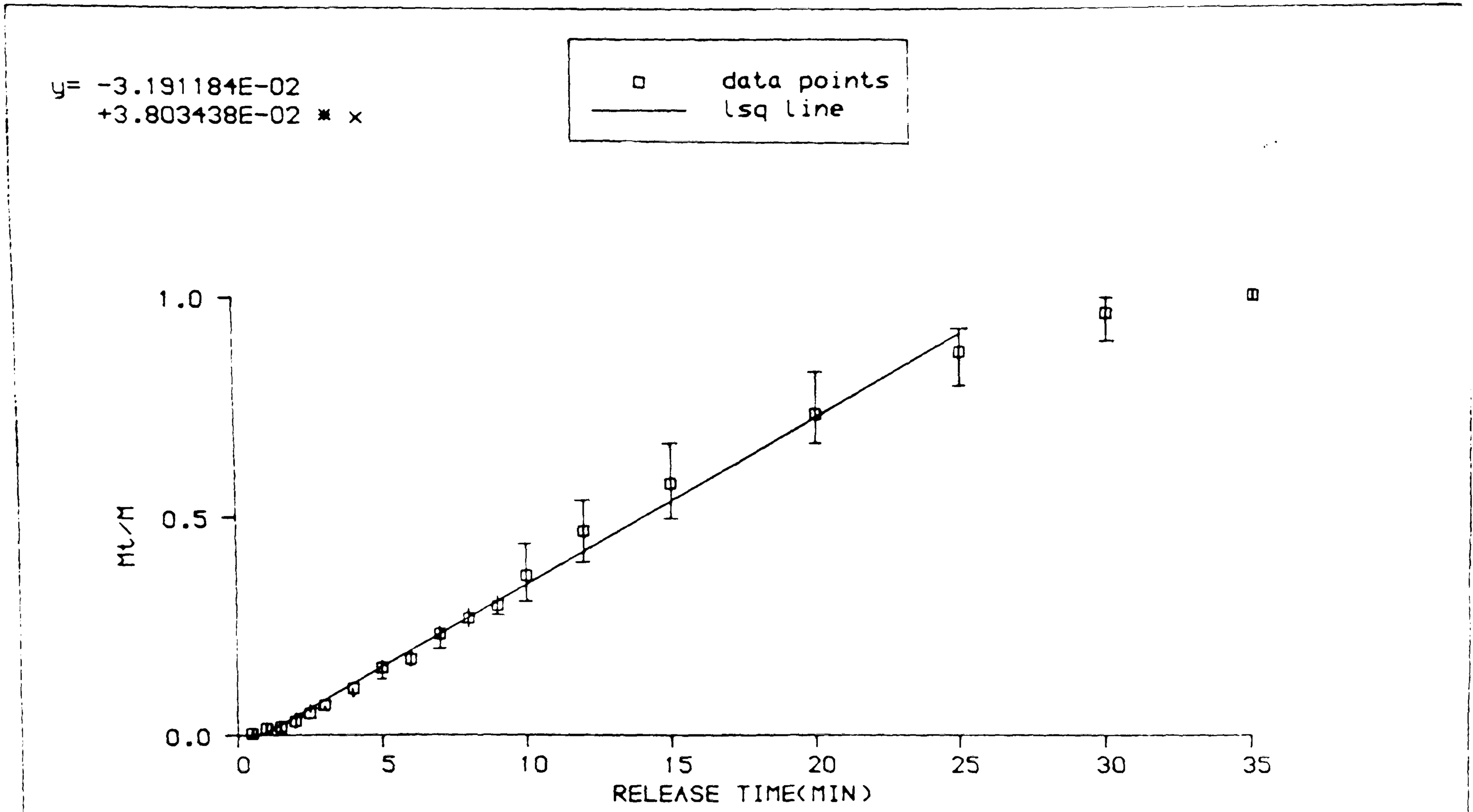

Fig. 8.5 RELEASE OF KCl (250um) THROUGH C1 POLYMER(% 0.8 W/W)

Calculation

Release rate = 3.77×10^{-4} g/sec

The total surface area of the experimental weight (0.6 g) used of the coated KCl = 441.6 cm^2

Thickness (l) of the capsule wall (membrane) = 1.16×10^{-5} cm

Concentration (ΔC) of the saturated solution of KCl = 38.78×10^{-2} g/ml

But flux through a membrane (J) = release rate/unit area

$J = 3.77 \times 10^{-4}/441.6 = 8.54 \times 10^{-7}$ g/cm^2/sec

and $J = (P/l)\ \Delta C$ (1)

where P is the permeability of the membrane.

$\therefore\ 8.54 \times 10^{-7} = P/1.16 \times 10^{-5} \times 38.78 \times 10^{-2}$

$\therefore\ P = 2.56 \times 10^{-11}$ cm^2/sec

8.3.2 *In Vitro* Release of Encapsulated β-Estradiol

The cumulative fractional release of the β-estradiol through polystyrene, GMA, Epikote 828 and C1 polymers, made with and without surfactant, in water at 37°C is illustrated in Fig. 8.6. The dissolution rate of the non-coated β-estradiol is also presented in the figure. Figure 8.7 illustrates the standard curve for the HPLC calibration.

As β-estradiol has poor solubility in water (concentration of the saturated solution = 2.1 μg/ml), it is important to present the values of the range of the concentration which were obtained from the amount of β-estradiol released in the

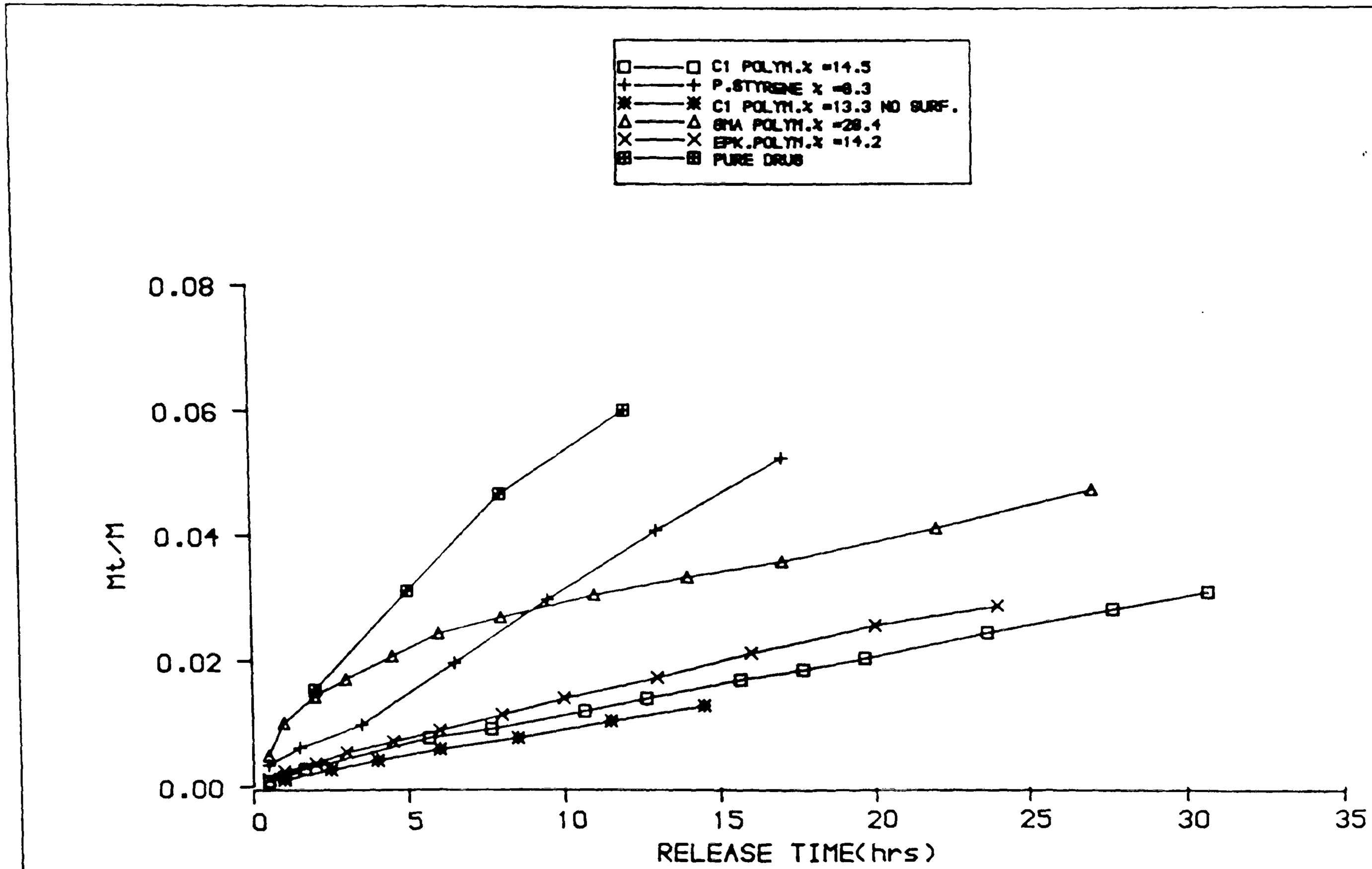

Fig. 8:6 RELEASE OF B-ESTRADIOL THROUGH VARIOUS POLYMERS

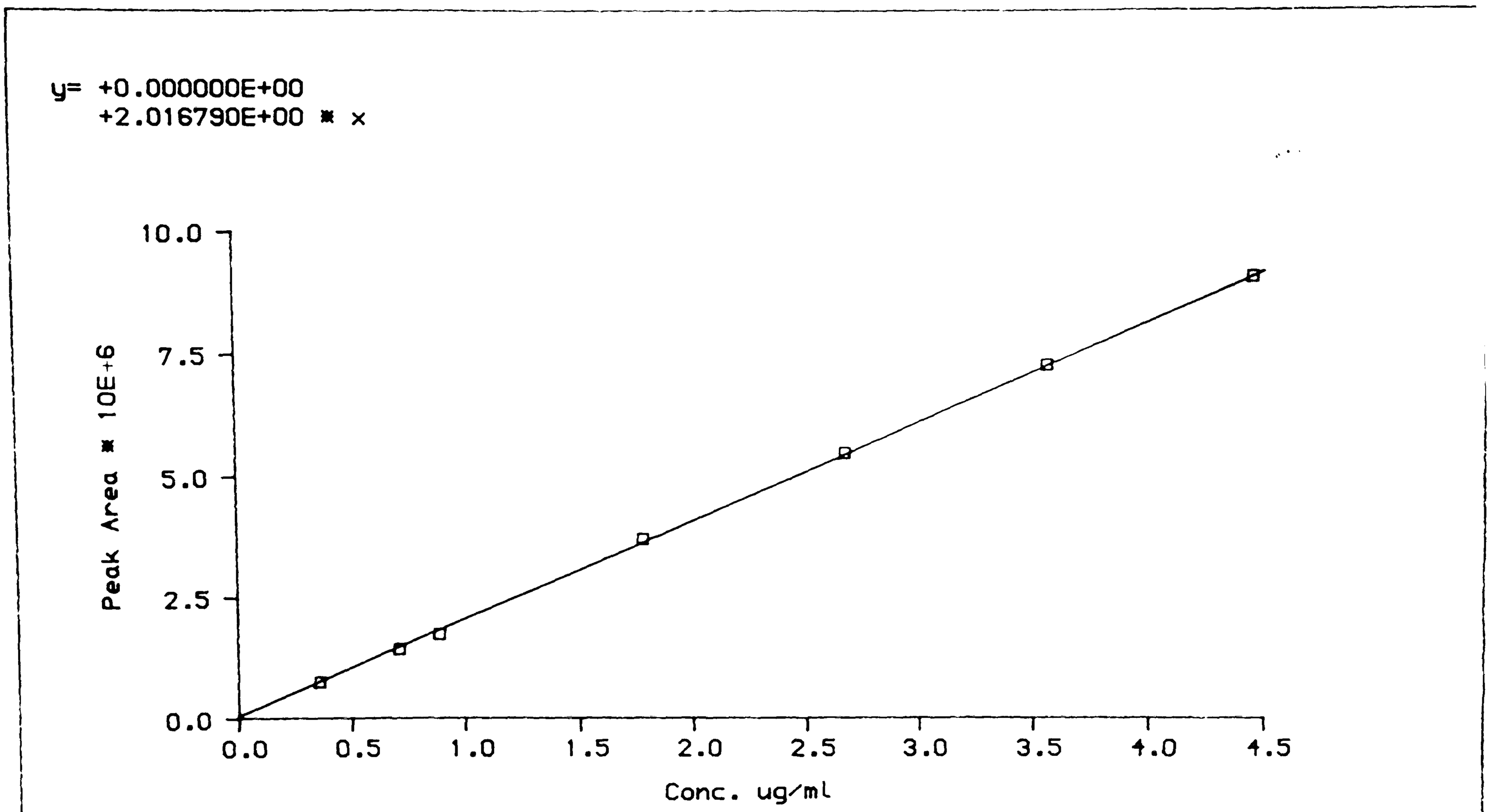

Fig. 8.7	STANDARD CURVE OF HPLC CALIBRATION FOR B-ESTRADIOL

release medium for each polymer and also for the dissolution of non coated drug. Table 8.1 presents the range of concentration found in each case.

Table 8.1 Concentration range of β–estradiol in water (release medium) in collected samples

Sample	Concentration range (μg/ml)
1. β-estradiol/C1 polymer	0.08 - 0.58
2. β-estradiol/C1 polymer without surfactant	0.14 - 0.33
3. β-estradiol/Epikote polymer	0.16 - 0.54
4. β-estradiol/GMA polymer	0.25 - 0.61
5. β-estradiol/polystyrene	0.36 - 1.48
6. β-estradiol pure	1.36 - 1.60

Mechanism of β–Estradiol Release

The kinetics of the release of β–estradiol at time (t) can be expressed by the use equation

$$M_t/M_\infty = kt^n \quad (10) \qquad (2)$$

where

M_t/M_∞ – fraction of drug released at time (t)

k – rate constant

t – time

n = slope of plot constructed from the log of amount released versus the log of the release time

If n = 1 this means that the release is constant per unit time i.e. zero order rate constant.

but

if n = 0.5 then the kinetics of the release are those commonly obtained when Fick's Law of Diffusion apply to monolithic shapes such as slabs, cylinders and spheres.

Table (8.2) illustrates the n values of the release kinetics of β–estradiol through the various polymers. Fig. 8.8 illustrates the kinetics of release of β–estradiol through C1 polymer. The equation of the straight line showing the slope is given in the figure.

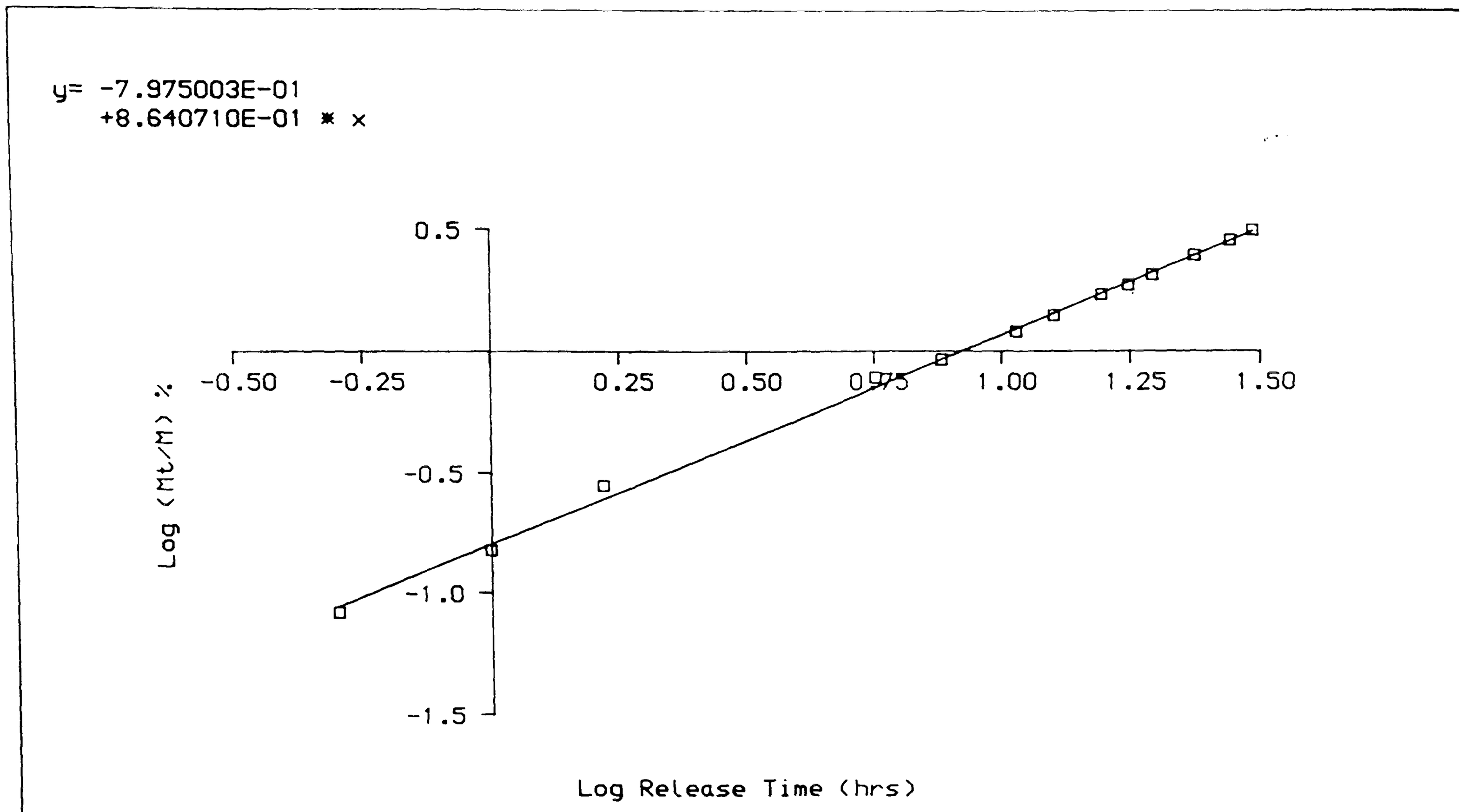

Fig. 8.8	RELEASE OF B-ESTRADIOL THROUGH C1 POLYMER

Table 8.2 Release of β–estradiol through various polymers

Wall Material	Slope of the log plot of the release fraction versus time (n)
1. C1 Polymer	0.86
2. C1 polymer without surfactant	0.89
3. Epikote 828 polymer	0.79
4. GMA polymer	0.50
5. Polystyrene	0.78

8.3.3 *In vitro* Release of Encapsulated 5–Aminosalicylic Acid

Fig. 8.9 illustrates the standard curve constructed by plotting the standard concentrations of 5–aminosalicylic acid in water versus their UV absorbance at 297 nm. This calibration curve was used to assay the amount of the drug released through various polymers. The dissolution of the non–encapsulated drug was also run as a control.

Figure 8.10 illustrates the dissolution of the uncoated acid and the release profile of the encapsulated drug through C1 polymers (with and without surfactant) and GMA polymer.

Release Mechanism

The release kinetics of 5–aminosalicylic acid through C1 and GMA polymer was indicated from the slope of the dissolution profile from the polymeric wall materials. The slope values are given in Table 8.3 and Fig. 8.11 illustrates an example of the release kinetics of 5–aminosalicylic acid through C1 polymer. The

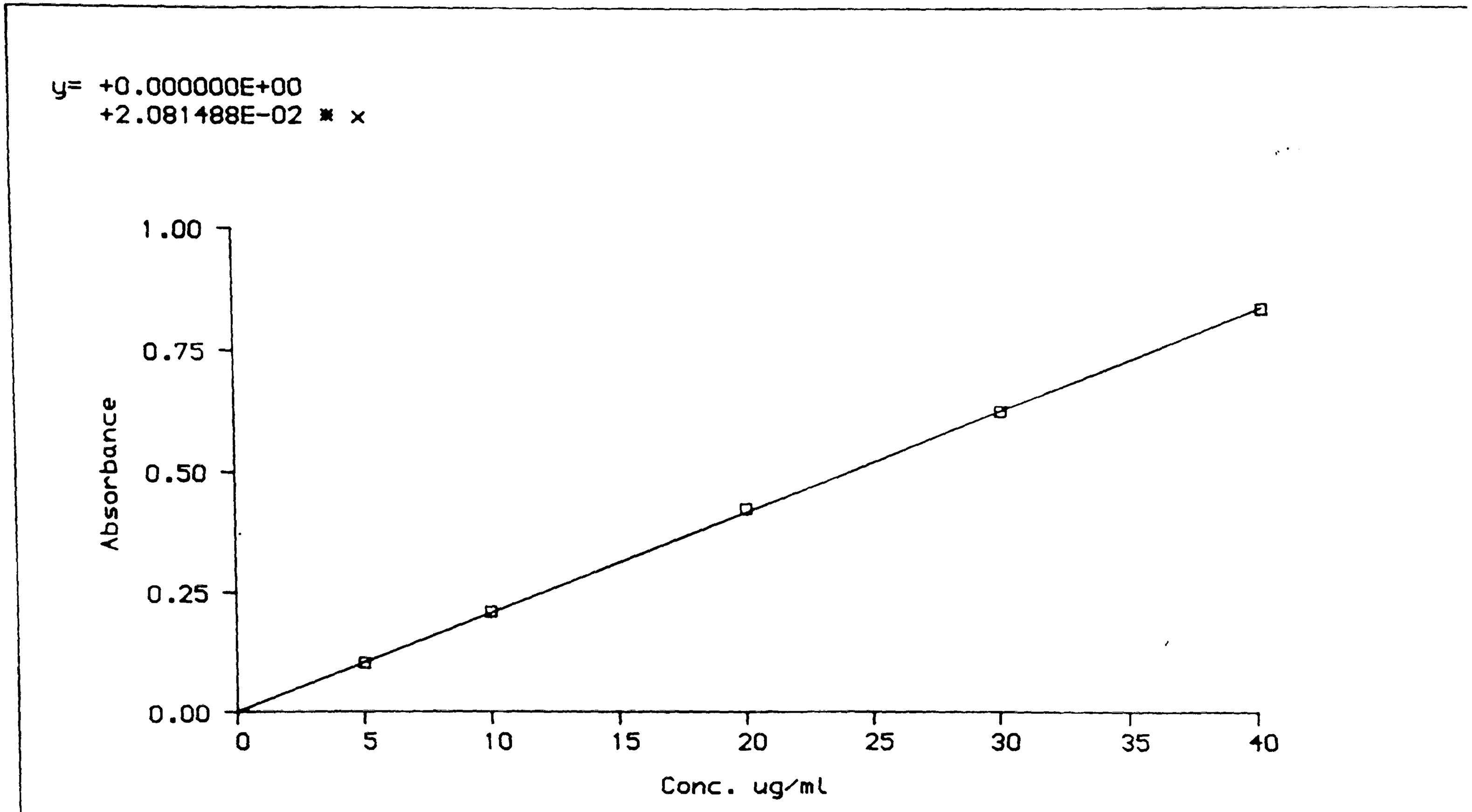

Fig. 8.9	STANDARD CURVE OF 5-AMINOSALICYLIC ACID

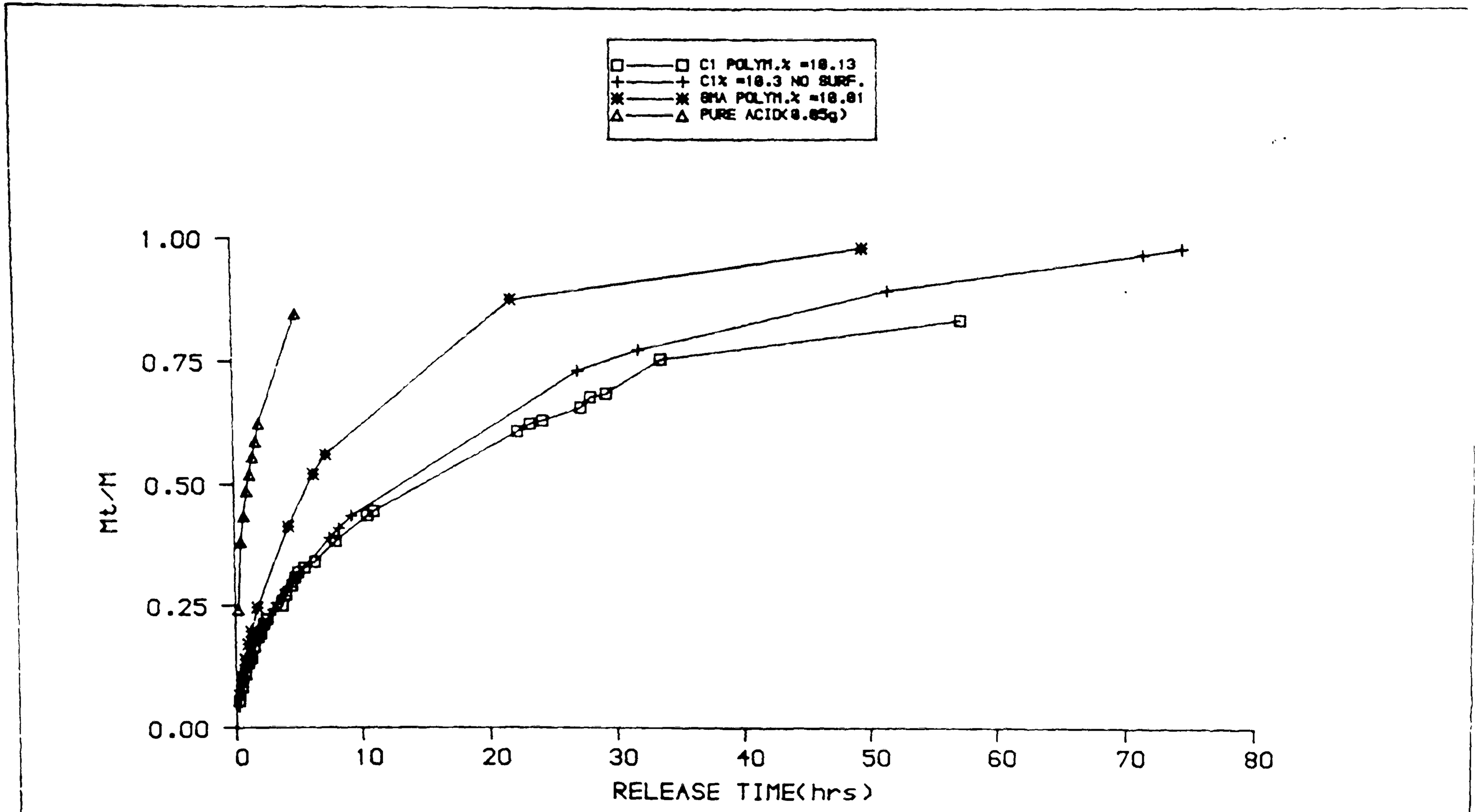

Fig.8.10 DISSOLUTION OF 5-AMINOSALICYLIC ACID AND ITS RELEASE THROUGH POLYMERS

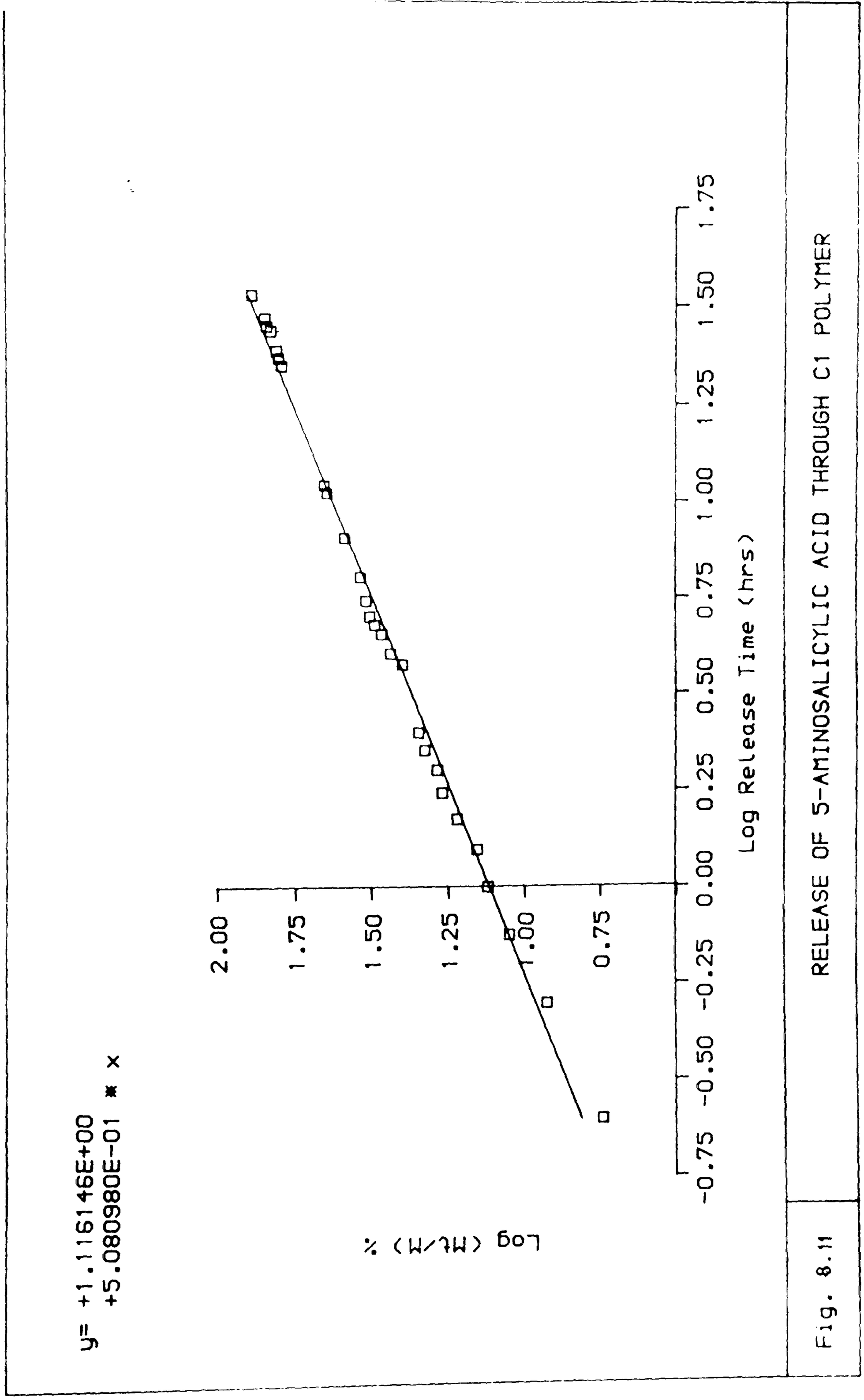
RELEASE OF 5-AMINOSALICYLIC ACID THROUGH C1 POLYMER
Log (Mt/M) %
Log Release Time (hrs)
2.00
1.75
1.50
1.25
1.00
0.75
-0.75 -0.50 -0.25 0.00 0.25 0.50 0.75 1.00 1.25 1.50 1.75
y= +1.1161146E+00
+5.0809980E-01 * x

Fig. 8.11

equation of the straight line illustrating the slope is given on the figure.

Table 8.3 Release of 5-aminosalicylic acid through C1 and GMA polymers

Wall material	Slope of the release profile (n)
1. C1 polymer	0.50
2. C1 polymer without surfactant	0.56
3. GMA polymer	0.59

8.4 Discussion

The *in vitro* release patterns of the drugs from the different polymers throws light on the different nature of each one. The C1 polymer significantly delayed the dissolution rate of potassium chloride compared to polystyrene, GMS and Epikote 828 polymers as illustrated in Fig. 8.1 for potassium chloride of particle size 250 μm. The release profile through C1 polymer indicates a constant rate of dissolution, i.e. a zero-order release rate as illustrated by Fig. 8.5. The progress of dissolution of KCl showing the membrane envelope is illustrated in Fig. 8.12. Polystyrene did not provide a sustained release even over a short period of time (5 minutes) as it showed an instant disintegration and rupture exposing the core (drug particle) to a direct contact to the release medium (water) in which KCl is highly soluble as shown in the micrograph, Fig. 8.13. This could be attributed to the very brittle nature of polystyrene.

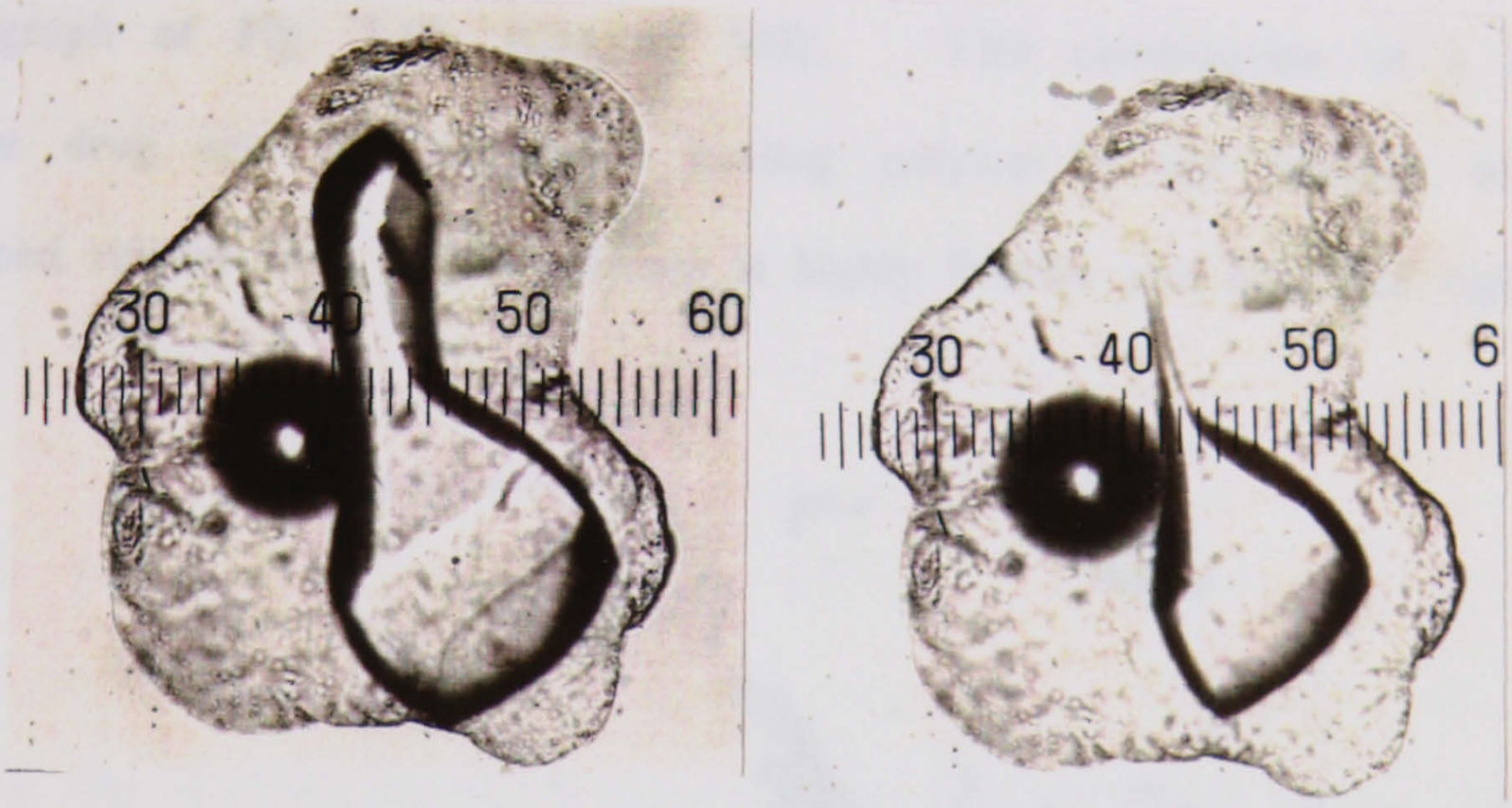

Fig. 8.12 Release progress of KCl through C1 polymer

The three polystyrene microcapsule samples prepared at three different temperature (Room Temperature, zero and −12°C) Fig. 8.1 did not show significant differences in the release profiles.

Although GMA polymer was expected to be less brittle than polystyrene, it still showed an accelerated release rate of KCl during the initial test period because GMA provided a porous coating on the KCl surface as illustrated in the micrograph of Fig. 7.15, (Chapter VII). This combination of a highly water soluble drug and a microporous coating polymer is not suitable to achieve a sustained release even if the polymer is highly flexible and does not rupture.

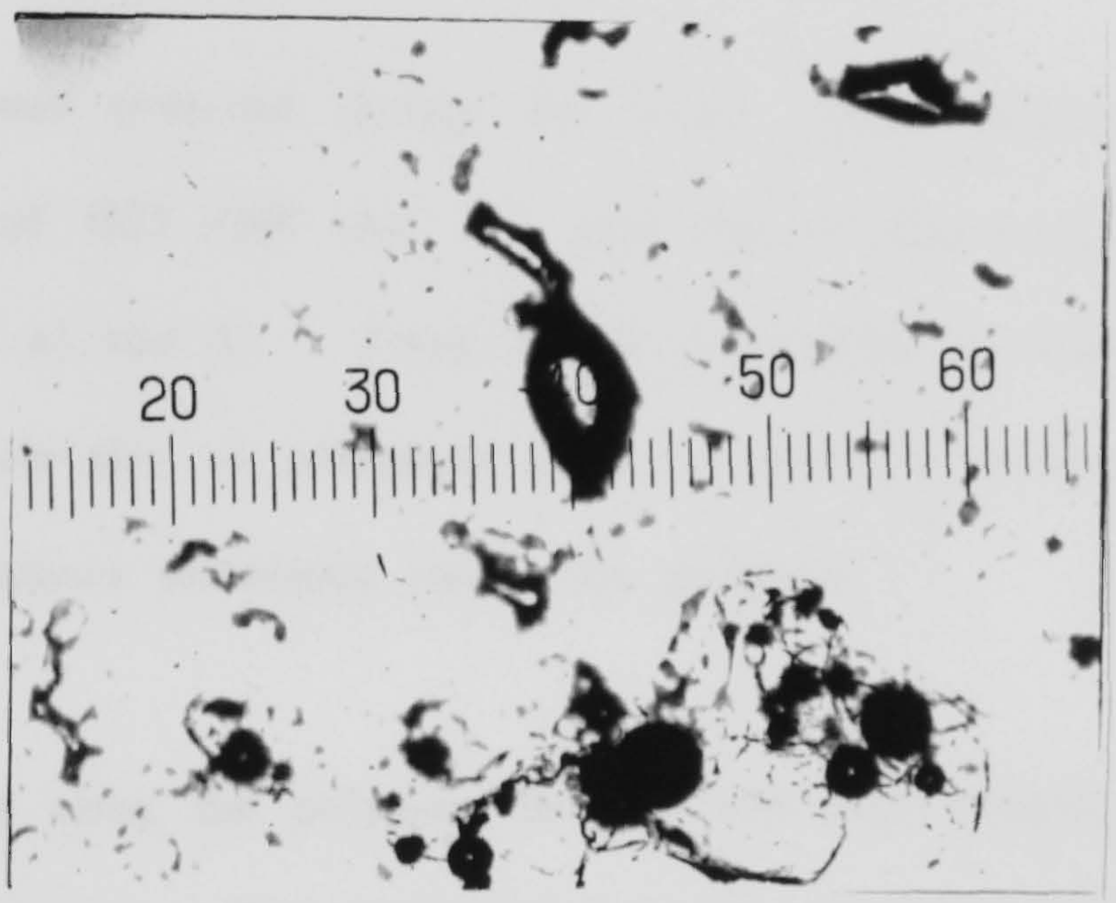

Fig. 8.13 Disintegration of polystyrene shell

The polymeric coating made from Epikote 828 monomer shows a slightly improved release profile but still not significantly delayed as 60% of the drug was dissolved in less than 10 minutes. The Epikote polymer, creates a continuous film coating on the drug surface as shown by micrograph Fig. 7.16, (Chapter VII). This might be due to low flexibility and film rupture as a result of osmotic pressure. So the Epikote polymer might show better release profiles with less soluble drugs.

As the dissolution rate of a powder is proportional to the total surface area of the

crystals offered to the dissolution medium, a powder system with low specific surface area should show a low dissolution rate, i.e. an increase in particle size should consequently reduce the dissolution rate. This could be utilized to delay the release. This did not work for the release profiles obtained from the C1 microencapsulated potassium chloride of two chosen larger particle sizes (500 and 710 μm) as shown in Fig. 8.3. The release of KCl (250 μm) through C1 polymer is included again in the figure for comparison.

A shell rupture was observed during the initial release period of these different coating materials of KCl (500 and 710 μm) and is illustrated by the micrograph given in Fig. 8.14 a) and b). From this it is possible to conclude that there is a limit on the particle size of potassium chloride before a catastrophic failure caused by the osmotic pressure developed inside the particles.

The release profile using the polymers formed with and without surfactant provided almost the same results. This indicates that the surfactant does not have a major effect on the coating or the release properties. The C1 polymer membrane encapsulating KCl (250 μm) of wall thickness 0.11 μm and permeability (P) = 2.56 x 10^{-11} cm^2/sec was found to be the optimum choice for KCl encapsulation among the other polymers as it controlled the release at a constant rate over a period of 25 minutes. The advantage of encapsulating potassium chloride is to solve the problem that raw KCl is very irritating agent to the mucosal lining. This is important for the patient who may take up to three grams KCl daily to correct a condition of hypokalemia. In human clinical studies, where fecal blood loss indicates ulceration, microencapsulated potassium chloride did not increase the normal fecal blood loss but raw potassium chloride increased the fecal blood loss

a) Micrograph of C1 polymer empty shells in water

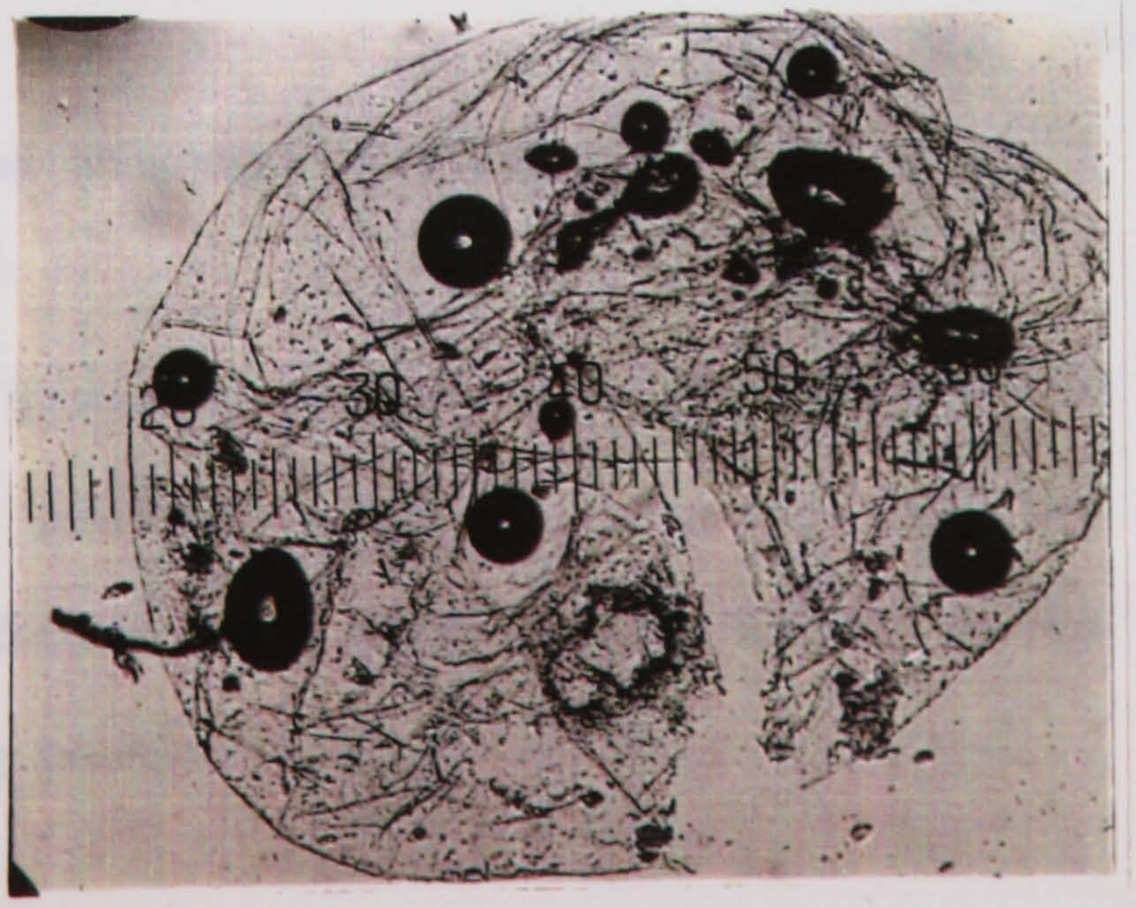

Fig. 8.14 b) Optical micrograph of a ruptured C1 polymer shell

by 500% as was reported by Maggi[4]. A zero order release rate of potassium chloride polymer matrix coated with a multiporous membrane was reported by Shah et al[5]. The polymeric matrix provided a backbone to the multiporous membrane which increased resistance of the membrane to rupture. Water-based diffusion coating of potassium chloride crystals as controlled release dosage formulation was demonstrated by Hansen et al[6]. Potassium chloride was also coated with polymer suspensions using fluidized bed equipment to achieve controlled dissolution[7].

The release patterns of β-estradiol from the various capsules used Fig. 8.6 were found to be sustained; although a zero-order release rate was not, at least initially, obtained. This suggests that the four different polymer materials used for encapsulation did not serve as rate controlling barriers. The boundary layer in the aqueous phase may be thick compared to the film coating and become rate controlling. So the permeability of the boundary layer would control the release rate much more than the polymer membrane. This would explain why the same release profiles were obtained from the different wall materials although their permeabilities and thicknesses were different.

The significant accelerated dissolution through GMA polymer is attributed to the fact that GMA polymer provides a microporous membrane coating as described earlier. This feature could allow the pumping out of the drug solution by an osmotic pumping process.

It is important to mention here that the technique used to study the release allowed the particles to settle instead of being suspended in the release medium.

The settling of the particles into a multiparticulate layer would convert an otherwise constant release into a rate which would decrease with time. Also, the frequency of collecting fractions from some of the releases allowed the concentration of the drug to reach up to 1.48 μg/ml as shown in Table 8.1. These relatively high concentrations approach the saturated solution concentrations of β–estradiol in water, 2.1 μg/ml, and cause the decrease in the release rate.

The concentration of β–estradiol in the fraction collected from the dissolution study of unencapsulated particles ranged between 1.36–1.60 μg/ml as explained in Table 8.1. These values are excessively high, the curve was included in Fig. 8.6 just as a reference to compare the dissolution profile with that of the encapsulated particles.

In order to have a better understanding of the release profiles of poorly water–soluble drugs like β–estradiol, the release studies should be preferably carried out under conditions which would allow the particles to be suspended individually in the release medium. Also, the release medium concentration should not exceed 10% of the value of the saturated solution during any release period. If these two conditions could be achieved, the dissolution rate of the encapsulated particles would be faster and possibly constant as expected.

Definitely, under such conditions the uncoated particle would dissolve faster compared to the results obtained in Fig. 8.6.

Release of encapsulated β–estradiol in buffer solutions at different temperatures was studied by Rashid[8]. Also, its release in different organic medium was studied

by Friend et al[9].

The *in vitro* release profile of 5-aminosalycylic acid indicates a Fickian diffusion controlled as Mt α $t^{\frac{1}{2}}$ as illustrated in Fig. 8.11 and 8.12 and also from Table 8.3. The release of the drug through C1 and GMA polymer was sustained but not constant. Although the weight of the drug in the coated samples used for release studies was precalculated not to exceed the 10% value of the saturated solution which is 137 μg/ml, the release rate was surprisingly not constant. This is probably due to the fact the 5-aminosalicylic acid particles formed agglomerates and particles of different shapes and sizes. In addition the release technique which was used allowed the particles to settle after a short period from the start of the release experiment and this would cause deviation from that giving a constant rate.

As GMA polymer membrane is microporous, this explains the relatively accelerated release compared to that of C1 membrane.

8.5 Conclusion

From the *in vitro* release profile mentioned above of the drug models of three different water solubilities used in this study, it is possible to conclude that C1 polymer forms a continuous coating with adequate flexibility and low permeability. It was a good model as a capsule membrane for the three drug systems and would be expected to give faster but constant release for the low water solubility drugs under the improved release technique conditions. The improved conditions would provide maintenance of low concentration during the release period and would allow the particles to be suspended in the release medium.

Styrene polymer provides a porous brittle coating which ruptures very easily if a significant osmotic pressure develops in the system. This would occur in cases of highly water soluble drug.

GMA polymer provides a microporous and apparently flexible membrane coating. This makes it a recommended choice with a low solubility drug.

Epikote 828 polymer provides a continuous coating film with less flexibility than C1 polymer but better than polystyrene. It would be applicable with a low solubility drug to avoid osmotic rupture.

References

1. I. Lipowsky, Australian patent 109, 438, November 22, (1938)

2. J.R. Robinson, Sustained and Controlled Release Drug Delivery System Marcel Dekker, Inc., New York and Basel (1978)

3. W.S. Frederik and L.J. Cass, J. New Drugs, 5, 138, (1965)

4. G.G. Maggi; G. Coppi; Curr. Ther. Res. Clin. Exp., 21, 676 (1977)

5. N.H. Shah, M.H. Infeld and A.W. Malick, Proceed. Intern. Symp. Control Rel. Bioact. Mater., 15, 38-39 (1988)

6. N.G. Hansen, F.N. Christensen, K. Kjarnaes, D. Willumsen, Proceed. Intern. Symp. Control. Rel. Bioact. Mater., 15, 366-367 (1988)

7. H.U. Petereit, K. Lehmann, D. Dreher, Proceed. Intern. Symp. Control Rel. Bioact. Mater., 15, 336 (1988)

8. "Some Aspects of Surface Chemistry, Microencapsulation and In Vitro Evaluation of β-Estradiol from an Injectable Formulation" MSc Thesis by Abdul Rashid, University of Strathclyde (1980)

9. D.R. Friend, P. Catz, and J. Heller, Proceed. Intern. Symp. Control Rel. Bioact. Mater. 15, 152-153 (1988)

10. N.A. Peppas, Pharm. Acta. Helv. 60, N-4, 110-111 (1985)

Overall Conclusion

The results cited in this study indicated that microencapsulation of potassium chloride, β-estradiol and 5-aminosalicylic acid took place in absence and in presence of α-monoolein surfactant, i.e. the surfactant did not have a major role in controlling the polymerization process.

The four polymers obtained in this study formed thin polymer films enveloping each particle of the drugs used.

Polystyrene film was microporous and of poor mechanical properties. It ruptured easily as a result of osmotic pressure developed from highly water soluble drug. It did not look practically promising as a rate controlling layer.

The C1 polymer provided a continuous film of calculated thickness of 0.11 μm. The permeability of C1 polymer to KCl was found to be 2.5×10^{-11} cm^2/sec. The results obtained indicated that there is a limit on the particle size of highly water soluble drugs, otherwise osmotic rupture would occur.

The GMA polymer provided a rubbery microporous film which could be used as a release rate controlling layer of low water solubility drugs. The structure of the polymer and its chemical properties require more investigation, as both the epoxy group and the double bond polymerized during the microencapsulation process.

Epikote 828 polymer formed a glassy continuous film of better resistance to osmotic pressure than polystyrene but still inferior to C1 polymer.

Increasing the thickness of polymer film is expected to improve the release profile of the highly water soluble drugs. This could be achieved by double coating, i.e. carrying out the microencapsulation process twice. In such case the surfactant might be important in the second process to improve the adsorption of the reactants onto the drug surface. This investigation is in progress.

Dedicated to Mama and my brothers,

Sultan, Sayed, Mohammed and Osama